TARGETING ANGIOGENESIS TO TREAT AUTOIMMUNE DISEASES AND CANCER

EDITED BY: Michal Amit Rahat, Vijaya Iragavarapu-Charyulu and Julia Kzhyshkowska

PUBLISHED IN: Frontiers in Immunology and Frontiers in Physiology

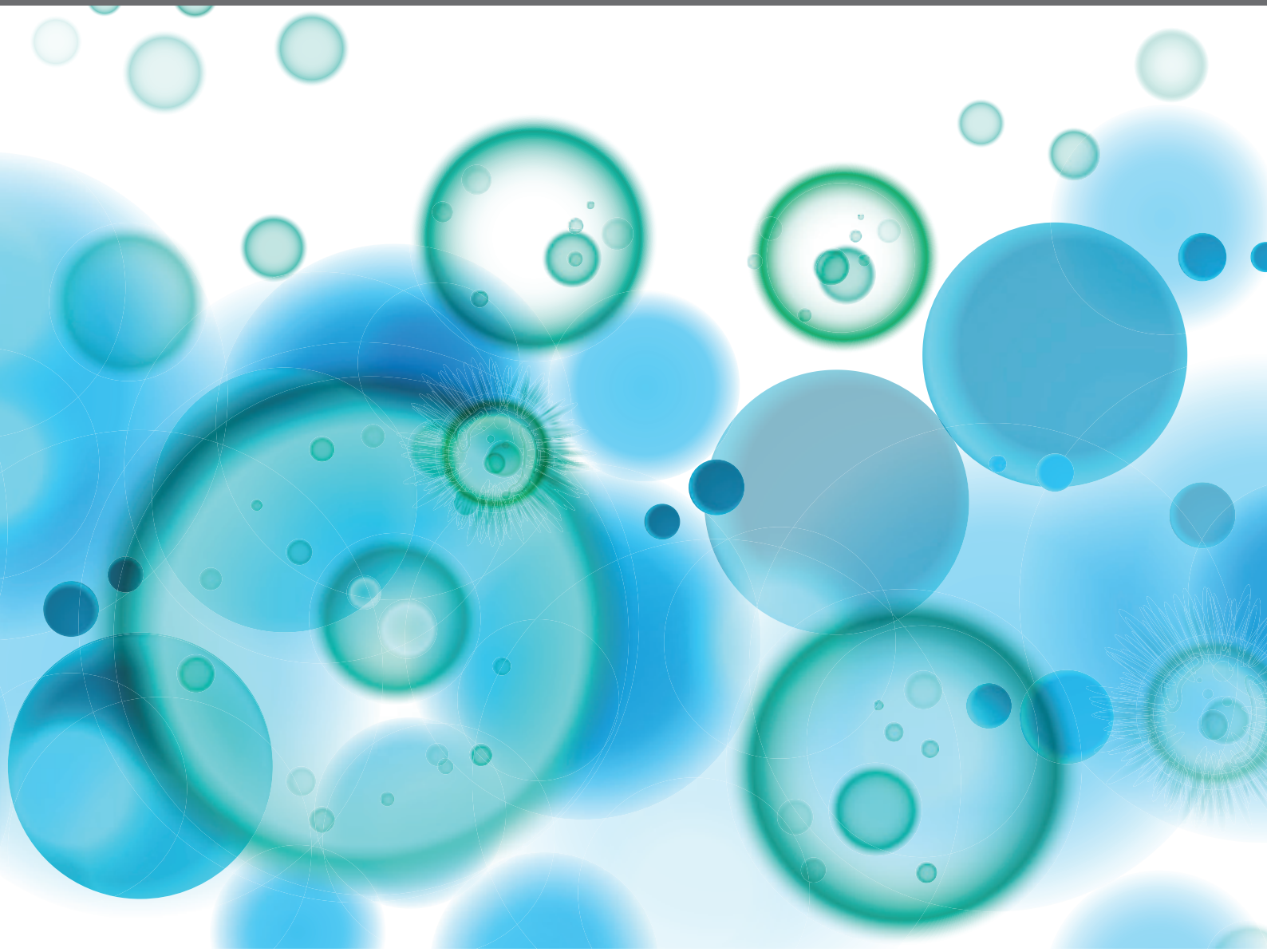

frontiers Research Topics

frontiers

ISSN 1664-8714
ISBN 978-2-88963-827-7
DOI 10.3389/978-2-88963-827-7

About Frontiers

Frontiers is more than just an open-access publisher of scholarly articles: it is a pioneering approach to the world of academia, radically improving the way scholarly research is managed. The grand vision of Frontiers is a world where all people have an equal opportunity to seek, share and generate knowledge. Frontiers provides immediate and permanent online open access to all its publications, but this alone is not enough to realize our grand goals.

Frontiers Journal Series

The Frontiers Journal Series is a multi-tier and interdisciplinary set of open-access, online journals, promising a paradigm shift from the current review, selection and dissemination processes in academic publishing. All Frontiers journals are driven by researchers for researchers; therefore, they constitute a service to the scholarly community. At the same time, the Frontiers Journal Series operates on a revolutionary invention, the tiered publishing system, initially addressing specific communities of scholars, and gradually climbing up to broader public understanding, thus serving the interests of the lay society, too.

Dedication to Quality

Each Frontiers article is a landmark of the highest quality, thanks to genuinely collaborative interactions between authors and review editors, who include some of the world's best academicians. Research must be certified by peers before entering a stream of knowledge that may eventually reach the public - and shape society; therefore, Frontiers only applies the most rigorous and unbiased reviews.
Frontiers revolutionizes research publishing by freely delivering the most outstanding research, evaluated with no bias from both the academic and social point of view. By applying the most advanced information technologies, Frontiers is catapulting scholarly publishing into a new generation.

What are Frontiers Research Topics?

Frontiers Research Topics are very popular trademarks of the Frontiers Journals Series: they are collections of at least ten articles, all centered on a particular subject. With their unique mix of varied contributions from Original Research to Review Articles, Frontiers Research Topics unify the most influential researchers, the latest key findings and historical advances in a hot research area! Find out more on how to host your own Frontiers Research Topic or contribute to one as an author by contacting the Frontiers Editorial Office: researchtopics@frontiersin.org

TARGETING ANGIOGENESIS TO TREAT AUTOIMMUNE DISEASES AND CANCER

Topic Editors:
Michal Amit Rahat, Technion Israel Institute of Technology, Israel
Vijaya Iragavarapu-Charyulu, Florida Atlantic University, United States
Julia Kzhyshkowska, Heidelberg University, Germany

Citation: Rahat, M. A., Iragavarapu-Charyulu, V., Kzhyshkowska, J., eds. (2020). Targeting Angiogenesis to Treat Autoimmune Diseases and Cancer. Lausanne: Frontiers Media SA. doi: 10.3389/978-2-88963-827-7

Table of Contents

frontiers in Immunology

EDITORIAL
published: 21 May 2020
doi: 10.3389/fimmu.2020.01005

Editorial: Targeting Angiogenesis to Treat Autoimmune Diseases and Cancer

Michal A. Rahat[1,2]*, *Julia Kzhyshkowska*[3,4,5] *and Vijaya Iragavarapu-Charyulu*[6]

[1] Immunotherapy Laboratory, Carmel Medical Center, Haifa, Israel, [2] The Ruth and Bruce Rappaport Faculty of Medicine, Technion-Israel Institute of Technology, Haifa, Israel, [3] Institute of Transfusion Medicine and Immunology, Medical Faculty Mannheim, University of Heidelberg, Mannheim, Germany, [4] German Red Cross Blood Service Baden-Württemberg—Hessen, Mannheim, Germany, [5] Laboratory of Translational Cellular and Molecular Biomedicine, National Research Tomsk State University, Tomsk, Russia, [6] Department of Biomedical Sciences, Florida Atlantic University, Boca Raton, FL, United States

Keywords: angiogenesis, autoimmunity, semaphorins, MMPs, EMMPRIN, TRPs, YKL-39, VEGF

OPEN ACCESS

Edited and reviewed by:
Denise Doolan,
James Cook University, Australia

***Correspondence:**
Michal A. Rahat
mrahat@netvision.net.il;
rahat_miki@clalit.org.il

Specialty section:
This article was submitted to Vaccines and Molecular Therapeutics, a section of the journal Frontiers in Immunology

Received: *16 March 2020*
Accepted: *28 April 2020*
Published: *21 May 2020*

Citation:
Rahat MA, Kzhyshkowska J and Iragavarapu-Charyulu V (2020) Editorial: Targeting Angiogenesis to Treat Autoimmune Diseases and Cancer. Front. Immunol. 11:1005. doi: 10.3389/fimmu.2020.01005

Editorial on the Research Topic

Targeting Angiogenesis to Treat Autoimmune Diseases and Cancer

Angiogenesis is the process where new blood vessels sprout from existing ones to address increased demand for oxygen and nutrients. Angiogenesis is physiologically required in development and wound healing, and is pathologically associated with many chronic inflammatory diseases, autoimmune diseases, and cancer (1). Within the tumor or inflamed microenvironment, epithelial, or cancer cells interact with stromal cells to determine which factors are secreted and to what extent. The balance between pro- and anti-angiogenic factors determines neovascularization. When pro-angiogenic factors are in excess over anti-angiogenic ones, the "angiogenic switch" is turned on resulting in the activation, proliferation, and migration of endothelial cells, and their spatial organization as new blood vessels. These vessels that feed the tissue are often leaky and permeable (2), and enable the infiltration of immune cells to the site, promoting a state of chronic inflammation.

Interventions designed to block angiogenesis were developed and some are in clinical use. Vascular endothelial growth factor (VEGF) or its receptors are targeted using monoclonal antibodies or small molecule tyrosine kinase inhibitors (3, 4). However, too often inhibition was transient, accompanied by off-target toxicities and a "rebound effect" of enhanced disease progression upon treatment withdrawal. This highlighted the redundancies of pro-angiogenic factors and the activation of compensatory mechanisms (5), and exemplified the complexity of the system, and therefore requiring new and more efficient strategies. This Research Topic provides an updated overview of new pro-angiogenic molecules and approaches to target familiar molecules.

First, the advantages of using active peptide vaccination against angiogenic targets is reviewed by Rahat. This strategy is generally considered a simple approach, with high specificity, reduced costs, easy synthesis, safe, and well-tolerated in comparison to traditional use of monoclonal antibodies against such targets. However, this strategy did not yield significant clinical benefits, and the review discusses reasons for this failure, including the choice of target, the type of peptides, the adjuvants, and the delivery methods used. This analysis is then followed by practical recommendations for peptide vaccinations.

The extracellular matrix (ECM) consisting of basement membrane (BM) and the underlying stroma plays an important role in angiogenesis. Members in the family of matrix metalloproteinases (MMPs), MMP-9, MMP-14, and MMP-2 that are strongly associated with angiogenesis, degrade the ECM allowing migration of endothelial cells. Fields describes different classes of selective MMP inhibitors, including antibodies and their fragments, triple-helical peptides, and small molecule compounds, developed specifically against these three MMPs and the principle of their inhibitory activity. Since MMPs can also activate anti-angiogenic factors (e.g., angiostatin, endostatin) that promote vessel normalization and/or regression, Fields reminds us that the correct timing or "window of opportunity" for the use of such inhibitors should be carefully determined.

Smani et al. explored the role of transient receptor potential (TRP) channels expressed by endothelial cells in growth-factor-induced angiogenesis. TRP channels are activated by pro-angiogenic factors resulting in rise of intracellular ions such as Ca^{2+} and activation of signaling pathways that promote angiogenesis. Thus, selective pharmacological TRP channel blockers may be additional strategies for anti-angiogenic therapies.

Angiogenesis is closely associated with intracranial aneurysm recurrence after surgery using the stent-jailing and stent-jack techniques. Exploring the difference between these two techniques, Xu et al. show that stent-jack causes higher mechanical forces in cerebral vessels than stent-jailing. They demonstrate lower micro-vessel density, TGFβ and Smad 2, 3, and 4 levels in the stent-jailing group compared to the stent-jack group, and conclude that the choice in surgical technique of stent-jailing could reduce shear stress, TGFβ signaling, and angiogenesis.

The role of angiogenesis in autoimmune diseases is beginning to unfold, and new approaches to its targeting are described in the next set of papers. Iragavarapu-Charyulu et al. review the role of different classes of semaphorins, axonal guidance molecules, with respect to their angiogenic activity and autoimmunity. Classes 3, 4, and 5 mediate either angiogenic or anti-angiogenic effects by signaling through neuropilins or plexins, and class 7 mediate angiogenic effects through binding to β1-integrin and Plexin-C1. Different strategies to target semaphorins to control angiogenesis and autoimmune diseases are addressed in this paper. In another paper, Adi et al. demonstrate that administration of Semaphorin 3A in an ovalbumin-induced mouse model of allergic asthma effectively reduced lung angiogenesis, eosinophil infiltration of lung bronchioles and arteries, and inflammatory cells in broncho-alveolar lavage. Another approach to targeting angiogenesis is demonstrated by Simanovich et al. A novel prophylactic peptide epitope was used to vaccinate against the pro-angiogenic protein EMMPRIN/CD147 in a murine model of DSS-induced colitis which mimics human Ulcerative Colitis. This vaccine resulted in improved clinical symptoms, reduced EMMPRIN expression and suppression of angiogenesis.

The critical role of angiogenesis in cancer is reviewed in the next three papers. In a mini-review, Barbosa de Aguiar and Zveiter de Moraes provide a perspective on targeting VEGF with bevacizumab, a humanized monoclonal antibody against VEGF, as both an angiogenesis inhibitor and modulator of the immune response in the tumor microenvironment, and discuss the contribution of the Fc and Fab domains of the antibody to this effect. Another family called chitinase-like proteins are glycoproteins whose levels are elevated in cancer patients and associated with poor prognosis. YKL-39 (chitinase 3-like protein 2), produced by tumor-associated macrophages (TAMs), is chemotactic for monocytes and stimulates angiogenesis. Kzhyshkowska et al. report that YKL-39 expression in tumors was found to be prognostic for metastasis after neoadjuvant chemotherapy in patients with breast cancer, suggesting YKL-39 as a target for anti-angiogenesis therapy. In the last paper, Huijbers et al. used a different approach to target CD99, a protein expressed by activated endothelial cells. Use of a conjugate vaccine that induced antibodies against CD99, resulted in reduced tumor micro-vessel density and functionality, and inhibition of tumor growth in two tumor models with high and low CD99 expression.

This collection of articles shows the tremendous diversity of pro-angiogenic molecules orchestrating angiogenesis in autoimmune diseases and in cancer, contributing to disease progression. To find cures for these diseases, new targets, and new approaches are required, and this collection suggests some new and exciting therapeutic possibilities.

AUTHOR CONTRIBUTIONS

All authors listed have made a substantial, direct and intellectual contribution to the work, and approved it for publication.

ACKNOWLEDGMENTS

We wish to convey our appreciation to all the authors who have participated in this Research Topic and to the reviewers for their hard work and insightful comments.

REFERENCES

1. Carmeliet P, Jain RK. Molecular Mechanisms and and clinical applications of angiogenesis. *Nature.* (2011) 473:298–307. doi: 10.1038/nature10144
2. Gacche RN. Compensatory angiogenesis and tumor refractoriness. *Oncogenesis.* (2015) 4:e153. doi: 10.1038/oncsis.2015.14
3. Yang J, Yan J, Liu B. Targeting VEGF/VEGFR to modulate antitumor immunity. *Front Immunol.* (2018) 9:978. doi: 10.3389/fimmu.2018.00978
4. Wu JB, Tang YL, Liang XH. Targeting VEGF pathway to normalize the vasculature: an emerging insight in cancer therapy. *Onco Targets Ther.* (2018) 11:6901–9. doi: 10.2147/OTT.S172042
5. Allen E, Missianen R, Bergers G. Trimming the vascular tree in tumors : metabolic and immune adaptations. *Cold Spring Harb Symp Quant Biol.* (2016) 81:21–9. doi: 10.1101/sqb.2016.81.030940

Conflict of Interest: The authors declare that the research was conducted in the absence of any commercial or financial relationships that could be construed as a potential conflict of interest.

frontiers in Physiology

REVIEW
published: 03 December 2018
doi: 10.3389/fphys.2018.01731

TRP Channels in Angiogenesis and Other Endothelial Functions

Tarik Smani[1,2†], *Luis J. Gómez*[3†], *Sergio Regodon*[3], *Geoffrey E. Woodard*[4], *Geraldine Siegfried*[5], *Abdel-Majid Khatib*[5*‡] and *Juan A. Rosado*[6*‡]

[1] Department of Medical Physiology and Biophysic, Institute of Biomedicine of Seville, University of Seville, Sevilla, Spain, [2] CIBERCV, Madrid, Spain, [3] Department of Animal Medicine, University of Extremadura, Cáceres, Spain, [4] Department of Surgery, Uniformed Services University of the Health Sciences, Bethesda, MD, United States, [5] INSERM U1029, University of Bordeaux, Bordeaux, France, [6] Cell Physiology Research Group, Department of Physiology, University of Extremadura, Cáceres, Spain

Angiogenesis is the growth of blood vessels mediated by proliferation, migration, and spatial organization of endothelial cells. This mechanism is regulated by a balance between stimulatory and inhibitory factors. Proangiogenic factors include a variety of VEGF family members, while thrombospondin and endostatin, among others, have been reported as suppressors of angiogenesis. Transient receptor potential (TRP) channels belong to a superfamily of cation-permeable channels that play a relevant role in a number of cellular functions mostly derived from their influence in intracellular Ca^{2+} homeostasis. Endothelial cells express a variety of TRP channels, including members of the TRPC, TRPV, TRPP, TRPA, and TRPM families, which play a relevant role in a number of functions, including endothelium-induced vasodilation, vascular permeability as well as sensing hemodynamic and chemical changes. Furthermore, TRP channels have been reported to play an important role in angiogenesis. This review summarizes the current knowledge and limitations concerning the involvement of particular TRP channels in growth factor-induced angiogenesis.

Keywords: angiogenesis, endothelial cells, VEGF, TRP channels, TRPC, TRPV, TRPM

OPEN ACCESS

Edited by:
Vijaya Iragavarapu-Charyulu, Florida Atlantic University, United States

Reviewed by:
Alexander Dietrich, Ludwig Maximilian University of Munich, Germany
Tim Murphy, University of New South Wales, Australia

***Correspondence:**
Abdel-Majid Khatib
majid.khatib@inserm.fr
Juan A. Rosado
jarosado@unex.es

[†] *These authors have contributed equally to this work*

[‡] *These authors share senior authorship*

Specialty section:
This article was submitted to Vascular Physiology, a section of the journal Frontiers in Physiology

Received: *23 June 2018*
Accepted: *16 November 2018*
Published: *03 December 2018*

Citation:
Smani T, Gómez LJ, Regodon S, Woodard GE, Siegfried G, Khatib A-M and Rosado JA (2018) TRP Channels in Angiogenesis and Other Endothelial Functions. Front. Physiol. 9:1731. doi: 10.3389/fphys.2018.01731

THE ANGIOGENIC PROCESS

The endothelium is a monolayer of endothelial cells (ECs) that line the internal surface of the vascular wall. In addition to serve as a barrier between circulation and the vascular smooth muscle cells, the endothelium plays a relevant role sensing hemodynamic and chemical changes in blood, regulating hemostasis and participating in the formation of new blood vessels, a process called angiogenesis. To create new vessels, ECs need to proliferate, to migrate, and to be organized in three dimensions. There are distinct processes of angiogenesis. The most rapid angiogenic mechanism is known as intussusception. Common in vascular remodeling during development, intussusception is the splitting of a preexisting vessel into two new smaller vessels. This occurs by penetration of smooth muscle cells through the endothelial cell layer (Burri et al., 2004). The formation of new vessels in adult during both physiological and pathological angiogenesis was also attributed to circulating bone marrow—derived endothelial precursor cells (EPCs). Although EPCs are mainly found in active sites of angiogenesis following a chemotactic signal (Patenaude et al., 2010), these cells act as collaborator cells in close proximity to the endothelium and are not incorporated into the vessel (Grunewald et al., 2006). Other angiogenic mechanisms occur during sprouting angiogenesis. Indeed, special ECs of a preexisting vessel acquire the capacity to invade the surrounding tissue

by forming an angiogenic sprout. The later is composed of leading cells known as tip cells and trailing stalk cells. These cells are required for the orientation and growth toward the source of an angiogenic factor (Gerhardt and Betsholtz, 2005). As soon as two sprouts anastomose, sprouting is accomplished by lumen formation and the initiation of blood circulation (Fantin et al., 2010). The maturation of newly formed sprouts into differentiated blood vessels requires the recruitment of mural cells, the development of the surrounding matrix and specialization of ECs in organ-specific manner. Pericytes participate in the stabilization of the newly formed blood vessels through direct physical contact and paracrine signaling.

Angiogenesis is regulated by a balance between stimulatory and inhibitory factors. When this balance shifts in favor of positive stimuli the "angiogenic switch" occurs (Hickey and Simon, 2006). To date several negative regulators of angiogenesis have been identified, however little is known about their exact role during physiological angiogenesis. Among these regulators, thrombospondin, previously reported to be secreted by epithelial cells, was found to inhibit tumor growth angiogenesis (Henkin and Volpert, 2011). Lately other anti-angiogenesis agents were also identified including endostatin, tumstatin, vasostatin, and lately anti-vascular endothelial growth factor (VEGF) (Norden et al., 2009). In the adult, under physiological conditions blood ECs are quiescent due to the increased levels of anti-angiogenic factors (thrombospondin and endostatin) compared to proangiogenic forces, such as the VEGF-A, placental growth factor (PlGF), platelet-derived growth factor (PDGF), and others. During pathological situations, including carcinogenesis and chronic inflammation, angiogenic factors are upregulated, and become more prominent than anti-angiogenic agents.

VEGF FAMILY MEMBERS AND THEIR RECEPTORS

The growth factors VEGFs, PDGF-BB, and PlGF are all grouped in the VEGF superfamily (McDonald and Hendrickson, 1993), and contain a cystine knot motif in their amino acid sequence. In mammals five VEGF members have been identified, namely VEGF-A, -B, -C, -D, and PlGF (McDonald and Hendrickson, 1993) (**Figure 1**). These growth factors mediate their function on vascular and lymphatic ECs through their cognate receptors VEGFR-1, -2, and -3 and the NP co-receptors. VEGF-A is able to activate both VEGFR-1 and VEGFR-2, whereas VEGF-B and PlGF are selective ligands for VEGFR-1 (Takahashi and Shibuya, 2005). VEGF-C and -D are the only known ligands for VEGFR-3 and are also able to activate VEGFR-2 (Tammela et al., 2005). The different expression of these receptors in various tissues seemed to be responsible for the relatively specific function of their ligands. Indeed, VEGFR-1 and VEGFR-2 are mainly found in vascular ECs, VEGFR-3 is largely restricted to lymphatic endothelium. Thus, according to their affinities for VEGFR-1 and -2, VEGF-A, -B, and PlGF exert angiogenic activities, while VEGF-C and -D predominantly act as lymphangiogenic growth factors by activating VEGFR-3. The interaction of VEGF with VEGFR (Jakobsson et al., 2006) leads to receptor dimerization leading to conformational changes and phosphorylation of their tyrosine residues, which is important for downstream signal mediators activation. The activation cascades outcome is the elaboration of various VEGF biological responses such as cell proliferation, survival, migration and ECs arrangement to form vascular tubes. The activation of VEGFR can be repressed by its dephosphorylation mediated by various phosphotyrosine phosphatases (PTPs), including density enhanced phosphatase 1 (DEP1) and vascular endothelial PTP (VEPTP) (Kappert et al., 2005).

VEGFR1

VEGFR1 (also known as Fms-like tyrosine kinase 1, Flt1,) binds VEGF-A, VEGF-B, and PlGF (Wiesmann et al., 1997). Activation of this receptor was found to induce various kinases including phosphoinositide 3′ kinase (PI3K)/protein kinase B (PKB/AKT), extracellular signal-regulated kinase (ERK)/mitogen-activated protein kinase (MAPK), and the stress kinase p38MAPK (Tchaikovski et al., 2008). VEGFR1 exists as a soluble form (sFlt1) (Kendall and Thomas, 1993), that exhibits higher affinity for VEGFA than VEGFR2. As a result, sFlt1 operates as a negative regulator of angiogenesis by reducing VEGFA/VEGFR2 interaction (Ambati et al., 2006).

VEGFR2

VEGFR2 [KDR (kinase insert domain receptor, human) and Flk1 (fetal liver kinase-1, mouse)]. Actively involved in vascular permeability, this receptor is crucial for ECs function during development. VEGFR2 is expressed most prominently in vascular ECs, with highest expression levels during embryonic vasculogenesis and angiogenesis (Millauer et al., 1993). VEGFR2 expression was also found increased during pathological processes associated with neovascularization such as tumor angiogenesis (Plate et al., 1993). VEGFR2 binds VEGF-A via its extracellular Ig-like domains 2 and 3, but with a lower affinity than VEGFR1 (Fuh et al., 1998). In contrast to VEGFR1, VEGFR2 binds also VEGF-C and VEGF-D (McColl et al., 2003) and represses binding to VEGFR3, which results in the inhibition of the proliferation of lymphatic ECs (Albuquerque et al., 2009). Interaction of VEGF-A and VEGFR2 promotes receptor dimerization (Yang et al., 2010), allowing receptor activation leading to several signaling mediators activation like PLCγ (Cunningham et al., 1997), and the adapter proteins SHB and SCK (Warner et al., 2000). These signals are required for various EC functions including proliferation, cell survival and migration, and vascular permeability.

VEGFR3

(also known as Flt4) binds VEGF-C and VEGF-D. Produced as precursor proteins, when proteolytically cleaved show increased affinity for both VEGFR2 and VEGFR3 (Joukov et al., 1997). VEGF-C and VEGFR3 interaction is critical for lymphendothelial function. Expressed in vascular ECs VEGFR3 is up-regulated during active angiogenesis. Binding of VEGF-C or VEGF-D to VEGFR3 leads to various kinases activation in VEGFR3 (Dixelius et al., 2003) and the activation of the PI3K/AKT pathway (Mäkinen et al., 2001), critical in lymphendothelial cell

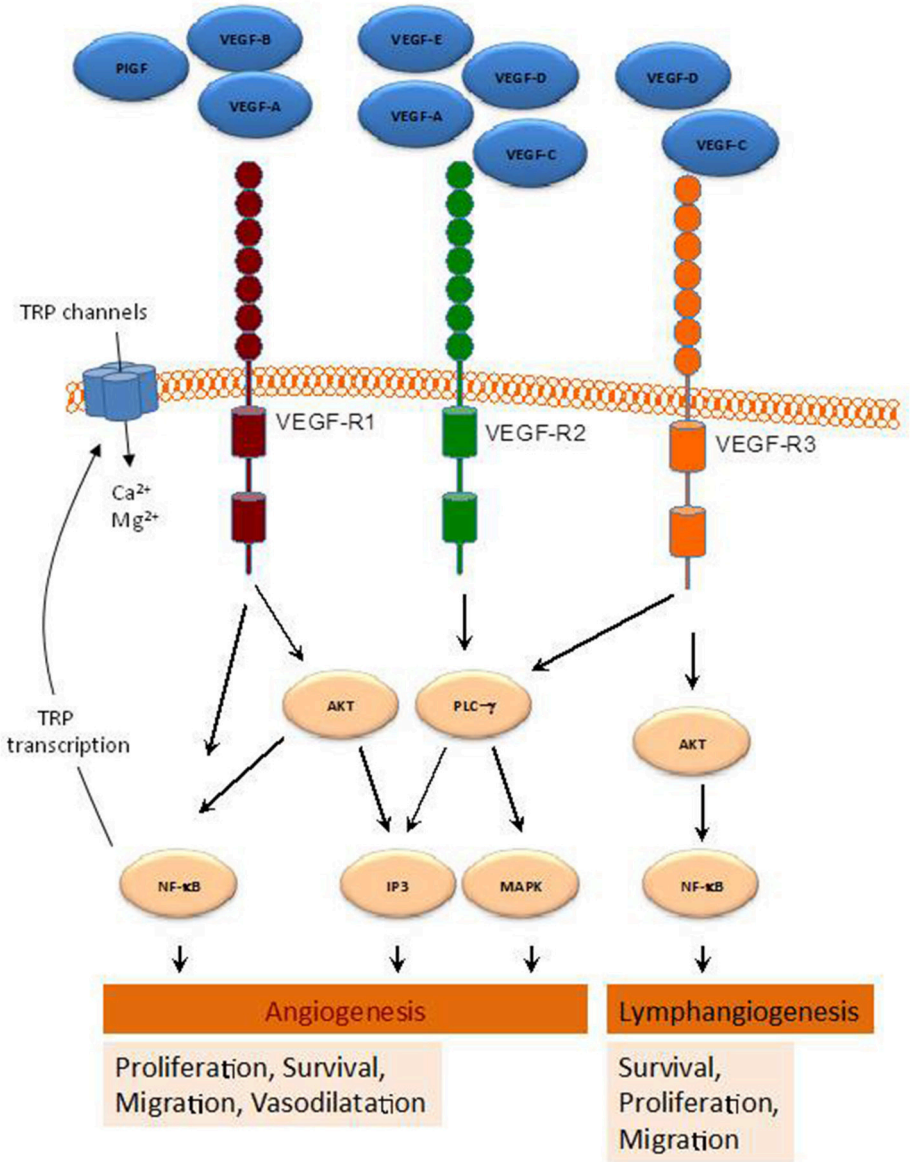

FIGURE 1 | Schematic representation of various pathways activated by the VEGF-family members. By binding to their receptors (VEGFR1-3), indicated VEGF members activate several intracellular pathways involved in a range of cellular functions leading to angiogenesis and lymphangiogenesis.

migration and sprouting of lymph EPCs and development of the lymphatic system (Karkkainen et al., 2004). Furthermore, VEGF-C-mediated AKT activation is required for embryonic and adult lymphangiogenesis (Zhou et al., 2010).

Compelling evidence demonstrated that VEGFRs increase intracellular Ca^{2+} concentration ($[Ca^{2+}]_i$), through the activation of TRP and other Ca^{2+} channels, which modulates signaling pathways leading to angiogenesis (Simons et al., 2016). For instance, VEGF-A enhances inositol 1,4,5-trisphosphate (IP_3) generation, which results in Ca^{2+} store depletion and the activation of store-operated Ca^{2+} entry in ECs and EPCs (SOCE) (Faehling et al., 2002; Moccia et al., 2014a). Consistent with this, SOCE inhibition or removal of extracellular Ca^{2+} has been reported to prevent VEGF-mediated Ca^{2+} oscillations in endothelial colony forming cells (Dragoni et al., 2011). Moreover, TRPC6 has been found to mediate VEGF-induced Ca^{2+} influx in microvessel ECs (Pocock et al., 2004), and both TRPC3 and TRPC6 mediate Ca^{2+} entry by VEGF in human microvascular ECs *in vivo* (Cheng et al., 2006). Furthermore, Mg^{2+} influx through TRP family members, such as TRPM6 and TRPM7, has been provided to be relevant for EC proliferation and angiogenesis (Nilius et al., 2003). TRP channels and VEGF signaling exhibit a cross relationship, so that VEGFRs activation has been reported to induce NFκB-mediated activation of

transcription of certain *TRP* genes (Santoni et al., 2011) (**Figure 1**), while Ca^{2+} influx via TRP channels has been found to stimulate the transcription of genes encoding different growth factors, including VEGF and PDGF, in ECs (Yao and Garland, 2005).Therefore, TRP channels play a relevant role in VEGF-mediated signaling in ECs, as summarized below.

OVERVIEW OF THE TRP SUPERFAMILY OF CATION CHANNELS

In 1969, Cosens and Manning reported their findings concerning a blind mutant strain of *Drosophila melanogaster* whose external appearance and histological sections of retinal structure were indistinguishable from the wild-type strain but exhibited abnormal electroretinogram (Cosens and Manning, 1969). Further studies revealed that while short stimuli induce a similar response in the wild-type and mutant fly, the response in the mutant fly to longer light stimulation was characterized by a marked decay in the receptor potential in the presence of illumination. The *trp* mutant, called so due to the transient receptor potential in response to light found in the retinular cells of the mutant strain, as compared to the more sustained receptor potential recorded in the wild-type fly, exhibited a defect in the process that links excitation to the membrane conductance (Minke et al., 1975; Minke, 1977). Later on, the light-sensitive conductance in *Drosophila* photoreceptors was found to be mediated by the Na^+ and Ca^{2+}-permeable channel trp and its homolog trpl (Hardie and Minke, 1992; Phillips et al., 1992), and comprises two distinct currents: one is conducted by the highly Ca^{2+} selective trp channel while the second is conducted by the trpl channel, which is supposed to be responsible for the residual light-sensitive current in the trp mutants (Katz et al., 2017).

The first mammalian homolog of *Drosophila* trp was identified in mouse in 1995 (Petersen et al., 1995) and two independent groups identified the first human transient receptor potential (TRP) channel, called TRPC1, (Wes et al., 1995; Zhu et al., 1995). Since the discovery of the first TRP channel in mammalian cells 28 TRP genes have been identified, which can be grouped into three subfamilies closely related to *Drosophila* trp (TRPC, TRPV, and TRPM), two more distantly related subfamilies (TRPP and TRPML), and a less related TRPN group expressed in flies and worms (Montell et al., 2002; Salido et al., 2011).

All TRP channels show a common architecture. They are membrane proteins with six putative transmembrane domains (TM1–TM6) and present a cation-permeable pore region created by a loop between TM5 and TM6 (**Figure 2**). The N- and C-termini are located intracellularly and show a great variability both in length and amino acid sequence among the different TRP members. The N- and C- terminal sequences include a variety of functional domains (Ramsey et al., 2006), including: (1) a variable number of ankyrin repeats (present in the members of TRPA, TRPC, TRPV, and TRPN subfamilies) that have been found to play a relevant role in channel sensing and gating (Gaudet, 2008); (2) TRPC, TRPM and TRPN exhibit a "TRP domain" sequence adjacent to the TM6, which shows highly conserved sequences called TRP boxes 1 and 2, and has been shown to be required for channel tetramerization and function (Venkatachalam and Montell, 2007). Similarly, the TRPV1, TRPA1, and TRPP channels show a TRP-like domain, which shows a similar α-helical configuration and function to TRP domains (García-Sanz et al., 2004; Zheng et al., 2018); (3) an α-kinase domain present in TRPM6 and TRPM7 that regulates channel function and sensitivity to Mg^{2+}·ATP (Clark et al., 2008; Zhang et al., 2014); (4) an ADPR hydrolase domain (Nudix-like domain or NUDT9 homology domain) in TRPM2, which has been reported to sense ADP-ribose concentration and convey this information to the cell by activation of cation entry (Scharenberg, 2005); (5) a calmodulin- and IP_3 receptor (IP_3R)-binding site (CIRB, present in TRPC, members), a domain that has been reported to be involved in the modulation of TRPC6 channel function by IP_3R and Ca^{2+}/calmodulin (Dionisio et al., 2011) and to modulate plasma membrane location of TRPC3 channels via an IP_3R-independent pathway (Wedel et al., 2003); (6) an EF-hand Ca^{2+}-binding domain (present in members of the TRPP, TRPML, and TRPA1) (Zurborg et al., 2007); (7) a large extracellular loop between TM1 and TM2 in TRPP and TRPML, which has recently been reported to play an essential role in channel assembly and function (Salehi-Najafabadi et al., 2017); and, (8) coiled-coil domains located in the C-terminal region (for TRPV, TRPM, TRPA1, and TRPP) or in the N- and C-terminal domains (for TRPC) (García-Sanz et al., 2004; Li et al., 2011a) (**Figure 2**), which have been found to be involved in subunit-subunit interaction (Launay et al., 2004), as well as in the interaction of TRPs with channel modulators, such as the interaction of TRPC proteins with the endoplasmic reticulum Ca^{2+} sensor, STIM1 (Lee et al., 2014).

Mammalian TRP channels are permeable to monovalent and divalent cations, with a permeability for Ca^{2+} over Na^+ (ratio P_{Ca}/P_{Na}) that ranges from channels that are selective for monovalent cations, such as TRPM4 and TRPM5, to highly Ca^{2+} selective channels, including TRPV5 and TRPV6, which exhibit a ratio P_{Ca}/P_{Na} over 100 (Freichel et al., 2012). It has also been reported that TRP channels are permeable to metal ions, such as manganese, magnesium, zinc, barium, strontium, nickel or cobalt, and, certain TRP members exhibit a greater relative permeability for these ions than for Ca^{2+} (for an extensive review see Bouron et al., 2015).

TRP channels have been reported to be activated and/or modulated by a number of chemical and physical stimuli, such as extracellular and intracellular ions (including H^+, Ca^{2+} and Mg^{2+}) (Liman, 2007; Zhang et al., 2014) and ligands, both intracellular molecules [such as diacylglycerol (Hofmann et al., 1999), phosphoinositide-4,5-bisphosphate (PIP_2) (Nilius et al., 2006; Jardín et al., 2008a)] and exogenous natural and synthetic ligands (for a review see Harteneck et al., 2011; Vetter and Lewis, 2011), temperature and mechanical stretch (Venkatachalam and Montell, 2007). Furthermore, TRPC channels have been reported to be activated by intracellular Ca^{2+} store depletion via the interaction with STIM1 and Orai1, the key elements for the activation of store-operated Ca^{2+} entry (SOCE) (Zhang et al., 2005; Feske et al., 2006). Ca^{2+} entry through SOCE is conducted by two types of channels: the highly Ca^{2+} selective CRAC (Ca^{2+} release-activated Ca^{2+}) channel, involving Orai1 subunits, and

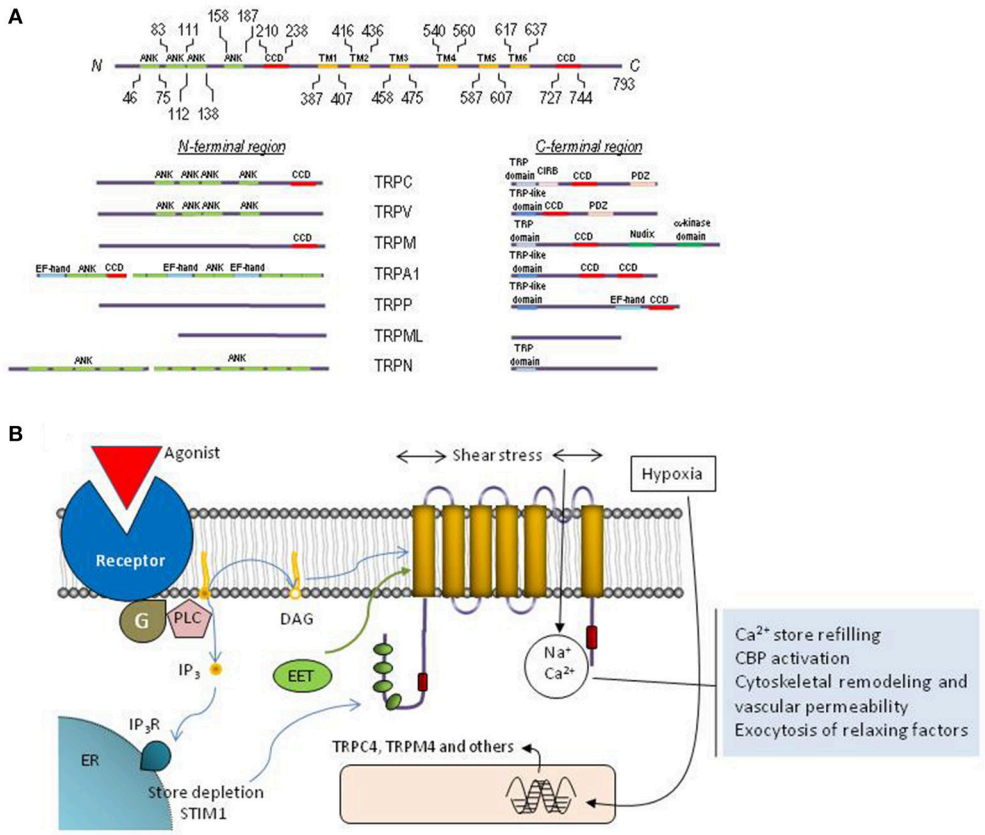

FIGURE 2 | Molecular structure and function of TRP channels. **(A)** Schematic representation of TRPC1 depicting functionally relevant domains. The cytoplasmic N- and C-termini of each TRP family contain different structural and functional domains as indicated. **(B)** Cartoon representing the topology of a TRP monomer within the plasma membrane, activation and functions associated to TRP channels in endothelial cells. The protein exhibits six transmembrane domains (TM1-TM6) with the pore located between transmembrane domains 5 and 6, and both N-terminal and C-terminal domains located in the cytosol. Endothelial TRP channels can be activated by receptor occupation, which, in turn, leads to the activation of phospholipase C and the generation of DAG and inositol 1,4,5-trisphosphate (IP_3). DAG is an endogenous activator of certain TRP channels and Ca^{2+} store depletion results in STIM1-dependent activation of TRPC1. Furthermore, TRP channels in endothelial cells can be activated by shear stress and the different EETs or their expression can be upregulated by hypoxia. Calcium influx via TRP channels is involved in Ca^{2+} store refilling, activation of Ca^{2+}-binding proteins (CBP), cytoskeletal remodeling and the regulation of vascular permeability as well as the exocytosis of smooth muscle cell relaxing factors.

the less selective store-operated Ca^{2+} (SOC) channels (Desai et al., 2015). Despite the participation of TRPC channels in SOCE has been a matter of intense debate in the past, there is now a general consensus that TRPC1 is a component of the SOC channels, forming a ternary complex with Orai1 and STIM1, which confers store depletion sensitivity to SOC channels (Huang et al., 2006; Jardin et al., 2008b; Desai et al., 2015; Ambudkar et al., 2017).

TRP CHANNELS IN THE ENDOTHELIUM

ECs have been reported to express at the transcript and/or protein level most of the mammalian TRP isoforms identified, including TRPC1, 3, 4, 5, 6, and 7, TRPV1, 2, and 4, TRPP1 and 2, TRPA1 and TRPM1, 2, 3, 4, 6, 7, and 8, although differences in the expression profile have been reported for different vasculatures and species (Wong and Yao, 2011; Cao et al., 2018).

TRP channels contribute to the Ca^{2+} influx induced by a plethora of vasoactive agents, including thrombin, ATP, angiotensin II or bradykinin (Bishara and Ding, 2010; Sundivakkam et al., 2013). Ca^{2+} entry through TRP channels has been found to be involved in the activation of a number of signaling pathways and cellular functions. Among the major functional roles of ECs is the modulation of the vascular tone through the release of a variety of factors that induce relaxation of smooth muscle cells. TRP channels have been reported to play an important role in this process, for instance, irisin, an exercise-induced myokine, has been reported to induce vasodilatation of rat mesenteric arteries through the activation of endothelial TRPV4 channels, which are involved in Ca^{2+} influx induced by irisin in primary cultured rat mesenteric artery ECs (Ye et al., 2018). Furthermore, TRPV4-deficient mice exhibit attenuated acetylcholine-induced endothelium-dependent vasodilatation associated to a reduced nitric oxide (NO) release (Zhang et al., 2009).

TRP channels have also been found to play a relevant role in vascular permeability, a cellular process that is based on transcellular and paracellular pathways, being the later regulated by the balance between cell-cell adhesive forces and contractile forces generated by the endothelial cytoskeleton (Wong and Yao, 2011). Probably, one of the most widely investigated TRP channels for its implication in endothelial permeability is TRPC6, which has been shown to be involved in lung ischemia-reperfusion-induced edema in mice (Weissmann et al., 2012), as well as in endotoxin-induced lung vascular permeability (Tauseef et al., 2012). TRPC1 and TRPC4 have also been found to be involved in vascular permeability. Expression of TRPC1 induced by TNFα has been reported to enhanced Ca^{2+} influx and vascular permeability (Paria et al., 2003) and TRPC4-deficient mice where thrombin-evoked Ca^{2+} signals and endothelial permeability were reduced (Tiruppathi et al., 2002). Other TRP channels, such as TRPV4 or TRPM4, have been reported to play a relevant role in vascular permeability. In isolated rat lung, activation of TRPV4 by 4α-phorbol 12,13-didecanoate (4α-PDD), as well as by 5,6- or 14,15-epoxyeicosatrienoic acids, has been found to increase lung endothelial permeability in a Ca^{2+} entry-dependent manner, which indicates that TRPV4 is involved in the disruption of the alveolar septal barrier. Consistent with this, the effect of the TRPV4 agonists was impaired in TRPV4-deficient mice (Alvarez et al., 2006). TRPM4 has been reported to be up-regulated in the ECs of blood vessels following spinal cord injury, which has been associated to secondary hemorrhage and progressive hemorrhagic necrosis (Gerzanich et al., 2009). Although the mechanism underlying the role of TRPM4 in vascular permeability remains unclear, there is a body of evidence supporting that TRPM4 expression is involved in post-trauma secondary hemorrhage, i.e., after spinal cord injury in rats, *in vivo* gene suppression using Trpm4 antisense was found to preserve capillary integrity and impair secondary hemorrhage, and similar results were observed in TRPM4-deficient mice (Gerzanich et al., 2009). Furthermore, 17β-estradiol, which attenuates TRPM4 and sulfonylurea receptor-1, has been reported to suppress disruption of the blood-spinal cord barrier and attenuate secondary hemorrhage after spinal cord injury (Lee et al., 2015).

Finally, TRP channels have also been reported to play a functional role in the ability of the ECs to sense hemodynamic and chemical changes. Flow shear force results in rises in cytosolic Ca^{2+} concentration ($[Ca^{2+}]_i$), which, in turn, lead to the release of vasodilating factors. A number of TRP channels are sensitive to flow shear stress, such as TRPV4. It has been reported that flow shear stress induces relaxation of the carotid artery, an effect that is mimicked by the TRPV4 activator 4α-PDD and is prevented by the non-selective TRPV4 inhibitor ruthenium red (Köhler et al., 2006). The involvement of TRPV4 in endothelial-dependent vascular dilation was confirmed in TRPV4-deficient mice, which exhibit attenuated response to stimulation with endothelium-derived hyperpolarizing factor (Loot et al., 2008) and, more recently, with studies reporting that TRPV4-TRPC1 heteromeric channels mediate flow shear-induced endothelial Ca^{2+} influx by a mechanism that might involve an upstream mechanosensitive pathway including phospholipase A2 and cytochrome P450 epoxygenase activity (Loot et al., 2008; Ma et al., 2010). The TRPP1-TRPP2 complex has also been suggested to play a role in flow-induced ECs-mediated vascular dilation, as Ca^{2+} influx and NO production in response to flow is significantly reduced by TRPP1 or TRPP2 expression silencing (Nauli et al., 2008; AbouAlaiwi et al., 2009); although the mechanism underlying the activation of TRPP2-mediated Ca^{2+} entry by flow shear forces in ECs remains unclear. A more recent study has identified the formation of a heteromeric channel including the flow-sensitive TRPV4 and both TRPC1 and TRPP2, which mediates the flow-induced Ca^{2+} influx in native vascular ECs (Du et al., 2014). TRP channels also play a relevant role sensing chemical blood components. For instance, TRPC3, TRPC4, TRPM2, TRPM7, and TRPA1 have been reported to be activated by oxidative stress, leading to Na^+ and Ca^{2+} entry and, thus, mediating the vascular effects associated to reactive oxygen species (ROS) (Wong and Yao, 2011). On the other hand, in addition to sensing ROS, TRPA1 channels have been found to detect molecular oxygen and are essential for hyperoxia- and hypoxia-induced vagal responses (Takahashi et al., 2011). The mechanistic details of the activation of TRPA1 by O_2 as well as the transduction pathway remain unclear; however, in cerebral arteries, TRPA1 in the endothelium is mostly located within myoendothelial junction sites, where TRPA1-mediated Ca^{2+} influx is associated to endothelium-dependent smooth muscle cell vasodilatation through the activation of Ca^{2+}-activated K^+ channels ($K_{Ca}3.1$), which, in turns, results in ECs hyperpolarization that is conducted via myoendothelial gap junctions to hyperpolarize the adjacent smooth muscle cell, resulting in myocyte relaxation (Earley, 2012).

TRP CHANNELS IN ANGIOGENESIS

TRP channels have also been found to play a relevant role in angiogenesis. Compelling evidence demonstrated that angiogenic growth factors activate TRP channels, causing a subsequent rise in endothelial $[Ca^{2+}]_i$, which modulates the signal transduction pathways leading to angiogenesis (Kwan et al., 2007). It is known that both tumor and physiological angiogenesis are initiated in hypoxic environment principally due to secretion of several growth factors, such as VEGF. These growth factors stimulate proliferation, migration, and tube formation of ECs, resulting in the generation of new capillary (Kohn et al., 1995). Most studies used particularly VEGF to investigate neovascularization in different experimental model. Briefly, tyrosine phosphorylation of VEGFR triggers activation of phospholipase C (PLC), inositol 1,4,5-triphosphate (InsP3) and diacylglycerol (DAG) generation. The consequent Ca^{2+} entry following the classic Ca^{2+} release modulates signaling pathways leading to angiogenesis (Simons et al., 2016). Several reports demonstrated that VEGF-induced Ca^{2+} entry through different isoforms of TRP in several cell types, such as TRPC3 and TRPC6 (Hamdollah Zadeh et al., 2008; Andrikopoulos et al., 2017); TRPM2 through reactive oxygen generation (Mittal et al., 2015); or TRPV1 (Garreis et al., 2016). Certainly, in ECs some TRPs associate to others isoforms forming heteromeric channels (Loot et al., 2008; Nauli et al., 2008; AbouAlaiwi et al., 2009; Ma et al.,

2010), however most studies of angiogenesis focused on only one isoform of TRPs as detailed below.

Role of TRPCs

The participation of TRPC3 in angiogenesis has been characterized in Human Umbilical Vein ECs (HUVEC) treated with VEGF. TRPC3 inhibition or its silencing with siRNA attenuated VEGF activation of ERK1/2 phosphorylation, and stimulation of $[Ca^{2+}]_i$ transients in HUVEC. Additionally, siRNA of TRPC3 significantly suppressed endothelial tube formation, an indicator of angiogenesis (Andrikopoulos et al., 2017). This study suggests that TRPC3 is activated by the generation of DAG downstream of VEGFR in HUVECs, causing Na^+ influx by subsequent activation of the Na^+/Ca^{2+} exchanger in reversal mode, contributing ultimately to angiogenesis (Andrikopoulos et al., 2017). The role of TRPC3 in angiogenesis has also been evaluated in EPCs (Dragoni et al., 2013). As stated above, EPCs are adult stem cells having the ability to differentiate into ECs, and thereby they promote postnatal vasculogenesis and endothelial repair after vascular intima injury (Djohan et al., 2018). Molecular and pharmacological inhibition of TRPC3, using siRNA and Pyr3 respectively, abrogated VEGF-induced Ca^{2+} response and inhibited proliferation of EPCs (Dragoni et al., 2013). The selectivity of Pyr3 on TRPC3 might be questioned, nevertheless the effect of TRPC3 silencing suggest that this channels might be relevant for vasculogenesis.

Independently of ECs stimulation with VEGF, silencing the expression of TRPC3, TRPC4, or TRPC5 also prevented spontaneous $[Ca^{2+}]_i$ oscillations and inhibited tube formation in human umbilical vein-derived EC line EA.hy926 and HUVECs (Antigny et al., 2012). A recent study performed in retina microvascular ECs showed that hypoxia, a potent trigger of angiogenesis, enhanced the expression of TRPC4, whose silencing inhibited VEGF-induced ECs proliferation and migration and *in vitro* angiogenesis evaluated by tube formation (Song et al., 2015). More recently, silencing of TRPC4 attenuated oxLDL-induced human coronary ECs proliferation; migration and *in vit*ro angiogenesis-tube formation on matrigel, suggesting that suppression of TRPC4 might be an alternative therapeutic strategy for atherosclerotic neovascularization (Qin et al., 2016).

TRPC6 seems also critical for angiogenesis and Ca^{2+} entry in response to VEGF and 1-oleoyl-2-acetyl-sn-glycerol (OAG, a membrane-permeant DAG analog) in human microvascular ECs and in HUVEC. Experiments using a dominant-negative mutant of TRPC6, made with three mutations in the pore region, reduced ECs proliferation, migration and sprouting in matrigel assay (Hamdollah Zadeh et al., 2008). Similar results were observed in HUVEC, where a dominant-negative form of TRPC6 inhibited VEGF-induced cation current, HUVEC growth and proliferation, as well as VEGF-evoked capillary formation *in vitro* (Ge et al., 2009). The role of TRPC6 in ECs proliferation and tube formation was also observed when 11,12-EET (11,12-cis-epoxyeicosatrienoic acid) was used to stimulate ECs (Ding et al., 2014).

Other studies have focused on the role of TRPC1 in angiogenesis. Indeed, a proangiogenic role for TRPC1 has been described *in vivo* in zebrafish, where authors have identified severe angiogenic defects in intersegmental vessel sprouting after knockdown of TRPC1 (Yu et al., 2010). Furthermore, TRPC1 likely controls cell proliferation and tubulogenesis in normal EPCs and in those isolated from peripheral blood of tumor patients (Moccia et al., 2014b). Recently, *in vivo* matrigel assay confirmed that EPCs isolated from TRPC1 knockout mice has substantially reduced functional activities, including migration and tube formation, indicating that TRPC1 plays an important role in angiogenesis (Du et al., 2018). Nevertheless, other studies suggested that TRPC1 is not relevant for angiogenesis. The use of siRNAs, dominant-negative mutants or neutralizing antibodies, failed to demonstrate that TRPC1 is required for VEGF-induced Ca^{2+} increase in HUVECs and tube formation (Li et al., 2011b; Antigny et al., 2012). Interestingly, TRPC1 knockout mice developed normal vasculature (Schmidt et al., 2010). Therefore, more investigations are still required to clarify the real role of TRPC1 in the angiogenic processes.

Role of TRPVs

TRPV4 has long been known to regulate angiogenesis and neovascularization by stimulating ECs proliferation and migration as reviewed recently (Moccia, 2018). TRPV4 plays an important role in cytoskeletal reorganization and changes in cell adhesion, which coordinate ECs proliferation and motility via mechanotransduction (Köhler et al., 2006; Reddy et al., 2015; Adapala et al., 2016; Thoppil et al., 2016). TRPV4 is dramatically up-regulated in breast tumor-derived ECs, and is required for arachidonic acid (AA)-evoked Ca^{2+} entry, which increase the rate of ECs migration and motility as compared to control ECs (Fiorio Pla et al., 2012). Moreover, the absence of TRPV4 in knockout mice was associated with an increase in basal Rho/Rho kinase activity, significant increase in ECs proliferation, migration, and abnormal tube formation *in vitro* (Thoppil et al., 2016). Interestingly, another study from the same group confirmed that overexpression or pharmacological activation of TRPV4, using GSK1016790, restored the aberrant ECs mechanosensitivity, migration and normalized tube formation in matrigel assay. TRPV4 activation and overexpression likely normalized the abnormal angiogenesis evoked by tumor ECs through the inhibition of the exacerbated Rho activity (Adapala et al., 2016). Therefore, TRPV4 activation seems relevant to normalize tumor angiogenesis via modulation of Rho/Rho kinase pathway.

TRPV1 has been found to be pro-angiogenic. Intraperitoneal injection of mice with a TRPV1 ligand, evodiamine, promoted vascularization in matrigel plugs used *in vivo* in wild type mice. In contrast, the induced angiogenesis was markedly reduced in TRPV1 knockout mice (Ching et al., 2011). Similarly, using knockout mice TRPV1 appears crucial for 14,15-EET-induced Ca^{2+} influx, NO production and angiogenesis evaluated by tube formation and *in vivo* matrigel assays (Su et al., 2014a). In addition, in human microvascular ECs TRPV1 activation is involved in simvastatin-activated Ca^{2+} influx, which induced the activation of CaMKII signaling and enhanced the formation of TRPV1–eNOS complex, leading to NO production and *in vitro* angiogenesis-tube formation (Su et al., 2014b).

Role of TRPMs

TRPM2, TRPM4, and TRPM7 have also been found to be involved in angiogenesis (Zhou et al., 2014). Recently, a study demonstrated that VEGF stimulated ECs migration and induced ROS-dependent Ca^{2+} entry through TRPM2 activation. In addition, they showed that matrigel plugs supplemented with VEGF injected subcutaneously in TRPM2 knockout mice presented significantly reduced vessel formation compared to wild type mice. Using the mouse aortic ring assay, they also observed defective capillary sprouting and reduced capillary lengths isolated from TRPM2 knockout mouse rings as compared with WT mice, indicating that TRPM2 was required for angiogenesis and ischemic neovascularization (Mittal et al., 2015). Moreover, TRPM4 is upregulated in vascular endothelium following hypoxia/ischemia *in vitro* and *in vivo*, and in HUVECs following oxygen–glucose deprivation. Pharmacological blocking of TRPM4, or its silencing with siRNA, enhanced tube formation on matrigel and improved capillary integrity *in vivo* (Loh et al., 2014). Previously, a report demonstrated that silencing of TRPM7, mimics the effect of Mg^{2+} deficiency in microvascular ECs growth and migration, proposing magnesium and TRPM7 as a modulator of angiogenesis (Baldoli and Maier, 2012).

Others TRPs' Role in Angiogenesis

Little is known regarding the participation of TRPA and TRPP isoforms in the angiogenic process. Few years ago, TRPA1 was suggested as the downstream effector for simvastatin—evoked activation of TRPV1-Ca^{2+} signaling in ECs, since its inhibition markedly decreased eNOS activation, NO production and *in vitro* angiogenesis-tube formation (Su et al., 2014b). The role of TRPA1 was further confirmed using matrigel plugs *in vivo* in TRPA1 knockout mice, whereby simvastatin—induced angiogenesis was partially reduced (Su et al., 2014b).

CONCLUSION

ECs activity, such as proliferation, migration, and survival is required for angiogenesis under both physiological conditions, (vessel growth and renewal) and pathological conditions, (cardiovascular diseases and tumors initiation and progression). Alteration of these functions resulted from exaggerated or reduced bioavailability of various downstream effectors of VEGF receptors. For example increased Akt and ERK activation following sustained VEGFRs-VEGF interaction induces tumor angiogenesis and growth, whereas, reduced Nitric oxide (NO) production seemed to cause endothelial dysfunction such as deficiency in vascular relaxation. It is now evident that TRP channels are critically involved in physiological and pathological angiogenic process. By controlling Ca^{2+} homeostasis, different TRP isoforms are activated by pro-angiogenic stimuli that evoke ECs proliferation and migration, as well as the formation of new capillary derived either from ECs or from EPCs. Nevertheless, considerable work is needed to fully understand why many TRPs from different subfamilies are activated by similar pro-angiogenic stimuli such as VEGFs, and whether these TRPs might associate between them to promote their angiogenic effect. To the best of our knowledge, and from the point of view of angiogenesis, the organization and interactions between closely related TRP channels have not been addressed. Several questions still remain unsolved concerning the role or TRP channels in angiogenesis such as are different TRPs located in microdomains with different VEGF-receptors? Are different Ca^{2+} signals generated by these TRP complexes inducing different cellular functions? Further studies will definitely clarify these and other functional aspects.

In light of the reported findings, the search of selective pharmacological blockers or activator of TRP channels stands out among the strategies for obtaining promising molecular drugs to normalize angiogenesis or for anti-angiogenic therapies to prevent tumor neovascularization.

AUTHOR CONTRIBUTIONS

TS, A-MK, and JR conceived the concept of the review. TS, A-MK, LG, GS, and JR wrote the review. SR, GW, and A-MK designed and formatted the figures. TS, LG, SR, GW, GS, A-MK, and JR read and edited the review manuscript.

ACKNOWLEDGMENTS

This work was supported by MINECO [Grants BFU2016-74932-C2], by the Institute of Carlos III [Grant PI15/00203], by the Andalusia Government [Grant: PI-0313-2016] and Junta de Extremadura-FEDER (IB16046 and GR18061). This study was co-financed by FEDER Funds.

REFERENCES

AbouAlaiwi, W. A., Takahashi, M., Mell, B. R., Jones, T. J., Ratnam, S., Kolb, R. J., et al. (2009). Ciliary polycystin-2 is a mechanosensitive calcium channel involved in nitric oxide signaling cascades. *Circ. Res.* 104, 860–869. doi: 10.1161/CIRCRESAHA.108.192765

Adapala, R. K., Thoppil, R. J., Ghosh, K., Cappelli, H. C., Dudley, A. C., Paruchuri, S., et al. (2016). Activation of mechanosensitive ion channel TRPV4 normalizes tumor vasculature and improves cancer therapy. *Oncogene* 35, 314–322. doi: 10.1038/onc.2015.83

Albuquerque, R. J., Hayashi, T., Cho, W. G., Kleinman, M. E., Dridi, S., Takeda, A., et al. (2009). Alternatively spliced vascular endothelial growth factor receptor-2 is an essential endogenous inhibitor of lymphatic vessel growth. *Nat. Med.* 15, 1023–1030. doi: 10.1038/nm.2018

Alvarez, D. F., King, J. A., Weber, D., Addison, E., Liedtke, W., and Townsley, M. I. (2006). Transient receptor potential vanilloid 4-mediated disruption of the alveolar septal barrier: a novel mechanism of acute lung injury. *Circ. Res.* 99, 988–995. doi: 10.1161/01.RES.0000247065.11756.19

Ambati, B. K., Nozaki, M., Singh, N., Takeda, A., Jani, P. D., Suthar, T., et al. (2006). Corneal avascularity is due to soluble VEGF receptor-1. *Nature* 443, 993–997. doi: 10.1038/nature05249

Ambudkar, I. S., de Souza, L. B., and Ong, H. L. (2017). TRPC1, Orai1, and STIM1 in SOCE: friends in tight spaces. *Cell Calcium* 63, 33–39. doi: 10.1016/j.ceca.2016.12.009

Andrikopoulos, P., Eccles, S. A., and Yaqoob, M. M. (2017). Coupling between the TRPC3 ion channel and the NCX1 transporter contributed to VEGF-induced ERK1/2 activation and angiogenesis in human primary endothelial cells. *Cell. Signal.* 37, 12–30. doi: 10.1016/j.cellsig.2017.05.013

Antigny, F., Girardin, N., and Frieden, M. (2012). Transient receptor potential canonical channels are required for *in vitro* endothelial tube formation. *J. Biol. Chem.* 287, 5917–5927. doi: 10.1074/jbc.M111.295733

Baldoli, E., and Maier, J. A. (2012). Silencing TRPM7 mimics the effects of magnesium deficiency in human microvascular endothelial cells. *Angiogenesis* 15, 47–57. doi: 10.1007/s10456-011-9242-0

Bishara, N. B., and Ding, H. (2010). Glucose enhances expression of TRPC1 and calcium entry in endothelial cells. *Am. J. Physiol. Heart Circ. Physiol.* 298, H171–H178. doi: 10.1152/ajpheart.00699.2009

Bouron, A., Kiselyov, K., and Oberwinkler, J. (2015). Permeation, regulation and control of expression of TRP channels by trace metal ions. *Pflugers Arch.* 467, 1143–1164. doi: 10.1007/s00424-014-1590-3

Burri, P. H., Hlushchuk, R., and Djonov, V. (2004). Intussusceptive angiogenesis: its emergence, its characteristics, and its significance. *Dev. Dyn.* 231, 474–488. doi: 10.1002/dvdy.20184

Cao, S., Anishkin, A., Zinkevich, N. S., Nishijima, Y., Korishettar, A., Wang, Z., et al. (2018). Transient receptor potential vanilloid 4 (TRPV4) activation by arachidonic acid requires protein kinase A-mediated phosphorylation. *J. Biol. Chem.* 293, 5307–5322. doi: 10.1074/jbc.M117.811075

Cheng, H. W., James, A. F., Foster, R. R., Hancox, J. C., and Bates, D. O. (2006). VEGF activates receptor-operated cation channels in human microvascular endothelial cells. *Arterioscler. Thromb. Vasc. Biol.* 26, 1768–1776. doi: 10.1161/01.ATV.0000231518.86795.0f

Ching, L. C., Kou, Y. R., Shyue, S. K., Su, K. H., Wei, J., Cheng, L. C., et al. (2011). Molecular mechanisms of activation of endothelial nitric oxide synthase mediated by transient receptor potential vanilloid type 1. *Cardiovasc. Res.* 91, 492–501. doi: 10.1093/cvr/cvr104

Clark, K., Middelbeek, J., Dorovkov, M. V., Figdor, C. G., Ryazanov, A. G., Lasonder, E., et al. (2008). The alpha-kinases TRPM6 and TRPM7, but not eEF-2 kinase, phosphorylate the assembly domain of myosin IIA, IIB and IIC. *FEBS Lett.* 582, 2993–2997. doi: 10.1016/j.febslet.2008.07.043

Cosens, D. J., and Manning, A. (1969). Abnormal electroretinogram from a Drosophila mutant. *Nature* 224, 285–287. doi: 10.1038/224285a0

Cunningham, S. A., Arrate, M. P., Brock, T. A., and Waxham, M. N. (1997). Interactions of FLT-1 and KDR with phospholipase C gamma: identification of the phosphotyrosine binding sites. *Biochem. Biophys. Res. Commun.* 240, 635–639. doi: 10.1006/bbrc.1997.7719

Desai, P. N., Zhang, X., Wu, S., Janoshazi, A., Bolimuntha, S., Putney, J. W., et al. (2015). Multiple types of calcium channels arising from alternative translation initiation of the Orai1 message. *Sci. Signal.* 8:ra74. doi: 10.1126/scisignal.aaa8323

Ding, Y., Fromel, T., Popp, R., Falck, J. R., Schunck, W. H., and Fleming, I. (2014). The biological actions of 11,12-epoxyeicosatrienoic acid in endothelial cells are specific to the R/S-enantiomer and require the G(s) protein. *J. Pharmacol. Exp. Ther.* 350, 14–21. doi: 10.1124/jpet.114.214254

Dionisio, N., Albarran, L., Berna-Erro, A., Hernandez-Cruz, J. M., Salido, G. M., and Rosado, J. A. (2011). Functional role of the calmodulin- and inositol 1,4,5-trisphosphate receptor-binding (CIRB) site of TRPC6 in human platelet activation. *Cell. Signal.* 23, 1850–1856. doi: 10.1016/j.cellsig.2011.06.022

Dixelius, J., Makinen, T., Wirzenius, M., Karkkainen, M. J., Wernstedt, C., Alitalo, K., et al. (2003). Ligand-induced vascular endothelial growth factor receptor-3 (VEGFR-3) heterodimerization with VEGFR-2 in primary lymphatic endothelial cells regulates tyrosine phosphorylation sites. *J. Biol. Chem.* 278, 40973–40979. doi: 10.1074/jbc.M304499200

Djohan, A. H., Sia, C. H., Lee, P. S., and Poh, K. K. (2018). Endothelial progenitor cells in heart failure: an authentic expectation for potential future use and a lack of universal definition. *J. Cardiovasc. Transl. Res.* 11, 393–402. doi: 10.1007/s12265-018-9810-4

Dragoni, S., Laforenza, U., Bonetti, E., Lodola, F., Bottino, C., Berra-Romani, R., et al. (2011). Vascular endothelial growth factor stimulates endothelial colony forming cells proliferation and tubulogenesis by inducing oscillations in intracellular Ca^{2+} concentration. *Stem Cells* 29, 1898–1907. doi: 10.1002/stem.734

Dragoni, S., Laforenza, U., Bonetti, E., Lodola, F., Bottino, C., Guerra, G., et al. (2013). Canonical transient receptor potential 3 channel triggers vascular endothelial growth factor-induced intracellular Ca^{2+} oscillations in endothelial progenitor cells isolated from umbilical cord blood. *Stem Cells Dev.* 22, 2561–2580. doi: 10.1089/scd.2013.0032

Du, J., Ma, X., Shen, B., Huang, Y., Birnbaumer, L., and Yao, X. (2014). TRPV4, TRPC1, and TRPP2 assemble to form a flow-sensitive heteromeric channel. *FASEB J.* 28, 4677–4685. doi: 10.1096/fj.14-251652

Du, L. L., Shen, Z., Li, Z., Ye, X., Wu, M., Hong, L., et al. (2018). TRPC1 deficiency impairs the endothelial progenitor cell function via inhibition of calmodulin/eNOS pathway. *J. Cardiovasc. Transl. Res.* 11, 339–345. doi: 10.1007/s12265-018-9798-9

Earley, S. (2012). TRPA1 channels in the vasculature. *Br. J. Pharmacol.* 167, 13–22. doi: 10.1111/j.1476-5381.2012.02018.x

Faehling, M., Kroll, J., Fohr, K. J., Fellbrich, G., Mayr, U., Trischler, G., et al. (2002). Essential role of calcium in vascular endothelial growth factor A-induced signaling: mechanism of the antiangiogenic effect of carboxyamidotriazole. *FASEB J.* 16, 1805–1807. doi: 10.1096/fj.01-0938fje

Fantin, A., Vieira, J. M., Gestri, G., Denti, L., Schwarz, Q., Prykhozhij, S., et al. (2010). Tissue macrophages act as cellular chaperones for vascular anastomosis downstream of VEGF-mediated endothelial tip cell induction. *Blood* 116, 829–840. doi: 10.1182/blood-2009-12-257832

Feske, S., Gwack, Y., Prakriya, M., Srikanth, S., Puppel, S. H., Tanasa, B., et al. (2006). A mutation in Orai1 causes immune deficiency by abrogating CRAC channel function. *Nature* 441, 179–185. doi: 10.1038/nature04702

Fiorio Pla, A., Ong, H. L., Cheng, K. T., Brossa, A., Bussolati, B., Lockwich, T., et al. (2012). TRPV4 mediates tumor-derived endothelial cell migration via arachidonic acid-activated actin remodeling. *Oncogene* 31, 200–212. doi: 10.1038/onc.2011.231

Freichel, M., Almering, J., and Tsvilovskyy, V. (2012). The role of TRP proteins in mast cells. *Front. Immunol.* 3:150. doi: 10.3389/fimmu.2012.00150

Fuh, G., Li, B., Crowley, C., Cunningham, B., and Wells, J. A. (1998). Requirements for binding and signaling of the kinase domain receptor for vascular endothelial growth factor. *J. Biol. Chem.* 273, 11197–11204. doi: 10.1074/jbc.273.18.11197

García-Sanz, N., Fernandez-Carvajal, A., Morenilla-Palao, C., Planells-Cases, R., Fajardo-Sanchez, E., Fernandez-Ballester, G., et al. (2004). Identification of a tetramerization domain in the C terminus of the vanilloid receptor. *J. Neurosci.* 24, 5307–5314. doi: 10.1523/JNEUROSCI.0202-04.2004

Garreis, F., Schroder, A., Reinach, P. S., Zoll, S., Khajavi, N., Dhandapani, P., et al. (2016). Upregulation of transient receptor potential vanilloid type-1 channel activity and Ca^{2+} influx dysfunction in human pterygial cells. *Invest. Ophthalmol. Vis. Sci.* 57, 2564–2577. doi: 10.1167/iovs.16-19170

Gaudet, R. (2008). A primer on ankyrin repeat function in TRP channels and beyond. *Mol. Biosyst.* 4, 372–379. doi: 10.1039/b801481g

Ge, R., Tai, Y., Sun, Y., Zhou, K., Yang, S., Cheng, T., et al. (2009). Critical role of TRPC6 channels in VEGF-mediated angiogenesis. *Cancer Lett.* 283, 43–51. doi: 10.1016/j.canlet.2009.03.023

Gerhardt, H., and Betsholtz, C. (2005). How do endothelial cells orientate? *EXS* 94, 3–15. doi: 10.1007/3-7643-7311-3_1

Gerzanich, V., Woo, S. K., Vennekens, R., Tsymbalyuk, O., Ivanova, S., Ivanov, A., et al. (2009). *De novo* expression of Trpm4 initiates secondary hemorrhage in spinal cord injury. *Nat. Med.* 15, 185–191. doi: 10.1038/nm.1899

Grunewald, M., Avraham, I., Dor, Y., Bachar-Lustig, E., Itin, A., Jung, S., et al. (2006). VEGF-induced adult neovascularization: recruitment, retention, and role of accessory cells. *Cell* 124, 175–189. doi: 10.1016/j.cell.2005.10.036

Hamdollah Zadeh, M. A., Glass, C. A., Magnussen, A., Hancox, J. C., and Bates, D. O. (2008). VEGF-mediated elevated intracellular calcium and angiogenesis in human microvascular endothelial cells *in vitro* are inhibited by dominant negative TRPC6. *Microcirculation* 15, 605–614. doi: 10.1080/10739680802220323

Hardie, R. C., and Minke, B. (1992). The trp gene is essential for a light-activated Ca^{2+} channel in Drosophila photoreceptors. *Neuron* 8, 643–651. doi: 10.1016/0896-6273(92)90086-S

Harteneck, C., Klose, C., and Krautwurst, D. (2011). Synthetic modulators of TRP channel activity. *Adv. Exp. Med. Biol.* 704, 87–106. doi: 10.1007/978-94-007-0265-3_4

Henkin, J., and Volpert, O. V. (2011). Therapies using anti-angiogenic peptide mimetics of thrombospondin-1. *Expert Opin. Ther. Targets* 15, 1369–1386. doi: 10.1517/14728222.2011.640319

Hickey, M. M., and Simon, M. C. (2006). Regulation of angiogenesis by hypoxia and hypoxia-inducible factors. *Curr. Top. Dev. Biol.* 76, 217–257. doi: 10.1016/S0070-2153(06)76007-0

Hofmann, T., Obukhov, A. G., Schaefer, M., Harteneck, C., Gudermann, T., and Schultz, G. (1999). Direct activation of human TRPC6 and TRPC3 channels by diacylglycerol. *Nature* 397, 259–263. doi: 10.1038/16711

Huang, G. N., Zeng, W., Kim, J. Y., Yuan, J. P., Han, L., Muallem, S., et al. (2006). STIM1 carboxyl-terminus activates native SOC, I(crac) and TRPC1 channels. *Nat. Cell Biol.* 8, 1003–1010. doi: 10.1038/ncb1454

Jakobsson, L., Kreuger, J., Holmborn, K., Lundin, L., Eriksson, I., Kjellen, L., et al. (2006). Heparan sulfate in trans potentiates VEGFR-mediated angiogenesis. *Dev. Cell.* 10, 625–634. doi: 10.1016/j.devcel.2006.03.009

Jardin, I., Lopez, J. J., Salido, G. M., and Rosado, J. A. (2008b). Orai1 mediates the interaction between STIM1 and hTRPC1 and regulates the mode of activation of hTRPC1-forming Ca^{2+} channels. *J. Biol. Chem.* 283, 25296–25304. doi: 10.1074/jbc.M802904200

Jardín, I., Redondo, P. C., Salido, G. M., and Rosado, J. A. (2008a). Phosphatidylinositol 4,5-bisphosphate enhances store-operated calcium entry through hTRPC6 channel in human platelets. *Biochim. Biophys. Acta* 1783, 84–97. doi: 10.1016/j.bbamcr.2007.07.007

Joukov, V., Sorsa, T., Kumar, V., Jeltsch, M., Claesson-Welsh, L., Cao, Y., et al. (1997). Proteolytic processing regulates receptor specificity and activity of VEGF-C. *EMBO J.* 16, 3898–3911. doi: 10.1093/emboj/16.13.3898

Kappert, K., Peters, K. G., Bohmer, F. D., and Ostman, A. (2005). Tyrosine phosphatases in vessel wall signaling. *Cardiovasc. Res.* 65, 587–598. doi: 10.1016/j.cardiores.2004.08.016

Karkkainen, M. J., Haiko, P., Sainio, K., Partanen, J., Taipale, J., Petrova, T. V., et al. (2004). Vascular endothelial growth factor C is required for sprouting of the first lymphatic vessels from embryonic veins. *Nat. Immunol.* 5, 74–80. doi: 10.1038/ni1013

Katz, B., Payne, R., and Minke, B. (2017). "TRP channels in vision," in *Neurobiology of TRP Channels, 2nd Edn.,* ed T. L. R. Emir (Boca Raton, FL: CRC Press/Taylor & Francis) 27–63.

Kendall, R. L., and Thomas, K. A. (1993). Inhibition of vascular endothelial cell growth factor activity by an endogenously encoded soluble receptor. *Proc. Natl. Acad. Sci. U.S.A.* 90, 10705–10709. doi: 10.1073/pnas.90.22.10705

Köhler, R., Heyken, W. T., Heinau, P., Schubert, R., Si, H., Kacik, M., et al. (2006). Evidence for a functional role of endothelial transient receptor potential V4 in shear stress-induced vasodilatation. *Arterioscler. Thromb. Vasc. Biol.* 26, 1495–1502. doi: 10.1161/01.ATV.0000225698.36212.6a

Kohn, E. C., Alessandro, R., Spoonster, J., Wersto, R. P., and Liotta, L. A. (1995). Angiogenesis: role of calcium-mediated signal transduction. *Proc. Natl. Acad. Sci. U.S.A.* 92, 1307–1311. doi: 10.1073/pnas.92.5.1307

Kwan, H. Y., Huang, Y., and Yao, X. (2007). TRP channels in endothelial function and dysfunction. *Biochim. Biophys. Acta* 1772, 907–914. doi: 10.1016/j.bbadis.2007.02.013

Launay, P., Cheng, H., Srivatsan, S., Penner, R., Fleig, A., and Kinet, J. P. (2004). TRPM4 regulates calcium oscillations after T cell activation. *Science* 306, 1374–1377. doi: 10.1126/science.1098845

Lee, J. Y., Choi, H. Y., Na, W. H., Ju, B. G., and Yune, T. Y. (2015). 17beta-estradiol inhibits MMP-9 and SUR1/TrpM4 expression and activation and thereby attenuates BSCB disruption/hemorrhage after spinal cord injury in male rats. *Endocrinology* 156, 1838–1850. doi: 10.1210/en.2014-1832

Lee, K. P., Choi, S., Hong, J. H., Ahuja, M., Graham, S., Ma, R., et al. (2014). Molecular determinants mediating gating of Transient Receptor Potential Canonical (TRPC) channels by stromal interaction molecule 1 (STIM1). *J. Biol. Chem.* 289, 6372–6382. doi: 10.1074/jbc.M113.546556

Li, J., Cubbon, R. M., Wilson, L. A., Amer, M. S., McKeown, L., Hou, B., et al. (2011b). Orai1 and CRAC channel dependence of VEGF-activated Ca^{2+} entry and endothelial tube formation. *Circ. Res.* 108, 1190–1198. doi: 10.1161/CIRCRESAHA.111.243352

Li, M., Yu, Y., and Yang, J. (2011a). Structural biology of TRP channels. *Adv. Exp. Med. Biol.* 704, 1–23. doi: 10.1007/978-94-007-0265-3_1

Liman, E. R. (2007). "The Ca(2+)-activated TRP channels: TRPM4 and TRPM5," in *TRP Ion Channel Function in Sensory Transduction and Cellular Signaling Cascades,* eds W. B. Liedtke and S. Heller (Boca Raton: CRC Press/Taylor & Francis).

Loh, K. P., Ng, G., Yu, C. Y., Fhu, C. K., Yu, D., Vennekens, R., et al. (2014). TRPM4 inhibition promotes angiogenesis after ischemic stroke. *Pflugers Arch.* 466, 563–576. doi: 10.1007/s00424-013-1347-4

Loot, A. E., Popp, R., Fisslthaler, B., Vriens, J., Nilius, B., and Fleming, I. (2008). Role of cytochrome P450-dependent transient receptor potential V4 activation in flow-induced vasodilatation. *Cardiovasc. Res.* 80, 445–452. doi: 10.1093/cvr/cvn207

Ma, X., Qiu, S., Luo, J., Ma, Y., Ngai, C. Y., Shen, B., et al. (2010). Functional role of vanilloid transient receptor potential 4-canonical transient receptor potential 1 complex in flow-induced Ca^{2+} influx. *Arterioscler. Thromb. Vasc. Biol.* 30, 851–858. doi: 10.1161/ATVBAHA.109.196584

Mäkinen, T., Veikkola, T., Mustjoki, S., Karpanen, T., Catimel, B., Nice, E. C., et al. (2001). Isolated lymphatic endothelial cells transduce growth, survival and migratory signals via the VEGF-C/D receptor VEGFR-3. *EMBO J.* 20, 4762–4773. doi: 10.1093/emboj/20.17.4762

McColl, B. K., Baldwin, M. E., Roufail, S., Freeman, C., Moritz, R. L., Simpson, R. J., et al. (2003). Plasmin activates the lymphangiogenic growth factors VEGF-C and VEGF-D. *J. Exp. Med.* 198, 863–868. doi: 10.1084/jem.20030361

McDonald, N. Q., and Hendrickson, W. A. (1993). A structural superfamily of growth factors containing a cystine knot motif. *Cell* 73, 421–424. doi: 10.1016/0092-8674(93)90127-C

Millauer, B., Wizigmann-Voos, S., Schnurch, H., Martinez, R., Moller, N. P., Risau, W., et al. (1993). High affinity VEGF binding and developmental expression suggest Flk-1 as a major regulator of vasculogenesis and angiogenesis. *Cell* 72, 835–846. doi: 10.1016/0092-8674(93)90573-9

Minke, B. (1977). Drosophila mutant with a transducer defect. *Biophys. Struct. Mech.* 3, 59–64. doi: 10.1007/BF00536455

Minke, B., Wu, C., and Pak, W. L. (1975). Induction of photoreceptor voltage noise in the dark in Drosophila mutant. *Nature* 258, 84–87. doi: 10.1038/258084a0

Mittal, M., Urao, N., Hecquet, C. M., Zhang, M., Sudhahar, V., Gao, X. P., et al. (2015). Novel role of reactive oxygen species-activated Trp melastatin channel-2 in mediating angiogenesis and postischemic neovascularization. *Arterioscler. Thromb. Vasc. Biol.* 35, 877–887. doi: 10.1161/ATVBAHA.114.304802

Moccia, F. (2018). Endothelial Ca(2+) signaling and the resistance to anticancer treatments: partners in crime. *Int. J. Mol. Sci.* 19:E217. doi: 10.3390/ijms19010217

Moccia, F., Dragoni, S., Poletto, V., Rosti, V., Tanzi, F., Ganini, C., et al. (2014b). Orai1 and transient receptor potential channels as novel molecular targets to impair tumor neovascularization in renal cell carcinoma and other malignancies. *Anticancer. Agents Med. Chem.* 14, 296–312. doi: 10.2174/1871520613139990315

Moccia, F., Tanzi, F., and Munaron, L. (2014a). Endothelial remodelling and intracellular calcium machinery. *Curr. Mol. Med.* 14, 457–480. doi: 10.2174/1566524013666131118113410

Montell, C., Birnbaumer, L., Flockerzi, V., Bindels, R. J., Bruford, E. A., Caterina, M. J., et al. (2002). A unified nomenclature for the superfamily of TRP cation channels. *Mol. Cell* 9, 229–231. doi: 10.1016/S1097-2765(02)00448-3

Nauli, S. M., Kawanabe, Y., Kaminski, J. J., Pearce, W. J., Ingber, D. E., and Zhou, J. (2008). Endothelial cilia are fluid shear sensors that regulate calcium signaling and nitric oxide production through polycystin-1. *Circulation* 117, 1161–1171. doi: 10.1161/CIRCULATIONAHA.107.710111

Nilius, B., Droogmans, G., and Wondergem, R. (2003). Transient receptor potential channels in endothelium: solving the calcium entry puzzle? *Endothelium* 10, 5–15. doi: 10.1080/10623320303356

Nilius, B., Mahieu, F., Prenen, J., Janssens, A., Owsianik, G., Vennekens, R., et al. (2006). The Ca^{2+}-activated cation channel TRPM4 is regulated by phosphatidylinositol 4,5-biphosphate. *EMBO J.* 25, 467–478. doi: 10.1038/sj.emboj.7600963

Norden, A. D., Drappatz, J., Muzikansky, A., David, K., Gerard, M., McNamara, M. B., et al. (2009). An exploratory survival analysis of anti-angiogenic therapy for recurrent malignant glioma. *J. Neurooncol.* 92, 149–155. doi: 10.1007/s11060-008-9745-8

Paria, B. C., Malik, A. B., Kwiatek, A. M., Rahman, A., May, M. J., Ghosh, S., et al. (2003). Tumor necrosis factor-alpha induces nuclear factor-kappaB-dependent TRPC1 expression in endothelial cells. *J. Biol. Chem.* 278, 37195–37203. doi: 10.1074/jbc.M304287200

Patenaude, A., Parker, J., and Karsan, A. (2010). Involvement of endothelial progenitor cells in tumor vascularization. *Microvasc. Res.* 79, 217–223. doi: 10.1016/j.mvr.2010.01.007

Petersen, C. C., Berridge, M. J., Borgese, M. F., and Bennett, D. L. (1995). Putative capacitative calcium entry channels: expression of Drosophila trp and evidence

for the existence of vertebrate homologues. *Biochem. J.* 311 (Pt 1), 41–44. doi: 10.1042/bj3110041

Phillips, A. M., Bull, A., and Kelly, L. E. (1992). Identification of a Drosophila gene encoding a calmodulin-binding protein with homology to the trp phototransduction gene. *Neuron* 8, 631–642. doi: 10.1016/0896-6273(92)90085-R

Plate, K. H., Breier, G., Millauer, B., Ullrich, A., and Risau, W. (1993). Up-regulation of vascular endothelial growth factor and its cognate receptors in a rat glioma model of tumor angiogenesis. *Cancer Res.* 53, 5822–5827.

Pocock, T. M., Foster, R. R., and Bates, D. O. (2004). Evidence of a role for TRPC channels in VEGF-mediated increased vascular permeability *in vivo*. *Am. J. Physiol. Heart Circ. Physiol.* 286, H1015–1026. doi: 10.1152/ajpheart.00826.2003

Qin, W., Xie, W., Xia, N., He, Q., and Sun, T. (2016). Silencing of transient receptor potential channel 4 alleviates oxLDL-induced angiogenesis in human coronary artery endothelial cells by inhibition of VEGF and NF-kappaB. *Med. Sci. Monit.* 22, 930–936. doi: 10.12659/MSM.897634

Ramsey, I. S., Delling, M., and Clapham, D. E. (2006). An introduction to TRP channels. *Annu. Rev. Physiol.* 68, 619–647. doi: 10.1146/annurev.physiol.68.040204.100431

Reddy, K., Khaliq, A., and Henning, R. J. (2015). Recent advances in the diagnosis and treatment of acute myocardial infarction. *World J. Cardiol.* 7, 243–276. doi: 10.4330/wjc.v7.i5.243

Salehi-Najafabadi, Z., Li, B., Valentino, V., Ng, C., Martin, H., Yu, Y., et al. (2017). Extracellular loops are essential for the assembly and function of polycystin receptor-ion channel complexes. *J. Biol. Chem.* 292, 4210–4221. doi: 10.1074/jbc.M116.767897

Salido, G. M., Jardin, I., and Rosado, J. A. (2011). The TRPC ion channels: association with Orai1 and STIM1 proteins and participation in capacitative and non-capacitative calcium entry. *Adv. Exp. Med. Biol.* 704, 413–433. doi: 10.1007/978-94-007-0265-3_23

Santoni, G., Morelli, M. B., Santoni, M., and Nabissi, M. (2011). New deals on the transcriptional and post-transcriptional regulation of TRP channel target genes during the angiogenesis of glioma. *J. Exp. Integr. Med.* 1, 221–234. doi: 10.5455/jeim.290711.ir.006

Scharenberg, A. M. (2005). TRPM2 and TRPM7: channel/enzyme fusions to generate novel intracellular sensors. *Pflugers Arch.* 451, 220–227. doi: 10.1007/s00424-005-1444-0

Schmidt, K., Dubrovska, G., Nielsen, G., Fesus, G., Uhrenholt, T. R., Hansen, P. B., et al. (2010). Amplification of EDHF-type vasodilatations in TRPC1-deficient mice. *Br. J. Pharmacol.* 161, 1722–1733. doi: 10.1111/j.1476-5381.2010.00985.x

Simons, M., Gordon, E., and Claesson-Welsh, L. (2016). Mechanisms and regulation of endothelial VEGF receptor signalling. *Nat. Rev. Mol. Cell Biol.* 17, 611–625. doi: 10.1038/nrm.2016.87

Song, H. B., Jun, H. O., Kim, J. H., and Fruttiger, M. (2015). Suppression of transient receptor potential canonical channel 4 inhibits vascular endothelial growth factor-induced retinal neovascularization. *Cell Calcium* 57, 101–108. doi: 10.1016/j.ceca.2015.01.002

Su, K. H., Lee, K. I., Shyue, S. K., Chen, H. Y., Wei, J., and Lee, T. S. (2014a). Implication of transient receptor potential vanilloid type 1 in 14,15-epoxyeicosatrienoic acid-induced angiogenesis. *Int. J. Biol. Sci.* 10, 990–996. doi: 10.7150/ijbs.9832

Su, K. H., Lin, S. J., Wei, J., Lee, K. I., Zhao, J. F., Shyue, S. K., et al. (2014b). The essential role of transient receptor potential vanilloid 1 in simvastatin-induced activation of endothelial nitric oxide synthase and angiogenesis. *Acta Physiol. (Oxf).* 212, 191–204. doi: 10.1111/apha.12378

Sundivakkam, P. C., Natarajan, V., Malik, A. B., and Tiruppathi, C. (2013). Store-operated Ca^{2+} entry (SOCE) induced by protease-activated receptor-1 mediates STIM1 protein phosphorylation to inhibit SOCE in endothelial cells through AMP-activated protein kinase and p38beta mitogen-activated protein kinase. *J. Biol. Chem.* 288, 17030–17041. doi: 10.1074/jbc.M112.411272

Takahashi, H., and Shibuya, M. (2005). The vascular endothelial growth factor (VEGF)/VEGF receptor system and its role under physiological and pathological conditions. *Clin. Sci.*109, 227–241. doi: 10.1042/CS20040370

Takahashi, N., Kuwaki, T., Kiyonaka, S., Numata, T., Kozai, D., Mizuno, Y., et al. (2011). TRPA1 underlies a sensing mechanism for O2. *Nat. Chem. Biol.* 7, 701–711. doi: 10.1038/nchembio.640

Tammela, T., Enholm, B., Alitalo, K., and Paavonen, K. (2005). The biology of vascular endothelial growth factors. *Cardiovasc. Res.* 65, 550–563. doi: 10.1016/j.cardiores.2004.12.002

Tauseef, M., Knezevic, N., Chava, K. R., Smith, M., Sukriti, S., Gianaris, N., et al. (2012). TLR4 activation of TRPC6-dependent calcium signaling mediates endotoxin-induced lung vascular permeability and inflammation. *J. Exp. Med.* 209, 1953–1968. doi: 10.1084/jem.20111355

Tchaikovski, V., Fellbrich, G., and Waltenberger, J. (2008). The molecular basis of VEGFR-1 signal transduction pathways in primary human monocytes. *Arterioscler. Thromb. Vasc. Biol.* 28, 322–328. doi: 10.1161/ATVBAHA.107.158022

Thoppil, R. J., Cappelli, H. C., Adapala, R. K., Kanugula, A. K., Paruchuri, S., and Thodeti, C. K. (2016). TRPV4 channels regulate tumor angiogenesis via modulation of Rho/Rho kinase pathway. *Oncotarget* 7, 25849–25861. doi: 10.18632/oncotarget.8405

Tiruppathi, C., Freichel, M., Vogel, S. M., Paria, B. C., Mehta, D., Flockerzi, V., et al. (2002). Impairment of store-operated Ca^{2+} entry in TRPC4(-/-) mice interferes with increase in lung microvascular permeability. *Circ. Res.* 91, 70–76. doi: 10.1161/01.RES.0000023391.40106.A8

Venkatachalam, K., and Montell, C. (2007). TRP channels. *Annu. Rev. Biochem.* 76, 387–417. doi: 10.1146/annurev.biochem.75.103004.142819

Vetter, I., and Lewis, R. J. (2011). Natural product ligands of TRP channels. *Adv. Exp. Med. Biol.* 704, 41–85. doi: 10.1007/978-94-007-0265-3_3

Warner, A. J., Lopez-Dee, J., Knight, E. L., Feramisco, J. R., and Prigent, S. A. (2000). The Shc-related adaptor protein, Sck, forms a complex with the vascular-endothelial-growth-factor receptor KDR in transfected cells. *Biochem. J.* 347, 501–509. doi: 10.1042/bj3470501

Wedel, B. J., Vazquez, G., McKay, R. R., St, J. B. G., and Putney, J. W. Jr. (2003). A calmodulin/inositol 1,4,5-trisphosphate (IP3) receptor-binding region targets TRPC3 to the plasma membrane in a calmodulin/IP3 receptor-independent process. *J. Biol. Chem.* 278, 25758–25765. doi: 10.1074/jbc.M303890200

Weissmann, N., Sydykov, A., Kalwa, H., Storch, U., Fuchs, B., Mederos y Schnitzler, M., et al. (2012). Activation of TRPC6 channels is essential for lung ischaemia-reperfusion induced oedema in mice. *Nat. Commun.* 3:649. doi: 10.1038/ncomms1660

Wes, P. D., Chevesich, J., Jeromin, A., Rosenberg, C., Stetten, G., and Montell, C. (1995). TRPC1, a human homolog of a Drosophila store-operated channel. *Proc. Natl. Acad. Sci. U.S.A.* 92, 9652–9656. doi: 10.1073/pnas.92.21.9652

Wiesmann, C., Fuh, G., Christinger, H. W., Eigenbrot, C., Wells, J. A., and de Vos, A. M. (1997). Crystal structure at 1.7 A resolution of VEGF in complex with domain 2 of the Flt-1 receptor. *Cell* 91, 695–704. doi: 10.1016/S0092-8674(00)80456-0

Wong, C. O., and Yao, X. (2011). TRP channels in vascular endothelial cells. *Adv. Exp. Med. Biol.* 704, 759–780. doi: 10.1007/978-94-007-0265-3_40

Yang, Y., Xie, P., Opatowsky, Y., and Schlessinger, J. (2010). Direct contacts between extracellular membrane-proximal domains are required for VEGF receptor activation and cell signaling. *Proc. Natl. Acad. Sci. U.S.A.* 107, 1906–1911. doi: 10.1073/pnas.0914052107

Yao, X., and Garland, C. J. (2005). Recent developments in vascular endothelial cell transient receptor potential channels. *Circ. Res.* 97, 853–863. doi: 10.1161/01.RES.0000187473.85419.3e

Ye, L., Xu, M., Hu, M., Zhang, H., Tan, X., Li, Q., et al. (2018). TRPV4 is involved in irisin-induced endothelium-dependent vasodilation. *Biochem. Biophys. Res. Commun.* 495, 41–45. doi: 10.1016/j.bbrc.2017.10.160

Yu, P. C., Gu, S. Y., Bu, J. W., and Du, J. L. (2010). TRPC1 is essential for *in vivo* angiogenesis in zebrafish. *Circ. Res.* 106, 1221–1232. doi: 10.1161/CIRCRESAHA.109.207670

Zhang, D. X., Mendoza, S. A., Bubolz, A. H., Mizuno, A., Ge, Z. D., Li, R., et al. (2009). Transient receptor potential vanilloid type 4-deficient mice exhibit impaired endothelium-dependent relaxation induced by acetylcholine *in vitro* and *in vivo*. *Hypertension* 53, 532–538. doi: 10.1161/HYPERTENSIONAHA.108.127100

Zhang, S. L., Yu, Y., Roos, J., Kozak, J. A., Deerinck, T. J., Ellisman, M. H., et al. (2005). STIM1 is a Ca^{2+} sensor that activates CRAC channels and migrates from the Ca^{2+} store to the plasma membrane. *Nature* 437, 902–905. doi: 10.1038/nature04147

Zhang, Z., Yu, H., Huang, J., Faouzi, M., Schmitz, C., Penner, R., et al. (2014). The TRPM6 kinase domain determines the Mg.ATP sensitivity

of TRPM7/M6 heteromeric ion channels. *J. Biol. Chem.* 289, 5217–5227. doi: 10.1074/jbc.M113.512285

Zheng, W., Cai, R., Hofmann, L., Nesin, V., Hu, Q., Long, W., et al. (2018). Direct binding between pre-S1 and TRP-like domains in TRPP channels mediates gating and functional regulation by PIP2. *Cell Rep.* 22, 1560–1573. doi: 10.1016/j.celrep.2018.01.042

Zhou, F., Chang, Z., Zhang, L., Hong, Y. K., Shen, B., Wang, B., et al. (2010). Akt/Protein kinase B is required for lymphatic network formation, remodeling, and valve development. *Am. J. Pathol.* 177, 2124–2133. doi: 10.2353/ajpath.2010.091301

Zhou, W., Guo, S., Xiong, Z., and Liu, M. (2014). Oncogenic role and therapeutic target of transient receptor potential melastatin 7 channel in malignancy. *Expert Opin. Ther. Targets* 18, 1177–1196. doi: 10.1517/14728222.2014.940894

Zhu, X., Chu, P. B., Peyton, M., and Birnbaumer, L. (1995). Molecular cloning of a widely expressed human homologue for the Drosophila trp gene. *FEBS Lett.* 373, 193–198. doi: 10.1016/0014-5793(95)01038-G

Zurborg, S., Yurgionas, B., Jira, J. A., Caspani, O., and Heppenstall, P. A. (2007). Direct activation of the ion channel TRPA1 by Ca^{2+}. *Nat. Neurosci.* 10, 277–279. doi: 10.1038/nn1843

Conflict of Interest Statement: The authors declare that the research was conducted in the absence of any commercial or financial relationships that could be construed as a potential conflict of interest.

frontiers in Immunology

ORIGINAL RESEARCH
published: 10 December 2018
doi: 10.3389/fimmu.2018.02919

Active Vaccination With EMMPRIN-Derived Multiple Antigenic Peptide (161-MAP) Reduces Angiogenesis in a Dextran Sodium Sulfate (DSS)-Induced Colitis Model

Elina Simanovich[1], *Vera Brod*[1] *and Michal A. Rahat*[1,2*]

[1] *Immunotherapy Laboratory, Carmel Medical Center, Haifa, Israel,* [2] *The Ruth and Bruce Rappaport Faculty of Medicine, Technion-Israel Institute of Technology, Haifa, Israel*

OPEN ACCESS

Edited by:
Sandip D. Kamath,
James Cook University, Australia

Reviewed by:
Aya C. Taki,
James Cook University, Australia
Lionel Hebbard,
James Cook University, Australia

***Correspondence:**
Michal A. Rahat
mrahat@netvision.net.il;
rahat_miki@clalit.org.il

Specialty section:
This article was submitted to Vaccines and Molecular Therapeutics, a section of the journal Frontiers in Immunology

Received: *21 August 2018*
Accepted: *28 November 2018*
Published: *10 December 2018*

Citation:
Simanovich E, Brod V and Rahat MA (2018) Active Vaccination With EMMPRIN-Derived Multiple Antigenic Peptide (161-MAP) Reduces Angiogenesis in a Dextran Sodium Sulfate (DSS)-Induced Colitis Model. Front. Immunol. 9:2919. doi: 10.3389/fimmu.2018.02919

Ulcerative colitis (UC) is an autoimmune disease that affects the colon and shares many clinical and histological features with the dextran sulfate sodium (DSS)-induced colitis model in mice. Angiogenesis is a critical component in many autoimmune diseases, as well as in the DSS-induced colitis model, and is it partially mediated by EMMPRIN, a multifunctional protein that can induce the expression of both the potent pro-angiogenic vascular endothelial growth factor (VEGF) and matrix metalloproteinases (MMPs). We asked whether targeting EMMPRIN by active vaccination, using a novel, specific epitope in the protein, synthesized as a multiple antigenic peptide (MAP), could trigger beneficial effects in the DSS-induced colitic C57BL/6J mice. Mice were vaccinated with four boost injections (50 μg each) of either 161-MAP coding for the EMMPRIN epitope or the scrambled control peptide (Scr-MAP) emulsified in Freund's adjuvant. We show that male mice that were vaccinated with 161-MAP lost less weight, demonstrated improved disease activity indices (DAI), had reduced colitis histological score, and their colons were longer in comparison to mice vaccinated with the Scr-MAP. The 161-MAP vaccination also reduced serum and colon levels of EMMPRIN, colon concentrations of VEGF, MMP-9, and TGFβ, and vessel density assessed by CD31 staining. A similar effect was observed in female mice vaccinated with 161-MAP, including weight loss, colitis histological score, colon length, colon levels of EMMPRIN and colon concentrations of VEGF. However, for female mice, the changes in DAI values, EMMPRIN serum levels, and MMP-9 and TGFβ colon concentrations did not reach significance. We conclude that our strategy of alleviating autoimmunity in this model through targeting angiogenesis by actively vaccinating against EMMPRIN was successful and efficient in reducing angiogenesis.

Keywords: angiogenesis, multiple antigenic peptide (MAP), active peptide vaccination, DSS-induced colitis, EMMPRIN/CD147

INTRODUCTION

Inflammatory bowel disease (IBD) is a group of chronic inflammatory diseases, with the two major diseases being Crohn's disease (CD) and ulcerative colitis (UC). UC is believed to be an autoimmune disease that primarily affects the large intestine, with unknown etiology. However, a local increase in the concentrations of reactive oxygen species (ROS) and pro-inflammatory cytokines (primarily, TNFα, IL-1β, and IL-17), was identified in UC patients, and these were speculated to increase the risk of colorectal cancer in chronic inflammation (1–3).

The DSS-induced colitis model used in rats and mice is widely used as an experimental model of IBD that demonstrates clinical and histopathological features similar to the human autoimmune UC (3, 4). DSS is thought to induce a chemical injury in intestinal epithelial cells, which causes them to lose barrier functions and consequently exposes the Lamina Propria (LP) to antigens and intestinal bacteria that enhance inflammation (1). Different concentrations of DSS, usually ranging between 1 and 3%, have been used to achieve moderate, mild or severe intestinal injury, varying time of healing and repair accordingly (5). Similar to UC, the pro-inflammatory response and increased reactive oxygen species (ROS) are implicated in the continued tissue damage caused in DSS-induced colitis (2).

Angiogenesis has been linked to chronic inflammation, and has been shown to be a critical component of the pathogenesis of DSS-induced colitis and is associated with disease severity, as it promotes leukocyte influx and supplies the necessary oxygen and nutrients to the inflamed tissue (6). VEGF is a known potent pro-angiogenic factor that links angiogenesis and inflammation by promoting endothelial cell proliferation, migration, tube formation and vascular permeability, as well as increasing neutrophil adhesion through the activation of NF-κB and increased expression of adhesion molecules (7, 8). Matrix metalloproteinases (MMPs) can remodel the ECM to facilitate endothelial cell migration, release VEGF that is bound to the ECM, or conversely, degrade collagen XVIII to produce the anti-angiogenic factor endostatin (9). Thus, both VEGF and MMPs, particularly MMP-9, promote angiogenesis. Increased permeability, characteristic of angiogenic vessels, further contributes to UC progression, as it reduces barrier functions and allows interaction of lumen bacteria with LP immune cells (10).

EMMPRIN (also called CD147 or basigin) is a transmembranal protein with multiple functions. Depending on the protein it binds to, EMMPRIN can be involved in cell metabolism when it chaperones the monocarboxylate transporters MCT-1 and MCT-4, it can serve as a leukocyte chemoattractant when it binds to extracellular cyclophilin A/B, and it becomes an adhesion molecule when it binds to integrins and to E-selectin, to name just a few functions (11–13). However, its most familiar activity is mediated through homophilic interactions of membranal-soluble or membranal-membranal EMMPRIN molecules (14), which induce the expression of VEGF and several types of MMPs, rendering EMMPRIN an important pro-angiogenic factor (15–18).

We have recently identified a novel epitope in the EMMPRIN protein extracellular domain I, which is specifically responsible for the induction of both VEGF and MMP-9 (19). We have synthesized this epitope as an octa-branched multiple antigenic peptide (designated 161-MAP), and used it either in a therapeutic or a prophylactic manner to vaccinate mice that were implanted with the CT26 colon carcinoma tumors subcutaneously, or that were intravenously injected with this cell line to generate an experimental metastasis model. Vaccination against EMMPRIN resulted in the inhibition, and even regression of both tumors and metastases, partly through the reduction in vessel density, and through reduced expression of EMMPRIN, VEGF and MMP-9, cumulatively decreasing angiogenesis. In view of the importance of angiogenesis in colitis, we now ask whether the same vaccination against EMMPRIN could also affect chronic inflammation in a mouse DSS-induced colitis model.

RESULTS

161-MAP Active Vaccination Ameliorates Disease Severity in DSS-Induced Colitis

We have chosen to vaccinate the mice with Scr-MAP or 161-MAP in a prophylactic manner, before the induction of colitis by DSS, to allow the adaptive immunity to prepare fully to the DSS challenge. Four days after the last vaccine injection the mice were supplied with DSS dissolved in their drinking water for 5 consecutive days, and 15 days after the introduction of DSS we euthanized the mice. The design of the experiment is shown (**Figure 1A**). DSS induced colonic damage that was manifested both by weight loss and by the disease activity index (DAI), which was calculated by factoring in weight loss, diarrhea, and occult blood or rectal bleeding. In the Scr-MAP vaccinated control mice, weight loss and DAI gradually increased and peaked around day 9 both in male and female mice. Following this peak, mice exhibited reduction in the change of weight and in the DAI (Figure 1B), suggesting that repair of the colonic damage had begun. A similar trend was observed for the weight loss of the161-MAP vaccinated mice, but although the peak was evident on the same days as the control group, it was reduced in comparison (by 1.65-fold, $p < 0.01$ for the male mice, by 2.9-fold, $p < 0.05$ for the female mice). Disease severity, assessed by the DAI, showed significant results only for male mice. It gradually elevated and peaked around day 9, and then moderately declined in both Scr-MAP and 161-MAP vaccinated mice, but not back to the levels prior to DSS administration. However, in days 9 through 12, the disease in the control group was more severe (by 23 and 35%, $p < 0.05$, **Figure 1C**). This observation suggests that damage and inflammation are still preset 10 days after mice were no longer exposed to DSS, and that the 161-MAP active vaccination exerted a protective influence. It is also noteworthy that starting on day 10, the Scr-MAP vaccinated females demonstrated significantly reduced change in weight ($p < 0.001$) and DAI scores ($p < 0.01$), in comparison to the Scr-MAP vaccinated males, suggesting that the females exhibited reduced inflammation.

Histological analysis of the colon in the control groups revealed damage to the epithelial layer, crypt loss and destruction,

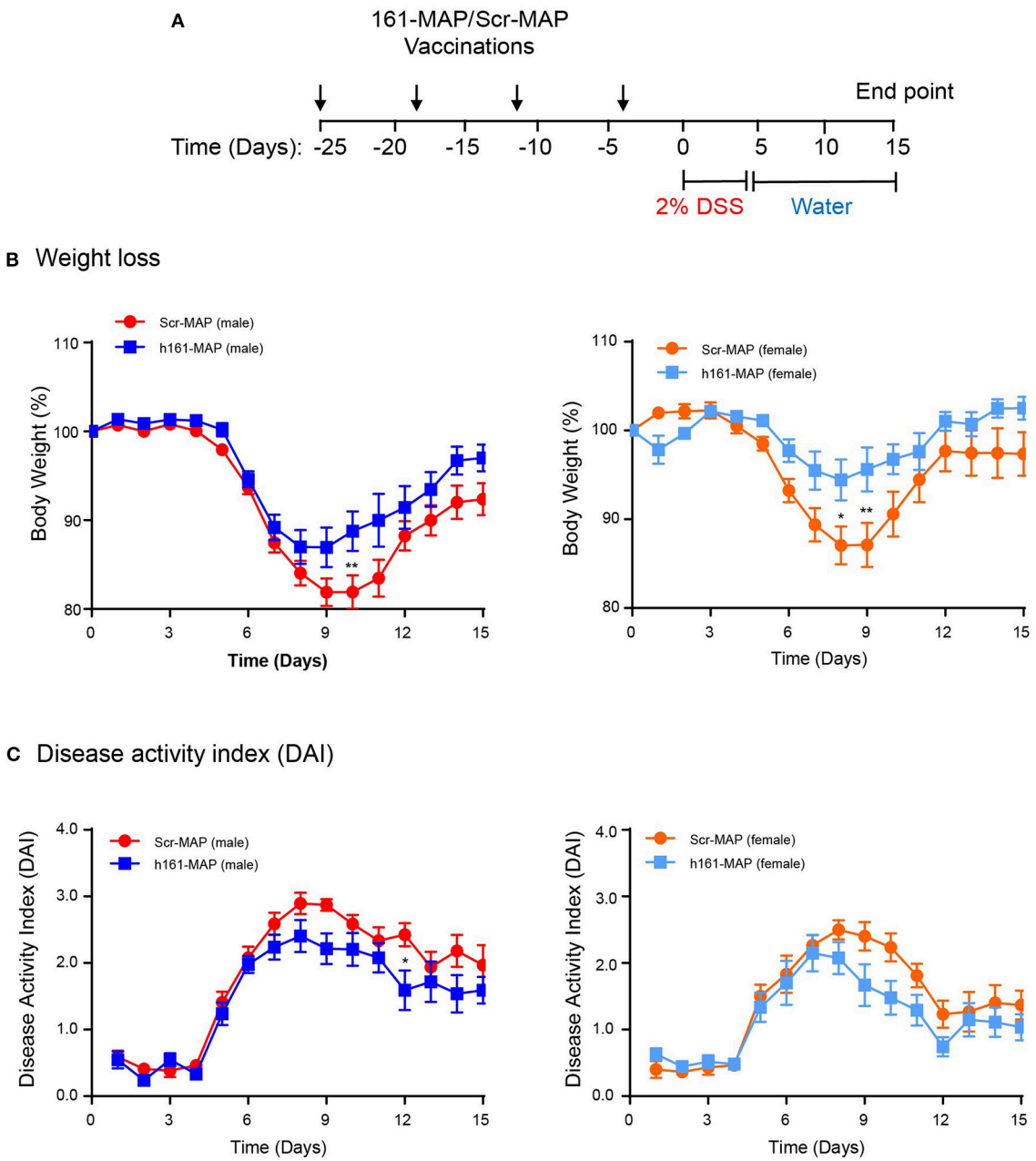

FIGURE 1 | 161-MAP active vaccination improves disease severity. **(A)** The experimental design is shown. Male and female C57Bl/6J mice were randomly assigned to the Scr-MAP vaccinated control group, or to the 161-MAP vaccinated experimental group. Mice received four vaccine boost injections every 7 days (arrows) prior to administration of 2% DSS in their drinking water for 5 consecutive days (marked). For the remaining time the mice received regular water, and after 10 days they were euthanized. After receiving DSS, mice were monitored daily and their **(B)** loss of weight or **(C)** the disease activity index (DAI) were observed ($n = 12$ for male mice, $n = 9$ for female mice). *$p < 0.05$, **$p < 0.01$ relative to the Scr-MAP vaccinated mice at the same day.

and increased leukocyte infiltration to the lamina propria (LP) and to the submucosa (**Figures 2A,B**). In comparison, in the 161-MAP vaccinated groups, crypt structures and epithelial lining were less damaged, and the immune infiltrate was reduced, as was reflected in the histological scores (**Figure 2B**, 95% CI for males [1.6, 10.15], 95% CI for females [0.1, 5.02]). Additionally, colon length, where shortening is a marker of inflammation, was increased in the 161-MAP vaccinated mice (by 12% in both male and female mice, $p < 0.05$, 95% CI for males [0.14, 1.6], and for females [0.4, 1.6], **Figures 2C,D**).

161-MAP Active Vaccination Reduces Angiogenesis

To examine whether the 161-MAP active vaccination targeted the EMMPRIN protein in the colon, we stained for the protein in the colon tissue sections. EMMPRIN is highly expressed in the colon,

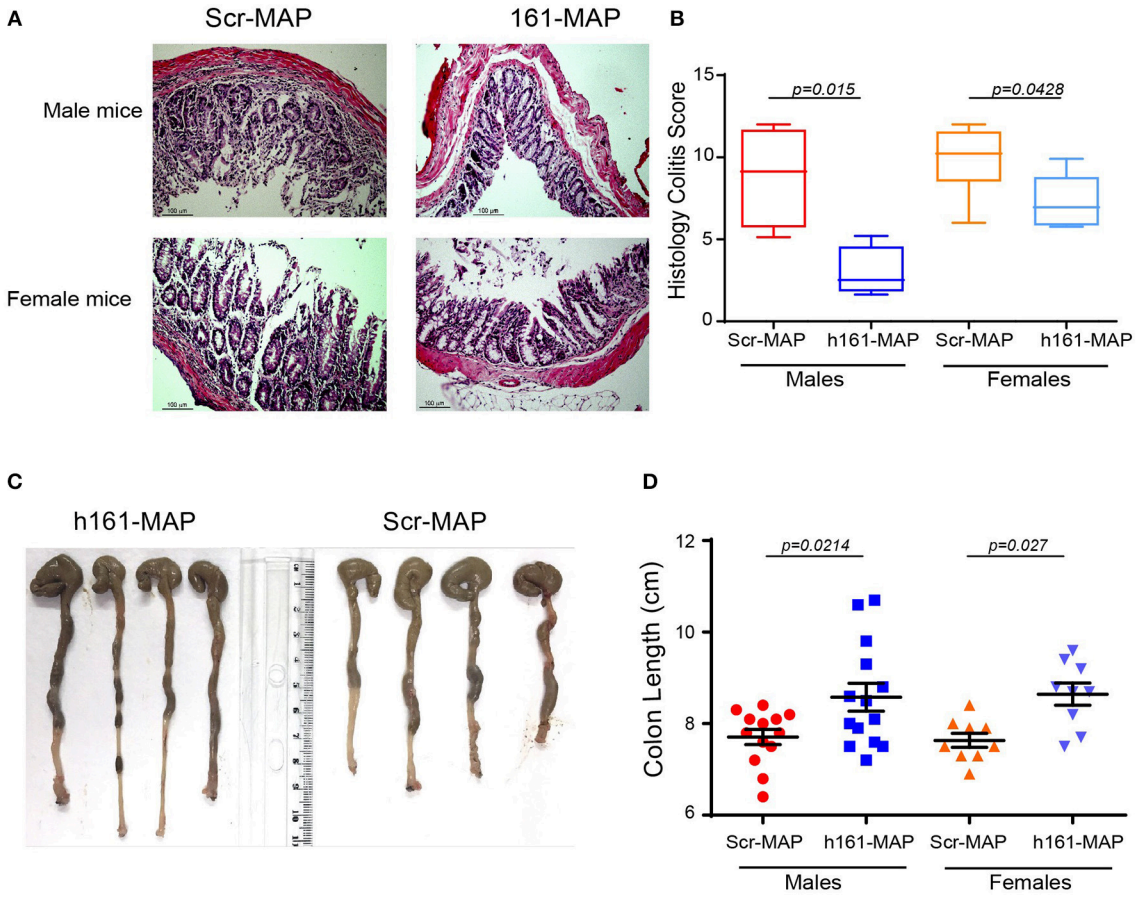

FIGURE 2 | 161-MAP active vaccination prevents damage and extends colon length. Fifteen days after the beginning of DSS-treatment, mice were euthanized and their colons were harvested, formalin-fixed and paraffin-embedded. Colon tissue sections were H&E stained and analyzed for their histological scores. **(A)** Representative images and **(B)** the assessment of the histological score ($n = 6$ in each group). Scale bar is 100 μm. **(C)** Representative images of the entire colon removed from male mice, and **(D)** measurement of the colon lengths ($n = 12$ for the male groups, $n = 9$ for the female groups).

and therefore, staining in both cases was strong. However, the immune reactive score (H-score), which takes into account both the intensity of the staining and the number of cells stained with each intensity, allowed us to observe a reduction in EMMPRIN expression in the 161-MAP vaccinated group (**Figure 3A**), in both male (by 1.6-fold, $p = 0.0022$, 95% CI [7.16, 25.43]) and female mice (by 1.8-fold, $p < 0.0001$, 95% CI [19.9, 30.45]). Moreover, reduced EMMPRIN expression is clearly visualized in the crypts' epithelial cells from 161-MAP vaccinated mice, whereas an increase in infiltrating macrophages is clearly seen in the LP (**Figure 3B**). Lastly, determination of EMMPRIN levels in the colon lysates (**Figure 3C**) showed a marked reduction in the 161-MAP vaccinated male (by 1.45-fold, $p = 0.0248$, 95% CI [140, 1878]) and female (by 1.36-fold, $p = 0.03$, 95% CI [89.1, 1596]) mice, whereas EMMPRIN levels in the circulation were markedly reduced only in the male group (by 1.3-fold, $p = 0.037$).

Angiogenesis was evaluated by the microvessel density that was assessed by CD31 staining. In the control Scr-MAP vaccinated groups, blood vessels were abundant in the muscularis mucosa, and infiltrated into the LP (**Figure 4A**). In contrast, both male and female 161-MAP vaccinated mice exhibited reduced amount of blood vessels in both the muscularis mucosa and in the LP (by 1.6-fold, $p < 0.001$, 95% CI for male 4.5, 8.9], and for females [5.9, 9.2]. As expected, the reduction in EMMPRIN levels, a known inducer of VEGF and MMPs expression, led to a similar reduction in local VEGF levels in both male and female mice (by 3- and 5-fold, respectively, $p < 0.05$, 95% CI for male [0.08, 2.5] and for female [0.2, 1.35]), whereas in the serum VEGF was hardly detected in both genders for both 161-Scr-MAP and 161-MAP vaccinated mice (**Figure 4B**). However, colon MMP-9 levels were reduced only in the 161-MAP male vaccinated group (by 3-fold, $p = 0.0383$, 95% CI [6.3, 197.6]), but not in the female vaccinated group. Although the local reduction of EMMPRIN levels was reflected in the serum, MMP-9 serum levels and the lack of VEGF serum levels were unchanged by the 161-MAP vaccination.

To demonstrate the involvement of EMMPRIN in the angiogenic potential, we subjected the extracted proteins to bEND3 endothelial scratch assay. The ability of the lysates to trigger wound healing, that requires endothelial cell proliferation

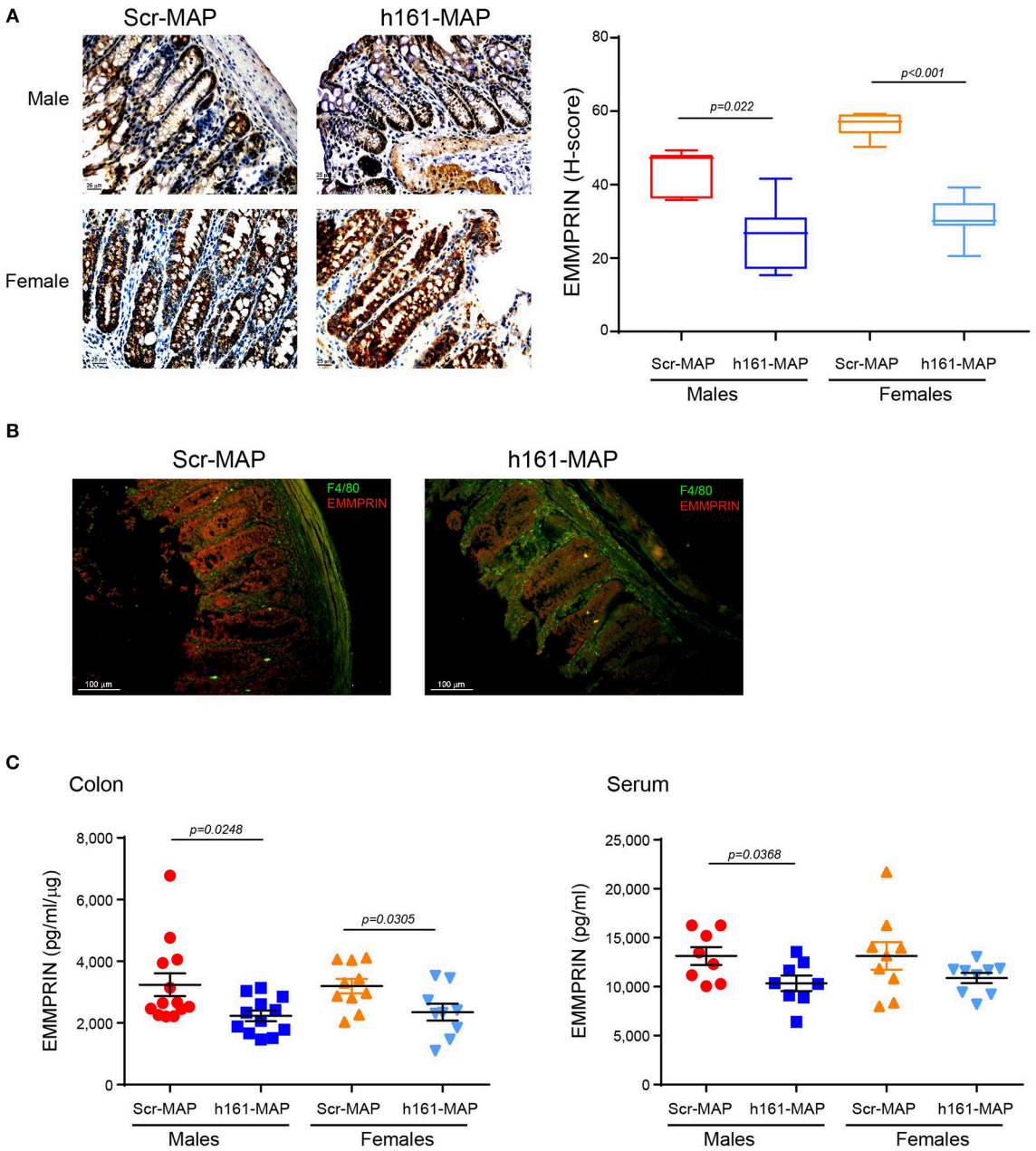

FIGURE 3 | 161-MAP active vaccination reduces EMMPRIN expression in the colon. **(A)** Representative images of colon sections stained for EMMPRIN and their quantification using the H-score ($n = 5$ per group). Scale bar is 25 µm **(B)** Representative image of fluorescently labeled EMMPRIN (red) and macrophages (green). Scale bar is 100 µm. **(C)** Determination of EMMPRIN concentrations in colon lysates ($n = 9$–10 per group), and in serum samples ($n = 8$–9 per group) by ELISA.

and migration, was assessed by measuring the area to which bEND3 cells had migrated, and the involvement of EMMPRIN was demonstrated by the neutralizing activity of the anti-EMMPRIN antibody (161-pAb). The baseline values of bEND3 cell migration, without addition of any protein extract, were similar and not different from the control Scr-MAP group (mean migration area 306,085 ± 20,493 mm). Relative to lysates obtained from the male Scr-MAP control group, the 161-MAP vaccinated male group reduced the migration of endothelial cells (by 1.42-fold, $p < 0.047$, 95% CI [23,426, 157,945], **Figure 4C**), and the addition of the antibody to male Scr-MAP lysates had a similar effect ($p < 0.045$). Likewise, the 161-MAP vaccination reduced migration in the female mice (1.6-fold, $p < 0.019$, 95% CI [133,284, 474,369]) (data not shown). However, addition of the antibody to the 161-MAP colon lysates in both male and female mice did not show any additional effect (**Figure 4C**), suggesting that the vaccination already neutralized EMMPRIN in these lysates.

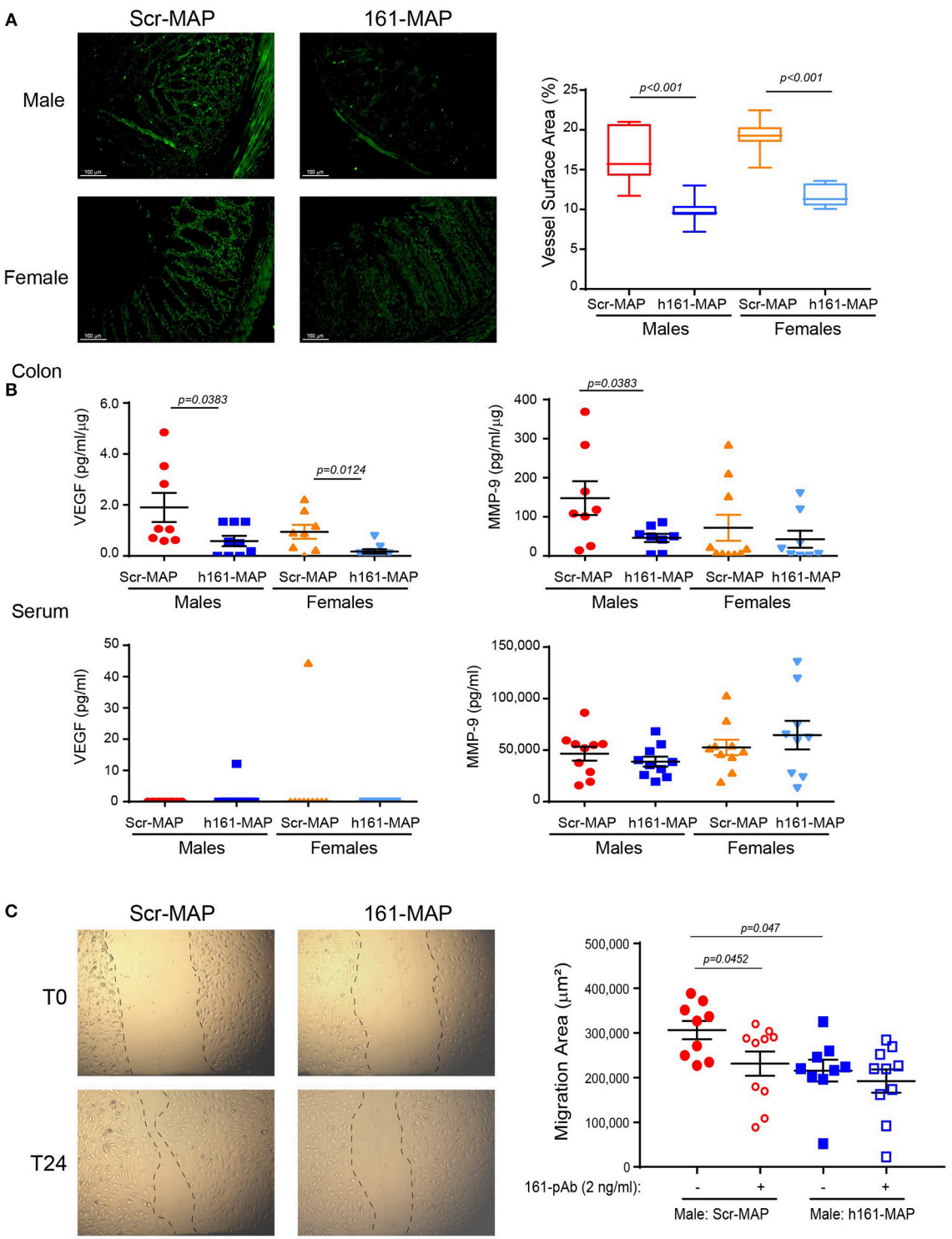

FIGURE 4 | 161-MAP active vaccination reduces angiogenesis. **(A)** Colon sections were stained for CD31 and the vessel surface area was calculated ($n = 4$ per group). Scale bar is 100 μm. **(B)** Concentrations of VEGF and MMP-9 were determined in serum sample by ELISA, and in the colon lysates, normalized to the total protein amounts ($n = 9$ per group). **(C)** Wound scratch assay: colon lysates (25 μg of total protein) were diluted (1:4) and applied onto a confluent layer of the mouse bEND3 endothelial cells (10^5 cells/ 96-plate well) that was scratched with a toothpick. Images were acquired at the beginning of the experiment (T0) and at the end after 24h (T24). The migration area was calculated by subtracting the area of the wound at T24, after endothelial cell migrated and partially closed the wound, from the area of the wound at T0. An EMMPRIN specific blocking antibody (161-pAb) was added to some of the wells as indicated. ($n = 9$–10 for the male mice, $n = 8$ for the female mice). Magnification is x4.

161-MAP Vaccination Changes Immune Cell Infiltration, the Microenvironment, and Cell Viability

As DSS-induced colitis is an inflammatory disease, and the vaccination process is likely to stimulate immune cells, we next stained colon sections for the presence of $CD8^+$ T cells, macrophages and neutrophils. As expected, infiltration of $CD8^+$ T cells, reflecting the stimulation of the adaptive immune system, was increased in the 161-MAP vaccinated mice in comparison to the control mice (by 3.3-fold, $p = 0.012$ for the males, 95% CI [0.3, 0.76], by 2.5-fold, $p = 0.0071$ for the females, 95% CI [0.14, 0.59] **Figure 5A**). Likewise, infiltration of macrophages was also increased (by 2.2-fold, $p = 0.0016$ for the males, 95% CI [0.41, 1.4], by 2.8-fold, $p < 0.001$ for the females, 95% CI [1.2, 2.1], **Figure 5B**). In contrast, neutrophil infiltration, that is characteristic of the innate immunity in acute inflammation, remained unchanged (data not shown).

To learn about the mode of activation of these cells, we next evaluated cytokine concentrations in serum samples and locally in the colon lysates. Concentrations of IL-1β, TNFα, and IL-10 in the serum and the colon were not different between the control and the 161-MAP vaccinated mice, in both males and females (**Figures 5C,D**), suggesting that the pro-inflammatory process was no longer active at this late stage. In contrast, levels of TGFβ were reduced in colon lysates of 161-MAP vaccinated male mice in comparison to the Scr-MAP vaccinated mice (by 3-fold, $p = 0.03$, 95% CI [0.4, 1.7]), whereas in female mice this trend (2-fold difference) did not reach significance. In the serum samples, TGFβ was reduced in both male and female 161-MAP vaccinated mice relative to their respective controls (by 1.4-fold and 1.5-fold, $p < 0.05$, 95% CI for male [4,357, 42,198] and for female [3,703, 42,412]). The high levels of TGFβ in the control Scr-MAP vaccinated mice together with no change in the low levels of the pro-inflammatory cytokines suggest that by day 15, the pro-inflammatory response was already replaced with a regeneration program. The relative reduction in those TGFβ levels in 161-MAP vaccinated mice suggests that a moderate repair program was in place.

Staining the colon sections for Ki-67 revealed that proliferation in the 161-MAP vaccinated groups was reduced relative to the Scr-MAP controls (by 3.7-fold, $p < 0.001$ for males 95% CI [0.016, 0.03], and by 2.4-fold, $p < 0.001$ for females, 95% CI [0.009, 0.015], **Figure 6A**). In contrast, the number of apoptotic cells, as assessed by the TUNEL assay, was increased in the 161-MAP vaccinated mice relative to the Scr-MAP vaccinated controls (by 2.5-fold, $p = 0.0005$ for males, 95% CI [176.6, 544.6], by 2.3-fold, $p = 0.0001$ for females, 95% CI [191.2, 507.3], **Figure 6B**).

DISCUSSION

The mechanisms that drive UC and its analogous model of DSS-induced colitis are not fully understood, although increased ROS and pro-inflammatory cytokines, pathological angiogenesis, as well as the composition of the microbiota in the gut have been implicated (4, 6). In many of the treated patients, the drugs currently in use do not exert sufficient beneficial effects, suggesting that additional pathological mechanisms, that could potentially be targeted, are at play. Here we demonstrate that by selectively targeting EMMPRIN, a multifunctional protein that is primarily involved in angiogenesis, we reduced angiogenesis and ameliorated clinical manifestations of the DSS-induced colitis model, including weight loss and disease severity, pointing to the central role that angiogenesis plays in this model.

EMMPRIN is highly expressed in the colon, especially in the crypt base columnar cells. As the chaperon of the monocarboxylate transporter family (particularly of MCT-1 and MCT-4) it has an important function in the transport of monocarboxylate anions, such as lactate, pyruvate, ketone bodies and the short-chain fatty acids acetate, propionate and butyrate (20), all of which are particularly important in intestinal function. Additionally, EMMPRIN may help in recruiting leukocytes to the inflamed site, and support their adhesion to endothelial cells. Despite its important role, this is the first demonstration of the involvement of EMMPRIN in colitis, to the best of our knowledge. We show here that targeting EMMPRIN reduces angiogenesis, but the reduction in EMMPRIN expression in the 161-MAP vaccinated mice suggests that other functions of EMMPRIN may also be affected. These aspects deserve additional exploration that is outside the scope of the current work.

The vaccination reduced EMMPRIN expression and led to reduced microvessel density and angiogenesis. Angiogenesis is a necessary process, as it promotes and sustains inflammation by supplying nutrients, allowing increased leukocyte influx and promoting endothelial cell local production of chemokines, cytokines, and MMPs. In fact, many mediators exhibit a dual role as pro-angiogenic and pro-inflammatory, linking the two processes. For example, VEGF, which is a potent pro-angiogenic factor as well as a chemoattractant for macrophages, has been shown to increase mucosal angiogenesis, promote leukocyte adhesion and worsen the clinical outcome in both IBD patients and in a DSS-induced colitis model (7). Pathogenic angiogenesis and elevated levels of both VEGF and MMP-9 were demonstrated in different models of UC, including a DSS-induced colitis model (7, 21). Furthermore, VEGF has been implicated in increasing vascular permeability, which in the context of colitis may have an additional effect by allowing bacteria to invade into the LP, thus enhancing the inflammatory process (10, 22).

In the past, attempts have been made to target VEGF or its receptor VEGFR2. For example, targeting VEGFR2 with the monoclonal DC101 antibody in a DSS-induced colitis model did not inhibit angiogenesis or improve disease severity, probably due to VEGF-independent compensatory pathways that maintained downstream signaling events (23). The authors suggested that this monotherapy might have had better effects if used in combination with another monoclonal antibody that targeted another angiogenic mediator. This may have been the case in our EMMPRIN vaccination, as EMMPRIN is a mediator upstream of VEGF that also induces MMP-9. Indeed, we show a reduction (at least in the male groups) of both VEGF and MMP-9, two potent pro-angiogenic mediators. Thus, in contrast to the previous study, we succeeded in improving disease

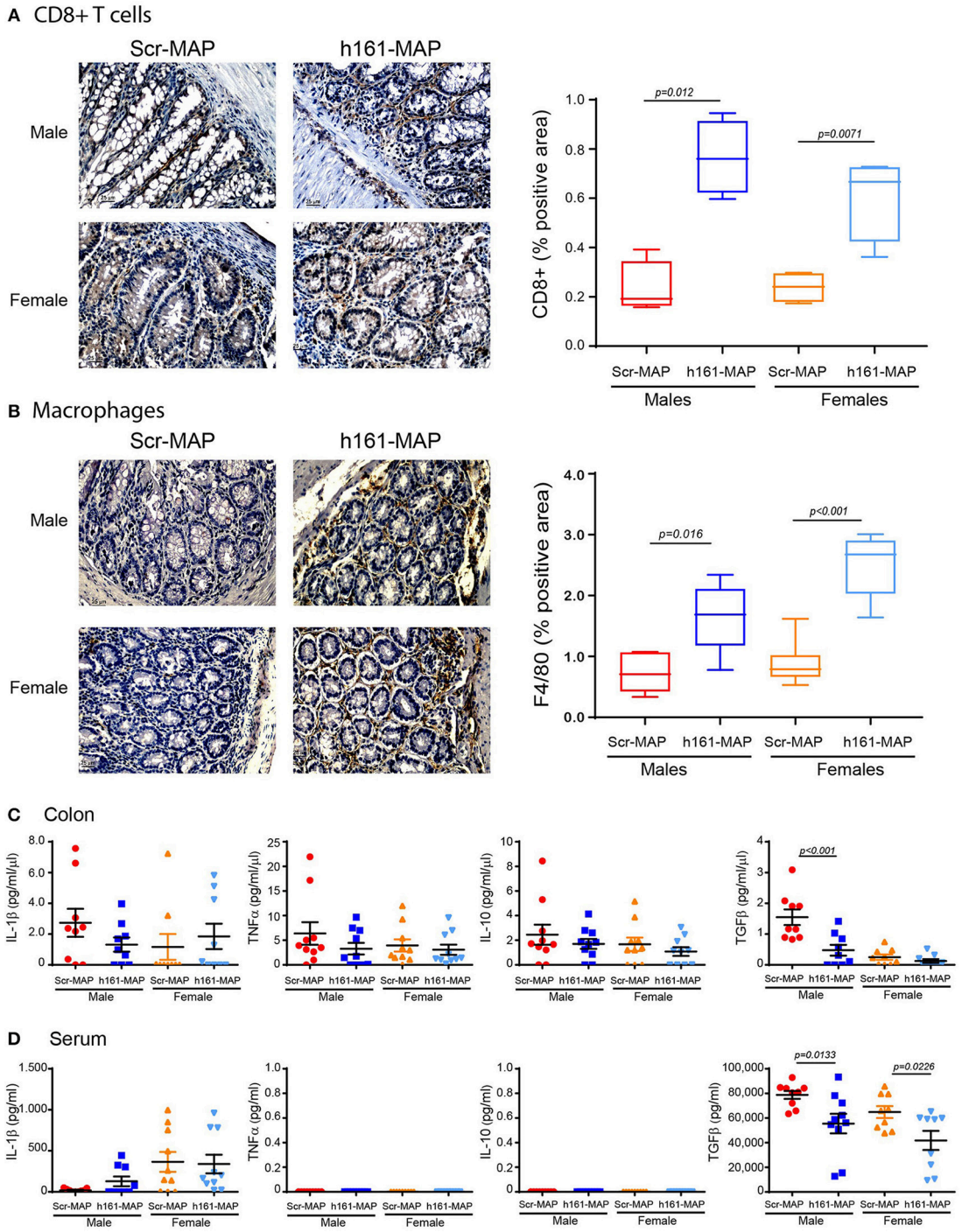

FIGURE 5 | 161-MAP active vaccination increases infiltration of $CD8^+$ T cells and macrophages, and reduces TGFβ concentrations. Colon tissue sections were stained for **(A)** $CD8^+$ or **(B)** for F4/80, and analyzed for their distribution ($n = 4–5$ in each group). Scale bar is 25 μm. **(C)** Proteins were extracted from colon segments and the concentrations of IL-1β, TNFα, IL-10 and TGFβ were determined in the lysates by ELISA and normalized to the total protein ($n = 9–10$). **(D)** Concentrations of the same cytokines were determined in the serum samples ($n = 9–10$).

severity and in reducing angiogenesis, while demonstrating again the importance of VEGF in the DSS-induced colitis model.

Since inflammation and angiogenesis are interconnected processes, we expected that targeting angiogenesis through EMMPRIN vaccination would also reduce inflammation. For

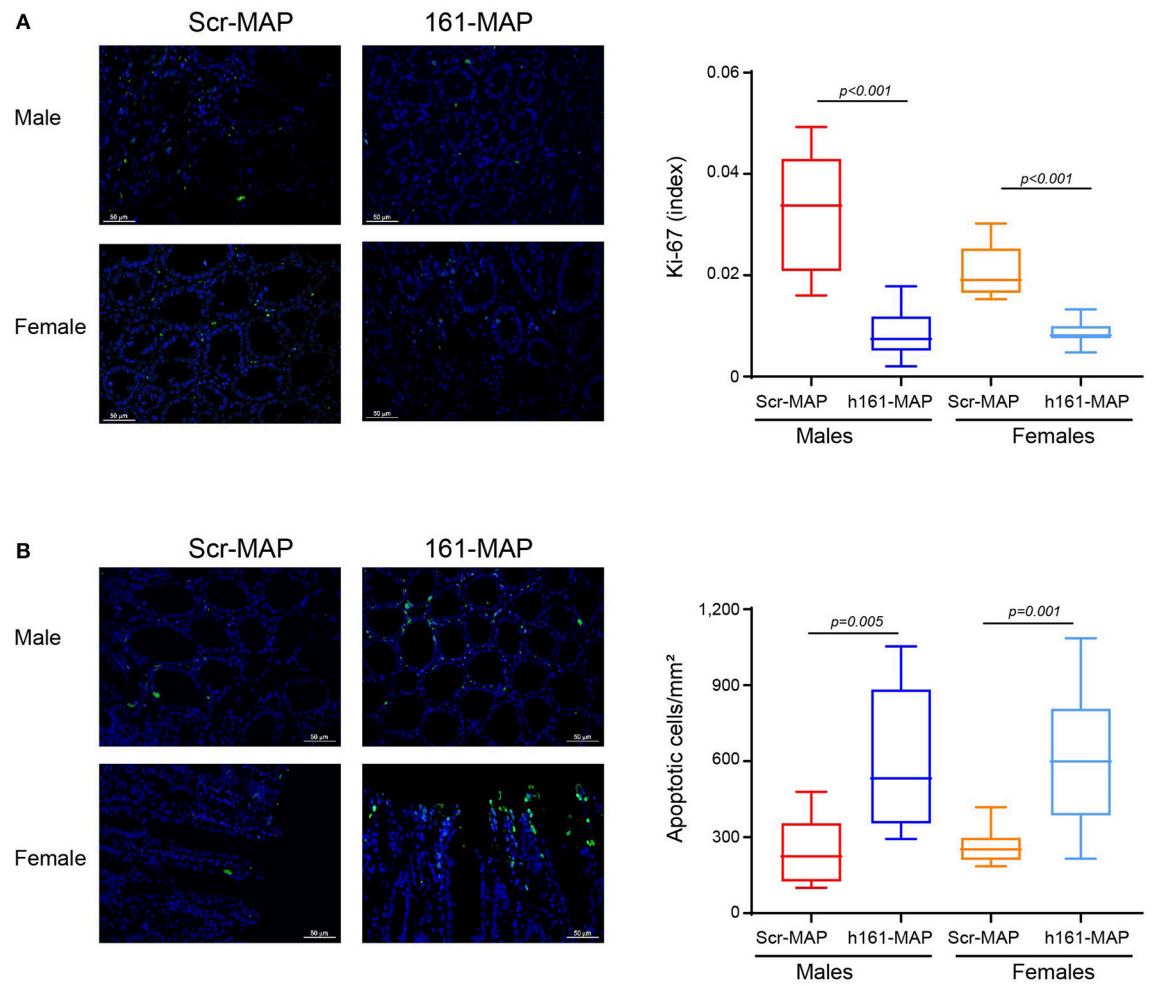

FIGURE 6 | 161-MAP active vaccination reduces proliferation and enhances apoptosis. Colon tissue sections were stained for Ki-67 or DNA strand breaks (TUNEL assay). **(A)** Representative images of Ki-67 staining (scale bar is 50 μm) and their quantitation (Green, proliferating cells; blue, DAPI staining of nuclei; white, merged co-localization, $n = 3$–4 in each group). **(B)** Representative images of the TUNEL assay and their quantitation. (Green, apoptotic cells; blue, DAPI staining of nuclei; white, merged co-localization, $n = 3$–4 in each group). Scale bar is 50 μm.

example, reduction of VEGF using anti-VEGF antibody has reduced vascular permeability and influx of immune cells into the colon in an experimental colitis model (22). EMMPRIN itself has a role in recruiting leukocytes, and therefore, targeting it was expected to reduce immune infiltrate. However, we show that 15 days after the onset of inflammation by the DSS, more macrophages and $CD8^+$ T cells were present in the LP, and colonic levels of pro-inflammatory cytokines, such as TNFα and IL-1β, were unchanged by the vaccination. We suggest that these results can be explained by the duration of the model. Most studies, with or without interventions, follow a design where DSS is administered for 5–7 consecutive days and then the mice are immediately euthanized without a DSS-free period that allows regeneration and repair. Thus, the status of immune activation is measured at the peak of the innate inflammatory response. In our experimental design, the mice are allowed to drink DSS-free water after 5 days of exposure, giving them the chance to repair intestinal damage. In this kinetics, disease is most severe around day 9, 4 days after DSS is no longer administered. It might be argued that since we stimulated the adaptive immune system prior to DSS administration, it is possible that the innate and adaptive immune responses occur simultaneously, prolonging the time of maximal damage. However, since the irritation to the intestine was stopped after 5 days by supplying DSS-free drinking water, the mice have entered into a repair or healing stage. Thus, the intestinal milieu was probably reflecting a resolution state, rather than a pro-inflammatory response with high cytokine concentrations, even if the inflammatory cells were still physically present in the microenvironment. Supporting our premise are studies of DSS-induced colonic tissue that show reduced cytokine production at the mRNA or protein levels in the resolution phase compared to the acute phase of inflammation (24–26).

Several evidences support our conclusion that the immune response is at the repair stage. First, the low number of

infiltrating neutrophils in the colon samples did not change upon vaccination, suggesting that the system was no longer in acute inflammation. In contrast, during the acute phase of DSS-induced colitis model the innate immune cells, especially neutrophils and macrophages, massively infiltrate the LP, and elevated levels of the pro-inflammatory cytokines they secrete, such as TNFα, IL-1β, and IL-17 are observed (27). However, upon removal of DSS, the acute response gradually changes into a chronic response, pro-inflammatory cytokines are decreased, and Th2 cytokine levels are increased (1, 2). In particular, IL-4 and TGFβ have been shown to be critical for regeneration of intestinal epithelial cells (28, 29). Comparing vaccinated and control mice, we found no change in the amount of infiltrating neutrophils, but $CD8^+$ T cells and macrophages were increased, suggesting that the adaptive immune response, rather than the innate immunity, was specifically increased in the 161-MAP vaccinated mice. The levels of TNFα, IL-1β, and IL-10 were low and showed no difference between the groups, whereas TGFβ levels were reduced compared to the Scr-MAP vaccinated control mice. This is consistent with the importance of this cytokine in tissue regeneration, and suggests that the damage in the vaccinated mice during the early stages was relatively reduced, leading to a reduced need for regeneration. Furthermore, turnover of the surface epithelium in the colon takes about 5–8 days. Although signs of inflammation are clearly visible in the vaccinated mice, they also demonstrate restoration of the crypts and epithelium, suggesting reduced inflammation and damage. Alternatively, we surmise that the 161-MAP vaccination triggered an early EMMPRIN-specific pro-inflammatory response, allowing for DSS-damaged epithelial cells that express EMMPRIN to be cleared faster, and helping to promote a rapid regeneration, which was reflected by the reduced loss of weight and disease activity scores.

DSS is believed to directly kill intestinal epithelial cells, cause barrier dysfunction and induce innate immunity, all leading to enhanced epithelial injury during acute inflammation (3, 4, 30). Studies show that relative to control mice without colitis, DSS-induced colitis increases apoptosis and decreases cell proliferation at the early stages of acute colitis, thus contributing to the barrier dysfunction (31). However, once DSS is removed, the intestine begins to proliferate, in order to regenerate the epithelial layer and restore epithelial barrier function. Increased proliferation underlies an attempt to regenerate the epithelial layer and restore barrier functions (3, 5). Thus, we would expect increased proliferation and reduced apoptosis during the regeneration phase in the 161-MAP group. In contrast, we demonstrate reduced proliferation and enhanced apoptosis in the 161-MAP vaccinated mice relative to the control Scr-MAP vaccinated mice. We suggest that the high proliferation in the Scr-MAP groups reflects an ongoing regeneration at this time point (10 days after cessation of DSS administration), whereas the relatively reduced proliferation observed in the 161-MAP vaccinated groups indicates earlier recovery and a reduced need for regeneration at this time. Likewise, the enhanced apoptosis observed in the 161-MAP vaccinated groups may reflect the death of both epithelial and non-epithelial cells, for example neutrophils, which typically appears at the end of the regeneration phase. As apoptotic neutrophils have been shown to shift macrophage activation toward a healing phenotype (32), and based on the improvement in the DAI and weight loss in the 161-MAP vaccinated groups, we propose that the increase in apoptotic cells may in fact protect the colon and help reduce inflammation.

The protective effects of the 161-MAP vaccination in the DSS-induced colitis model are comparable to our recent results with the same vaccine in implanted and metastatic tumor models, where we used the CT26 colon carcinoma cells among others. We demonstrated there that relative to Scr-MAP vaccinated mice, tumors or metastases were reduced and even eliminated, angiogenesis and its mediators VEGF and MMP-9 were reduced, more $CD8^+$ T cells and macrophages infiltrated the tumors and were engaged in killing tumor cells, TGFβ was reduced and an increase in a Th1/M1 gene signature was detected (33). However, tumor models represent an ongoing chronic inflammation, with continuous exposure to inflammation-inciting triggers and mediators. In contrast, in our design of the DSS-induced colitis model, we allowed enough time for regeneration following cessation of DSS administration. To delineate the full spectrum of the protective effects of the 161-MAP vaccination in the DSS-induced model, a follow-up study looking at multiple time points during the dynamic healing process should be conducted, and immune cells should be isolated from the LP to phenotype and characterize their exact mode of activation.

Many autoimmune diseases are known for their gender bias, generating our interest to examine this phenomenon in our DSS-induced colitis model. Indeed, we observed that despite the basic similarities in kinetics, the female group generally exhibited a more moderate inflammation, reflected by less severe weight loss and DAI scores. This is in agreement with other studies that found that male mice respond faster and develop a more significant and aggressive colitis relative to female mice when exposed to DSS (3), and that STAT-1 deficiency or IRAK-1 deficiency render male, but not female, mice more resistant to DSS-induced colitis (34, 35). However, not all parameters were consistent with this trend, as the histology score and the colon length were similar between males and females. Other studies that showed difference in weight loss but no difference in colon length between the genders attributed these findings to mild colitis being induced (35, 36).

In summary, we show that the critical component of angiogenesis can be targeted in DSS-induced colitis, by vaccinating against the pro-angiogenic mediator EMMPRIN protein. This vaccination improved disease severity, reduced angiogenesis and expedited regeneration, although a direct effect on inflammatory cytokines was not observed.

MATERIALS AND METHODS

Experimental Mouse Model, Vaccination and Disease Activity Index (DAI)

C57BL/6J OlaHsd male and female mice (8 weeks old, Envigo Laboratories, Jerusalem, Israel), were housed in specific pathogen free (SPF) conditions and kept with a 12 h light/dark cycle and access to food and water *ad libitum*. To vaccinate mice we used the synthetic multiple antigenic peptide (MAP) derived

from the human sequence of the EMMPRIN protein (sequence: GHRWLKGGVVLC, designated h161-MAP), or a peptide with the same amino acids in a scrambled order used as a negative control (sequence: WCRGGGLKMRVH, designated Scr-MAP). Peptides were synthesized by the standard stepwise solid-phase procedure using Fmoc chemistry on β-Ala-Wang resin, conjugating the peptides onto an octa-branched lysine core (Yuan Yu Bio-Teck), and purity was confirmed by HPLC and mass spectroscopy. Using the human sequence, rather than the mouse sequence, reflected the homology between the two sequences, and was shown before to trigger an equally effective EMMPRIN-specific response (33). For the first vaccine injection, the 161-MAP and Scr-MAP (50 μg each) were emulsified in complete Freund's adjuvant (CFA) for the first vaccine injection, and additional three vaccination injections where the same amount of MAPs was emulsified in incomplete Freund's adjuvant (IFA), were administered subcutaneously to each mouse every 7 days. Four days after the last boost injection, colitis was induced with 2% DSS (MW 36–50 kDa, cat. No. 160110, MP Biomedicals, LLC Solon, OH) administered in the drinking water for five consecutive days, after which their drinking water were replaced with regular water, and the mice were left for additional 10 days. At the end of the experiment, mice were euthanized and their colon tissue and serum were harvested for later analyses. Disease activity index (DAI) was calculated as the average of loss of weight, stool consistency and bleeding and evaluated daily for each mouse. Change in weight relative to the weight of each mouse on the first day of DSS administration was given the scores: 0, if $<$ 1%; 1, 1–5%, 2, 5–10%, 3, 10–15%; 4, $>$15%; Consistency of the stool was assigned the scores: 0, normal stool; 2, loose or pasty pellets; 4, diarrhea. Presence of occult blood (measured with Hemooccult, SENSA, Beckman Coulter, Brea, CA) was given the following scores: 0, normal; 2, positive occult blood; 4, rectal bleeding.

Histology and Scoring

Colon sections were fixed in 4% formalin and paraffin embedded, and then 4 μM sections were stained with hematoxylin and eosin (H&E). Histological scoring, assessing the severity of the model, was based on four parameters. Epithelial loss was scored as follows: 0, no epithelial loss; 1, loss of up to 5% of the epithelial surface; 2, loss of 5–10% of the epithelial surface; 3, loss of $>$10% of the epithelial surface. Crypt integrity was evaluated as follows: 0, Intact crypt; 1, loss of 0–10% of the crypts; 2, loss of 10–20% of the crypts, 3, loss of $>$20% of the crypts. Inflammatory infiltrate was assigned the following score: 0, no infiltration; 1, mild leukocyte infiltrate; 2, moderate leukocyte infiltrate; 3, severe leukocyte infiltrate. Depletion of Goblet cells was estimated as: 0, no depletion of Goblet cells; 1, mild depletion of Goblet cells; 2, moderate depletion of Goblet cells; 3, severe depletion of Goblet cells.

Immunohistochemistry, Immunofluorescence, and Immune Reactive Score

Four-micron thick paraffin embedded tissue sections were deparaffinized on a glass slide with xylene substitute K-Clear Plus (Kaltex) and rehydrated with decreasing ethanol immersions. Antigen retrieval for Ki-67 and F4/80 was performed by microwave heating in citrate buffer pH 6.0, for CD31 by immersing the slides in 42 mg/mL Proteinase XXIV solution (Sigma-Aldrich, Rehovot, Israel) for 10 min at 37°C, or in 20 mg/mL of Proteinase K in Tris buffer, pH 8.0 for the TUNEL kit. Endogenous peroxidase was quenched in 3% H_2O_2 solution for 10 min, slides were blocked with 5% BSA and incubated overnight at 4°C with the following primary antibodies: rat anti-mouse EMMPRIN (R&D systems, MAB772, Minneapolis, MN, USA) diluted 1:250; rat monoclonal anti-F4/80 (Abcam, ab6640, Cambridge, UK) diluted 1:200; rabbit polyclonal anti-CD8 (Bioss, bs-0648R, Woburn, MA, USA) diluted 1:400. After washing, the antibodies were detected with HRP-Polymer anti-rabbit (Zytomed, Berlin, Germany) or with the N-Histofine Simple Stain Mouse MAX PO (Rat) (Nichirei Bioscience, Tokyo, Japan) for 1 h and the DAB substrate Kit (Zytomed systems). All sections were counterstained with hematoxylin (Sigma) and coverslips were applied using Pertex mounting medium (Histolab Products AB). For the CD31 and Ki-67, we used the primary antibodies rat monoclonal anti-CD31 (Acris Antibodies, BM4086, Herford, Germany) diluted 1:50 and rabbit monoclonal anti-Ki67 (Abcam, ab16667) diluted 1/140. Secondary antibodies were donkey Alexa Fluor 488-conjugated anti-rat IgG (Abcam, ab150153), or donkey Alexa Fluor 488-conjugated anti-rabbit (Abcam, ab150061), respectively, diluted 1:500. Nuclei were stained with 300 nM DAPI (MP Biochemicals, LLC Solon, OH) and coverslips were applied using the fluorescent mounting medium (Agilent Dako, Carpinteria, CA). The TUNEL staining was performed using the *in situ* death detection kit POD (Roche Life Science, Mannheim, Germany) according to manufacturer's instructions. All sections were viewed under the bright field trinocular microscope (Olympus BX-60, Tokyo, Japan) and images were acquired with the MS60 camera and the MShot Image Analysis System V1 (MSHOT, Guangzhou Micro-shot Technology Co., Guangzhou, China). Vessel densities were assessed in CD31 stained sections by using a Weibel grid to calculate vessel surface area (37), and the fraction of Ki-67-positive tumor cells was calculated by the digital image analysis web application ImageJS (38). EMMPRIN expression was assessed using the modified H-score, which assigns an immune reactive score on a continuous scale of 0–300, based on the percentage of positive cells expressing the protein at different intensities. Staining was divided into three categories: 1 for "light staining," 2 for "intermediate staining," and 3 for "strong staining." The percentage of positive cells was determined according to the positive surface area of cells measured with ImagePro plus 4.5 software, and the score was calculated using the formula: $1 \times$ (%1 positive cells) $+ 2 \times$ (%2 positive cells) $+ 3 \times$ (%3 positive cells).

Sandwich ELISA

The mouse cytokines were determined using ELISA kits (R&D systems,) according to the manufacturer's instructions. Serum samples were diluted 1:4 (for IL-1β, IL-10, and TNF) or 1:100 (for TGFβ, MMP-9, and VEGF), and tissue lysate samples were normalized to the total protein. Serum EMMPRIN

concentrations were measured with an ELISA kit (Abcam, ab215405) at a dilution of 1:200, according to the manufacturer's instructions, or normalized to total protein in tissue lysates.

In vitro Wound Scratch Assay

In vitro wound scratch assay was performed as described before (17), with the mouse bEND3 endothelial cell monolayers (10^5 cells) seeded in 96-well dishes and incubated with 25 mg of total protein extracted from colon samples of the control or 161-MAP vaccinated mice groups. To demonstrate EMMPRIN involvement, we added the rabbit anti-mouse EMMPRIN polyclonal antibody (161-pAb, 2 ng/ml) that we previously produced (19), to some of the wells. Images of the field of injury were acquired at the beginning of the experiment (T0) and after 24 h (T24) using the ImagePro plus 4.5 software (Media Cybernetics, Inc., Rockville, MD, USA), and the wound area was measured at both times. The migration area, reflecting the area to which endothelial cells migrated in order to close the wound, was calculated by the subtraction of the area at T24 from the area at T0.

Statistical Analyses

All values are presented as means ± SE and all comparisons are presented with the 95% CI for the difference between the means. Significance between two groups was determined using the two-tailed unpaired *t*-test. Differences between experimental groups accounting for time and treatment were analyzed using two-way analysis of variance (ANOVA) and the *post hoc* Bonferroni's multiple comparison test. *P*-values exceeding 0.05 were not considered significant.

ETHICS STATEMENT

Mice were cared for in accordance with the procedures outlined in the NIH Guideline for the Care and Use of laboratory Animals, and all experiments were performed under the approved protocol (IL-0350315) issued by the Animal Care and Use Committee of the Technion-Israel Institute of Technology.

AUTHORS CONTRIBUTIONS

ES performed the animal experiments and carried out all ELISA analyses, as well as wound assays. VB was in charge of the immunohistochemical staining. MAR designed the study, analyzed and interpreted the results, and wrote the manuscript.

FUNDING

This study was supported by the KAMIN project from the Office of the Chief Scientist in Israel's Ministry of Economy (Grant No. 53642), by the Israel Science Foundation (Grant No. 1392/14), and by the Israel Cancer Association (Grant No. 20180051 made available by the ICA USA Board of Directors).

ACKNOWLEDGMENTS

This publication was made possible through core services and support provided by Drs. Levin-Ashkenazi and Schlensinger-Laufer from the Pre-Clinical Research Authority at the Technion-Israel Institute for Technology.

REFERENCES

1. Eichele DD, Kharbanda KK. Dextran sodium sulfate colitis murine model: an indispensable tool for advancing our understanding of inflammatory bowel diseases pathogenesis. *World J Gastroenterol.* (2017) 23:6016–29. doi: 10.3748/wjg.v23.i33.6016
2. Ma J, Yin G, Lu Z, Xie P, Zhou H, Liu J, et al. Casticin prevents DSS induced ulcerative colitis in mice through inhibitions of NF-kappaB pathway and ROS signaling. *Phytother Res.* (2018) 32:1770–83. doi: 10.1002/ptr.6108
3. Chassaing B, Aitken JD, Malleshappa M, Vijay-Kumar M. Dextran Sulfate Sodium (DSS)-induced colitis in mice. *Curr Protoc Immunol.* (2014) 104:15.25.1–14. doi: 10.1002/0471142735.im1525s104
4. Perse M, Cerar A. Dextran sodium sulphate colitis mouse model : traps and tricks. *J Biomed Biotechnol.* (2012) 2012:718617. doi: 10.1155/2012/718617
5. Rose WA, Sakamoto K, Leifer CA. Multifunctional role of dextran sulfate sodium for *in vivo* modeling of intestinal diseases. *BMC Immunol.* (2012) 13:4–6. doi: 10.1186/1471-2172-13-41
6. Cromer WE, Mathis JM, Granger DN, Chaitanya G V, Alexander JS. Role of the endothelium in inflammatory bowel diseases. *World J Gastroenterol.* (2011) 17:578–93. doi: 10.3748/wjg.v17.i5.578
7. Scaldaferri F, Vetrano S, Sans M, Arena V, Straface G, Stigliano E, et al. VEGF-A links angiogenesis and inflammation in inflammatory bowel disease pathogenesis. *Gastroenterology* (2009) 136:585–95.e5. doi: 10.1053/j.gastro.2008.09.064
8. Alkim C, Alkim H, Koksal AR, Boga S, Sen I. Angiogenesis in inflammatory bowel disease. *Int J Inflam.* (2015) 2015:970890. doi: 10.1155/2015/970890
9. O'Sullivan S, Gilmer JF, Medina C. Matrix metalloproteinases in inflammatory bowels disease: an update. *Meditors of Infalm.* (2015) 2015:964131. doi: 10.1155/2015/964131
10. Deng X, Szabo S, Khomenko T, Tolstanova G, Paunovic B, French S W, et al. Novel pharmacologic approaches to the prevention and treatment of ulcerative colitis. *Curr Pharm Des.* (2012) 19:17–28. doi: 10.2174/13816128130105
11. Grass GD, Toole BP. How, with whom and when: an overview of CD147-mediated regulatory networks influencing matrix metalloproteinase activity. *Biosci Rep.* (2016) 36:e00283. doi: 10.1042/BSR20150256
12. Weidle UH, Scheuer W, Eggle D, Klostermann S, Stockinger H. Cancer-related issues of CD147. *Cancer Genomics Proteomics* (2010) 7:157–69.
13. Yurchenko V, Constant S, Eisenmesser E, Bukrinsky M. Cyclophilin-CD147 interactions: a new target for anti-inflammatory therapeutics. *Clin Exp Immunol.* (2010) 160:305–17. doi: 10.1111/j.1365-2249.2010.04115.x
14. Belton RJ, Chen L, Mesquita FS, Nowak RA. Basigin-2 is a cell surface receptor for soluble basigin ligand. *J Biol Chem.* (2008) 283:17805–14. doi: 10.1074/jbc.M801876200
15. Wang Z, Zhao Z, Jiang T, Chen Y, Huang C. The multistep functions of EMMPRIN / CD147 in the tumor angiogenesis. *Cell Mol Med.* (2016) 2:1–5. doi: 10.21767/2573-5365.100012
16. Voigt H, Vetter-Kauczok CS, Schrama D, Hofmann UB, Becker JC, Houben R. CD147 impacts angiogenesis and metastasis formation. *Cancer Invest.* (2009) 27:329–33. doi: 10.1080/07357900802392675
17. Tang Y. Regulation of vascular endothelial growth factor expression by EMMPRIN via the PI3K-Akt signaling pathway. *Mol Cancer Res.* (2006) 4:371–7. doi: 10.1158/1541-7786.MCR-06-0042
18. Zhou J, Zhu P, Jiang JL, Zhang Q, Wu ZB, Yao XY, et al. Involvement of CD147 in overexpression of MMP-2 and MMP-9 and enhancement of invasive potential of PMA-differentiated THP-1. *BMC Cell Biol.* (2005) 6:25–35. doi: 10.1186/1471-2121-6-25

19. Walter M, Simanovich E, Brod V, Lahat N, Bitterman H, Rahat MA. An epitope-specific novel anti-EMMPRIN polyclonal antibody inhibits tumor progression. *Oncoimmunology* (2015) 5:e1078056. doi: 10.1080/2162402X.2015.1078056
20. Kirat D, Kondo K, Shimada R, Kato S. Dietary pectin up-regulates monocaboxylate transporter 1 in the rat gastrointestinal tract. *Exp Physiol.* (2009) 94:422–433. doi: 10.1113/expphysiol.2009.046797
21. Tolstanova G, Deng X, Khomenko T, Garg P, Paunovic B, Chen L, et al. Role of anti-angiogenic factor endostatin in the pathogenesis of experimental ulcerative colitis. *Life Sci.* (2011) 88:74–81. doi: 10.1016/j.lfs.2010.10.026
22. Tolstanova G, Khomenko T, Deng X, Chen L, Tarnawski A, Ahluwalia A, et al. Neutralizing anti-vascular endothelial growth factor (VEGF) antibody reduces severity of experimental ulcerative colitis in rats : direct evidence for the pathogenic role of VEGF. *Rev Lit Arts Am.* (2009) 328:749–57. doi: 10.1124/jpet.108.145128
23. Knod L, Donovan EC, Chernoguz A, Crawford KM, Dusing MR, Frischer JS. Vascular endothelial growth factor receptor-2 inhibition in experimental murine colitis. *J Surg Res.* (2013) 184:101–7. doi: 10.1016/j.jss.2013.04.026
24. Bento AF, Leite DFP, Marcon R, Claudino RF, Dutra RC, Cola M, et al. Evaluation of chemical mediators and cellular response during acute and chronic gut inflammatory response induced by dextran sodium sulfate in mice. *Biochem Pharmacol.* (2012) 84:1459–69. doi: 10.1016/j.bcp.2012.09.007
25. Lan A, Blais A, Coelho D, Capron J, Maarouf M, Benamouzig R, et al. Dual effects of a high-protein diet on DSS-treated mice during colitis resolution phase. *Am J Physiol Liver Physiol.* (2016) 311:G624–33. doi: 10.1152/ajpgi.00433.2015
26. Meers GK, Bohnenberger H, Reichardt HM, Lühder F, Reichardt SD. Impaired resolution of dss-induced colitis in mice lacking the glucocorticoid receptor in myeloid cells. *PLoS ONE* (2018) 13:e0190846. doi: 10.1371/journal.pone.0190846
27. Zhang X, Wei L, Wang J, Qin Z, Wang J, Lu Y, et al. Suppression colitis and colitis-associated colon cancer by anti-S100a9 antibody in mice. *Front Immunol.* (2017) 8:1774. doi: 10.3389/fimmu.2017.01774
28. Iizuka M, Konno S. Wound healing of intestinal epithelial cells. *World J Gastroenterol.* (2011) 17:2161–71. doi: 10.3748/wjg.v17.i17.2161
29. Stevceva L, Pavli P, Husband A, Ramsay A. Dextran sulphate sodium-induced colitis is amelioratedin Interleukin 4 Deficient Mice. *Genes Immun.* (2001) 2:309–16. doi: 10.1038/sj.gene.6363782
30. Yuan B, Zhou S, Lu Y, Liu J, Jin X, Wan H, et al. Changes in the expression and distribution of claudins, increased epithelial apoptosis, and a mannan-binding lectin-associated immune response lead to barrier dysfunction in dextran sodium sulfate-induced rat colitis. *Gut Liver* (2015) 9:734–40. doi: 10.5009/gnl14155
31. Araki Y, Mukaisyo K-I, Sugihara H, Fujiyama Y, Hattori T. Increased apoptosis and decreased proliferation of colonic epithelium in dextran sulfate sodium-induced colitis in mice. *Oncol Rep.* (2010) 24:869–74. doi: 10.3892/or_00000932
32. Greenlee-Wacker MC. Clearance of apoptotic neutrophils and resolution of inflammation. *Immunol Rev.* (2016) 273:357–70. doi: 10.1111/imr.12453
33. Simanovich E, Brod V, Rahat MM, Drazdov E, Miriam W, Shakya J, et al. Inhibition of tumor growth and metastasis by EMMPRIN Multiple Antigenic Peptide (MAP) vaccination is mediated by immune modulation. *Oncoimmunology* (2017) 6:e1261778.doi: 10.1080/2162402X.2016.1261778
34. Berglund M, Thomas JA, Fredin MF, Melgar S, Hörnquist EH, Hultgren OH. Gender dependent importance of IRAK-1 in dextran sulfate sodium induced colitis. *Cell Immunol.* (2009) 259:27–32. doi: 10.1016/j.cellimm.2009.05.009
35. Crnčec I, Modak M, Gordziel C, Svinka J, Scharf I, Moritsch S, et al. STAT1 is a sex-specific tumor suppressor in colitis-associated colorectal cancer. *Mol Oncol.* (2018) 12:514–28. doi: 10.1002/1878-0261.12178
36. Wagnerova A, Babickova J, Liptak R, Vlkova B, Celec P, Gardlik R. Sex differences in the effect of resveratrol on DSS-induced colitis in mice. *Gastroenterol Res Pract.* (2017) 2017:8051870. doi: 10.1155/2017/8051870
37. Weibel ER, Kistler GS, Scherle WF. Practical stereological methods for morphometric cytology. *J Cell Biol.* (1966) 30:23–38. doi: 10.1083/jcb.30.1.23
38. Almeida JS, Iriabho EE, Gorrepati VL, Wilkinson SR, Grüneberg A, Robbins DE, et al. ImageJS: personalized, participated, pervasive, and reproducible image bioinformatics in the web browser. *J Pathol Inf.* (2012) 3:25–32. doi: 10.4103/2153-3539.98813

Conflict of Interest Statement: ES and VB declare that the research was conducted in the absence of any commercial or financial relationships that could be construed as a potential conflict of interest. MR is an inventor of a patent (US Grant US9688732B2, EP application EP2833900A4) related to the research described in the manuscript.

frontiers in Physiology

ORIGINAL RESEARCH
published: 08 January 2019
doi: 10.3389/fphys.2018.01862

Stent-Jailing Technique Reduces Aneurysm Recurrence More Than Stent-Jack Technique by Causing Less Mechanical Forces and Angiogenesis and Inhibiting TGF-β/Smad2,3,4 Signaling Pathway in Intracranial Aneurysm Patients

*Ning Xu, Hao Meng, Tianyi Liu, Yingli Feng, Yuan Qi, Donghuan Zhang and Honglei Wang**

Department of Neurosurgery, The First Hospital of Jilin University, Changchun, China

OPEN ACCESS

Edited by:
Michal Amit Rahat, Technion – Israel Institute of Technology, Israel

Reviewed by:
Hiroshi Suzuki, Showa University, Japan
Zhenhuan Ma, The First People's Hospital of Yunnan Province, China
Weiping Zhou, General Hospital of Shenyang Military Command, China

***Correspondence:**
Honglei Wang
wanghongleimd@163.com

Specialty section:
This article was submitted to Vascular Physiology, a section of the journal Frontiers in Physiology

Received: *18 September 2018*
Accepted: *11 December 2018*
Published: *08 January 2019*

Citation:
Xu N, Meng H, Liu T, Feng Y, Qi Y, Zhang D and Wang H (2019) Stent-Jailing Technique Reduces Aneurysm Recurrence More Than Stent-Jack Technique by Causing Less Mechanical Forces and Angiogenesis and Inhibiting TGF-β/Smad2,3,4 Signaling Pathway in Intracranial Aneurysm Patients. Front. Physiol. 9:1862. doi: 10.3389/fphys.2018.01862

Background: Stent-jailing and stent-jack are used for stent-assisted coil embolism (SCE) in intracranial aneurysm (IA) therapy, and cause different incidences of IA recurrence. Angiogenesis strongly correlates with aneurysm accumulation. Stent-jack causes higher mechanical forces in cerebral vessels than stent-jailing. Mechanical forces, as well as TGF-β/Smad2,3,4 signaling pathway, may play an important factor in IA recurrence by affecting angiogenesis.

Methods: We explored the effects of stent-jailing or stent-jack technique on IA recurrence by investigating mechanical forces, TGF-β/Smad2,3,4 signaling pathway and the incidence of angiogenesis in IA patients. One-hundred-eighty-one IA patients were assigned into stent-jailing (n = 93) and stent-jacket groups (n = 88). The clinical outcome was evaluated using Glasgow Outcome Score (GOS) and aneurysm occlusion grades. The percentage of $CD34^+$EPCs (releasing pro-angiogenic cytokines) in peripheral blood was measured by flow cytometer. Endothelial cells were separated from cerebral aneurysm and malformed arteries via immunomagnetic cell sorting. Angiogenesis was measured by microvessel density (MVD) using anti-CD34 monoclonal antibody staining before using the stent, immediately after surgery and 2 years later. Meanwhile, the mechanical forces in cerebral vessels were determined by measuring endothelial shear stress (ESS) via a computational method. TGF-β and Smad2,3,4 were measured by real-time qPCR and Western Blot. Tube formation analysis was performed to test the relationship between angiogenesis and TGF-β, and the effects of different techniques on angiogenesis.

Results: After a 2-year follow-up, 85 and 81 patients from stent-jailing and stent-jack groups, respectively, completed the experiment. Stent-jailing technique improved GOS and reduced aneurysm occlusion grades higher than the stent-jack technique ($P < 0.05$). The counts of $CD34^+$EPCs and MVD values in the stent-jailing group

were lower than the stent-jack group ($P < 0.05$). ESS values in sent-jailing group were lower than the stent-jack group ($P < 0.05$), and positively correlated with MVD values ($P < 0.05$). TGF-β and Smad2,3,4 levels in sent-jailing group were also lower than the stent-jack group ($P < 0.05$). TGF-β was associated with angiogenesis incidence and stent-jack caused angiogenesis incidence more than stent-jailing.

Conclusion: Stent-jailing technique reduces IA recurrence more than stent-jack by causing less mechanical forces, angiogenesis and inhibiting TGF-β/Smad2,3,4 signaling in IA patients.

Keywords: intracranial aneurysm, stent-jailing, stent-jack, angiogenesis, TGF-β, Smad2,3,4, endothelial shear stress, microvessel density

INTRODUCTION

Intracranial aneurysm (IA) is a common cerebral disease, which involves various organs and becomes more prevalent with high-level morbidity and mortality (Piotin et al., 2018). With the development of medical devices, endovascular stents have been widely used in the prevention of IA (Bakhsheshian et al., 2018; Takahashi et al., 2018). Stent-assisted coil embolization (SCE) techniques are becoming popular and may be feasible and effective for such postoperatively complicated aneurysms (Takeshita et al., 2017).

Stent-jailing technique represents an efficacious adjuvant technique for treating wide-necked persistent trigeminal artery aneurysm (Rong-Bo et al., 2013), in which IAs are "jailed." For some small aneurysms, stent-jailing technique has been often considered. Nevertheless, the technique should be used carefully and may be unsuccessful occasionally (Yoon et al., 2013). Stent-jack is another technique for complicated aneurysmal treatment. The first coil can be detached into aneurysm dome after the stent is positioned (de Paula Lucas et al., 2008). The technique has been proved to be effective in treating the aneurysms with a ratio of dome height to neck width less than 1.5 (de Paula Lucas et al., 2008).

Complicated IAs are often existed in the internal and middle cerebral artery. Embolization of irregular and complicated IAs is still a challenge. The stent-jailing technique (Tsai et al., 2018) or stent-jack (Lozen et al., 2009) can facilitate efficient embolization of aneurysms. Although stent-jailing and stent-jack techniques are safe and effective for aneurysm therapy but the effects of these techniques on IA recurrence, and associated molecular mechanism remains unknown. Stent-jailing and stent-jack techniques can cause different mechanical forces in cerebral blood vessels. Mechanical forces regulate transforming growth factor-β (TGF-β) and Smads (Maeda et al., 2011). TGF-β is the prototype of structurally related cytokines and control proliferation, differentiation and migration of various cells (Jin et al., 2018). TGF-β has a positive association with the levels of VEGF, and can enhance cellular angiogenesis (Li et al., 2016) while angiogenesis is associated with aneurysm formation (Baumann et al., 2013). SMAD is a family of proteins that play an important role in signal transduction pathways of TGF-β (Huang et al., 2018). Smad2/3 and Smad4 are direct mediators of TGF-β signaling pathway (Ungefroren et al., 2011). Smad2 activates TGF-β type I receptor (TβR-I) and Smad2 phosphorylation is necessary for its nuclear translocation (Rostam et al., 2018). Smad3 is structurally associated with Smad2. Smad4 forms heteromeric complexes with Smad2 or Smad3 and appears to be part of TGF-β signaling pathway (Kretschmer et al., 2003). TGF-β is involved in blood vessel formation while Smad2/3 signaling in endothelial cells is indispensable to keep vessel integrity (Itoh et al., 2012). Angiogenesis is the growth of new blood vessels from the existing vessels and may play an important role in the development of aneurysms (Hoh et al., 2014). IAs can recure or grow after SCE, and TGF-β/Smad2,3,4 signaling pathway, as well as mechanical forces, may play an important factor in the process of angiogenesis.

Stent-Jailing technique and stent-jacket technique may affect the recurrence and regrowth of IA since stent can induce angiogenesis (Zhang et al., 2014), which is associated with aneurysm development (Hoh et al., 2014). Therefore, we explored the effects of stent-Jailing and stent-jacket techniques on the angiogenesis of IA recurrence. Here, we showed that different stent techniques affected angiogenesis of IA patients by affecting mechanical forces in cerebral blood vessels and TGF-β/Smad2,3,4 pathways.

MATERIALS AND METHODS

Reagents

Rabbit anti-Smad2 (ab63576), anti-Smad2 around the phosphorylation site of serine 467 (ab63576), Anti-Smad3 (EP568Y), anti-Smad3 phosphorylated on Serine 423 and 425 (ab52903), anti-Smad4 (EP618Y), anti-CD31 (ab28364), anti-CD34 (ab8536) and goat anti-rabbit HRP (IgG H&L) (ab6721) antibodies were purchased from Abcam trading (Shanghai) co., ltd. (Shanghai, China). Anti-CD 146-coated dynabeads were purchased from Invitrogen Corporation (CA, United States).

Participants

Before the present experiment, all steps were approved by Human Research Ethics Committee of the First Hospital of Jilin University (Approval No. 2015JLUMPZ), and all patients agreed to sign the informed consent. IAs were measured via digital subtraction angiography (DSA), magnetic resonance

angiography (MRA) and computed tomographic angiography (CTA). CTA and MRA can locate the position and show characteristics of IAs. DSA can improve the accuracy of the diagnoses. Severity of IA was evaluated by using Glasgow Outcome Scale (GOS) (Gotoh et al., 1993).

Inclusion Criteria

The following patients were included: (Piotin et al., 2018) > 18 years; (Takahashi et al., 2018) Modified Rankin Scale (MRS) score < 3; (Bakhsheshian et al., 2018) Clinical symptoms of severe headache, unconsciousness and focal neurological deficits; (Takeshita et al., 2017) the IA identified with CTA.

Exclusion Criteria

The following excluding criteria were used: (Piotin et al., 2018) the patients had severe medical illness (such as myocardial infarction and psychiatric illness) and or severe sequelae of stroke; (Takahashi et al., 2018) the patients had a history of allergy to aspirin or clopidogrel, and or intracerebral hemorrhage; (Bakhsheshian et al., 2018) besides of aspirin or clopidogrel, the patients took other antiplatelet or anti-inflammatory drugs; and (Takeshita et al., 2017) the patients were pregnant or lactating women.

Preoperative Treatment

Nimodipine was used and act to inhibit cerebral vasospasm. IA subjects were orally administered with 80-mg clopidogrel (daily) and 100-mg aspirin (daily) 3 days before surgery. Before half-an-hour surgery, patients were injected with one-mg atropine sulfate to prevent gland secretion.

Patients Grouping

After inclusion and exclusion criteria, 181 IA patients were assigned into stent-jailing ($n = 93$) and stent-jack groups ($n = 88$) based on self-selection after consulting with the brain aneurysm specialists. To eliminate the self-selection bias, a little adjustment was performed to keep no significant difference for IA types and clinical characteristics between two groups after receiving individual agreement (**Table 1**).

With CTA, IA location, size and the diameter of parent artery were examined. Based on the results, the angle, path and corresponding stent technique were chosen. The stent-jailing technique was employed in 93 patients. A stent and coils were employed in two microcatheters, and reached IA dome, respectively. The coils were positioned in the IA dome and covered by the stent, and IA was completely packed. Finally, coil microcatheter was withdrawn, and coils were encaged between the stent and parent artery.

Stent-jack technique was also performed in other 88 IA patients according. A first coil in microcatheter was deployed and self-expandable stent was delivered across IA neck, and first coil was detached when the stent was deployed. The technique constrains the coil loops within IA dome before detachment of the first coil.

Treatment After SCE Intervention

All patients took intraoperative heparinization therapy and orally administrated with 80-mg clopidogrel and 100-mg aspirin daily. Angiography was observed after half year and angiography indicated no symptoms or stent stenosis. The patients would still receive 100-mg aspirin daily during 2-year follow-up.

Clinical Evaluation of SCE

The embolic and ruptured IA events were evaluated before and immediately postoperative imaging. According to occlusion grades, IAs were classified as complete, sub-complete, partial occlusion and no occlusion grades. Clinical outcomes were measured by using the Glasgow Outcome Scale (GOS) (Tsao et al., 2005). GOS categories 1–3 were regarded as unfavorable and GOS categories 4 and 5 were favorable. The outcome was measured based on IA occlusion grades before and immediately after surgery, and 2 years later.

Measurement of Peripheral Blood $CD34^+$EPCs (Endothelial Progenitor Cells)

$CD34^+$EPCs are involved with the release of pro-angiogenic cytokines and associated with pathological angiogenesis (Calzi et al., 2010), and thus the counts of the cells in peripheral blood were measured. One-hundred-microliter peripheral blood was taken from a vein of each patient before and after immediate stent implantation, and 2-year follow-up. Two-microliter mouse anti-human PE-CD34 antibody was added to each tube, and incubated at 4°C overnight; the mixture was centrifuged at 1500 rpm/min at 4°C for 5 min, and the supernatant was discarded. The cells were resuspended in 2 ml PBS, and centrifuged at 2000 rpm/min for 5 min at 4°C, and the supernatant was discarded for 2 times; finally, the blood cells were resuspended in 100 μl of PBS. The cells were stored at 4°C and the number of EPCs was measured on a flow cytometer (Beckman Coulter, Brea, CA, United States).

Endothelial Cells Isolation

The physicians used real-time X-ray technology to visualize the patient's vascular system and locate IA inside the blood vessel. A solitaire stent retriever (Covidien, Irvine, CA, United States) was used for biopsy specimens' retrieval from an occluded IA. Cerebral aneurysm and malformed arteries were isolated from cerebral arties using a cutting plane and separating the surfaces on either side of the plane by using a minimally invasive technique. Endothelial cells were derived from human cerebral aneurysm and malformed arteries, and separated with immunomagnetic cell sorting. Briefly, Anti-CD 146-coated Dynabeads (Invitrogen, CA, United States) were prepared according to manufacturer's instruction and stored at 4°C. Fifty-mg aneurysms were ground with glass pestle and mortar with one-millilter PBS buffer, 0.1% bovine serum albumin, 0.1% sodium azide, and 0.1% a standard broad-spectrum inhibitor cocktail at 4°C. Ten-microliter FcR-blocking agent (Miltenyi, Bergisch Gladbach, Germany) and 25-microliter antibody-coated Dynabeads were added and mixed thoroughly. The samples were mixed in a mixer for 1 h at 4°C and washed four times with

PBS inside the Big Easy Magnet (EasySep, United States) at 4°C. Between each washing procedure, the endothelial cells were flushed out with MACS buffer (PBS with 0.5% BSA and 2 mM EDTA, pH 7.0) 10 times in a 100-μL pipette.

Microvessel Density (MVD) Assay

Angiogenesis is associated with MVD and can be evaluated by MVD (Zhang et al., 2018). For MVD assay, CD31 is considered to be a marker of MVD (Bösmüller et al., 2018; Xing et al., 2018). Isolated arteriovenous malformation and IA tissues were fixed in 10% formalin and embedded in paraffin blocks. Sections were deparaffinized in xylene and rehydrated in a series of different concentrations of ethanol. After deparaffinization, antigen-retrieval procedure and blocking of endogenous peroxidase, 5-μm sections were incubated for 20 min with CD31 antibody. Subsequently, the sample was incubated with HRP secondary antibody for 10 min, DAB for 15 min and stained with Mayer's hematoxylin for 5 min. MVD was measured by choosing five regions of each sample at 40× magnification.

Measurement of Mechanical Forces

The mechanical forces caused by different stent techniques could not be measured *in vivo* exactly. However, the mechanical forces mainly produced shear stress due to blood flow (Ohashi and Sato, 2005), while shear stress could be measured by combining with a computational method. Thus, the mechanical forces in cerebral vessels were analyzed by measuring shear

TABLE 1 | Clinical characteristics between two groups.

Characteristics		Stent-jailing (*n* = 85)	Stent-jack (*n* = 81)	χ^2 or *t*-value	*P*-value
Sex, male (%)		50 (58.82)	47 (58.02)	0.011	0.917
Age, years		58.8 ± 22.9	57.6 ± 21.4	0.481	0.258
Hypertension		10 (11.76)	11 (13.58)	0.124	0.725
Diabetes		11 (12.94)	13 (16.05)	0.324	0.569
Dyslipidemia		14 (16.47)	12 (14.81)	0.086	0.769
Coronary artery disease		9 (10.59)	11 (13.58)	0.350	0.554
Smoking		13 (15.29)	15 (18.52)	0.308	0.579
Drinking		12 (14.12)	10 (12.35)	0.113	0.736
Body mass index (kg/m^2)		17.5 – 29.3 (23.1 ± 2.7)	19.3 – 28.6 (21.8 ± 3.4)	0.353	0.060
Cr (mg/dL)		0.42 – 1.41 (0.80 ± 0.28)	0.46 – 1.35 (0.83 ± 0.21)	0.026	0.174
CCr (mL/min)		37.6 – 113.6 (61.4 ± 25.2)	36.3 – 110.6 (59.3 ± 23.4)	0.554	0.141
Aspirin		73 (85.88)	71 (87.65)	0.113	0.736
Clopidogrel		12 (14.12)	10 (12.35)		
Location	BTA	35 (41.18)	36 (44.44)	0.244	0.970
	VAA	18 (21.18)	17 (20.99)		
	PCAA	19 (22.35)	16 (19.75)		
	PICAA	13 (15.29)	12 (14.81)		
Unruptured/ruptured aneurysm		82/3	79/2	0.003	0.956
GOS score					
1		2 (2.35)	2 (2.47)	0.546	0.969
2		6 (7.06)	7 (8.64)		
3		17 (20)	15 (18.52)		
4		28 (32.94)	26 (32.1)		
5		27 (31.76)	31 (38.27)		
Aneurysm classification					
Fusiform	Simple	4 (4.71)	3 (3.7)	0.685	0.953
	Complex	1 (1.18)	1 (1.23)		
Saccular	No branch	35 (41.18)	34 (41.98)		
	Side Branch	25 (29.41)	23 (28.4)		
	Bifurcation	16 (18.82)	20 (24.69)		
Size	<15 mm	48 (56.47)	45 (55.56)	0.188	0.910
	15-25 mm	24 (28.24)	25 (30.86)		
	>25 mm	13 (15.29)	11 (13.58)		
Stent	Solitaire	63 (74.12)	60 (74.07)	0.001	0.999
	Enterprise	21 (24.71)	20 (24.69)		
	Neuroform	1 (1.18)	1 (1.23)		

BTA, basilar tip aneurysms; VAA, vertebral artery aneurysm; PCAA, posterior cerebral artery aneurysm; and PICAA, posterior inferior cerebellar artery aneurysm. GOS, Glasgow Outcome Scale. The statistical difference was significant if $P < 0.05$.

stress. A three-dimension (3D) reconstruction of the target aneurysm vessel was obtained by using an Intravascular Doppler ultrasound catheter (GE Healthcare, Fremont, CA, United States) and biplane cerebral angiogram before and after stent implantation to measure endothelial shear stress (ESS). The catheter was advanced into the cerebral artery and, before starting pull-back, and a biplane cerebral angiogram with contrast injection was performed. The images of the simultaneous electroencephalograph (EEG) signals were recorded. From the data, a computer algorithm was used to calculate the EES via three-dimensional intravascular ultrasound software (Life Imaging Systems, Inc., London, ONT, Canada). The reconstructed cerebral blood vessels were used for 3D geometry calculation and fluid dynamics remodeling. In this way, the values of ESS were measured before and after stent surgery. To avoid different stent length would produce different ESS (LaDisa et al., 2006), six territories proximal to the stent (within 10 mm) were measured.

Real-Time Quantitative Reverse Transcription-PCR (Real-Time qRT-PCR)

Total RNA was extracted from isolated endothelial cells by using total RNA Isolation Kit (TIANGEN, Beijing, China). The isolated RNA was digested by DNase I (TaKaRa, Dalian, China) according to the manufacturer's instructions. Two-microliter total RNA was used for reverse transcription to cDNA with the reverse transcription kit (Takara, Dalian, China). The primers for specific genes and β-actin were listed in **Table 2**. Real-time PCR was performed on LightCycler 2.0 instrument (Roche, Germany). qPCR was performed as follows, 95°C 2 min, and 45 cycles of 95°C for 20 s, 55°C for 15 s, and 72°C for 20 s. Relative gene expression was calculated as $2^{-\Delta\Delta Ct}$.

Western Blot

Frozen samples endothelial cells were lysed in RIPA buffer containing 1% (w/v) of protease/phosphatase inhibitor cocktail (Thermo Scientific, Madison, WT, United States). Protein concentration was measured by BCA detection kit (Beyotime, Beijing, China). The mixed proteins (100 μg) were separated by using SDS-PAGE and transferred to a PVDF membrane for 20 min. Antibodies were incubated overnight at 4°C. The membrane was blocked by using 5% non-fat milk in PBST buffer for 1 h. Secondary antibodies were further incubated and protein bands were visualized chemiluminescence (ECL) system (Bio-Rad, Richmond, CA, United States).

TABLE 2 | The primers used in the present study.

Genes	Primers	Sequences (5′–3′)	Size (bp)
TGF-β	Forward	CAGGGCTTCTCCTACCCCTA	160
	Reverse	GATGGTGGTAGCGTGGGTGG	
Smad2	Forward	CCCCGACACACCGAGATCCT	130
	Reverse	CTGATATATCCAGGAGGTGG	
Smad3	Forward	CCACGCCACACAGAGATCCC	200
	Reverse	AGGTTTGGAGAACCTGCGTC	
Smad4	Forward	ACCATCCAGCATCCACCAAG	200
	Reverse	CCTGGCTGAGGCCCTGATGC	
Actin	Forward	GACATGGAGAAAATCTGGCA	130
	Reverse	AAGGTCTCAAACATGATCTG	

Tube Formation Analysis

HUVECs were purchased from Shanghai Institutes for Biological Sciences (Cat. No. ECV304) were cultured in RPMI-1640 medium (Gibco Life Technologies, Shanghai, China) supplemented with 10% fetal calf serum at a density of 4×10^3 cells in 96 wells overnight. The cells were treated with 2 μM TGF-β inhibitor (SB505124) (Selleckchem Co., Shanghai, China), or 10 ng/mL TGF-β [Sigma-Aldrich (Shanghai) Trading Co., Ltd., Shanghai, China], the sample supernatants from stent-jailing and stent jack groups for 48 h. A 96-well plate was coated with Matrigel (BD Biosciences) and was cultured at 37°C for half an hour to let Matrigel solidify. HUVECs were plated onto the plate coated by Matrigel. After 20-h culture, the HUVECs were recorded using Olympus IX71 Inverted Compound Microscope (Tokyo, Japan).

Statistical Analysis

The statistical analysis was carried out by using SPSS 20.0. The possible factors associated with IA risks and postoperative symptoms were analyzed by using univariate and multi-factor analysis. The relationship between the levels of MVD values and ESS values was analyzed using Spearman's correlation coefficient test.

TABLE 3 | The effects of coil embolism techniques on aneurysm occlusion grades.

Occlusion grades	Stent-Jailing technique	Stent-Jack technique	χ^2 values	*P*-values
Before aneurysm coil embolization			0.626	0.429
Complete	65 (76.47)	66 (81.48)		
Sub-complete	20 (23.53)	15 (18.52)		
Partially	0 (0)	0 (0)		
No	0 (0)	0 (0)		
After aneurysm coil embolism, cases (%)			0.263	0.967
Complete	2 (2.35)	3 (3.7)		
Sub-complete	12 (14.12)	11 (13.58)		
Partially	18 (21.18)	17 (20.99)		
No	53 (62.35)	50 (61.73)		
2-year follow up			14.865	0.002
Complete	2 (2.35)	8 (9.88)		
Sub-complete	9 (10.59)	21 (25.93)		
Partially	22 (25.88)	23 (28.4)		
No	52 (61.18)	29 (35.8)		

Complete occlusion, no contrast agents in the aneurysm; sub-complete occlusion, partial contrast agents in aneurysmal dome; partial occlusion, contrast agents filling in the aneurysm dome; and no occlusion, contrast agents is full of in the aneurysm dome.

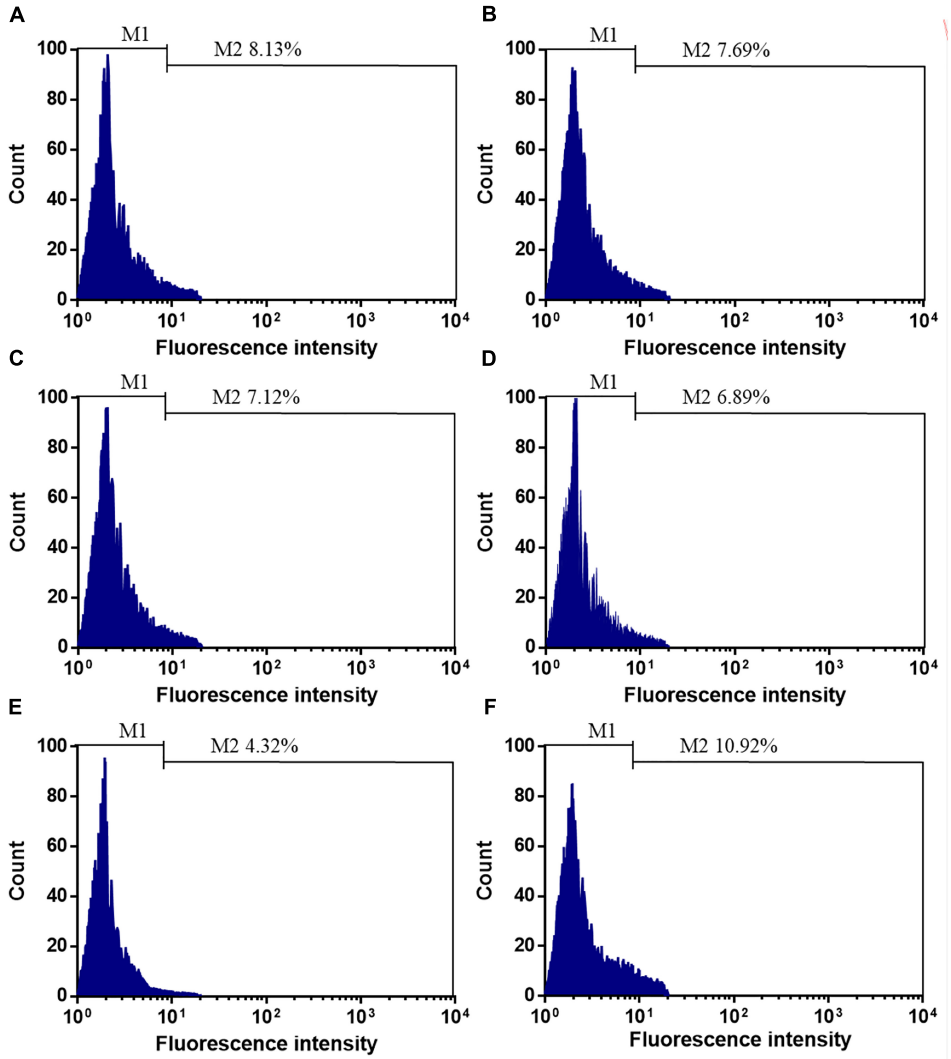

FIGURE 1 | The effects of different stent techniques on the counts of CD34$^+$EPCs. **(A)** The effects of stent-jailing techniques on the counts of CD34$^+$EPCs before SCE surgery. **(B)** The effects of stent-jack techniques on the counts of CD34$^+$EPCs before SCE surgery. **(C)** The effects of stent-jailing techniques on the counts of CD34$^+$EPCs after immediate SCE surgery. **(D)** The effects of stent-jack techniques on the counts of CD34$^+$EPCs after immediate SCE surgery. **(E)** The effects of stent-jailing techniques on the counts of CD34$^+$EPCs after a 2-year follow-up period. **(F)** The effects of stent-jack techniques on the counts of CD34$^+$EPCs after a 2-year follow-up period. G, the average percentage of CD34$^+$ cells between two groups.

RESULTS

Clinical Characteristics

From April 1st, 2016 to March 1st, 2017, 181 IA patients received SCE therapy, including 97 males and 69 females, aged 35.9–81.7 years. Complete coil embolization was 65 cases (76.47%) and 66 cases (81.48%) in stent-jailing and -jack groups, respectively. After a 2-year follow-up period, 6 and 4 patients withdrew from two groups, respectively. Two and 3 patients were died from two groups because of aneurysmal subarachnoid hemorrhage (SAH), respectively. Thus, 85 and 81 patients completed the study, respectively. The statistical differences for all parameters were insignificant between the two groups (**Table 1**, $P > 0.05$).

Primary Outcome

Stent-jailing and stent-jack surgery techniques were employed in IA therapy. Coils successfully covered the aneurysms after SCE surgery and the coils were stable even after a 2-year follow-up period. There were 3 and 5 cases of cerebrovascular vasospasm in stent-jailing group and stent-jack group, respectively. Papaverine (100–115 mg/day) or nimodipine (20–30 mg/day) was administrated to prevent the development of vasospasm. There were 4 and 2 cases of cerebral vascular occlusion in the two groups, respectively. Balloon was deployed to dilate blood vessels. There were 2 cases of embolism coil pop-up in stent-jack group and no case of embolism coil pop-up in stent-jailing group.

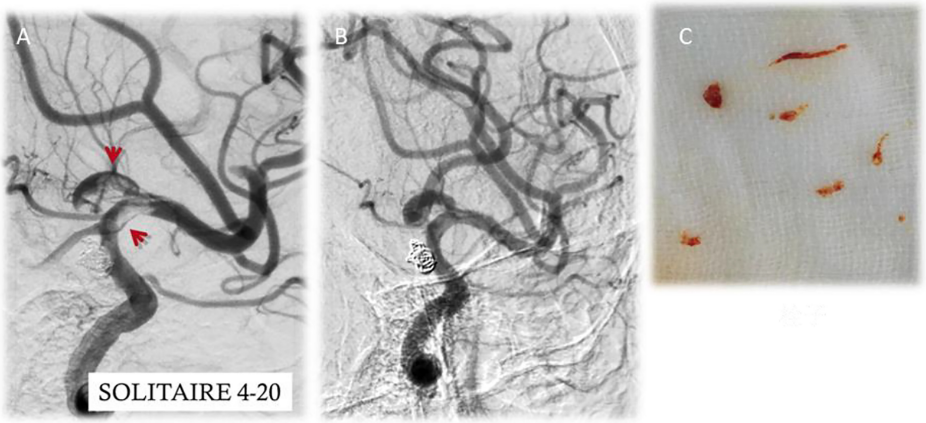

FIGURE 2 | Aneurysm tissues retrieval by a solitaire stent retriever in minimally invasive procedure. **(A)** First-time retrieval of IA biopsy specimens. **(B)** Second-time retrieval of IA biopsy specimens. **(C)** IA biopsy specimens. Red arrow showed the aneurysm.

Stent-Jailing Reduced the Incidences of Aneurysm Occlusion Grades More Than Stent-Jack

Aneurysm occlusion grades reflect the severity of ischemic stroke (Qureshi, 2002). The statistical differences for aneurysm occlusion grade were insignificant between two groups before the SCE surgery (**Table 3**, $P > 0.05$). In contrast, the statistical differences for aneurysm occlusion grade were still insignificant between two groups after immediate SCE surgery (**Table 3**, $P > 0.05$) but significant after 2-year follow-up (**Table 3**, $P < 0.05$). The results suggested that stent-jailing was more effective than stent-jack in the prevention of aneurysm occlusion.

The Effects of Different Stent Techniques on the Counts of $CD34^+$EPCs

Before SCE surgery and after immediate SCE surgery, the statistical difference for the counts of $CD34^+$EPCs was insignificant between stent-jailing and stent-jack groups (**Figures 1A–D**, $P > 0.05$). After 2-year follow-up, the counts of $CD34^+$EPCs in the stent-jailing group were lower than in the stent-jack group (**Figures 1E,F**, $P < 0.05$). The results suggest that stent-jack increases the counts of $CD34^+$EPCs, which may increase the incidence of angiogenesis.

Stent-Jack Increased More MVD Than Stent-Jailing

After first-time retrieval of IA biopsy specimens (**Figure 2A**) and second-time retrieval of IA biopsy specimens (**Figure 2B**), IA biopsy specimens were retrieved well (**Figure 2C**). Before SCE surgery and after immediate SCE surgery, the statistical difference for MVD levels was insignificant between stent-jailing and stent-jack groups ($P > 0.05$, **Figures 3A,B**). Mean MVD values were 107.58 ± 35.23 vessels/mm^2. After 2-year follow-up, MVD values in the stent-jailing group were lower than in the stent-jack group ($P < 0.05$, **Figure 3C**). Mean MVD values were 100.21 ± 37.45 vessels/mm^2 in stent-jailing group and 136.72 ± 41.98 vessels/mm^2 in stent-jack group.

Stent-Jack Increased ESS Values More Than Stent-Jailing

In total, 25 IA patients were analyzed from stent-jailing and stent-jack groups, respectively. The statistical difference for ESS was insignificant before stent implantation ($P > 0.05$, **Figure 4A**). The surgery caused a significant ESS increase in the entire aneurysm lesion after immediate surgery, and the ESS values in stent-jailing group were lower than in stent-jack group ($P < 0.05$, **Figure 4B**). Similarly, the ESS values in stent-jailing group were still lower than in stent-jack group after 2-year follow-up ($P < 0.05$, **Figure 4C**).

MVD Values Had a Positive Association With ESS Values

Pearson correlation coefficient analysis showed that ESS values were increased with the increase of MVD values. MVD values had a strong positive association with ESS values since Rho values were more than 0.5 ($P < 0.05$, **Figure 5**). The results suggested that ESS enhancement increased MVD values, which stand for angiogenic degree (Ames et al., 2016).

Relative mRNA Levels

Before SCE surgery and after immediate SCE surgery, the statistical difference for relative mRNA levels of TGF-β, Smad2, Smad3, and Smad4 was insignificant between stent-jailing and stent-jack groups ($P > 0.05$, **Figures 6A,B**). After 2-year follow-up, relative mRNA levels of TGF-β, Smad2, Smad3, and Smad4 were still comparable between stent-jailing and stent-jack groups ($P > 0.05$, **Figure 6C**). The results suggested that different stent techniques would not change relative mRNA levels of TGF-β, Smad2, Smad3, and Smad4.

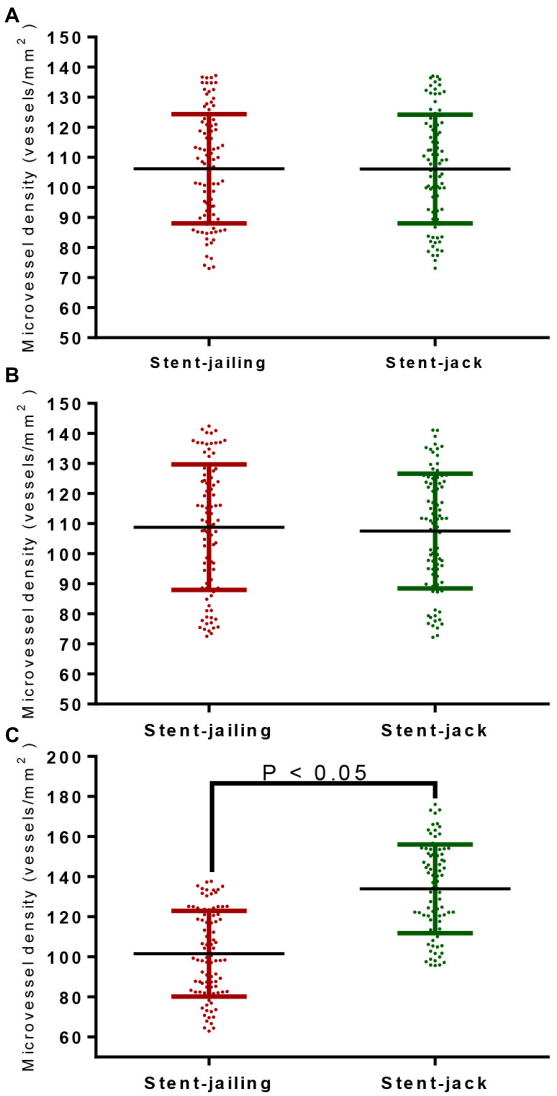

FIGURE 3 | The effects of different stent techniques on microvessel density (MVD) values. **(A)** The effects of different stent techniques on MVD values before SCE surgery. **(B)** The effects of different stent techniques on MVD values after immediate SCE surgery. **(C)** The effects of different stent techniques on MVD values after 2-year follow-up.

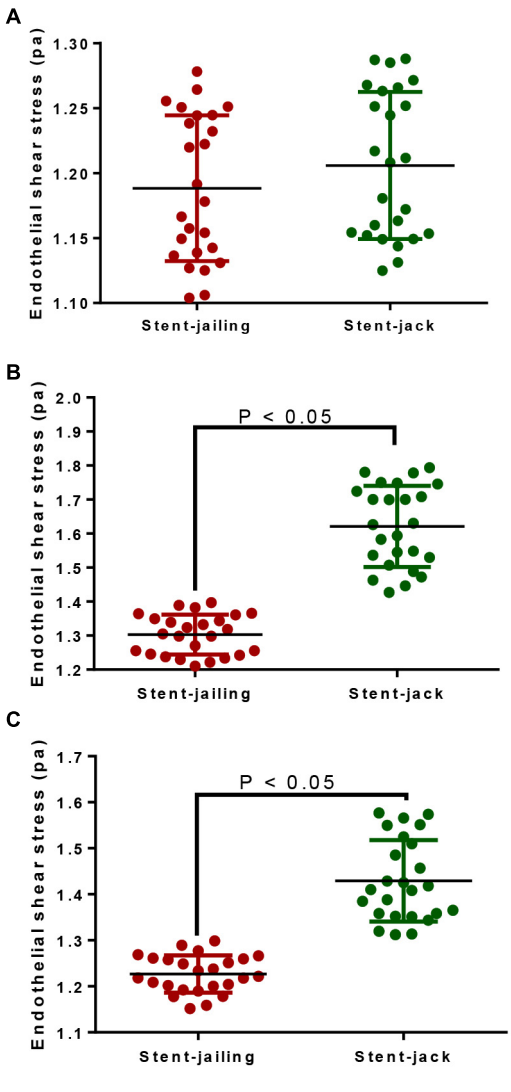

FIGURE 4 | Endothelial shear stress (ESS) values before and after stent implantation within 10-mm segments proximal to the stents. **(A)** ESS values before stent implantation within 10-mm segments proximal to the stents. **(B)** ESS values after immediate stent implantation within 10-mm segments proximal to the stents. **(C)** ESS values after 2-year stent implantation within 10-mm segments proximal to the stents.

Stent-Jack Promoted TGF−β− Promot Phosphorylation of Smad2 and Smad3

Relative protein levels of TGF-β, phospho-TGF-β, Smad2, phospho-Smad2, Smad3, phospho-Smad3 and Smad4 were analyzed by using Western Blot (**Figure 7A**). Before SCE surgery and after immediate SCE surgery, the statistical difference for relative protein levels of TGF-β (**Figure 7B**), phospho-TGF-β (**Figure 7C**), Smad2 (**Figure 7D**), phospho-Smad2 (**Figure 7E**), Smad3 (**Figure 7F**), phospho-Smad3 (**Figure 7G**), Smad4 (**Figure 7H**), and Phospho-Smad4 (**Figure 7I**) were insignificant between stent-jailing and stent-jack groups ($P > 0.05$). After 2-year follow-up, relative protein levels of TGF-β, Smad2, Smad3, and Smad4 were still comparable between stent-jailing and stent-jack groups ($P > 0.05$, **Figures 7B,D,F,H,I**). However, relative protein levels of phospho-TGF-β (**Figure 7C**), phospho-Smad2 (**Figure 7E**) and phospho-Smad3 (**Figure 7G**) in the stent-jailing group were lower than in the stent-jack group ($P < 0.05$).The results suggested that stent-jack promoted phosphorylated TGF−β−sphoryl phosphorylation of Smad2 and Smad3 when compared with stent-jailing technique.

Stent-Jailing Potently Reduced More Angiogenesis Than Stent-Jack

Transforming growth factor-β increased cellular proliferation and promoted angiogenesis when compared with controls (**Figures 8A,B,F**) ($P < 0.05$). In contrast, SB505124 potently

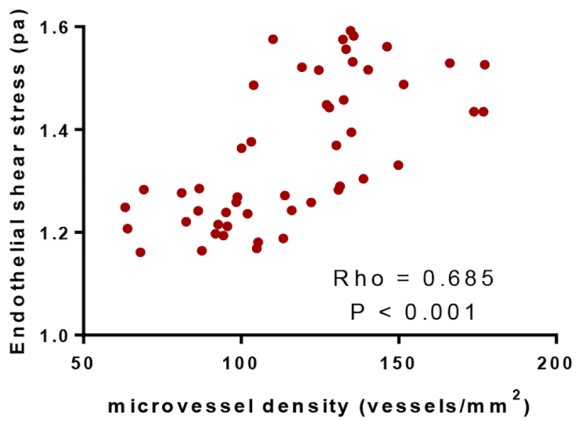

FIGURE 5 | Pearson correlation coefficient analysis of the relationship between the values of microvessel density and endothelial shear stress. There was positive correlation between the two variables if rho values were within 0.5 and 1.

inhibited the proliferation and tube formation of HUVECs (**Figures 8C,F**) ($P < 0.05$). Comparatively, stent-jailing potently reduced more angiogenesis than stent-jack (**Figures 8D–F**) ($P < 0.05$). The results proved that stent-jailing and stent-jack may cause different angiogenesis by affecting TGF-β.

DISCUSSION

Stent-assisted coil embolism is an important strategy in the therapy of IAs. Compared with craniotomy, endovascular embolization has the advantages of less trauma, fewer complications, lower mortality and short procedure time (Cohen et al., 2013). Although endovascular interventional therapy has been shown to be effective, the use of coil embolization alone remains a significant challenge for IA. With the development of techniques, stents have been used to assist coil embolization in the treatment of IAs, particularly wide-neck aneurysms (Feng et al., 2017).

There were 85 aneurysms treated by stent-jailing technology and 81 aneurysm treated by stent-jack in the present work. When stent-assisted embolism is carried out, the choice between the two methods will depend on the expert's experiences. Stent-jailing method has more advantages than stent-jack. Firstly, catheter placement into aneurysm dome is more difficult after the deployment of stent, especially for closed and small stents. Secondly, like a balloon, the deployed stent will avoid the kickback of the jailing catheter during coil embolism. Thirdly, the occurrence of coil herniation into the parent artery is low. Finally, unintended untangling of coils around the stent-jack can be avoided in stent-jailing technique. The main shortage of stent-jailing technique is that the catheter tip is forced out from aneurysm dome during stent deployment. More coil loops can be deployed to solve the drawback.

Stent-jack can be considered when it is difficult in the application of stent-jailing technique because the stent-jailing technique cannot be adjusted to a satisfactory location. Due to

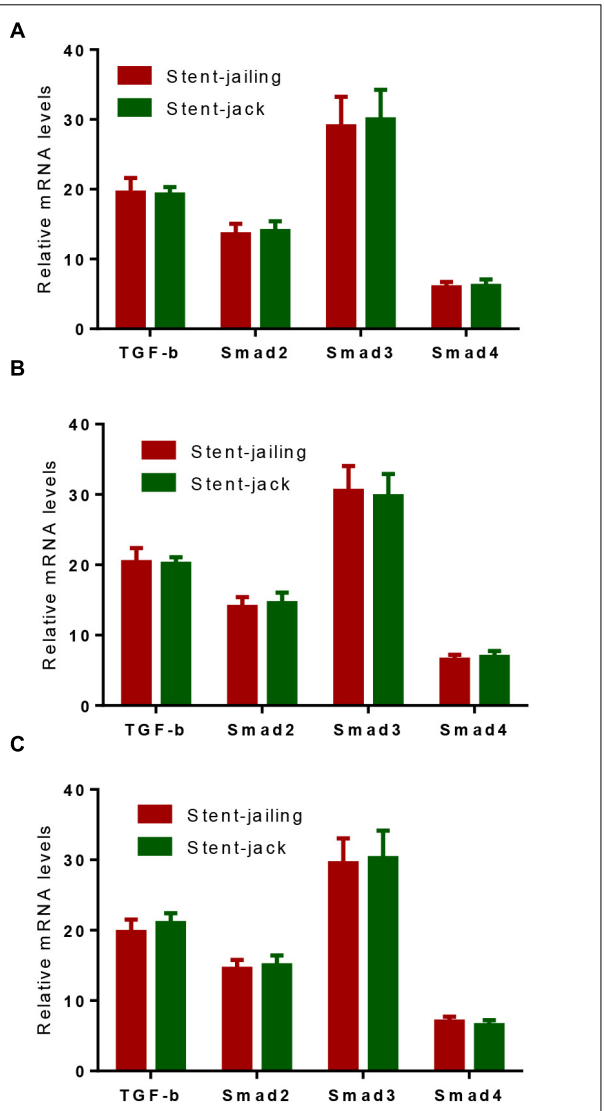

FIGURE 6 | Real-time qPCR analysis of the effects of different stent techniques on relative mRNA levels of TGF-β, Smad2, Smad3 and Smad4. **(A)** The effects of different stent techniques on relative mRNA levels of TGF-β, Smad2, Smad3, and Smad4 before SCE surgery. **(B)** The effects of different stent techniques on relative mRNA levels of TGF-β, Smad2, Smad3, and Smad4 after immediate SCE surgery. **(C)** The effects of different stent techniques on relative mRNA levels of TGF-β, Smad2, Smad3, and Smad4 after a 2-year follow-up period.

the small opening of aneurysms have been small, scaffold can enter the aneurysm dome via stent-jack. One main drawback for stent-jack is that the detached coil loops may herniate or move, and hang on stent when the stent retrieved.

Peripheral blood $CD34^+$ progenitor cells can be stimulated by many cytokines (Brugger et al., 1993). Surgery has been reported to induce the increase in EPC values (Scheubel et al., 2004). We proposed that stent-jack surgery might induce cytokines more than stent-jailing, resulting in high-level of EPCs. $CD34^+$EPCs did not increase much after stenting in IA patients between two groups (**Figures 1C,D**). After 2-year follow-up, the EPC values

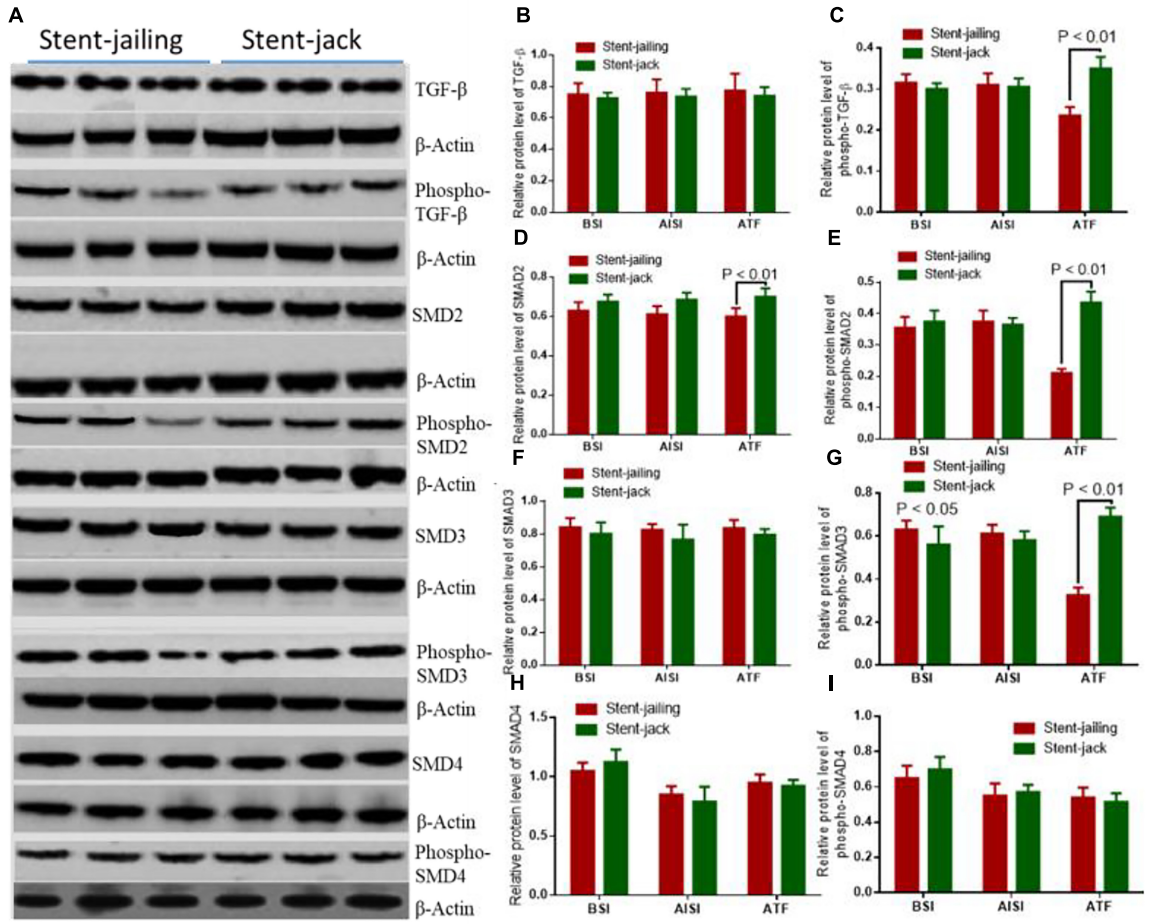

FIGURE 7 | Stent-Jack promoted TGF–β–nt-Jack promoted Smad4 after immediate SCEs. **(A)** The effects of different stent techniques on relative protein levels of TGF-GF-phospho-TGF-β, Smad2, phospho-Smad2, Smad3, phospho-Smad3, and Smad4 before SCE surgery. **(B)** Relative protein levels of TGF-β. **(C)** Relative protein levels of phospho-TGF-β. **(D)** Relative protein levels of Smad2. **(E)** Relative protein levels of phospho-Smad2. **(F)** Relative protein levels of Smad3. **(G)** Relative protein levels of phospho-Smad3. **(H)** Relative protein levels of Smad4. **(I)** Relative protein levels of phosphor-Smad4.BSI, before surgery intervention; AISI, immediately after surgery intervention; ATF, after a 2-year follow-up period. The statistical difference was significant if $^*P < 0.05$ and very significant if $^*P < 0.01$.

were increased significantly in stent-jack group (**Figure 1F**) when compared with other groups, whereas the values was reduced significantly in stent-jailing group (**Figure 1E**), suggesting other mechanism may be existed for the changes of EPC values. Peripheral blood EPCs can secrete many cytokines associated with angiogenic activities, such as vascular endothelial growth factor (Demetz et al., 2017), hepatocyte growth factor (Iwabayashi et al., 2012) and fibroblast growth factor (Huang et al., 2015).

We showed that stent-jailing rather than stent-jack reduced angiogenesis partly via reducing mechanical forces in cerebral blood vessels or the TGF-β/Smad2,3,4 pathway. The mechanical forces may stimulate endothelial-cell-inducing angiogenesis (Yang et al., 2018). Stent-jack increased ESS values more than stent-jailing technique ($P < 0.05$, **Figure 4**), suggesting stent-jack caused mechanical forces more than stent-jailing. The results led to the risk of angiogenesis in stent-jack group higher than in stent-jailing group (**Figure 9**). Phosphorylation of Smad has been widely reported to be associated with the activity of Smad signaling pathway (Seong et al., 2010; Hough et al., 2012). Stent-jailing techniques reduced the phosphorylation of TGF-β, Smad2 and Smad3, and resulted in the reduction of activity of TGF-β/Smad2,3,4 pathway (**Figure 9**). The decrease in the activity of TGF-β/Smad2,3,4 pathway would inhibit the angiogenesis of the patients (**Figure 9**) (Pen et al., 2008; Ji et al., 2014; Assis et al., 2015).

There were some limitations of the present work. The interaction of stents with the cerebral endothelial cells in a controlled environment has been widely reported (Sprague et al., 2017; Tefft et al., 2017; Ter Meer et al., 2017). The stent provides the potential attachment and promote the growth of endothelial cells. However, we could not directly detect the associate between the mechanical forces and angiogenesis or the activation of the TGF-β/Smad2,3,4 pathway because the measurement of the mechanical forces applied by each technique is still not feasible *in vivo*. Some long-term complications existed

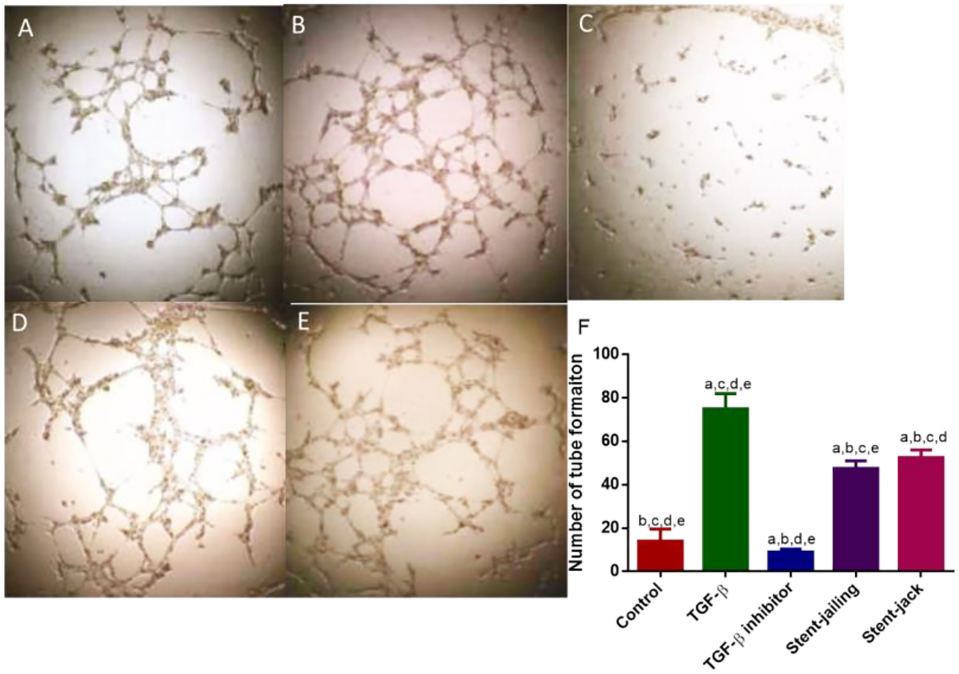

FIGURE 8 | Tube formation of HUVECs among different groups. **(A)** Control group. **(B)** The effect of TGF-β on tube formation in HUVECs. **(C)** The effect of TGF-β inhibitor on tube formation in HUVECs. **(D)** The effect of the supernatants from stent-jailing group on tube formation in HUVECs. **(E)** The effect of the supernatants from stent-jack group on tube formation in HUVECs. **(F)** The average number of tube formation among different groups. $^{a}P < 0.05$ vs. a control group, $^{b}P < 0.05$ vs. a TGF-β group, $^{c}P < 0.05$ vs. a TGF-β inhibitor group, $^{d}P < 0.05$ vs. a stent-jailing group, and $^{e}P < 0.05$ vs. a stent-jack group.

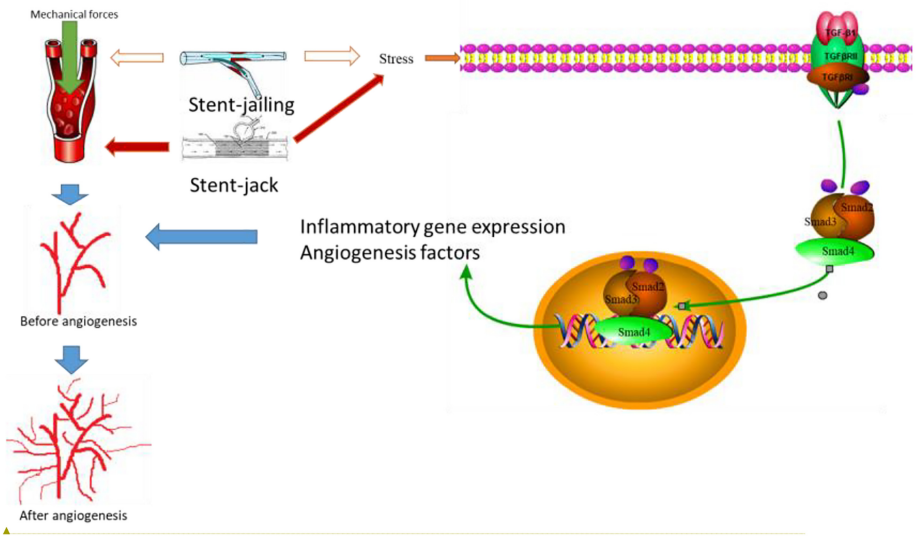

FIGURE 9 | The effects of different stent techniques on angiogenesis. Stent techniques affect angiogenesis via two main ways: different stents will produce different mechanical forces in blood vessel and result in the risk of angiogenesis; different stents will affect TGF-β/Smad2,3,4 signaling pathway differently. Smad2 and Smad3 forms complexes after interacting with TGF–βsignaling pathway diff, which is phosphorylated by T Smad2 and SmaHeteromeric complexes of Smads 2, 3 and 4 can translocated to the nucleus together, resulting in inflammatory gene expression and production of angiogenesis. Red arrows showed an increase in the activity and blank arrows shows no function in the activity.

for the patients that undergo aneurysm treatment. First, in-stent thrombosis may be a source of complications because of the angiogenesis caused by mechanical forces. Second, mechanical forces could be technically problematic and induced a further risk of complications. Thus, in-stent thrombosis may be higher. In the present study, aneurysm neck was mainly covered by stents.

Although angiogenesis is associated with aneurysm formation (Baumann et al., 2013), angiogenesis may exert good effect to promote endothelialization of the stent to cover the neck of the aneurysm in case of stent-jacket technique and angiogenesis may be required. Cons and pros of angiogenesis were not compared in the present work. Thus, further work is highly required to address these important issues.

CONCLUSION

Stent-jailing technique reduced aneurysm occlusion grades more than stent-jack technique after 2-year follow-up by controlling angiogenesis in IA patients. Stent-jailing technique was more effective than stent-jack technique in the treatment of IA patients by reducing mechanical forces and activity of TGF-β/Smad2,3,4 signaling pathway. To confirm the present conclusion, further work in highly demanded in a larger population in the future.

AUTHOR CONTRIBUTIONS

NX, HM, and TL performed the experiments, enrolled patients, and analyzed the related data. YF and YQ measured MVD and ESS values. DZ and HW contributed to design the techniques. NX, HM, TL, YF, YQ, and DZ performed the surgery. DZ and HW conceived the experimental plan and wrote the manuscript.

REFERENCES

Ames, J. J., Henderson, T., Liaw, L., and Brooks, P. C. (2016). Methods for analyzing tumor angiogenesis in the chick chorioallantoic membrane model. *Methods Mol. Biol.* 1406, 255–269.

Assis, P. A., De, Figueiredo-Pontes LL, Lima, A. S., Leão, V., Cândido, L. A., Pintão, C. T., et al. (2015). Halofuginone inhibits phosphorylation of SMAD-2 reducing angiogenesis and leukemia burden in an acute promyelocytic leukemia mouse model. *J. Exp. Clin. Cancer Res.* 34, 65–75. doi: 10.1186/s13046-015-0181-2

Bakhsheshian, J., Walcott, B. P., and Mack, W. J. (2018). Orthogonal catheter access for stent assisted coiling of posterior cerebral artery aneurysm. *Oper. Neurosurg.* 14:85.

Baumann, A., Devaux, Y., Audibert, G., Zhang, L., Bracard, S., Colnat-Coulbois, S., et al. (2013). Gene expression profile of blood cells for the prediction of delayed cerebral ischemia after intracranial aneurysm rupture: a pilot study in humans. *Cerebrovasc. Dis.* 36, 236–242. doi: 10.1159/000354161

Bösmüller, H., Pfefferle, V., Bittar, Z., Scheble, V., Horger, M., Sipos, B., et al. (2018). Microvessel density and angiogenesis in primary hepatic malignancies: differential expression of CD31 and VEGFR-2 in hepatocellular carcinoma and intrahepatic cholangiocarcinoma. *Pathol. Res. Pract.* 214, 1136–1141. doi: 10.1016/j.prp.2018.06.011

Brugger, W., Mocklin, W., Heimfeld, S., Berenson, R. J., Mertelsmann, R., and Kanz, L. (1993). Ex vivo expansion of enriched peripheral blood CD34+ progenitor cells by stem cell factor, interleukin-1 beta (IL-1 beta), IL-6, IL-3, interferon-gamma, and erythropoietin. *Blood* 81, 2579–2584.

Calzi, S. L., Neu, M. B., Shaw, L. C., Kielczewski, J. L., Moldovan, N. I., and Grant, M. B. (2010). EPCs and pathological angiogenesis: when good cells go bad. *Microvasc. Res.* 79, 207–216. doi: 10.1016/j.mvr.2010.02.011

Cohen, J. E., Moscovici, S., and Itshayek, E. (2013). The advantages of balloon assistance in endovascular embolization of spinal dural arteriovenous fistulas. *J. Clin. Neurosci.* 20, 141–143. doi: 10.1016/j.jocn.2012.09.004

de Paula Lucas, C., Piotin, M., Spelle, L., and Moret, J. (2008). Stent-jack technique in stent-assisted coiling of wide-neck aneurysms. *Neurosurgery* 62, ONS414–ONS416; discussion ONS416–ONS417. doi: 10.1227/01.neu.0000326028.47090.5f

Demetz, G., Oostendorp, R. A. J., Boxberg, A. M., Sitz, W., Farrell, E., Steppich, B., et al. (2017). Overexpression of insulin-like growth factor-2 in expanded endothelial progenitor cells improves left ventricular function in experimental myocardial infarction. *J. Vasc. Res.* 54, 321–328. doi: 10.1159/000479872

Feng, Z., Zuo, Q., Yang, P., Li, Q., Zhao, R., Hong, B., et al. (2017). Staged stenting with or without additional coils after conventional initial coiling of acute ruptured wide-neck intracranial aneurysms. *World Neurosurg.* 108, 506–512. doi: 10.1016/j.wneu.2017.09.040

Gotoh, O., Tamura, A., Oka, H., Tsujita, Y., Sano, K., Yasui, N., et al. (1993). Acute aneurysm surgery and the glasgow coma scale: relationship with 6-month outcome. *No Shinkei Geka* 21, 37–43.

Hoh, B. L., Hosaka, K., Downes, D. P., Nowicki, K. W., Wilmer, E. N., Velat, G. J., et al. (2014). Stromal cell-derived factor-1 promoted angiogenesis and inflammatory cell infiltration in aneurysm walls. *J. Neurosurg.* 120, 73–86. doi: 10.3171/2013.9.JNS122074

Hough, C., Radu, M., and Dore, J. J. (2012). Tgf-beta induced Erk phosphorylation of smad linker region regulates smad signaling. *PLoS One* 7:e42513. doi: 10.1371/journal.pone.0042513

Huang, L., Wang, F., Wang, Y., Cao, Q., Sang, T., Liu, F., et al. (2015). Acidic fibroblast growth factor promotes endothelial progenitor cells function via Akt/FOXO3a pathway. *PLoS One* 10:e0129665. doi: 10.1371/journal.pone.0129665

Huang, Y., Li, G., Wang, K., Mu, Z., Xie, Q., Qu, H., et al. (2018). Collagen type VI Alpha 3 chain promotes epithelial-mesenchymal transition in bladder cancer cells via transforming growth factor beta (TGF-beta)/Smad pathway. *Med. Sci. Monit.* 24, 5346–5354. doi: 10.12659/MSM.909811

Itoh, F., Itoh, S., Adachi, T., Ichikawa, K., Matsumura, Y., Takagi, T., et al. (2012). Smad2/Smad3 in endothelium is indispensable for vascular stability via S1PR1 and N-cadherin expressions. *Blood* 119, 5320–5328. doi: 10.1182/blood-2011-12-395772

Iwabayashi, M., Taniyama, Y., Sanada, F., Azuma, J., Iekushi, K., Okayama, K., et al. (2012). Inhibition of Lp(a)-induced functional impairment of endothelial cells and endothelial progenitor cells by hepatocyte growth factor. *Biochem. Biophys. Res. Commun.* 423, 79–84. doi: 10.1016/j.bbrc.2012.05.086

Ji, H., Li, Y., Jiang, F., Wang, X., Zhang, J., Shen, J., et al. (2014). Inhibition of transforming growth factor beta/SMAD signal by MiR-155 is involved in arsenic trioxide-induced anti-angiogenesis in prostate cancer. *Cancer Sci.* 105, 1541–1549. doi: 10.1111/cas.12548

Jin, Y. K., Li, X. H., Wang, W., Liu, J., Zhang, W., Fang, Y. S., et al. (2018). Follistatin-like 1 promotes bleomycin-induced pulmonary fibrosis through the transforming growth factor beta 1/mitogen-activated protein kinase signaling pathway. *Chin. Med. J.* 131, 1917–1925. doi: 10.4103/0366-6999.238151

Kretschmer, A., Moepert, K., Dames, S., Sternberger, M., Kaufmann, J., and Klippel, A. (2003). Differential regulation of TGF-beta signaling through Smad2. Smad3 and Smad4. *Oncogene* 22, 6748–6763.

LaDisa, J. F. Jr., Olson, L. E., Douglas, H. A., Warltier, D. C., Kersten, J. R., and Pagel, P. S. (2006). Alterations in regional vascular geometry produced by theoretical stent implantation influence distributions of wall shear stress: analysis of a curved coronary artery using 3D computational fluid dynamics modeling. *Biomed. Eng. Online* 5, 40–50.

Li, G. C., Zhang, H. W., Zhao, Q. C., Sun, L. I., Yang, J. J., Hong, L., et al. (2016). Mesenchymal stem cells promote tumor angiogenesis via the action of transforming growth factor beta1. *Oncol. Lett.* 11, 1089–1094.

Lozen, A., Manjila, S., Rhiew, R., and Fessler, R. (2009). Y-stent-assisted coil embolization for the management of unruptured cerebral aneurysms: report of six cases. *Acta Neurochir.* 151, 1663–1672. doi: 10.1007/s00701-009-0436-9

Maeda, T., Sakabe, T., Sunaga, A., Sakai, K., Rivera, A. L., Keene, D. R., et al. (2011). Conversion of mechanical force into TGF-β-mediated biochemical signals. *Curr. Biol.* 21, 933–941. doi: 10.1016/j.cub.2011.04.007

Ohashi, T., and Sato, M. (2005). Remodeling of vascular endothelial cells exposed to fluid shear stress: experimental and numerical approach. *Fluid Dyn. Res.* 37, 40–59.

Pen, A., Moreno, M. J., Durocher, Y., Deb-Rinker, P., and Stanimirovic, D. B. (2008). Glioblastoma-secreted factors induce IGFBP7 and angiogenesis by modulating Smad-2-dependent TGF-beta signaling. *Oncogene* 27, 6834–6844. doi: 10.1038/onc.2008.287

Piotin, M., Biondi, A., Sourour, N., Mounayer, C., Jaworski, M., Mangiafico, S., et al. (2018). The LUNA aneurysm embolization system for intracranial aneurysm treatment: short-term, mid-term and long-term clinical and angiographic results. *J. Neurointerv. Surg.* 10:e34. doi: 10.1136/neurintsurg-2018-013767

Qureshi, A. I. (2002). New grading system for angiographic evaluation of arterial occlusions and recanalization response to intra-arterial thrombolysis in acute ischemic stroke. *Neurosurgery* 50, 1405–1414; discussion14–1415.

Rong-Bo, Q., Hua, J., Kai, W., and Ze-Lin, S. (2013). Stent-Jail technique in endovascular treatment of wide-necked aneurysm. *Turk Neurosurg.* 23, 179–182. doi: 10.5137/1019-5149.JTN.6274-12.1

Rostam, M. A., Shajimoon, A., Kamato, D., Mitra, P., Piva, T. J., Getachew, R., et al. (2018). Flavopiridol inhibits TGF-beta-stimulated biglycan synthesis by blocking linker region phosphorylation and nuclear translocation of Smad2. *J. Pharmacol. Exp. Ther.* 365, 156–164. doi: 10.1124/jpet.117.244483

Scheubel, R., Zorn, H., Silber, R., Kuss, O., Morawietz, H., Holtz, J., et al. (2004). Age-dependent depression in circulating endothelial progenitor cells in patients under coronary artery bypass grafting. *Thorac. Cardiovasc. Surg.* 52, 2073–2080.

Seong, H. A., Jung, H., and Ha, H. (2010). Murine protein serine/threonine kinase 38 stimulates TGF-beta signaling in a kinase-dependent manner via direct phosphorylation of Smad proteins. *J. Biol. Chem.* 285, 30959–30970. doi: 10.1074/jbc.M110.138370

Sprague, E., Luo, J., and Palmaz, J. C. (2017). Static and flow conditions: endothelial cell migration onto metal stent surfaces. *J. Long Term Eff. Med. Implants* 27, 97–110. doi: 10.1615/JLongTermEffMedImplants.v27.i2-4.10

Takahashi, Y., Endo, H., Endo, T., Fujimura, M., Niizuma, K., and Tominaga, T. (2018). Patient with recurrent anterior cerebral artery dissecting aneurysm after stent-assisted coil embolization successfully treated with A3-A3 anastomosis. *World Neurosurg.* 109, 77–81. doi: 10.1016/j.wneu.2017.09.128

Takeshita, T., Nagamine, T., Ishihara, K., and Kaku, Y. (2017). Stent-assisted coil embolization of a recurrent posterior cerebral artery aneurysm following surgical clipping. *Neuroradiol. J.* 30, 99–103. doi: 10.1177/1971400916678243

Tefft, B. J., Uthamaraj, S., Harburn, J. J., Hlinomaz, O., Lerman, A., Dragomir-Daescu, D., et al. (2017). Magnetizable stent-grafts enable endothelial cell capture. *J. Magn. Magn. Mater.* 427, 100–104. doi: 10.1016/j.jmmm.2016.11.007

Ter Meer M, Daamen, W. F., Hoogeveen, Y. L., van, Son GJF, Schaffer, J. E., van, der Vliet JA, et al. (2017). Continuously grooved stent struts for enhanced endothelial cell seeding. *Cardiovasc. Intervent. Radiol.* 40, 1237–1245. doi: 10.1007/s00270-017-1659-4

Tsai, M. S., Chiang, M. T., Tsai, D. L., Yang, C. W., Hou, H. S., Li, Y. R., et al. (2018). Galectin-1 restricts vascular smooth muscle cell motility via modulating adhesion force and focal adhesion dynamics. *Sci. Rep.* 8, 11497–11510. doi: 10.1038/s41598-018-29843-3

Tsao, J. W., Hemphill, J. C. III, Johnston, S. C., Smith, W. S., and Bonovich, D. C. (2005). Initial glasgow coma scale score predicts outcome following thrombolysis for posterior circulation stroke. *Arch. Neurol.* 62, 1126–1129.

Ungefroren, H., Groth, S., Sebens, S., Lehnert, H., Gieseler, F., and Fändrich, F. (2011). Differential roles of Smad2 and Smad3 in the regulation of TGF-β1-mediated growth inhibition and cell migration in pancreatic ductal adenocarcinoma cells: control by Rac1. *Mol. Cancer* 10, 67–82.

Xing, J., He, W., Ding, Y. W., Li, Y., and Li, Y. D. (2018). Correlation between Contrast-Enhanced Ultrasound and Microvessel Density via CD31 and CD34 in a rabbit VX2 lung peripheral tumor model. *Med. Ultrason.* 1, 37–42. doi: 10.11152/mu-1234

Yang, H., Zhang, H., Ge, S., Ning, T., Bai, M., Li, J., et al. (2018). Exosome-derived miR-130a activates angiogenesis in gastric cancer by targeting C-MYB in vascular endothelial cells. *Mol. Ther.* 26, 2466–2475. doi: 10.1016/j.ymthe.2018.07.023

Yoon, S. G., Jin, S. C., Kim, S. H., Jeon, K. D., Kim, D. Y., Lee, S. I., et al. (2013). Jailing technique using a catheter-based open-cell stent system in internal carotid artery sidewall aneurysms unfeasible to simple coiling. *J. Cerebrovasc. Endovasc. Neurosurg.* 15, 293–298. doi: 10.7461/jcen.2013.15.4.293

Zhang, L., Zheng, F., Peng, Z., Hu, Z., and Yang, Z. (2018). A feasible method of angiogenesis assessment in gastric cancer using 3D microvessel density. *Stem Cells Int.* 2018:7813729. doi: 10.1155/2018/7813729

Zhang, M., Cresswell, N., Tavora, F., Mont, E., Zhao, Z., and Burke, A. (2014). In-stent restenosis is associated with neointimal angiogenesis and macrophage infiltrates. *Pathol. Res. Pract.* 210, 1026–1030. doi: 10.1016/j.prp.2014.04.004

Conflict of Interest Statement: The authors declare that the research was conducted in the absence of any commercial or financial relationships that could be construed as a potential conflict of interest.

frontiers in Immunology

ORIGINAL RESEARCH
published: 22 March 2019
doi: 10.3389/fimmu.2019.00550

Semaphorin 3A Is Effective in Reducing Both Inflammation and Angiogenesis in a Mouse Model of Bronchial Asthma

*Sabag D. Adi[1], Nasren Eiza[1], Jacob Bejar[2], Hila Shefer[2], Shira Toledano[3], Ofra Kessler[3], Gera Neufeld[3], Elias Toubi[1] and Zahava Vadasz[1]**

[1] *Proteomic Unit, The Division of Clinical Immunology and Allergy, Bnai-Zion Medical Center, Haifa, Israel,* [2] *The Department of Pathology, Faculty of Medicine, Bnai-Zion Medical Center, Haifa, Israel,* [3] *The Ruth and Bruce Rappaport Faculty of Medicine, Technion Israel Institute of Technology, Haifa, Israel*

OPEN ACCESS

Edited by:
Michal Amit Rahat, Technion Israel Institute of Technology, Israel

Reviewed by:
Guido Serini, Fondazione del Piemonte per l'Oncologia, Istituto di Candiolo (IRCCS), Italy
Jonathan S. Duke-Cohan, Dana–Farber Cancer Institute, United States

***Correspondence:**
Zahava Vadasz
zahava.vadas@b-zion.org.il

Specialty section:
This article was submitted to Vaccines and Molecular Therapeutics, a section of the journal Frontiers in Immunology

Received: *02 December 2018*
Accepted: *28 February 2019*
Published: *22 March 2019*

Citation:
Adi SD, Eiza N, Bejar J, Shefer H, Toledano S, Kessler O, Neufeld G, Toubi E and Vadasz Z (2019) Semaphorin 3A Is Effective in Reducing Both Inflammation and Angiogenesis in a Mouse Model of Bronchial Asthma. Front. Immunol. 10:550. doi: 10.3389/fimmu.2019.00550

Semaphorin 3A (sema3A) belongs to the sub-family of the immune semaphorins that function as regulators of immune-mediated inflammation. Sema3A is a membrane associated molecule on T regulatory cells and on B regulatory cells. Being transiently ligated to the cell surface of these cells it is suggested to be a useful marker for evaluating their functional status. In earlier studies, we found that reduced sema3A concentration in the serum of asthma patients as well as reduced expression by Treg cells correlates with asthma disease severity. Stimulation of Treg cells with recombinant sema3A induced a significant increase in FoxP3 and IL-10 expression. To find out if sema3A can be of benefit to asthma patients, we evaluated the effect of sema3A injection in a mouse model of asthma. BALB\c-mice were sensitized using ovalbumin (OVA) + adjuvant for 15 days followed by OVA aerosol inhalation over five consecutive days. Four hours following air ways sensitization on each of the above days- 15 of these mice were injected intraperitoneally with 50 μg per mouse of recombinant human sema3A-FR and the remaining 15 mice were injected with a similarly purified vehicle. Five days later the mice were sacrificed, broncheo-alveolar lavage (BAL) was collected and formalin-fixed lung biopsies taken and analyzed. In sema3A treated mice, only 20% of the bronchioles and arterioles were infiltrated by inflammatory cells as compared to 90% in the control group ($p = 0.0079$). In addition, eosinophil infiltration was also significantly increased in the control group as compared with the sema3A treated mice. In sema3A treated mice we noticed only a small number of mononuclear and neutrophil cells in the BAL while in the control mice, the BAL was enriched with mononuclear and neutrophil cells. Finally, in the control mice, angiogenesis was significantly increased in comparison with sema3A treated mice as evidenced by the reduced concentration of microvessels in the lungs of sema3A treated mice. To conclude, we find that in this asthma model, sema3A functions as a potent suppressor of asthma related inflammation that has the potential to be further developed as a new therapeutic for the treatment of asthma.

Keywords: semaphorin3A, asthma, inflammation, angiogenesis, BAL (bronco-alveolar lavage)

INTRODUCTION

Semaphorins were initially identified as axon guidance factors but have subsequently been characterized in addition as modulators of angiogenesis, and as modulators of immune responses. The involvement of some semaphorins such as sema3A and sema4D in both innate and adaptive immune responses resulted in their characterization as a semaphorin subgroup of "immune semaphorins" (1). Semaphorin 3A (sema3A), is a member of the secreted class-3 semaphorins (2). Following secretion sema3A binds to the neuropilin-1 receptor which in association with receptors of the plexin family form functional sema3A receptors in responsive cell types (2). Sema3A had been characterized as a regulator of immune mediated inflammation. Incubation of sema3A with stimulated T effector cells inhibits their proliferation and their ability to secrete pro-inflammatory cytokines (3). The transient ligation of sema3A on Tregs from patients suffering from rheumatoid arthritis (RA) is decreased in association with increased disease activity (4). Taken together, these findings establish sema3A as an indicator for Treg cells activation and as a target for the development of therapeutics targeting inflammatory diseases. When recombinant sema3A was injected into collagen-induced arthritic (CIA) mice, Treg cell function was restored and RA disease activity in these mice was inhibited (4). The concentration of sema3A was found to be reduced in serum of systemic lupus erythematosus (SLE) patients and in correlation with SLE disease activity (5). Furthermore, injection of sema3A into NZB/W mice (an animal model of SLE) reduced and delayed proteinuria, renal damage and prolonged the survival of these mice (6).

Airway inflammation in asthma patients is a complex process, mainly characterized by T helper-2 cells (Th2) hyper-activation. Consequently they display enhanced responses to environmental allergens, and over-produce pro-inflammatory cytokines. This is followed by the activation of allergen-specific B cells and the production of high amounts of specific IgEs, leading to mast cell degranulation (7). The concentration of Treg cells, as well as FoxP3 expression and IL-10 production are deficient in asthma thereby contributing to airway inflammation and disease activity. Upon treatment with corticosteroids and following Allergen Immunotherapy (AIT) the concentrations of the Treg cells and the expression of FoxP3 and IL-10 can be restored and clinical improvement of asthma achieved (8, 9). Subsequently, the concentration of T regulatory cells (CD4/CD25/highFoxP3+) were found to be reduced in induced sputum of atopic asthmatics found to be negatively correlated with airway hyper-responsiveness (10). In patients with active bronchial asthma, decreased amounts of Treg cells and altered expression of FoxP3 were found to be associated with increased level of Th17 cells. In this case, dexamethasone therapy was shown to correct this disturbed balance between Treg and Th17 cells (11). Chronic airway structural changes such as smooth muscle cells hypertrophy and angiogenesis are consequences of long-lasting inflammation in bronchial asthma and are considered to be part of the remodeling process (12). In contrast with the beneficial effect of inhaled corticosteroids in reducing lung T cell and eosinophil infiltration, it is still unclear if inhaled corticosteroids inhibit angiogenesis in bronchial asthma. Sema3A is a membrane associated molecule on Tregs and the newly defined Breg cells. Sema3A plays a regulatory role in experimental mouse models as well as in human models of allergic rhinitis, atopic dermatitis and asthma (13). We have found that low serum levels of sema3A are correlated with severe asthma. Incubation of recombinant sema3A with Treg cells increased the expression of FoxP3 in normal individuals but less so in Tregs of asthmatics (14). We assume that this regulatory effect of Sema3A on Treg cells is via its ligation to neuropilin-1, the known functional receptor of Sema3A on Treg cells. With this in mind we have evaluated in the present study the therapeutic immune-modulatory effects of sema3A following its injection into mice in which we have induced asthma using ovalbumin (OVA) adjuvant. We find that in this asthma model, sema3A functions as a potent suppressor of asthma related inflammation that in addition inhibits asthma associated angiogenesis.

MATERIALS AND METHODS

Production and Purification of Recombinant Point Mutated Human Furin Cleavage Resistant sema3A

The construction of a lentiviral expression vector directing the expression of point mutated furin like pro-protein convertases resistant sema3A containing a c-terminal 6xHis epitope tag (FR-sema3A) was previously described (15). Lentiviruses directing expression of FR-sema3A or control empty lentiviruses were used to infect HEK-293 cells. Conditioned medium from FR-sema3A producing and from control cells, was purified on nickel columns according to the manufacturer instructions. The purified FR-sema3A (FR-sema3A) and the corresponding fractions eluted from nickel columns loaded with control conditioned medium (vehicle) were then used in subsequent experiments.

Asthma Mouse Model

Thirty female Balb/c mice 6- to 7-old weeks were included in this study. OVA sensitization and airway challenge were performed as follows: the mice were sensitized intraperitoneally with 50 μg ovalbumin (OVA; grade V; Sigma-Aldrich) emulsified in 2 mg Alum-Hydroxide (Sigma-Aldrich) in 200 μl 0.9% sodium chloride (saline; Hospira) on Days 0, 7, and 14. On Days 22–25, the mice were placed in a box and were exposed each day for 20 min to an aerosol consisting of 1% (m\v) OVA dissolved in PBS, Ph-7.4 (16). Four hours following air ways sensitization on each of the above days- 15 of these mice were injected intraperitoneally with 50 μg per mouse of recombinant human sema3A-FR and the remaining 15 mice were injected with a similarly purified vehicle as described above. The mice were sacrificed 5 days after sema3A injection on day 30. Broncho-alveolar lavage (BAL) was collected and lung tissue taken for evaluation of treatment efficacy.

Inflammatory Cells in BAL

The BAL fluid was centrifuged at 2,000 rpm for 10 min. After discarding the supernatant the sediment was fixed on lysine-coated slides (Leica Biosystems, Germany), dried and stained

with hematoxilin-eosin. The total number of inflammatory cells was counted double blindly by two expert pathologists. They then scored these numbers to "grade"; above 100 cells\slide- graded as "3," 50–100 cells\slide- graded as "2," 10–50 cells\slide- graded as "1" and <10 cells\slide-graded as "0." The results are the average of these results.

Lung Biopsies

Lungs were formalin-fixed and paraffin embedded (FFPE). Five microns slides were cut and subjected to hematoxylin-eosin staining. The evaluation of the extent of the inflammatory process around blood vessels and bronchioles and the evaluation of the number of eosinophils per high power microscopic field (HPF) was performed by two expert pathologists. The results are expressed as the average of these results.

The Anti-angiogenic Effects of sema3A

Sections of the FFPE samples were mounted onto electrostatically charged microscope slides, dried at 60°C for 1 h, dewaxed and rehydrated as follows: Twice in 100% Xylene for 5 min, twice in 100% Ethanol for 5 min, once in Methanol+H_2O_2 for 20 min, once in 70% Ethanol for 5 min, once in 50% Ethanol for 5 min, once in 25% Ethanol for 5 min, and twice in distilled water (DW). The slides were transferred to a working surface and incubated in warm Trypsin-PBS 1:1 for 2 min then washed in PBSx1. The slides were then transferred into retrieval solution-10 mM Tris buffer PH = 8 and put in the microwave for 18 min, then cooled on the bench and washed with DW. The slides were blocked with 10% normal goat serum (NGS) for 1 h at room temperature, and incubated in primary antibody (rat anti-mouse CD31,Dianova, Hamburg, Germany, 1:100 diluted in 5% NGS) overnight at 4°C. The next day the slides were washed 3 × 5 min in PBS, incubated in secondary antibody conjugated to biotin(diluted in 5% NGS) for 1 h at room temperature, 3 × 5 min washed in PBS, then incubated in HRP Streptavidin antibody (diluted in 5% NGS) for 1 h in RT and washed 3 × 5 min in PBS. The slides were then stained with 3-amino-9-ethylcarbazole (AEC) staining for 15 min, washed in DW and stained with Hematoxylin for 30 s. The evaluation of angiogenic blood vessels in the tissue was performed by two expert pathologists and the results are the mean of their evaluation.

Statistical Analysis

A comparison between two groups was performed using the Mann–Whitney non-parametric test. A two-tailed *P*-value of 0.05 or less was considered to be statistically significant.

RESULTS

The Effect of sema3A Treatment on the Concentration of Inflammatory Cells in BAL

Mice were sensitized by OVA adjuvant injection followed by OVA inhalation to generate asthmatic mice. Mice were then divided into two groups and treated by injection of vehicle or sema3A as described in materials and methods. After 5 days the concentration of inflammatory cells in BAL fluid derived from vehicle treated mice or sema3A treated mice was compared by analysis of microscopic fields followed by grading as described in materials and methods. The BAL of sema3A treated mice contained a low concentration of inflammatory cells while the BAL of vehicle treated mice contained a significantly higher concentration ($P = 0.0081$) of inflammatory cells (see **Figure 1**).

The Effect of sema3A Treatment on Lung Inflammation and Eosinophils Induced by OVA Sensitization in Mice

Inflammation in tissues surrounding the bronchioles and blood vessels in lungs of mice sensitized by OVA and then treated with sema3A or vehicle was determined in histological sections obtained from the lungs of the mice. In sema3A treated mice only few bronchioles (25 ± 10%) were surrounded by invading inflammatory cell (**Figures 2A,C**) while in lungs derived from control mice most of the bronchioles (85 ± 10%) attracted inflammatory cells ($P = 0.0021$) (**Figures 2B,C**). The infiltration of eosinophils (**Figure 3A**, black arrows) was also compared between the two groups and was also more pronounced in the control group with 25 ± 8 eosinophils per HPF as compared with only 5 ± 2 eosinophils per HPF in the sema3A treated mice ($P = 0.033$) (**Figure 3B**).

Sema3A Inhibits Angiogenesis Induced by OVA Sensitization in the Asthmatic Mouse Model

Sema3A is a potent anti-angiogenic factor (17). We have therefore determined if sema3A can inhibit angiogenesis induced by OVA sensitization in the lungs of mice (18). Indeed the lungs of mice treated with sema3A contained a significantly reduced concentration of micro-vessels as compared to lungs of control mice (**Figures 4A,B**). In the vehicle-treated group the concentration of micro-capillaries was 10.22 ± 2.178\HPF as compared with a concentration of 2.46 ± 0.932 capillaries\HPF in lung biopsies derived from sema3A treated mice ($p = 0.0017$) (**Figure 4C**).

DISCUSSION

Airway inflammation in bronchial asthma is classically characterized by multiple inflammatory pathways involving both innate and adaptive immune responses. The hallmark of this inflammation is considered to be T-cell-driven, involving all T cell phenotypes. Increased IL-17 production was found to be responsible for the neutrophil influx into airways as well as for the depletion of Tregs in peripheral blood and in the inflamed airways of patients with bronchial asthma. IL-22 was also reported to be involved in airway hyper-reactivity and in the inflammation of asthmatic OVA-sensitized mice. Lungs of such mice were infiltrated with CD3+CD4+IL-22+T cells that co-expressed IL-17 and TNF-α in association with neutrophil airway infiltration (19–21). The involvement of Th2-type cytokines such as IL-4 and IL-5 was also reported to be important in the pathogenesis of asthma, and was found to shift the differentiation of naïve CD4+ T cells into Th2 cytokine-producing eosinophils

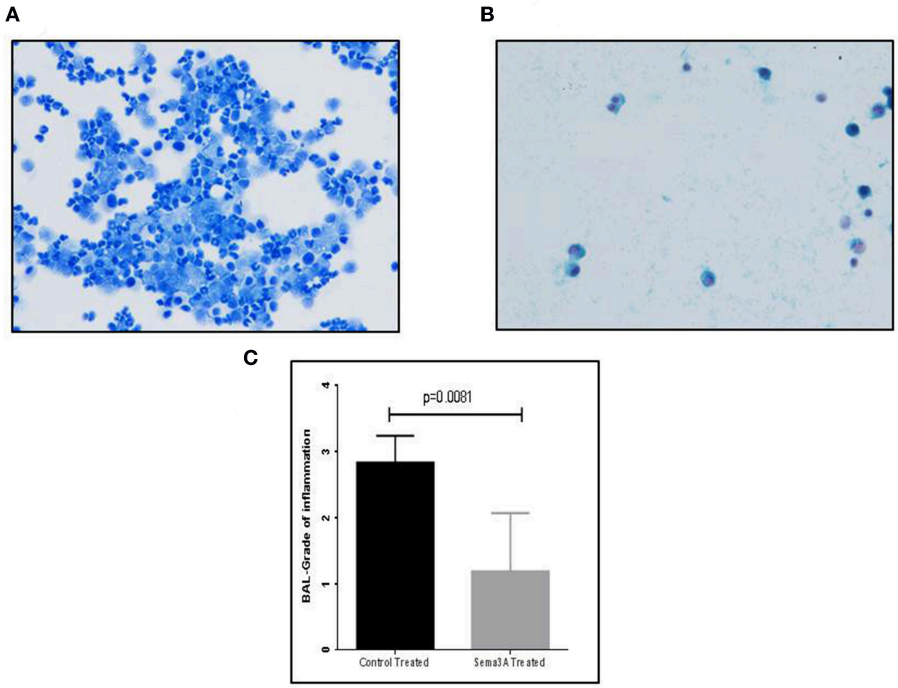

FIGURE 1 | The effect of sema3A treatment on the concentration of inflammatory cells in the BAL. **(A)** A representative picture of inflammatory cells in the BAL fluid of vehicle treated mice. **(B)** A representative picture of inflammatory cells in the BAL fluid of sema3A treated mice. **(C)** Comparison of the average grade of inflammatory cells in the BAL of vehicle vs. sema3A treated mice as determined by the counting of 3–5 microscope fields derived from 15 mice in each group followed by grading as described in materials and methods. Error bars represent the standard error of the mean. Statistical significance was determined using the Mann–Whitney non-parametric test.

and to promote eosinophil infiltration into the inflamed bronchial tree (22). Current therapeutic approaches in bronchial asthma are directed against all of the above-mentioned inflammatory pathways. They classically include corticosteroids (both inhaled and systemic), that are mainly beneficial in altering neutrophil and eosinophil infiltration in the bronchi. When steroids are insufficient, newly introduced anti-IgE or anti-IL-5 drugs are of additive value and reported to be effective in sparing steroids (23, 24). A new approach focused on the modulation of relevant regulatory pathways rather than on the use of immunosuppressive agents (such as steroids and cytotoxic drugs), for the treatment of immune-mediated inflammatory diseases is gaining popularity. In this context, sema3A was recently reported to be a good candidate (6). In previous studies we demonstrated the beneficial effect of sema3A as a down-regulator of the increased expression of TLR-9 in activated B cells from both normal individuals and from patients suffering from SLE (25). Subsequently we also found that sema3A increases the expression of CD72 (a regulatory molecule) on B cells, in addition to enhancement of Treg cell functions (26). These findings are in accordance with *in-vivo* studies in which the injection of recombinant sema3A effectively improved allergic rhinitis and atopic dermatitis in relevant mice models. In these models sema3A was shown to improve both clinical symptoms and tissue inflammation (27, 28). The present study is the first to show that sema3A also reduces efficiently the infiltration of both neutrophils and eosinophils in lung tissue inflammation and in BAL derived from OVA-sensitized mice. We assume that this effect is achieved by increasing local Treg functions, which subsequently reduces adaptive immune-mediated responses and pro-inflammatory cytokines. It is also possible that sema3A inhibits IL-17 production, indirectly leading to the reduced influx of neutrophils, although experimental proof for that is still required (29). So far there is no evidence for the presence of sema3A receptors on neutrophils and eosinophils. Long-lasting airway inflammation may lead to structural changes termed remodeling. These changes consist of sub-epithelial layer thickening, airway smooth muscle hyperplasia and increased angiogenesis induced by the expression of angiogenic factors such as VEGF and angiopoietin (30). Ongoing angiogenesis in the alveoli of asthmatic patients is usually followed by tissue edema and increased vascular permeability which is also triggered by VEGF. Inhaled corticosteroids and anti-leukotriens are of limited influence on angiogenesis and remodeling in most cases. The timing of anti-angiogenic therapy is crucial in attenuating this process and preventing irreversible tissue remodeling. The effect of biological therapies such as the anti-IgE omalizumab and the anti-IL-5 mepolizumab on remodeling is still ill defined and remains to be assessed (31, 32). Thus, new anti-angiogenic compounds such as sema3A are needed in order to control remodeling in asthma. Of the reported mechanisms by which sema3A inhibits angiogenesis, the most important is its high efficacy in inhibiting VEGF activity as a result of the activation of inhibitory intracellular pathways that inhibit

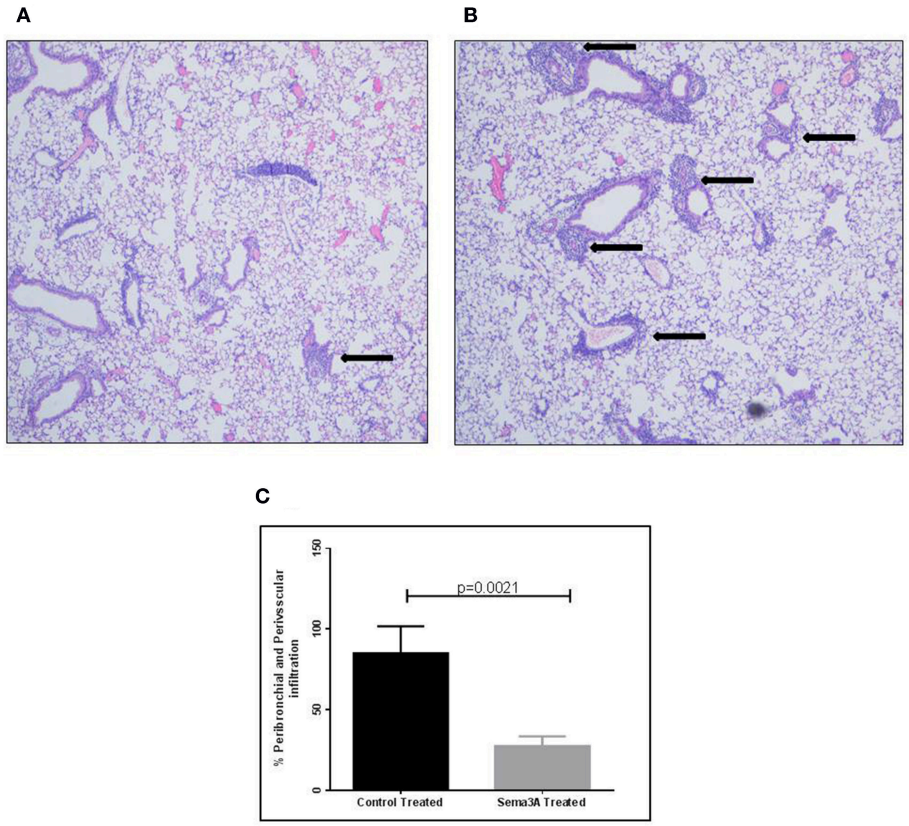

FIGURE 2 | Sema3A inhibits the infiltration of inflammatory cells into the lungs of OVA sensitized asthmatic mice. **(A)** Infiltration of inflammatory cells around bronchiole, in sema3A treated mice. Black arrow denotes inflammation (Magnification X20). **(B)** Infiltration of inflammatory cells around bronchioles and blood vessel, in vehicle treated mice. Black arrows denote massive inflammation (Magnification X20). **(C)** Percentage of bronchioles and blood vessels that are surrounded by inflammatory cells in HPF. The results are the mean value of 3–5 HPF, derived from 15 mice in each group.

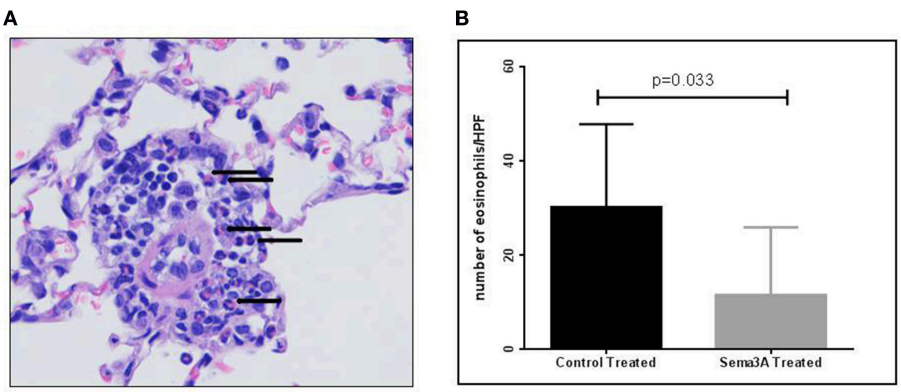

FIGURE 3 | Sema3A inhibits eosinophil infiltration into the lungs of OVA sensitized asthmatic mice. **(A)** Representative figure of eosinophil infiltrate in lungs of OVA sensitized asthmatic mice. Black arrows denote eosinophils (Magnification X40). **(B)** Number of eosinophils per HPF in the inflammatory cell infiltrates in vehicle vs.sema3A treated mice. The results are the average of 3–5 HPF, derived from 15 mice in each group.

VEGF signal transduction (33). Sema3A may also inhibit airway smooth muscle cell proliferation (34) and may in addition reduce angiogenesis by reducing expression of nitric oxide (NO). Diminished NO production was found to be in association with increased smooth muscle cell hyperplasia and with vascular remodeling of blood vessels. Reduced NO production was associated with reduced NO production in patients suffering from pulmonary vascular diseases thus supporting a possible role for NO deficiency in vascular remodeling (35, 36). This observation suggests that improved eNOS-NO pathway signaling may represent a beneficial outcome when considering possible sema3A therapy. The full understanding of all mechanisms

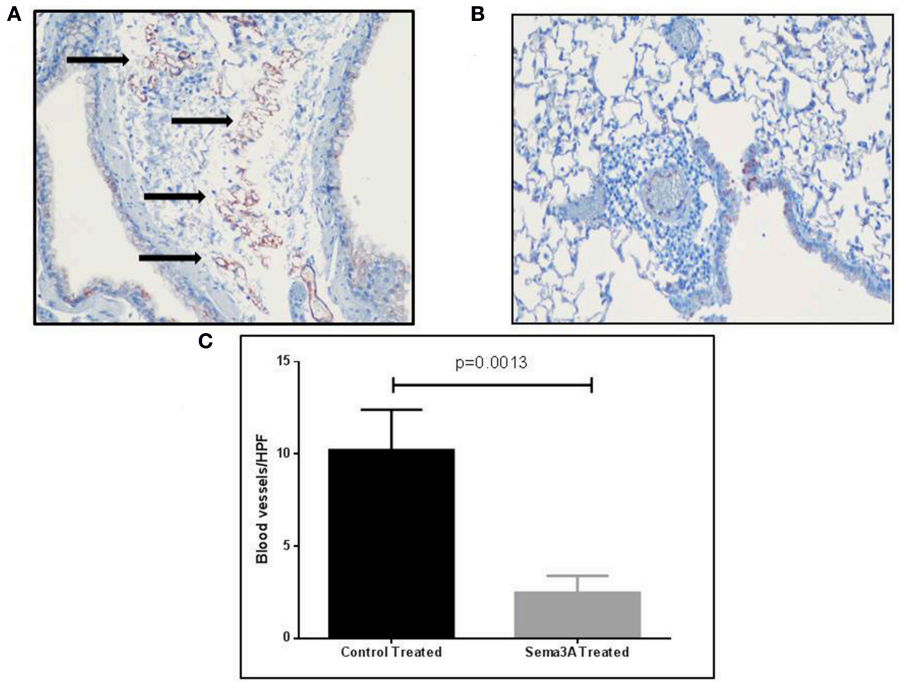

FIGURE 4 | The effect of sema3A on angiogenesis induced by OVA sensitization in lungs of mice. **(A)** Blood vessels in the lung tissue in vehicle treated mice were stained with an antibody directed against CD31 as described in materials and methods. Shown is a representative HPF. Black arrows denote microvessels. **(B)** Shown is a representative HPF. Blood vessels in the lung tissue in sema3A treated mice were stained similarly. Almost no blood vessels can be seen. **(C)** Quantification of the blood vessels concentration across all examined histological slides in vehicle treated and in sema3A treated mice (15 mice in each group, $P = 0.0013$).

by which sema3A decreases eosinophil infiltration in lung tissues and by which it inhibits angiogenesis is still ill defined. To summarize, our experiments indicate that sema3A should be considered as a possible novel therapeutic agent for the treatment of bronchial asthma. Future studies should focus on the strengthening of these results by demonstration of the benefit of sema3A for the improvement of lung functions in asthmatics.

ETHICS STATEMENT

This study was carried out in accordance with the recommendations of Ministry of Health-Israel-Ethical license. The protocol was approved by the Ministry of Health-Israel-Ethical committee.

AUTHOR CONTRIBUTIONS

ZV and ET conducted this research, participated in the experiments, and were responsible for this manuscript writing and editing. SA, NE, OK, and GN were responsible for analysis of results and participated in the experiments. JB and HS participated in the histological analysis of results. ST contributed to the manufacturing and purification of recombinant human sema3A.

ACKNOWLEDGMENTS

This study was supported partially by a grant from the Israel science foundation (ISF, Grant no. 188/16) (to GN).

REFERENCES

1. Nishide M, Kumanogoh A. The role of semaphorins in immune responses and autoimmune rheumatic diseases. *Nat Rev Rheumatol.* (2018) 14:19–31. doi: 10.1038/nrrheum.2017.201
2. Neufeld G, Mumblat Y, Smolkin T, Toledano S, Nir-Zvi I, Ziv K, et al. The role of the semaphorins in cancer. *Cell Adh Migr.* (2016) 10:652–74. doi: 10.1080/19336918.2016.1197478
3. Lepelletier Y, Moura IC, Hadj-Slimane R, Renand A, Fiorentino S, Baude C, et al. Immunosuppressive role of semaphorin3A on T cell proliferation is mediated by inhibition of actin cytoskeleton reorganization. *Eur J Immunol.* (2006) 36:1782–93. doi: 10.1002/eji.200535601
4. Catalano A. The neuroimmune semaphorin3A reduces inflammation and progression of experimental autoimmune arthritis. *J Immunol.* (2010) 185:6373–83. doi: 10.4049/jimmunol.0903527
5. Vadasz Z, Toubi E. Semaphorin3A – a marker for disease activity and a potential putative disease-modifying treatment in systemic lupus erythematosus. *Lupus.* (2012) 21:1266–70. doi: 10.1177/0961203312456753
6. Bejar J, Kessler O, Sabag AD, Sabo E, Itzhak OB, Neufeld G, et al. Semaphorin3A: a potential therapeutic tool for lupus nephritis. *Front Immunol.* (2018) 9:634. doi: 10.3389/fimmu.2018.00634

7. Schmidt-Weber CB, Blaser K. The role of FoxP3 transcription factor in the immune regulation of allergic asthma. *Curr Allergy Asthma Rep*. (2006) 5:356–61. doi: 10.1007/s11882-005-0006-z
8. Robinson DS. Regulatory T cells and asthma. *Clin Exp Allergy*. (2009) 39:1314–23. doi: 10.1111/j.1365-2222.2009.03301.x
9. Hartl D, Koller B, Mehlhorn AT, Reinhardt D, Nicolai T, Schendel DJ, et al. Quantitative and functional impairment of pulmonary CD4+CD25+regulatory T cells in pediatric asthma. *J Allergy Clin Immunol*. (2007) 119:1258–66. doi: 10.1016/j.jaci.2007.02.023
10. Kawayama T, Matsunaga K, Kaku Y, Yamaguchi K, Kinoshita T, O'Byrne PM, et al. Decreased CTLA4+ and FoxP3+ CD25hiCD4+ cells in induced sputum from patients with mild atopic asthma. *Allergol Int*. (2013) 62:203–13. doi: 10.2332/allergolint.12-OA-0492
11. Zhu J, Liu X, Wang W, Ouyang X, Zheng W, Wang Q. Altered expression of T regulatory and Th17 cells in murine bronchial asthma. *Exp Ther Med*. (2017) 14:714–22. doi: 10.3892/etm.2017.4519
12. Samitas K, Carter A, Kariyawasam HH, Xanthou G. Upper and lower airway remodelling mechanisms in asthma, allergic rhinitis and chronic rhinosinusitis: the one airway concept revisited. *Allergy*. (2018) 73:993–1002. doi: 10.1111/all.13373
13. Vadasz Z, Haj T, Toubi E. The role of B regulatory cells and semaphorin3A in atopic dermatitis. *Int Arch Allergy Immunol*. (2014) 163:245–51. doi: 10.1159/000360477
14. Cozacov R, Halasz K, Haj T, Vadasz Z. Semaphorin3A: is a key player in the pathogenesis of asthma. *Clin Immunol*. (2017) 184:70–2. doi: 10.1016/j.clim.2017.05.011
15. Lavi N, Kessler O, Ziv K, Nir-Zvi I, Mumblat Y, Eiza N, et al. Semaphorin-3A inhibits multiple myeloma progression in a mouse model. *Carcinogenesis*. (2018) 39:1283–91. doi: 10.1093/carcin/bgy106
16. Aravind TR, Lakshmi SP, Reddy RC. Murine model of allergen induced asthma. *J Vis Exp*. (2012) 63:3771. doi: 10.3791/3771
17. Acevedo LM, Barillas S, Weis SM, Gothert JR, Cheresh DA. Semaphorin 3A suppresses VEGF-mediated angiogenesis yet acts as a vascular permeability factor. *Blood*. (2008) 111:2674–80. doi: 10.1182/blood-2007-08-110205
18. Sun Y, Wang J, Li H, Sun L, Wang Y, Han X. The effects of budesonide on angiogenesis in a murine asthma model. *Arch Med Sci*. (2013) 9:361–7. doi: 10.5114/aoms.2013.33194
19. Newcomb DC, Peebles RS Jr. Th17-mediated inflammation in asthma. *Curr Opin Immunol*. (2013) 25:755–60. doi: 10.1016/j.coi.2013.08.002
20. Halawani R, Sultana A, Vazquez-Tello A, Jamhawi A, Al-Masri AA, Al-Muhsen S. Th17 regulatory cytokines IL-21, IL-23, and IL-6 enhance neutrophil production of IL-17 cytokines during asthma. *J Asthma*. (2017) 54:893–904. doi: 10.1080/02770903.2017.1283696
21. Leyva-Castillo JM, Yoon J, Geha RS. IL-22 promotes allergic airway inflammation in epicutaneously sensitized mice. *J Allergy Clin Immunol*. (2018) 143:619–30.e7. doi: 10.1016/j.jaci.2018.05.032
22. Tran TN, Zeiger RS, Peters SP, Colice G, Newbold P, Goldman M, Chipps BE. Overlap of atopic, eosinophilic, and Th2-high asthma phenotypes in a general population with current asthma. *Ann Allergy Asthma Immunol*. (2016) 116:37–42. doi: 10.1016/j.anai.2015.10.027
23. Busse WW. Biological treatments for severe asthma:Where do we stand? *Curr Opin Allergy Clin Immunol*. (2018) 18:509–18. doi: 10.1097/ACI.0000000000000487
24. Cabon Y, Molinari N, Marin G, Vachier I, Gamez AS, Chanez P, Bourdin A. Comparison of anti-interleukin-5 therapies in patients with severe asthma:global and indirect meta-analyses of randomized placebo-controlled trials. *Clin Exp Allergy*. (2017) 47:129–38. doi: 10.1111/cea.12853
25. Vadasz Z, Haj T, Halasz K, Rosner I, Slobodin G, Attias D, et al. Semaphorin3A is a marker for disease activity and potential immunoregulator in systemic lupus erythematosus. *Arthritis Res Ther*. (2012) 14:R146. doi: 10.1186/ar3881
26. Vadasz Z, Haj T, Balbir A, Peri R, Rosner I, Slobodin G, et al. A regulatory role for CD72 expression on B cells in systemic lupus erythematosus. *Semin Arthritis Rheum*. (2014) 43:767–71. doi: 10.1016/j.semarthrit.2013.11.010
27. Yamaguchi J, Nakamura F, Aihara M, Yamashita N, Usul H, Hida T, et al. Semaphorin3A alleviates skin lesions and scratching behavior in NC/Nga mice, an atopic dermatitis model. *J Invest Dermatol*. (2008) 128:2842–9. doi: 10.1038/jid.2008.150
28. Sawaki H, Nakamura F, Aihara M, Nagashima Y, Komori-Yamaguchi J, Yamashita N, et al. Intranasal administration of semaphorin-3A alleviates sneezing and nasal rubbing in a murine model of allergic rhinitis. *J Pharmacol Sci*. (2011) 117:34–44. doi: 10.1254/jphs.11005FP
29. Xiang R, Xu Y, Zhang W, Kong YG, Tan L, Chen SM, et al. Semaphorin 3A inhibits allergic inflammation by regulating immune responses in a mouse model of allergic rhinitis. *Int Forum Allergy Rhinol*. (2018). doi: 10.1002/alr.22274. [Epub ahead of print].
30. Palgan K, Bartuzi Z. Angiogenesis in bronchial asthma. *Int J Immunopathol Pharmacol*. (2015) 28:415–20. doi: 10.1177/0394632015580907
31. Girodet PO, Ozier A, Bara I, Tunon de Lara JM, Marthan R, Berger P. Airway remodeling in asthma:new mechanisms and potential for pharmacological interventions. *Pharmacol Ther*. (2011) 130:325–37. doi: 10.1016/j.pharmthera.2011.02.001
32. Durrani SR, Viswanathan RK, Busse WW. What effect does asthma treatment have on airway remodeling? *Curr Perspect J Allergy Clin Immunol*. (2011) 128:439–48. doi: 10.1016/j.jaci.2011.06.002
33. Guttmann-Raviv N, Shraga-Heled N, Varshavsky A, Guimaraes-Sternberg C, Kessler O, Neufeld G. Semaphorin-3A and semaphorin-3F work together to repel endothelial cells and to inhibit their survival by induction of apoptosis. *J Biol Chem*. (2007) 282:26294–305. doi: 10.1074/jbc.M609711200
34. Movassagh H, Tatari N, Shan L, Kousaih L, Alsubait D, Khattabi M, et al. Human airway smooth muscle cell proliferation from asthmatics is negatively regulated by semaphorin 3A. *Oncotarget*. (2016) 7:80238–251. doi: 10.18632/oncotarget.12884
35. Jaitovich A, Jourd'heuil D. A brief overview of nitric oxide and reactive oxygen species signaling in hypoxia-induced pulmonary hypertension. *Adv Exp Med Biol*. (2017) 967:71–81. doi: 10.1007/978-3-319-63245-2_6
36. Klinger JR, Kadowitz PJ. The nitric oxide pathway in pulmonary vascular disease. *Am J Cardiol*. (2017) 120:S71–9. doi: 10.1016/j.amjcard.2017.06.012

Conflict of Interest Statement: The authors declare that the research was conducted in the absence of any commercial or financial relationships that could be construed as a potential conflict of interest.

The handling editor declared a shared affiliation, though no other collaboration, with several of the authors GN, ST, and OK.

frontiers in Immunology

ORIGINAL RESEARCH
published: 02 April 2019
doi: 10.3389/fimmu.2019.00651

Targeting Tumor Vascular CD99 Inhibits Tumor Growth

*Elisabeth J. M. Huijbers[1], Inge M. van der Werf[2], Lisette D. Faber[1], Lena D. Sialino[1], Pia van der Laan[1], Hanna A. Holland[1], Anca M. Cimpean[3], Victor L. J. L. Thijssen[1], Judy R. van Beijnum[1] and Arjan W. Griffioen[1]**

[1] Angiogenesis Laboratory, Department of Medical Oncology, Cancer Center Amsterdam, VU University Medical Center, Amsterdam UMC, Amsterdam, Netherlands, [2] Hematology Laboratory, Department of Hematology, Cancer Center Amsterdam, VU University Medical Center, Amsterdam UMC, Amsterdam, Netherlands, [3] Department of Histology, Angiogenesis Research Center Timisoara, Victor Babeş University of Medicine and Pharmacy, Timisoara, Romania

CD99 (MIC2; single-chain type-1 glycoprotein) is a heavily O-glycosylated transmembrane protein (32 kDa) present on leukocytes and activated endothelium. Expression of CD99 on endothelium is important in lymphocyte diapedesis. CD99 is a diagnostic marker for Ewing's Sarcoma (EWS), as it is highly expressed by these tumors. It has been reported that CD99 can affect the migration, invasion and metastasis of tumor cells. Our results show that CD99 is also highly expressed in the tumor vasculature of most solid tumors. Furthermore, we found that *in vitro* CD99 expression in cultured endothelial cells is induced by starvation. Targeting of murine CD99 by a conjugate vaccine, which induced antibodies against CD99 in mice, resulted in inhibition of tumor growth in both a tumor model with high CD99 (Os-P0109 osteosarcoma) and low CD99 (CT26 colon carcinoma) expression. We demonstrated that vaccination against CD99 is safe, since no toxicity was observed in mice with high antibody titers against CD99 in their sera during a period of almost 11 months. Targeting of CD99 in humans is more complicated due to the fact that the human and mouse CD99 protein are not identical. We are the first to show that growth factor activated endothelial cells express a distinct human CD99 isoform. We conclude that our observations provide an opportunity for specific targeting of CD99 isoforms in human tumor vasculature.

Keywords: CD99, MIC2, angiogenesis, tumor vasculature, vaccination, immunotherapy, cancer

OPEN ACCESS

Edited by:
Michal Amit Rahat, Technion Israel Institute of Technology, Israel

Reviewed by:
Kang Chen, Wayne State University, United States
Supansa Pata, Chiang Mai University, Thailand

****Correspondence:***
Arjan W. Griffioen
a.griffioen@vumc.nl

Specialty section:
This article was submitted to Vaccines and Molecular Therapeutics, a section of the journal Frontiers in Immunology

Received: *02 November 2018*
Accepted: *11 March 2019*
Published: *02 April 2019*

Citation:
Huijbers EJM, van der Werf IM, Faber LD, Sialino LD, van der Laan P, Holland HA, Cimpean AM, Thijssen VLJL, van Beijnum JR and Griffioen AW (2019) Targeting Tumor Vascular CD99 Inhibits Tumor Growth. Front. Immunol. 10:651. doi: 10.3389/fimmu.2019.00651

INTRODUCTION

The CD99 antigen, also known as MIC2 or single-chain type-1 glycoprotein, is a 32 kDa transmembrane protein expressed in inflamed endothelium and at low levels in thymocytes and T cells. Several reports show that CD99 is involved in lymphocyte diapedesis (1–6). Furthermore, CD99 has been presented as a diagnostic marker for Ewing's Sarcoma (EWS), as it is highly expressed by most EWS tumors (7, 8). In EWS tumors CD99 has been described to have an oncogenic function (9–13). Also, CD99 has been found to be involved in the migration, invasion and metastasis of tumor cells (5, 12, 14, 15).

Previous studies suggest that CD99 is a promising therapeutic target. Guerzoni et al. showed that targeting of CD99 by a diabody (C7 dAbd) promoted cancer cell death of EWS tumor cells *in vitro* (16). In addition, knockdown of CD99 in EWS tumor cells reduced *in vivo* tumor growth in mouse xenograft experiments (12). Also, a monoclonal antibody against CD99 (0662 Mab) combined with doxorubicin showed enhanced inhibition of EWS tumor growth and metastasis formation in a xenograft model (17). Imaging of mice with a ^{64}Cu-labeled anti-mCD99 antibody detects subcutaneous Ewing sarcoma tumors and metastatic sites with high sensitivity (18). CD99 was also found to be highly expressed in acute lymphoblastic leukemia (ALL), acute myeloid leukemia (AML), myelodysplastic syndromes (MDS), and stem cells and anti-CD99 monoclonal antibodies show antileukemic activity in AML xenograft models (19–21). In atherosclerosis CD99 is expressed on activated endothelial cells that cover the plaque. Treatment of immunocompetent mice with an oral vaccine composed of attenuated *Salmonella typhimurium* transformed with pcDNA3-murineCD99 inhibited atherosclerotic plaque formation by induction of CD99 targeting cytotoxic T cells (22). Van Wanrooij et al. suggest that vaccination leads to removal of the CD99 expressing endothelial cells and thereby reduces atherosclerotic plaque formation. After vaccination a decreased expression of CD99 on leukocytes was observed and fewer leukocytes were recruited to the site of the plaque, whereas the total number of leukocytes was not affected. These observations indicate that CD99 can safely be used as a therapeutic target for vaccination.

In the current study, we explored the opportunity to use vaccination against CD99 as a treatment option against solid tumors. We showed that CD99 is heavily overexpressed on tumor endothelial cells in multiple human solid tumors. We developed a conjugate vaccine, based on a fusion protein technique published previously by Huijbers et al. (**Supplementary Figure 1B**) (23–25). In short, a fusion protein, consisting of the murine CD99 sequence and an engineered truncated version of bacterial thioredoxin (26), was made and used for vaccination. The vaccine induced an antibody response against CD99 by activation of specific CD99 auto-reactive B-cells. In two different immunocompetent mouse tumor models we found that vaccination against CD99 reduced tumor microvessel density and functionality, and resulted in suppressed tumor growth. No side-effects were observed after maintaining mice hyperimmune for almost a year.

For human CD99, two different isoforms have been described (27). A long full-length isoform (185 amino acids, 32 kDa, variant I; **Supplementary Figure 1C**) and a short truncated isoform (161 amino acids, 28 kDa, variant II), lacking most of the cytoplasmic domain, exist. The murine CD99 only shows 46% homology with human CD99 and resembles the human short isoform (28). However, it is unclear whether the CD99 isoforms have the same function in mouse as in humans (29). In the NCBI database six different protein coding human CD99 splice variants are suggested (Gene ID: 4267) (30). In this paper we dissected the expression of these splice variants in endothelial cells and EWS tumor cells. Our results show a difference in CD99 splicing in activated endothelial cells and EWS tumor cells, which provides opportunities for specific therapeutic targeting to treat cancer.

MATERIALS AND METHODS

Cell Culture

The murine osteosarcoma cell line Os-P0107, derived from a spontaneous osteosarcoma arising in a female *VEGF^{P}-GFP/C3H* transgenic mouse, was a kind gift of Dr. Dan Duda (Massachusetts General Hospital, Harvard Medical School, Boston, MA, USA) (31). The Os-P0107 cells were maintained in Dulbecco's modified eagle medium (DMEM) (cat no. BE12-604F, Lonza Biowhittaker, Leusden, The Netherlands) containing 15% Fetal bovine serum (FBS) (cat no. S1810-500, Biowest, Nuaillé, France) and 100 U/ml penicillin/streptomycin (pen/strep) (cat. no. DE17-602E Lonza Biowhittaker). CT26 murine colon carcinoma cells (CT26.WT) (ATCC no. CRL-2638, Manassas, VA, USA) were cultured in Roswell Park Memorial Institute (RPMI)-1640 supplemented with 2 mM L-glutamine (cat no. 17-605C, Lonza Biowhittaker) 10% FBS and 100 U/ml pen/strep.

The Ewing's Sarcoma cell lines EW7 and EWS-RDES were previously characterized by Dr. O. Delattre (Pathologie Moléculaire des Cancers, Institut Curie, Paris Cedex). Cells were maintained in RPMI-1640 supplemented with 10% FBS and 2 mM L-glutamine.

Human umbilical vein endothelial cells (HUVEC), isolated from umbilical cords by standard methods, were maintained in RPMI-1640 (Lonza Biowhittaker) medium supplemented with 10% FBS (Biowest), 10% human serum, 2 mM L-glutamine (Lonza Biowhittaker), and 100 U/ml pen/strep (Lonza Biowhittaker). HUVEC were cultured in 0.2% gelatin coated culture flasks.

HUVEC Starvation Assay

Six-well culture plates (VWR International, Radnor, PA, USA) were coated with 0.2% gelatin and 150,000 HUVEC were seeded in each well. Cells were allowed to adhere for 3–4 h before nutrient deprived medium was added containing only 10% FBS or 1% FBS (Lonza Biowhittaker) in RMPI-1640 medium (Lonza Biowhittaker). Cells were then harvested at 24 or 48 h and flow cytometry was performed. In addition, cell lysates were prepared from control treated cells and 48 h starved cells. To this end cells grown in a T75 culture flask were scraped off the bottom in 500 µl 2x Laemmli sample buffer (#1610737, Bio-Rad Laboratories B.V., Veenendaal, The Netherlands) plus β-mercaptoethanol (sc-202966, Santa Cruz Biotechnology Inc., Dallas, TX, USA) on ice. Lysates were stored at −20°C until use.

Flow Cytometry

HUVEC were harvested using trypsin/EDTA (Lonza Biowitthaker), washed with 0.1% BSA/PBS stained with rabbit anti-human CD99 polyclonal antibody (ab27271, 0.2 mg/ml, Abcam, Cambridge, UK) diluted 1:100 in 0.1% BSA/PBS for 30 min at RT. After a washing step cells were incubated with secondary anti-rabbit APC antibody (F0111, R&D Systems, Abingdon, UK).

Os-P0107 osteosarcoma and CT26 cells were collected with 0.5 M EDTA (Sigma Aldrich), centrifuged and resuspended in ice-cold PBS/10%FCS/0.1% sodium azide solution to prevent internalization of CD99. Cells were distributed into FACS tubes ($1*10^6$ cells per tube), washed and centrifuged for 5 min at 400 g and 4°C in a Rotina 420R centrifuge (Hettich Lab Technology, Tuttlingen, Germany). To detect CD99 expression, cells were incubated in a volume of 50 µl with primary goat anti-mouse CD99 polyclonal antibody (1:100; R&D systems; AF3905, 0.2 mg/ml) in 0.1% BSA/PBS for 30 min at 4°C. Cells were washed and centrifuged three times before and after being incubated with donkey anti-goat IgG Northern Lights 557 (1:1,000; R&D systems; NL001) for 30 min at 4°C in the dark. Subsequently cells were resuspended in ice-cold PBS/10%FCS/0.1% sodium azide solution.

Cells were analyzed with a FACSCalibur flow cytometer (Beckton Dickinson, Franklin Lakes, NJ, USA) and CellQuest Software. Data analysis was performed with FCSalyzer (SourceForge, La Jolla, CA, US). Fold increase of the mean fluorescence intensity (MFI) was determined by dividing the MFI of CD99 stained cells by the MFI of control stained cells.

Immunohistochemistry

Tumors and normal tissues were paraffin embedded and sectioned (5 µm) with a Leica RM 2135 microtome (Leica, Nieuw-Vennep, The Netherlands). Sections were dried overnight at 37°C, placed at 60°C for 1 h and baked for 10 min at 56°C before deparaffinization with xylene (VWR International) followed by 100% (Nedalco B.V., Bergen op Zoom, The Netherlands), 96 and 70% ethanol and rehydration in phosphate buffered saline (PBS). After treatment with 1% hydrogen peroxide (Hydrogen peroxide 30%, BDH Prolabo, VWR International, Amsterdam, The Netherlands) in PBS for 15 min at room temperature (RT), antigens were retrieved in 10 mM sodium citrate buffer pH 6.0. After cooling down, sections were washed in PBS and blocked with 3% Bovine Serum Albumin Fraction V (BSA, Roche Diagnostics, Penzberg, Germany)/PBS for 1 h at RT and incubated with rabbit anti-human CD99 polyclonal antibody (ab27271, Abcam) diluted 1:200 in 0.5% BSA/PBS overnight at 4°C. The next day, tissue sections were incubated with biotinylated swine anti-rabbit Ig antibody (E0353, 0.50 g/L, DakoCytomation, Glostrup, Denmark) diluted 1:500 for 45 min at RT. This was followed by incubation with Streptavidin-HRP (P0397, 0.82 g/L, DakoCytomation) diluted 1:200 in 0.5% BSA/PBS for 30 min at RT and 3,3′-diaminobenzidine tetrahydrochloride hydrate (DAB) staining (Sigma-Aldrich Chemie B.V., Zwijndrecht, The Netherlands).

Images of different tumor types and normal tissues stained for human CD99 were retrieved from the Human Protein Atlas (32, 33).

For staining of murine CD99, polyclonal goat anti-mouse CD99 antibody (AF3905, 0.2 mg/ml, R&D Systems,) diluted 1:50 was used. Endogenous peroxidase activity was blocked with 1% H_2O_2. After antigen retrieval with sodium citrate buffer, primary antibody was detected with biotinylated polyclonal rabbit anti-goat (E0466, 1.6 g/L, DakoCytomation) diluted 1:200 in 0.1% PBS-T, followed by Streptavidin-HRP (DakoCytomation) 1:400 in 0.1% PBS-T and DAB substrate. All sections stained with CD99 antibody, were counterstained with Mayer's hematoxylin (Klinipath, Duiven, The Netherlands) for 30 s and the reaction was stopped under running tap water for 10 min. Finally, sections were dehydrated in 70% ethanol, 96% ethanol and 100% ethanol for 2 min consecutively and mounted with Quick D mounting medium (Klinipath).

To determine vessel density and morphology, tumor tissue and organs, sections (3 µm) were stained for CD31 (34). To this end, cleared paraffin sections were incubated with 0.3% H_2O_2/PBS for 15 min at RT. Antigens were retrieved with sodium citrate buffer, slides were blocked with 3%BSA/PBS as described above and stained with rat anti-mouse CD31 antibody (DIA310M, clone SZ31, 0.2 mg/ml, Dianova GmbH, Hamburg, Germany), diluted 1:50 in 0.5% BSA/PBS overnight at 4°C. Tissue sections were subsequently incubated with biotinylated donkey anti-rat IgG antibody (product code: 712-067-003, 1.3 mg/ml, Jackson ImmunoResearch laboratories, Baltimore, PA, USA) diluted 1:500 in 0.5% BSA/PBS for 45 min at RT. Sections were washed in PBS and subsequently incubated with Streptavidin-HRP (1:200; DakoCytomation) in 0.5% BSA/PBS for 30 min at RT and developed with DAB substrate. Finally, sections were dehydrated in 70% ethanol, 96% ethanol, and 100% ethanol for 2 min consecutively and mounted with Quick D mounting medium (Klinipath).

Desmin Staining

After deparaffinization, osteosarcoma tumor sections were treated with 0.3% H_2O_2 for 15 min at RT, washed and boiled in citrate buffer. Sections were blocked with 3% BSA/PBS for 60 min at RT and incubated with primary rat anti-mouse CD31 antibody (1:50; Dianova) and goat anti-human/mouse desmin antibody (1:200; R&D systems; AF3844) in 3.0% BSA/PBS overnight at 4°C. Primary antibody was detected with secondary rabbit anti-rat HRP (1:100; DakoCytomation; P045001) and rabbit anti-goat biotinylated (1:200; DakoCytomation) in 3.0% BSA/PBS for 30 min at RT. After a washing step, sections were developed with DAB substrate to detect the CD31 staining. To detect the pericytes, sections were washed and incubated with strep-AP (1:500; Genmed Synthesis Inc. San Antonio, Texas, USA) in 10X TBS Solution (0.5 M Tris-Cl; 1.5 M NaCl, pH 7.6) for 30 min at RT. Washed in ddH_2O and developed with Fast Blue BB (Sigma Aldrich). Finally, sections were washed in ddH_2O, air-dried and embedded in Kaisers glycerol gelatin (Merck group).

Staining of Tumor Tissue With Serum of TRXtr-mCD99 Immunized Mice

Osteosarcoma tumor sections from TRXtr immunized mice were deparaffinized, treated with 1% H_2O_2 for 15 min at RT and boiled in citrate buffer. Sections were blocked with 20% horse serum (H-1138, heat inactivated, Sigma-Aldrich)/PBS for 1 h at RT. Consecutively, sections were incubated with goat F(ab) anti-mouse IgG H&L (ab6668, 1 mg/ml, Abcam) diluted 1:20 in PBS for 2 h at RT, to prevent non-specific binding of the mouse serum to the mouse tissue. A washing step with 0.05% PBS-T was performed and the sections

were stained with serum from TRXtr immunized or TRXtr-mCD99 immunized mice diluted 1:600 in 20% horse serum/PBS overnight at 4°C. Anti-CD99 antibodies in the serum were detected with biotinylated polyclonal goat anti-mouse Ig (E0433, Dako Cytomation) diluted 1:500 in 0.5% BSA/PBS, followed by Streptavidin-HRP (DakoCytomation) 1:200 in 0.5% BSA/PBS and DAB substrate. Sections were counterstained with Mayer's hematoxylin (Klinipath), dehydrated in an ethanol series and mounted with Quick D (Klinipath).

Hematoxylin/Eosin Staining

Sections were deparaffinized and dipped in diluted Mayer's Hematoxylin (Klinipath) (1:4 dilution in 5 mM sodium citrate buffer pH 6.0). After a rinse under flowing tap water for 5 min, sections were stained with 0.2% eosin Y solution (J.T. Baker, Avantor Performance Materials B.V., Deventer, The Netherlands) for 30 s. Sections were dehydrated with two changes of 70% ethanol, three changes of 96% ethanol, 100% ethanol for 5 min and xylene for 2 min. Consecutively sections were mounted with Quick D mounting medium (Klinipath).

Immunohistochemistry Quantification

Pictures were captured with an Olympus BX50 microscope (Olympus Optical Co. GmbH, Hamburg, Germany) equipped with a CMEX DC 5000C camera (Euromex microscopes, Arnhem, The Netherlands).

Only viable tumor tissue was used for analysis. Microvessel density was assessed by manual counting of tumor tissue stained for CD31. In total 3 fields/tumor (100x magnification) and 3–10 tumors per experimental group were counted. Images were used to manually count the number of vessels with a clear lumen in osteosarcoma tumors. Images were further analyzed with ImageJ (Laboratory for Optical and Computational Instrumentation, University of Wisconsin-Madison; Version 1.51s) to determine the vessel density of osteosarcoma and CT26 tumors. For pericyte (desmin) quantification, 10 fields per tumor were chosen (magnification 200x). Images were used to manually count the number of vessels with and without desmin staining/associated pericytes. Pericyte coverage was then determined by dividing the number of vessels with pericytes by the total vessel count.

Reverse Transcriptase Quantitative Polymerase Chain Reaction (RT-qPCR)

Total RNA was isolated using TRIzol Reagent (Life technologies, Carlsbad, CA, USA) according to the manufacturer's protocol. RNA concentration and quality were measured using a NanoDrop ND-1000 spectrophotometer (Isogen Life Science, Utrecht, The Netherlands). One microgram of the obtained RNA was reverse transcribed to cDNA using an iScript cDNA synthesis kit (Bio-Rad Laboratories, Hercules, CA, USA). The obtained cDNA was diluted 1:5 and RT-qPCR was performed using iQ SYBR Green Supermix (Bio-Rad Laboratories) and 0.2 μM of each primer (Eurogentec, Seraing, Belgium) (**Tables 1**, **2**). Primers were validated as previously described (35). Samples were run in duplicate and analyzed on the CFX96 Real Time System C1000 Thermal Cycler (Bio-Rad Laboratories). Data were analyzed with CFX Manager software (version 3.1, Bio-Rad Laboratories), and further processed in MS Excel. All samples were normalized to cyclophillin A, β-actin, and β2-microglobulin transcript expression (**Tables 3**, **4**) to account for variations in template input (35). The following formula was used to calculate the 2^{-dCt} value of the gene of interest: $2^{-(Ctvaluegeneofinterest-meanCtvaluereferencegenes)}$. Ratios of the different primer pairs and the k + l primers used to determine total CD99 were calculated by dividing the mean 2^{-dCt} value of each primer pair with the mean 2^{-dCt} value of the k + l primers.

TABLE 1 | Primers RT-qPCR endogenous mCD99 in mouse cell lines.

Primer	Sequence
mCD99fw	5′-GCCTCGCCTGAATATGCAAA-3′
mCD99rev	5′-GTCAGTTGTGGGCGGAGTCTT-3′

TABLE 2 | RT-qPCR Primers hCD99 isoforms.

Primer	Sequence
a	5′-TGCTGCTCTTCGGCCTGCTG-3′
b	5′-TTCTTGGGGATTGCAGTGGG-3′
c	5′-TCAAAGTCATCCCCAGGAAGG-3′
e	5′-TTGGCATTCCGGTGGCTCTC-3′
f	5′-GTTTCAGGTGGAGAAGCCGAC-3′
g	5′-TGATCCCCGGGATTGTGG-3′
h	5′-TTCTCTGCTCACCCCTAGGTC-3′
k	5′-AATGACGACCCACGACCACC-3′
l	5′-AACGCCATCCGCAAGGTCAG-3′

TABLE 3 | Mouse RT-qPCR reference gene primers.

Primer	Sequence
β-actin fw	5′- GAAGCTGTGCTATGTTGCTCTA−3′
β-actin rev	5′- GGAGGAAGAGGATGCGGCA−3′
β-2microglobulin fw	5′- CCGCCTCACATTGAAATCC−3′
β-2microglobulin rev	5′- CTCTGCAGGCGTATGTATCAG−3′
Cyclophilin A	5′- ATTTCTTTTGACTTGCGGGC−3′
Cyclophilin A	5′- AGCTAGACTTGAGGGGAATG−3′

TABLE 4 | Human RT-qPCR reference gene primers.

Primer	Sequence
β-actin fw	5′- CATTCCAAATATGAGATGCATT−3′
β-actin rev	5′- CCTGTGTGGACTTGGGAGAG−3′
β-2microglobulin fw	5′- TCGATCCGACATTGAAGTTG−3′
β-2microglobulin rev	5′- ACACGGCAGGCATACTCAT−3′
Cyclophilin A	5′- CTCGAATAAGTTTGACTTGTGTTT−3′
Cyclophilin A	5′- CTAGGCATGGGAGGGAACA−3′

Expression Vectors

The region encoding the extracellular part [amino acids (aa) 27–137] of murine CD99 (36) (GenBank TM/EBI Data Bank accession numbers BC019482) (UniProtKB-Q8VCN6 (CD99_mouse) (RefSeq NP_079860.2. NM_025584.2.; GI:

125660452), optimized for protein expression in bacteria (Genscript) (333 bp), was inserted downstream the bacterial truncated thioredoxin (TRXtr) (26) sequence (192 bp) containing an N-terminal 4xGS-linker sequence and His-tag (6xhistidine) into a pET21a (+) vector (Novagen; EMD Chemicals, Gibbstown, NJ, USA). The original pET21-TRX plasmid was a kind gift of Dr. Anna-Karin Olsson (Uppsala University, Uppsala, Sweden). The resulting expression vector was named pET21a-TRXtr-mCD99$_{extracellular}$ (**Supplementary Figure 1D**).

Murine CD99 extracellular part protein sequence (aa27-137) (36): ASDDFNLGDALEDPNMKPTPKAPTPKKPSGGFDLED ALPGGGGGGAGEKPGNRPQPDPKPPRPHGDSGGISDSDL ADAAGQGGGGAGRRGSGDEGGHGGAGGAEPEGTPQ

For construction of the pET21a-mCD99$_{extracellular}$ plasmid the extracellular part of murine CD99 was PCR amplified from the original pET21a-mCD99 vector (Genscript) using the following primers:

Nde1-His-extracellmCD99fw
5′-TAT-CAT-ATG-CAC-CAC-CAC-CAC-CAC-CAC-GCA-AGC-GAT-GAT-TTT-A-3′
Xho1-3x-stop-excellmCD99rev
5′-TAT-CTC-GAG-CTA-TTA-TCA-ACC-CTG-CGG-GGT-ACC-TTC-CGG-TTC-3′

After purification and restriction with *NdeI* and *XhoI* the mCD99$_{extracellular}$ sequence was ligated into a pET21a vector.

Vaccine Production and Purification

The recombinant vaccine proteins were produced and purified as previously described (23, 24). The pET21a expression vectors were transformed into *E. Coli* Rosetta gami (DE3) (Novagen; Merck Millipore, Darmstadt, Germany) for recombinant protein expression. Overnight cultures were diluted 1:3 and were grown until optical density 600 nm (OD_{600}) 0.5 was reached. Protein expression was induced with 1 mM isopropyl β-D-1-thiogalactopryanoside (IPTG, Invitrogen, Life Technologies, CA, USA) at 37°C for 4 h for TRXtr-mCD99$_{extracellular}$ and mCD99$_{extracellular}$ (for simplicity the resulting proteins are named TRXtr-mCD99 and mCD99). TRXtr expression was induced at 22°C for 15 h. Bacteria were harvested by centrifugation at 4,500 rpm (3,584 g), 10 min, 4°C (Hettich Rotina 420R) and washed five times with PBS. Bacterial pellets were dissolved in PBS (TRXtr-mCD99 and mCD99) or in 5 M urea (TRXtr) (Acros Organics/Thermo Fisher Scientific, Landsmeer, The Netherlands). The proteins (TRXtr-mCD99 and mCD99) were released by sonication (amplitude 22–26 microns, Soniprep 150 MSE, London, UK) on ice, 12 times for 30 s with breaks of 30 s, for the TRXtr protein 15 cycles of 20 s on and 30 s off were used. After centrifugation, 20 mM imidazole (J.T. Baker, Avantor Performance Materials B.V.) was added to the supernatant to reduce non-specific binding of background proteins to the nickel (Ni) agarose. No imidazole was added to the TRXtr supernatant during the Ni-agarose incubation step. Thereafter, 500 µl 50% Ni-NTA agarose slurry (Qiagen, Venlo, The Netherlands) was mixed with 25 ml supernatant (originating from 500 ml bacteria culture) and incubated "end-over-end" at 4°C for 3 h. After centrifugation at 3,000 rpm (Rotina 420R, Hettich), the agarose beads were washed with 250 ml wash buffer containing PBS pH 7.0/1 M NaCl /0.1% Tween-20. An additional washing step with PBS was performed to remove the detergent Tween (P1379, Sigma-Aldrich, Zwijndrecht, The Netherlands). Then, the beads were transferred to a 1 ml syringe (BD Plastipak, BD Biosciences, Madrid, Spain) with a glass filter (Sartorius Stedim Biotech, Göttingen, Germany) and washed again with PBS. The TRXtr-mCD99 protein was eluted with two 250 µl fractions of 50 mM and three fractions of 100 mM imidazole, dissolved in 20 mM Tris pH 8.0/0.1 M NaCl. The TRXtr and mCD99 protein were eluted with four 250 µl fractions of 100 mM imidazole solution. Protein content of the separate fractions was determined by SDS-PAGE using precast 4–20% gradient polyacrylamide gels (Mini-Protean TGX, Bio-Rad Laboratories). Gels were fixed and stained with home-made colloidal Coomassie brilliant blue R250 solution containing 20% methanol (VWR International). Destaining of the gels was performed with methanol for 1 min and ddH_2O for several hours. Fractions containing most protein were pooled and dialyzed against PBS (pH 7.0). The different recombinant proteins TRXtr-mCD99 (18 kDa), TRXtr (7.5 kDa; appears as a 15 kDa dimer on reduced SDS-PAGE) and mCD99 (11 kDa) as present on an SDS-PAGE gel after purification (**Figure 1G**).

For the TRXtr and TRXtr-mCD99 protein a Slide-A-Lyzer Dialysis cassette (M_w cut-off (MWCO) 7,000 Da; Thermo Fisher Scientific) was used. The mCD99 protein was dialyzed in snakeskin dialysis membrane (MWCO 3,500 Da; Thermo Fisher Scientific). Final protein concentrations were measured by micro BCA protein assay (Pierce Biotechnology, Rockford, IL, USA).

Production of Rosetta Gami Extract to Block Background Binding in ELISA

Rosetta gami extract for use in ELISA was produced from uninduced pET21a-TRX transformed overnight cultures. Bacteria were harvested at 4,500 rpm, 10 min, 4°C (Rotina 420R, Hettich) and washed 3 times with PBS. The pellet (originating from 200 ml overnight culture) was resuspended in 10 ml 0.5 M urea and sonicated for 15 cycles 20 s on and 30 s off (amplitude 22–26 microns, Soniprep 150 MSE). Bacterial lysates were centrifuged at 4,500 rpm, 10 min, 4°C (Rotina 420R, Hettich) and supernatants saved at −20°C until use.

Western Blot

Cell lysate of Os-P0107 and CT26 was obtained using RIPA buffer (Cell Signaling Technology, Danvers, MA, USA) with the addition of HALT protease/phosphatase inhibitor 1:100 (Thermo Fisher Scientific) and stored at −20°C until use. Protein concentration was measured by Nanodrop ND-1000 spectrophotometer (Isogen Life Science).

Samples were separated by SDS-PAGE on a precast 4–20% gradient polyacrylamide gel (Mini-Protean TGX gel, Bio-Rad Laboratories). Thereafter, proteins were transferred/blotted to a methanol activated nitrocellulose membrane [Immobilon® PVDF (polyvinylidene) membrane (Merck Millipore, Darmstadt, Germany)] in a Bio-Rad blotting system with transfer buffer

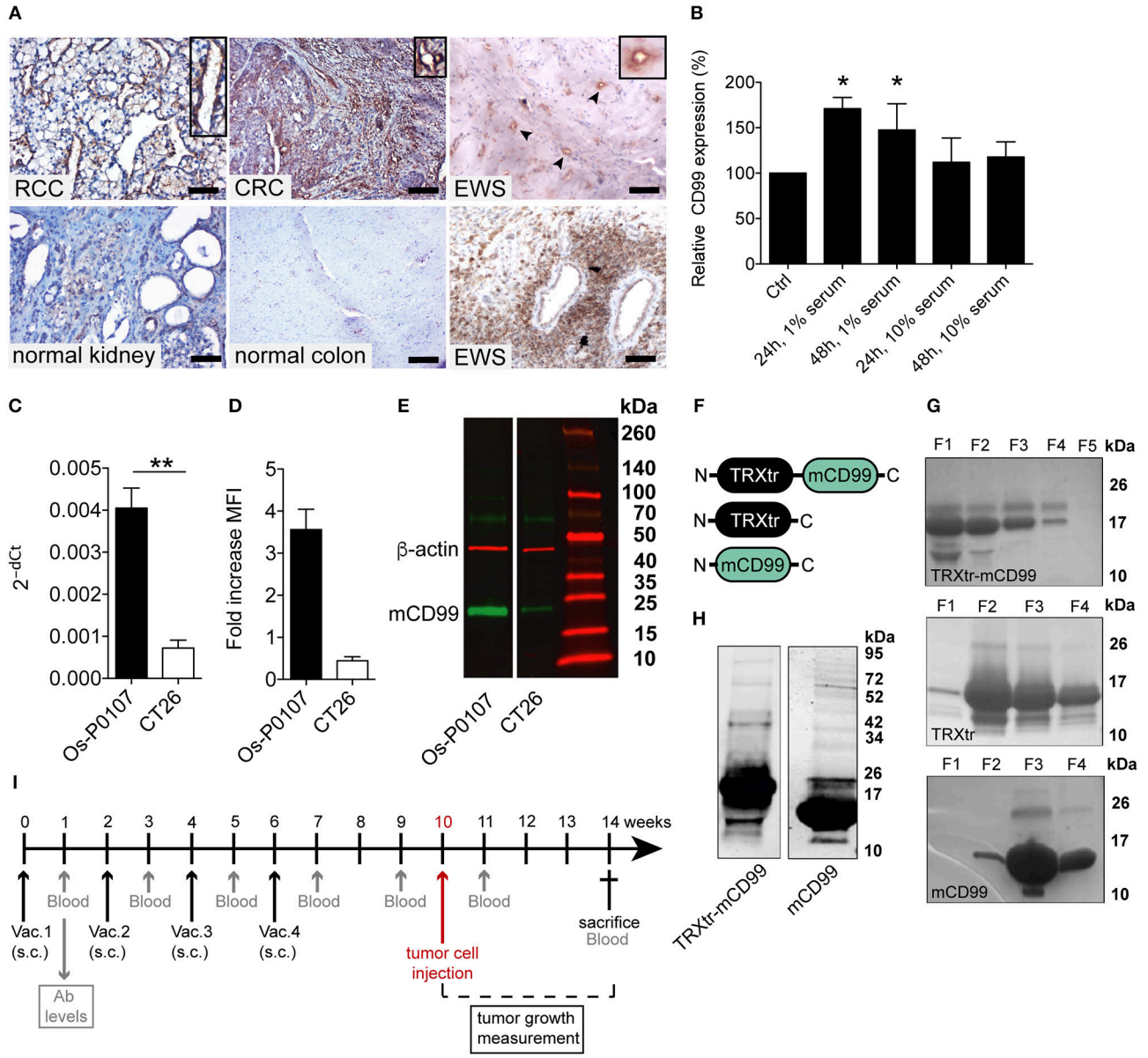

FIGURE 1 | CD99 expression in the vasculature of solid tumors and in the mouse tumor cell lines used; purification of vaccine proteins. **(A)** Tumor and normal tissue stained for CD99. Clear expression of CD99 in the tumor vasculature can be observed in renal cell carcinoma (RCC), colorectal cancer (CRC) and Ewing sarcoma (EWS) (upper row). Inlays show enlargement of CD99 staining in the tumor vessels. Normal healthy kidney and colon are devoid of CD99 (lower left panel and lower middle panel). In EWS both tumor cells (lower right panel) and the tumor endothelium (upper right panel, arrow heads and inlay) express CD99. (EWS, RCC, normal kidney: scale bar 50 μm; CRC and normal colon: scale bar 35 μm). **(B)** Expression of CD99 is increased in serum starved HUVEC. HUVEC were cultured for 24 or 48 h under normal conditions in culture medium supplemented with 20% serum (control, Ctrl) or in medium supplemented with only 1 or 10% serum ($n = 3$). CD99 expression was determined by flow cytometry analysis of non-fixated cells. Means were compared using a Mann-Whitney U test (*$P < 0.05$). **(C)** Relative expression (2^{-dCt}) of mouse CD99 mRNA in Os-P0107 (black bar) and CT26 tumor cells (white bar); **$P < 0.01$. **(D)** FACS analysis of CD99 surface expression in Os-P0107 and CT26 tumor cells. **(E)** Western blot analysis of total cell lysates of Os-P0107, and CT26 cells stained with antibodies against murine CD99 (24–30 kDa) and actin (42 kDa). Both Os-P0107 and CT26 cells show clear CD99 protein expression. CT26 cells have low levels of CD99. **(F)** Schematic representation of the recombinant fusion protein TRXtr-mCD99 used for vaccination of mice and the proteins TRXtr (used for vaccination of control mice) and mCD99 used to measure anti-CD99 antibodies in the sera of the vaccinated mice. **(G)** Appearance of TRXtr-mCD99 (18 kDa), TRXtr dimer (15 kDa) and mCD99 (11 kDa) proteins on reducing SDS-PAGE after elution from the Ni-NTA agarose with imidazole. For each protein all eluted fractions **(F)** are shown. **(H)** Western blot of TRXtr-mCD99 and mCD99 to confirm protein identity. **(I)** Illustration of the experimental set-up. Mice are vaccinated four times (Vac.; black arrows). At set time-points blood samples are taken for measurement of anti-mCD99 antibodies in the sera of the mice (blood; gray arrows). When anti-mCD99 levels are high, tumor cells are injected subcutaneously into the left flank of the mice (red arrow). Tumors are allowed to grow 3–4 weeks before the mice are sacrificed (cross).

(500 mM Glycine, 50 mM Tris-HCl, 0.01% SDS, 20% methanol; Bio-Rad) at 100 V for 2 h on ice. The membrane was washed with 0.05% Tween-20/PBS and blocked with 5% BSA (Roche, Woerden, The Netherlands)/PBS-T 0.05% for 1 h before incubation with the primary antibody, goat polyclonal anti-mouse CD99 (AF3905, R&D Systems) 1:1,000 in 1% BSA/PBS-T 0.05% overnight at 4°C. The next day the membrane was incubated with the secondary antibody, biotinylated rabbit polyclonal anti-goat antibody (E0466, 1.6 g/l Dako Cytomation) 1:600 in 1% BSA/PBS-T 0.05% for 45 min followed by Streptavidin IRDye 800CW (cat no. 926-32230, LI-COR Biosciences, Lincoln, NE, USA) 1:10 000 in 1% BSA/PBS-T 0.05% for 30 min, both at room temperature in the dark. After this step, the blot was washed overnight in PBS-T 0.05% and the next day incubated with rabbit anti-mouse β-actin antibody (cat no. 49675, Cell Signaling Technology, Leiden, The Netherlands), dilution 1:1,000, for 1 h at RT and donkey anti-mouse IRDye 680RD antibody (cat no. 925-68072, LI-COR Biosciences) diluted 1:10 000 for 30 min at RT. After each incubation step membranes were washed with 0.05% Tween-20/PBS and with PBS prior to imaging with the Odyssey Infrared Imaging System (Model 9120, LI-COR Biosciences).

For staining of human CD99 the membrane was blocked with 5% BSA/PBS-T 0.05% and incubated with rabbit anti-human CD99 polyclonal antibody (ab27271, Abcam) diluted 1:200 in 1% BSA/PBS-T 0.05% overnight at 4°C. The next day the membrane was incubated with goat anti-rabbit IRDye 800CW antibody (cat no. 926-32211, LI-COR Biosciences) diluted 1:10,000 in 1% BSA/PBS-T 0.05%. Washing steps were performed as described above. The blot was stored overnight in PBS and blocked the next day with 5% non-fat dry milk (blotting-grade blocker, cat no. 170-6404, Bio-Rad Laboratories)/PBS-T 0.1%. After that the membrane was stained overnight at 4°C with mouse monoclonal anti-human β-actin antibody (cat no. #3700, clone 3H10D10, Cell Signaling Technology, Leiden, The Netherlands) diluted 1:1,000 in 1% non-fat dry milk/PBS-T 0.1%. As final step the membrane was incubated with donkey anti-mouse IRDye 680D (cat no. 925-6872, LI-COR Biosciences) diluted 1:10,000 in 1% non-fat dry milk/PBS-T 0.1%. All washing steps were performed with PBS-T 0.1% and performed as described above. The membrane was imaged with the Odyssey Infrared Imaging System (LI-COR Biosciences).

Animal Studies

Animal experiments were approved by the local Animal Ethics Committee of the VU University and the national Central Animal Experiments Committee (CCD) (reg. no. AngL14-01 and CCD AVD114002016576). Approximately 8-week old female C3H/HeNCrL mice (Charles River Laboratories, Leiden, The Netherlands) or BALB/c mice (Envigo, Horst, The Netherlands) were immunized four times with an interval period of 2 weeks. Each vaccine emulsion (100 μl per mouse, 50 μl per groin) contained 40 μg TRXtr (control group) or 100 μg TRXtr-mCD99 in a volume of 50 μl mixed with 50 μl Freund's complete adjuvant (F-5881, Sigma Aldrich) (ratio 1:1, aqueous phase: oil phase) for the priming immunization and Freund's incomplete adjuvant (F-5506, Sigma Aldrich) for booster immunizations. Emulsions were mixed for 30 min on a Vortex Genie (Fisher Scientific) at full speed. Four weeks after the last immunization 2×10^6 osteosarcoma (Os-P0107) cells were inoculated subcutaneously in the left flank of C3H mice in a total volume of 100 μl (10% culture medium/PBS). For the CT26 model 2×10^5 CT26 colon carcinoma cells were inoculated in the left flank of BLALB/c mice. Blood samples were taken from the tail vein 1 week after each immunization, 1 week prior to tumor cell injection, and 1 week after tumor cell injection and at the end of the experiment. Tumor growth was measured by calipers. Tumor volume was calculated by the formula: $\text{width}^2 \times \text{length} \times \pi/6$. At the end of the experiment mice were euthanized and tumors and organs were removed and stored in 1% PFA/PBS (Aurion, Wageningen, the Netherlands) overnight and consecutively paraffin embedded.

Long-Term Follow-Up After CD99 Vaccination

To address the safety of exposure to high antibody titers against CD99; control vaccinated (TRXtr, $n = 5$) and TRXtr-mCD99 vaccinated mice (CD99; $n = 5$) were included in the study for 45 weeks. Approximately 8-week old female C57BL/6 mice (Envigo) were immunized three times with an interval period of 2 weeks as described above. Blood samples were taken from the tail vein 1 week after each immunization. During the rest of the follow-up period monthly blood samples were taken. When antibody levels dropped below 50% of the levels after the third vaccination mice were revaccinated. In addition, body weight of the mice was monitored regularly during the whole study period. At the end of the experiment mice were euthanized and organs were removed, stored in 1% PFA/PBS (Aurion) overnight and paraffin embedded.

ELISA

Indirect ELISA was performed to determine total anti-mCD99 antibody levels. Blood samples were coagulated overnight at 4°C and centrifuged twice at 7,000 rpm for 10 min at 4°C in a microcentrifuge. The supernatant (serum) was stored at −20°C until use. Volumes used per well in ELISA were 50 μl, unless indicated otherwise. 96-well ELISA plates (Nunc A/S, Roskilde, Denmark) were coated with 2 μg/ml mCD99 protein and then blocked with 100% horse serum (100 μl/well) (Sigma-Aldrich), both for 1 h at 37°C. After a single wash with PBS (B. Braun Medical, Oss, The Netherlands) for 1 min, the plates were incubated with serum of TRXtr-mCD99 or TRXtr-vaccinated mice for 45 min at 37°C, diluted 1:10 in 100% horse serum, which was further diluted 1:15 in 10% Rosetta Gami extract (final serum dilution 1:150) to reduce non-specific binding of the serum. Thereafter, plates were incubated with biotinylated polyclonal goat anti-mouse Ig (E0433, Dako Cytomation) for 45 min and streptavidin-horseradish peroxidase (Strep-HRP) (Dako Cytomation) for 30 min, both diluted 1:2,000 in 0.01% PBS-T at 37°C. After each incubation step, plates were washed four times with PBS. HRP activity was detected with TMB substrate (T-8665, Sigma-Aldrich) and absorbance was measured at 655 nm after 15 min using a Biotek Synergy HT microplate reader (Biotek).

Statistical Analysis

Means were compared using a Mann–Whitney *U*-test or two-tailed student's *t*-test, if Gaussian distribution could be assumed. For comparison of tumor growth, a two-way ANOVA with Bonferroni post-test was used for repeated measurements at different time points. Values are depicted as mean ± SEM. All statistical tests were executed using GraphPad Prism 5.0 (GraphPad Software Inc., La Jolla, CA, USA). Values of $P < 0.05$ were considered statistically significant.

RESULTS

CD99 Is a Marker of Tumor Blood Vessels and Is Induced by Starvation

The Ewing's sarcoma (EWS) tumor marker CD99 was found to be overexpressed in the vasculature of different solid tumor types (**Figure 1A**; **Supplementary Figure 1A**), but CD99 was not expressed in normal healthy tissues. In endothelial cells, cultured *in vitro*, CD99 expression was upregulated upon 24 and 48 h of starvation ($p < 0.05$) (**Figure 1B**).

Expression of CD99 in Murine Tumor Cell Lines

In order to determine the CD99 expression in the murine osteosarcoma (Os-P0107) and colon carcinoma (CT26) cell lines qPCR primers were designed to determine the expression of endogenous CD99 (mCD99; RefSeq NP_079860.2. NM_025584.2.; GI: 125660452) (**Table 1**). Expression of CD99 at the mRNA level was confirmed in both cell lines (**Figure 1C**). The CT26 cell line was observed to express significantly lower levels of CD99 than the Os-P0107 cell line [($^{**}P < 0.01$); **Figure 1C**, white bar]. At the protein level, flow cytometry was used to check for surface expression of CD99. These data indicated a higher surface expression of CD99 on Os-P0107 cells compared to the CT26 cell line (**Figure 1D**). In order to clearly distinguish any difference in CD99 protein level between the two cell lines we performed a Western blot analysis (**Figure 1E**) on cell lysate. Indeed, the Western blot confirmed that the osteosarcoma cells express high levels of murine CD99 (24 kDa, green band) and that CD99 expression in the CT26 cell line is much lower. β-actin (42 kDa, red band) was used as a loading control. In addition, the ratio of the CD99 and β-actin bands was quantified with ImageJ software and the osteosarcoma cell line showed a higher CD99/β-actin ratio than the CT26 cell line (Os-P0107 ratio: 1.77; CT26 ratio: 0.46) (**Table 5**).

TABLE 5 | Western blot quantification CD99 expression cell lines.

	Band area CD99	Band area b-actin	Ratio CD99/b-actin
Os-P0107	6045.447	3411.870	1.77
CT26	876.648	1891.920	0.46

Design/Construction of a CD99 Targeting Vaccine

The overexpression of CD99 in human tumor vasculature prompted us to study the role of the molecule in tumor growth. To that end, we planned to vaccinate against CD99, using the conjugate vaccine technology that we recently published (26). The extracellular part of murine CD99 ($mCD99_{extracellular}$, 111aa; RefSeq NP_079860.2. NM_025584.2.; GI: 125660452) (36) was used as the self-antigen to be fused to truncated bacterial thioredoxin (TRXtr, 58aa) (26), resulting in the fusion protein TRXtr-mCD99 (**Figure 1F**).

The TRXtr protein was produced for vaccination of control mice and mCD99 for detection of anti-mCD99 antibodies in serum by ELISA (**Figure 1F**). All proteins were soluble (**Figure 1G**). Protein identity of TRXtr-mCD99 and mCD99 was confirmed by Western blot analysis (**Figure 1H**).

Vaccination Against CD99 Inhibits Tumor Growth

C3H mice were vaccinated with TRXtr-mCD99 (CD99; $n = 10$) or TRXtr (control group; $n = 5$). At week 10, when the mice were hyperimmune and had high antibody titers against murine CD99 in their sera, osteosarcoma (Os-P0107) tumor cells were injected into the left flank (see experimental set-up **Figure 1I**). Blood samples were collected 1 week after each vaccination, 1 week prior to tumor cell injection, 1 week after tumor cell injection and at the end of the experiment. In two independent experiments the mice responded with the production of anti-mCD99 antibodies (**Figures 2A,B**; **Supplementary Figure 2A,B**). Indeed, when antibodies against CD99 were present in the sera of the mice, tumor growth of osteosarcoma (Os-P0107) was significantly inhibited compared to control vaccinated mice ($^{**}P < 0.01$; **Figure 2F**). We also investigated if tumor growth of the CD99 low CT26 colon carcinoma (**Figure 2D**, lower panel) could be inhibited after vaccination against CD99. All TRXtr-mCD99 (CD99 group; $n = 5$) vaccinated BALB/c mice responded with the production of anti-mCD99 antibodies (**Figure 2C**, one mouse died of unrelated cause). Also, in this study a significant difference in tumor growth between the TRXtr-mCD99 group and control group (TRXtr group; $n = 5$) could be observed ($^{**}P < 0.01$; **Figure 2I**), indicating that in this tumor model inhibition of tumor growth was mainly due to targeting of the tumor vasculature. During the study period no difference in body weight between the CD99 vaccinated and control-vaccinated mice was observed in all three different vaccination studies performed (**Supplementary Figure 2C**). This suggests that vaccination against CD99 is well-tolerated and safe. In addition, we investigated if the antibodies induced against CD99 would recognize native CD99 in tissue. Therefore, we stained tissue of Os-P0107 osteosarcoma tumors derived from TRXtr-vaccinated mice with serum of TRXtr-mCD99 (CD99) vaccinated mice or of control (TRXtr) vaccinated mice. A specific staining of CD99 in tumor tissue was observed as indicated by the arrows in the upper right panel of **Supplementary Figure 4A** and the arrowheads in the lower right panel (**Supplementary Figure 4A**).

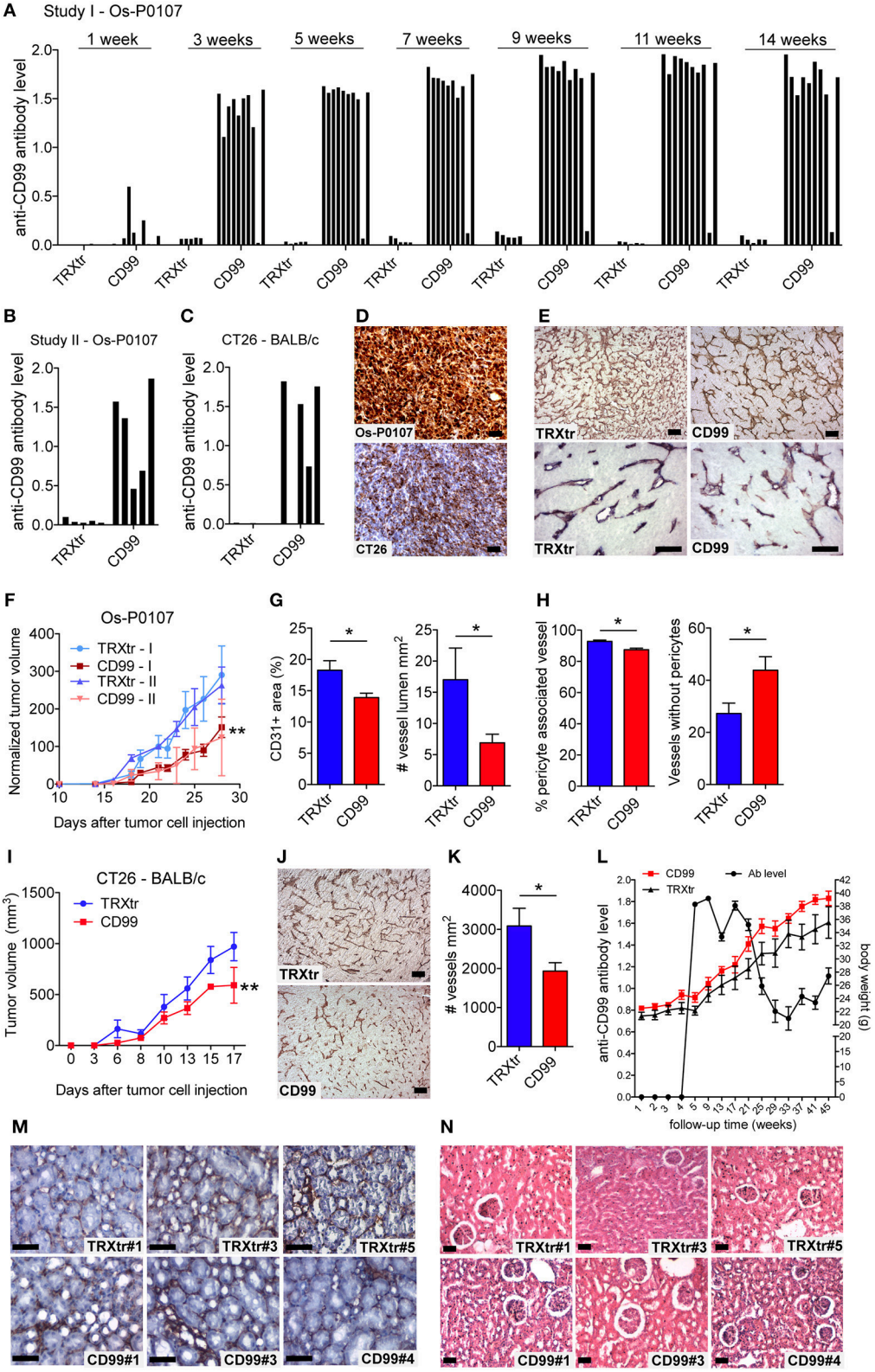

FIGURE 2 | Induction of a humoral immune response against CD99 inhibits tumor growth and is safe. **(A)** Anti-mCD99 antibody levels in the sera of the C3H mice (Os-P0107 model) at different time points (weeks) (1st study, Study I; $n = 10$, CD99). In the sera of TRXtr vaccinated mice ($n = 5$, TRXtr, control) no anti-mCD99

(Continued)

FIGURE 2 | antibodies were present. **(B)** Anti-mCD99 antibody levels in the sera of CH3 mice at time point week 9 (after four vaccinations, prior to tumor cell injection) (2nd study, Study II; $n = 5$, CD99). The control vaccinated mice ($n = 5$, TRXtr) did not have any anti-mCD99 antibodies. **(C)** Anti-mCD99 antibody levels in the sera of the BALB/c mice (CT26 model) after four vaccinations (week 7), prior to tumor cell injection. TRXtr-mCD99 vaccinated mice ($n = 4$, TRXtr-mCD99) responded with the production of anti-mCD99 antibodies, whereas in the sera of TRXtr vaccinated mice ($n = 5$, TRXtr, control) no anti-mCD99 antibodies were present. **(D)** Immunohistochemistry staining of CD99 of Os-P0107 (upper panel) and CT26 tumors (lower panel) (8 μm scale bar). CD99 expression in Os-P0107 is higher than in CT26 tumors. **(E)** Staining of the tumor vasculature (CD31) of Os-P0107 tumors of control vaccinated (TRXtr, left upper panel, scale bar 35 μm) and TRXtr-CD99 vaccinated mice (CD99, right upper panel, scale bar 35 μm). Lower panels show double staining of the tumor vasculature with CD31 (red) and desmin (blue), a pericyte marker (scale bars 50 μm). **(F)** Tumor growth curves of Os-P0107 in TRXtr-mCD99 vaccinated (CD99; red curves) and control vaccinated mice (TRXtr; blue curves). In both studies (Study I and II) tumor growth was significantly inhibited in TRXtr-mCD99 vaccinated compared to control vaccinated mice. Tumor volume was normalized and growth curves were compared by two-way ANOVA ($^{**}P < 0.01$). **(G)** Vessel density of osteosarcoma tumor tissue [CD31+ area (%)]. Vessel density was determined of 3 representative fields per tumor (magnification 100x). Tumors from TRXtr-mCD99 vaccinated mice (CD99; $n = 9$; red bars) had a lower vessel density compared to control vaccinated mice (TRXtr; $n = 4$; blue bars), (left panel, $^{*}P < 0.05$). The number of clear lumina found per field of osteosarcoma tumor (Os-P0107) tissue (magnification 100x, 3 fields per tumor). Mice vaccinated with TRXtr-mCD99 (CD99) had a significantly lower lumen count compared to control vaccinated mice (TRXtr) (right panel, $^{*}P = 0.05$). **(H)** Percentage of vessels associated with pericytes in osteosarcoma tumors. The number of vessels with and without pericytes was manually counted of 10 fields per tumor (magnification 200x). The number of vessels associated with pericytes was divided by the total number of vessels per tumor. Tumors of TRXtr-mCD99 vaccinated (CD99, red bars) mice had a significantly lower pericyte coverage compared to control vaccinated (TRXtr, blue bars) tumor tissue (left panel, $^{*}P < 0.05$). In addition, in tumors of TRXtr-mCD99 vaccinated mice significantly more vessels were found without pericytes than in tumors of control vaccinated mice (right panel, $^{*}P < 0.05$). **(I)** Tumor growth curves of CT26 in TRXtr-mCD99 vaccinated (CD99; red curve) and control vaccinated BALB/c mice (TRXtr; blue curve). Vaccination against CD99 significantly inhibited tumor growth in the CT26 tumor model as well (two-way ANOVA; $^{**}P < 0.01$). **(J)** Representative images of CD31 stained CT26 tumors of control vaccinated mice (TRXtr, upper panel) and TRXtr-mCD99 vaccinated mice (CD99, lower panel) (scale bars 35 μm). **(K)** Vessel density of CT26 tumor tissue. Vessel density was determined of 3 fields per tumor (magnification 100x). Significantly fewer vessels were counted in tumors of TRXtr-mCD99 vaccinated mice (CD99; $n = 4$; blue bar) compared to control vaccinated mice (TRXtr; $n = 3$; red bar) ($^{*}P < 0.05$). **(L)** Vaccinated mice with high anti-CD99 antibody levels in their blood (antibody level is shown on the left y-axis; curve with marked black circles) were followed-up for a period of 45 weeks. No difference in body weight (right y-axis) between TRXtr-mCD99 vaccinated (CD99, red curve, squares) and control vaccinated mice (TRXtr, black curve, triangles) was found between the groups. Values are depicted as mean ± SEM. **(M)** Kidneys stained for CD31 (brown-reddish staining) of TRXtr-mCD99 (CD99) and control vaccinated (TRXtr) mice from the long-term follow-up study (time point 45 weeks). Tissues were counter stained with Mayer's hematoxylin (blue) (scale bar 50 μm). No difference in tissue morphology was found between TRXtr-mCD99 vaccinated and control vaccinated mice. **(N)** Hematoxylin eosin staining of kidneys of TRXtr-mCD99 (CD99) and control vaccinated (TRXtr) mice from the long-term follow-up study (time point 45 weeks) (scale bar 35 μm). No difference in tissue morphology was observed between the CD99 and TRXtr group, indicating that vaccination against CD99 is safe.

Vaccination Affects the Tumor Vasculature

Osteosarcoma tumor tissue of the first vaccination study (study I) was stained for the vascular marker CD31 to determine the effect of vaccination against CD99 on the tumor vasculature (**Figure 2E**, upper panels). Vaccination with TRXtr-mCD99 seemed to have an effect on the morphology of the vasculature of osteosarcoma tumors (**Figure 2E**, upper panels). More specifically, tumors retrieved from TRXtr-mCD99 vaccinated mice (CD99, red bars) were found to have a significantly lower vessel density ($^{*}P < 0.05$) and lumen count ($^{*}P = 0.05$) compared to tumors retrieved from control vaccinated mice (TRXtr, blue bars) (**Figure 2G**). In the CD99 low CT26 tumor model also a significantly lower vessel density ($^{*}P < 0.05$) was found in tumors of CD99 vaccinated mice (**Figures 2J,K**).

Furthermore, we stained the osteosarcoma tumors for both the vessel marker CD31 and the pericyte marker Desmin to study the effect of vaccination on vessel functionality. As illustrated in **Figure 2E** (lower panels) and **Figure 2H**, a significantly lower pericyte coverage was found in TRXtr-mCD99 vaccinated tumor tissue (red bars) compared to TRXtr vaccinated tumor tissue (blue bars) ($^{*}P < 0.05$, **Figure 2H**, left panel). Furthermore, tumors of CD99 vaccinated mice were found to have more vessel without pericytes than control vaccinated mice ($^{*}P < 0.05$, **Figure 2H**, right panel).

Induction of a Humoral Immune Response Against CD99 Is Safe

During the experimental period of 14 weeks of the tumor growth study we did not observe any toxicity of the TRXtr-mCD99 vaccine as addressed by body weight or macroscopic and behavioral characteristics between CD99 vaccinated and control-vaccinated mice. However, to further investigate the safety of the vaccine we vaccinated healthy C57BL/6 mice against CD99 and monitored their body weight over a period of 45 weeks (**Figure 2L**). The mice were kept with high anti-CD99 antibody levels during the whole study period. Once the anti-CD99 antibody level dropped below 50% of the starting level (the antibody level after the third vaccination) the mice were re-vaccinated. Control mice were vaccinated with the TRXtr protein. During the whole study period we did not observe any difference in body weight between the CD99 group and the control vaccinated mice (**Figure 2L**). In addition, all except one mouse in the CD99 group, which was lost to follow-up at week 35, were healthy during the whole study period. We also looked at the morphology of the organs of CD99 vaccinated and control mice, but did not find any changes in tissue morphology after vaccination against CD99 (**Figures 2M,N**; **Supplementary Figures 2D, 3**). All together these observations indicate that vaccination against CD99 is safe.

A Distinct Human CD99 Isoform Is Present in Activated Endothelial Cells

In literature two different human CD99 isoforms have been described (27). A long full-length isoform (185 amino acids, 32 kDa, variant I; **Supplementary Figure 1C**) and a short truncated isoform (161 amino acids, 28 kDa, variant II), lacking most of the cytoplasmic domain. In the NCBI database six different protein coding human CD99 splice variants are suggested (Gene ID: 4267) (30) (**Figure 3A**). To distinguish the different human CD99 isoforms, as described in the NCBI database (**Table 6**),

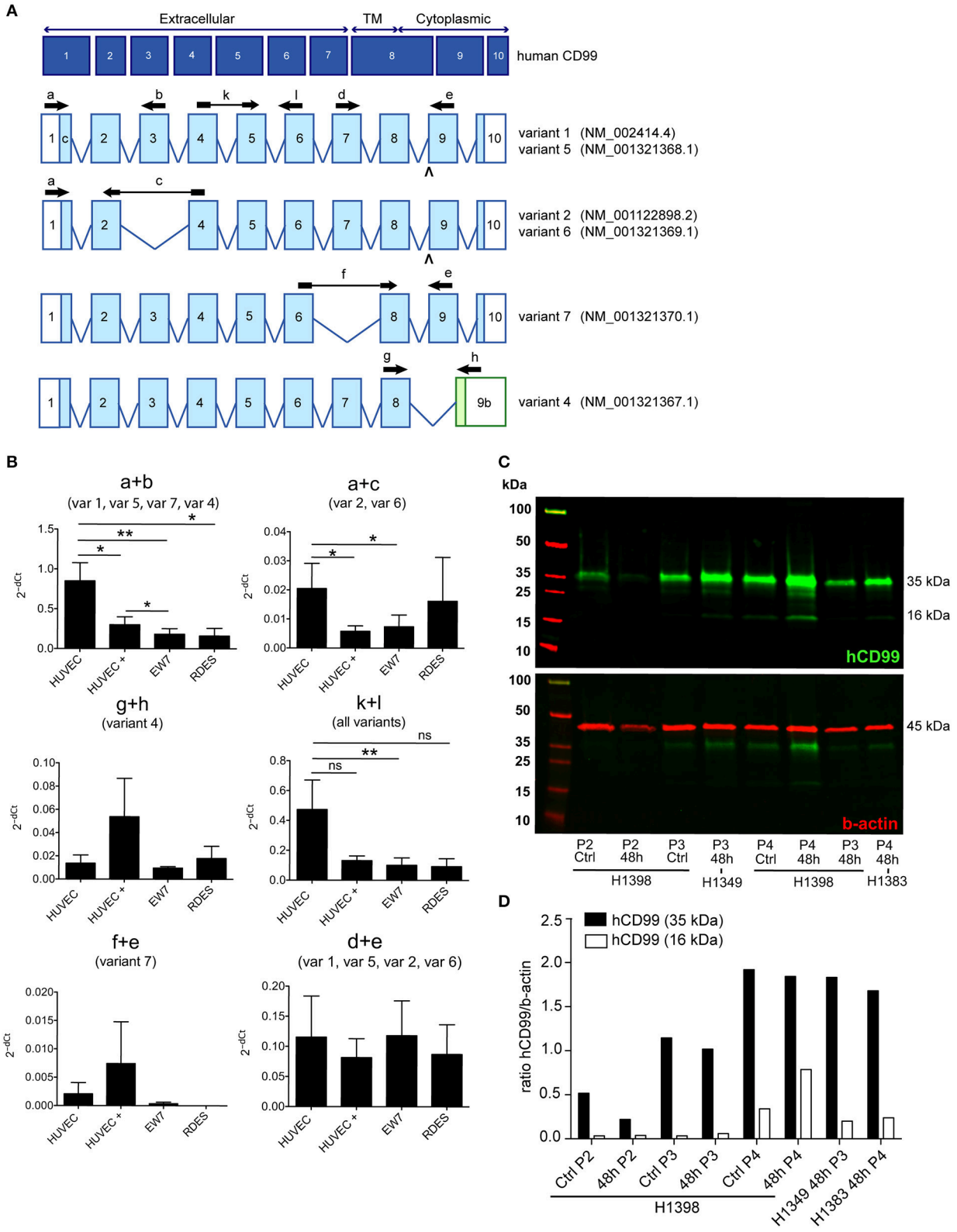

FIGURE 3 | A distinct human CD99 isoform is present in activated endothelial cells. **(A)** Schematic representation of the human CD99 molecule and its exons (dark blue). The extracellular part (extracellular), the transmembrane region (TM) and the cytoplasmic domain (cytoplasmic) are indicated. Depicted in light blue are the

(Continued)

FIGURE 3 | different human CD99 isoforms (variants) retrieved from the NCBI database (CD99 molecule *Homo sapiens*, Gene ID: 4267). Accession numbers of the individual isoforms are indicated in brackets. Light blue exons are protein coding; UTRs are depicted in white. The inverted "v" below exon 9 indicates the presence of an additional alanine at the start of the exon and thereby a different variant (var) (variant 5 or 6). RT-qPCR-primers used for identification: the primer pair k + l detects all human CD99 variants (pan; total CD99). Primer pair d + e identifies variant 1, 5, 2, and 6. Primer pair a + b was used to detect the full-length CD99 isoform (var 1, var 5) and the variants 7 and 4. Primer pair a + c detects variant 2 and 6, which lack exon 3 in the extracellular domain. Primer pair f + e was used to identify variant 7, lacking exon 7. Primer pair g + h detects the truncated CD99 isoform (var 4, isoform **(C)**. **(B)** In activated HUVEC (HUVEC +; $n = 9$), EW7 ($n = 11$) and EWS-RDES (RDES; $n = 3$) relative expression (2^{-dCt}) of total CD99 is downregulated on mRNA level (k + l; all variants). For native HUVEC (HUVEC; n=6) vs. EW7 this is statistically significant (**$P <$ 0.01) and for HUVEC vs. activated HUVEC (HUVEC +) [$P = 0.0905$; k + l)] and RDES ($P =$ 0.0833; k + l) there is a trend toward significance. The observed difference of a + c between native and activated HUVEC (*$P < 0.05$) and EW7 (*$P < 0.05$) is due to that there is more total CD99 present (k + l primers) in native HUVEC compared to activated HUVEC. The ratio a + c/k + l is similar for both cell types (HUVEC = 0.04327756; HUVEC + = 0.0440165). A higher signal for the a + b primer pair is observed in native HUVEC compared to activated HUVEC+ (*$P < 0.05$), EW7 (**$P < 0.01$) or RDES (*$P < 0.05$). However, the ratio a + b/k + l is similar for all cell types (**Table 7**). The main isoform present in growth factor activated HUVEC (HUVEC+) is variant 4 (the short CD99 isoform, isoform **(C)**, identified by primer pair g + h. **(C)** Western blot of cell lysates from control treated HUVEC (Ctrl) and HUVEC grown for 48 h in culture medium supplemented with 1% serum (48 h). Different passages (P2–P4) of the same HUVEC (H1398) were used and P3 and P4 of different HUVEC (H1349 and H1383, respectively). The upper panel shows CD99 expression in the cell lysates (green). A protein band of 35 kDa can be observed in all lysates, with increasing passages a 16 kDa band is induced. In the lower panel the same Western blot is shown as in the upper panel, but now stained for β-actin (45 kDa; red), which was used as a loading control. **(D)** Data of the Western blot were quantified with ImageJ software. Expression of CD99 is induced in activated HUVEC; cells in higher passages express more CD99 (35 kDa band, black bars). In addition, there is a trend toward induction of expression of the 16 kDa band (white bars, the short CD99 isoform; isoform **(C)** with higher passage and by starvation of the cells.

TABLE 6 | Human CD99 isoforms listed in the NCBI database.

Gene	Variant	Protein	Isoform	Size (kDa)
NM_002414.4	Variant 1	NP_002405.1	Isoform A	18.8
NM_001122898.2	Variant 2	NP_001116370.1	Isoform B	17.1
NM_001321367.1	Variant 4	NP_001308296.1	Isoform C	16.0
NM_001321368.1	Variant 5	NP_001308297.1	Isoform D	18.8
NM_001321369.1	Variant 6	NP_001308298.1	Isoform E	17.0
NM_001321370.1	Variant 7	NP_001308299.1	Isoform F	17.2

TABLE 7 | Ratio variant specific primers vs. total CD99 (k + l primers).

	Ratio a + b/k + l	Ratio a + c/k + l	Ratio g + h/k + l
HUVEC	1.640392	0.043278	0.0290038
HUVEC+	2.280937	0.044017	0.408618
EW7	1.794606	0.072968	0.0949811
RDES	1.736055	0.175196	0.1944184

we designed RT-qPCR primers specific for the different splice variants (**Figure 3A** and **Table 2**). In **Supplementary Figure 5** the different human CD99 splice variants retrieved from the NCBI database (**Supplementary Figure 5A**) and the Ensembl database (**Supplementary Figure 5B**) and their protein sequences (**Supplementary Figure 5C**) are depicted.

In activated HUVEC (HUVEC+; $n = 9$), EW7 ($n = 11$), and EWS-RDES (RDES; $n = 3$) expression of total CD99 (k + l primers; all variants) is downregulated on mRNA level (**Figure 3B**). For native HUVEC (HUVEC; $n = 6$) vs. EW7 this is statistically significant (**$P < 0.01$) and for HUVEC vs. activated HUVEC (ns $P = 0.09$) and RDES (ns $P = 0.08$) there is a trend toward significance. The difference in expression found with the a + b and a + c primers in native HUVEC is due to high expression of total CD99 (k + l primers) in native HUVEC compared to the other cell types; as determined by the ratio of a + b/k + l and a + c/k + l (**Table 7**). On mRNA level however, there is a trend toward a higher expression of the short human CD99 isoform variant 4 (g + h primers; **Table 7**).

Western blot was performed on cell lysates of growth factor activated and serum starved HUVEC to determine if the short CD99 isoform could be detected on protein level. In activated HUVEC, after several passages (>P2) in culture, an additional protein band around 16 kDa can be observed next to the 35 kDa band of human CD99 (**Figure 3C**, green bands, upper panel). β-actin was used as a loading control (**Figure 3C**, 45 kDa, red band, lower panel). We quantified the ratio of the human CD99 bands (35 kDa, black bars; and 16 kDa, white bars) and β-actin with ImageJ software (**Figure 3D**, **Table 8**) and found that expression of CD99 is induced in activated HUVEC; cells in higher passages express more CD99 (35 kDa band, black bars). In addition, there is a trend toward induction of expression of the 16 kDa band (white bars, the short CD99 isoform; isoform C) with higher passage and after starvation of the cells for 48h.

Peripheral blood mononuclear cells (PBMC) of healthy volunteers only express CD99 at low levels (**Supplementary Figure 4B**). The main CD99 variants detected in PBMC were variant 1, variant 5, variant 7, and variant 4 (primer pair a + b), of which variant 7 (primer pair f + e) was basically undetectable (data not shown).

We also isolated mRNA from human colorectal carcinoma and renal cell carcinoma and matching healthy tissue, but were not able to determine any conclusive CD99 isoform expression pattern. This is most likely due to the fact that only 1–2% of all cells present in a tumor are endothelial cells and therefore it is very difficult to pick up specific splice variants.

These results indicate that CD99 splicing is tissue specific and provide an opportunity for specific targeting of CD99 isoforms in human tumor vasculature.

DISCUSSION

It was previously described that CD99 is overexpressed in inflamed vasculature. Our study demonstrated that CD99 is also

TABLE 8 | Western blot quantification hCD99 expression in HUVEC.

	Band area b-actin	Band area hCD99 (35 kDa)	Band area hCD99 (16 kDa)	Ratio hCD99 (35 kDa)/b-actin	Ratio hCD99 (16 kDa)/b-actin
H1398 Ctrl P2	6835.426	3532.154	239.092	0.51674234	0.03497836
H1398 48 h P2	3108.770	686.284	116.950	0.22075741	0.03761938
H1398 Ctrl P3	5808.891	6647.004	199.971	1.14428107	0.03442499
H1398 48 h P3	5428.841	9946.832	1095.820	1.83222017	0.20185156
H1398 Ctrl P4	4948.770	9503.489	1683.820	1.92037395	0.34025020
H1398 48 h P4	5567.255	10257.631	4373.962	1.84249347	0.78565864
H1349 48 h P3	4026.698	4097.447	239.092	1.01756998	0.05937669
H1383 48 h P4	4014.113	6741.518	956.577	1.67945397	0.23830346

overexpressed in the vasculature of solid tumors. CD99 is also known as a marker of Ewing's sarcoma (EWS). A therapeutic vaccination approach against CD99 could be of benefit for EWS patients. In addition, vaccination against CD99 could be used to treat other solid tumors by means of targeting the tumor vasculature.

For construction of the vaccine fusion protein TRXtr-mCD99, we used the protein sequence of the extracellular part of murine CD99 as described in Bixel et al. (36). We show that it is possible to induce a polyclonal antibody response against the self-antigen CD99 in immunocompetent mice by vaccination. Vaccination induced high levels of anti-mCD99 antibodies in the sera of the mice. This confirms the findings of previous studies using the same vaccination strategy for the induction of antibodies against different self-antigens (23, 24, 37).

In three independent studies a significantly smaller tumor volume was measured in the TRXtr-mCD99 vaccinated mice compared to control vaccinated mice. In this context, it is important to keep in mind that our vaccination strategy induces a polyclonal antibody response that is much more effective in inducing immune system activation than monocloncal antibodies (38). A polyclonal antibody response induces antibody-dependent cellular cytotoxicity (ADCC) where the antibodies function as a recognition and binding site for non-specific toxic cells like natural killer cells and macrophages. It also induces complement-dependent cytotoxicity (CDC) where the antibodies activate the complement system which leads to the formation of the membrane attack complex (MAC) and subsequent lysis of the target cell (39, 40).

In the CT26 model only low levels of CD99 are expressed by the tumor cells as compared to the osteosarcoma model. However, in the CT26 model also a significantly lower vessel density was observed in tumors of CD99 vaccinated mice. It is therefore likely that tumor growth inhibition in the CT26 model is mainly due to targeting of the tumor vasculature by the CD99 vaccine. The osteosarcoma model highly expresses CD99 and therefore inhibition of tumor growth in this model is due to targeting of both the tumor vasculature and the tumor cells, which leads to a more pronounced anti-tumor effect.

Anti-CD99 antibodies induced by the TRXtr-mCD99 were able to detect native CD99 in osteosarcoma tumor tissue. However, a lot of background staining was observed when the sections were stained with serum from CD99 vaccinated mice. This can be explained by the fact that staining mouse tissue with murine antibodies is difficult. We therefore used a F(ab) fragment to prevent non-specific binding of the serum. However, with this approach still a lot of background staining was observed. We have considered to purify IgG from mouse serum or to specifically purify the anti-CD99 antibodies in the serum with antigen, but we did not have sufficient mouse serum to do so.

After vaccination against CD99 we found more vessels without pericytes in the osteosarcoma tumors. This indicates that vascular targeting leading to vessel destruction occurs rather than vascular normalization after which a higher pericyte coverage is expected (41, 42). Vascular normalization is characterized by neutralization of growth factors, such as vascular endothelial growth factor (VEGF) (43). Neutralization of VEGF results in a more quiescent vasculature with more pericyte coverage and improved vascular flow. Vascular targeting on the other hand, leads to killing of the tumor endothelial cells, since these are attacked and removed by the immune system. This would explain our observations of a lower number of vessels with a lumen and pericytes in the tumors of CD99 vaccinated mice. As, the target CD99 is a transmembrane molecule tissue bound frustrated phagocytosis will occur (23) and not only the endothelial cells will be destroyed but everything in their vicinity as well, including pericytes.

No toxicity of the vaccination against CD99 was observed. In the tumor growth studies, no weight loss of the mice occurred during the study period. In addition, we monitored the body weight and health condition of CD99 vaccinated mice, with constantly high anti-mCD99 antibody levels in their sera, and control vaccinated mice, for a period of 45 weeks. In this study one mouse (CD99#2) was lost to follow-up. Considering the good health of all other CD99 vaccinated mice, this was probably due to non-treatment related conditions. We scrutinized the morphology of the organs of control and CD99 vaccinated mice and did not observe any changes in tissue morphology related to the presence of anti-mCD99 antibodies, neither based on vessel staining (CD31) of kidney vasculature and hematoxylin eosin staining of heart, lung, kidney, and liver. For the mouse that

was lost to follow-up both the tissue and vessel morphology were normal/comparable to control vaccinated mice, implying that the loss of the mouse was probably not due side-effects of the vaccine. Taken together, our data suggest that vaccination against CD99 is safe, and provides a vascular targeting approach that lacks the risk of current angiostatic approaches for running into drug-induced resistance (44, 45).

Expression of CD99 was upregulated in growth factor activated HUVEC, resembling tumor endothelial cells, as determined by Western blot analysis. In addition, CD99 expression on cultured endothelial cells was induced by nutrient deprivation, which suggests that expression of CD99 in the tumor vasculature is most likely regulated by microenvironmental stress. We did not investigate if distinct CD99 isoforms are induced by starvation. To define which human CD99 isoform is the main variant present in the tumor vasculature we would need to perform a RT-qPCR on mRNA isolated from by flow cytometry sorted tumor endothelial cells. In literature, two distinct human CD99 isoforms have been described (27, 46). The full-length isoform (variant I, 32 kDa) and the truncated isoform (variant II, 28 kDa). Variant II includes a premature stop-codon caused by an insertion in the cytoplasmic domain and therefore lacks most of the cytoplasmic domain and is thought to be non-functional. The murine CD99 only shows 46% homology with human CD99 and resembles the human short isoform (28). However, if CD99 has the same function in mouse as in humans is unclear (29).

Currently, six different protein coding human CD99 isoforms are described in the NCBI database. We found contradictory results of CD99 expression on mRNA level and protein level in growth factor activated HUVEC. On mRNA level expression of CD99 seems to be downregulated in activated HUVEC, whereas on protein level CD99 expression is upregulated in activated HUVEC. On mRNA level the main CD99 isoform identified is variant 4, the short CD99 isoform, lacking part of the cytoplasmic domain. This is consistent with appearance of a 16 kDa protein band in higher passages of HUVEC and after starvation of the cells. If the 16 kDa protein band is a true splice variant of human CD99 is difficult to determine, since the anti-human CD99 antibody that we used is a polyclonal antibody that cannot distinguish between different splice variants. The human CD99 protein is highly O-glycosylated (47) and starvation of cells changes their glycosylation pattern (48), therefore the 16 kDa band observed in the Western blot might be nonglycosylated CD99. Also, in the Western blot a protein band between 35 and 25 kDa can be observed in some of the HUVEC cell lysates. We did however not further investigate if this could be a human CD99 splice variant.

In conclusion targeting of CD99 by vaccination inhibits tumor growth in different murine tumor models and is safe. Human CD99 is overexpressed in HUVEC and expression of CD99 is induced in culture and by nutrient deprivation. Also, a distinct human CD99 isoform is induced under these conditions, which is distinct form the isoforms expressed by EWS and healthy PBMC. These observations provide an opportunity for specific targeting of CD99 isoforms in human tumor vasculature.

DATA AVAILABILITY

All datasets generated for this study are included in the manuscript and/or the **Supplementary Files**.

AUTHOR CONTRIBUTIONS

EH designed research, performed experiments, analyzed data, and wrote the manuscript. IvdW, LF, LS, PvdL, and HH performed experiments, analyzed data, and edited the manuscript. JvB designed research, analyzed data, and edited the manuscript. VT designed research and edited the manuscript. AC performed experiments and edited the manuscript. AG designed research and wrote the manuscript.

ACKNOWLEDGMENTS

We thank the European Union (GENE-FP7-PEOPLE-2012-IEF, project ID: 328695 to EH) and the Dutch Cancer Society—Netherlands (VU 2012-5480 to JvB and AG and VU 2014-7234 to AG, VU 2018-2005412 to EH and AG) for financial support.

We also would like to thank Dr. Dan Duda, Dr. Peigen Huang, and Rakesh Ramjiawan from the Steele Laboratory for Tumor Biology, Department of Radiation Oncology, Massachusetts General Hospital, Harvard Medical School, Boston, USA for the murine Os-P0107 osteosarcoma cell line. We thank Tse Wong, Iris Koning, Karlijn van Loon, and Nadia Hammi for their valuable experimental contributions and Dr. Anna-Karin Olsson for the kind gift of the pET21-TRX vector.

SUPPLEMENTARY MATERIAL

The Supplementary Material for this article can be found online at: https://www.frontiersin.org/articles/10.3389/fimmu.2019.00651/full#supplementary-material

Supplementary Figure 1 | Expression of CD99 in the tumor vasculature and vaccination strategy. **(A)** Different tumor types and normal healthy tissues stained for CD99 obtained from the Human Protein Atlas (scale bar 10 μm) and own staining of Ewing's sarcoma (EWS, right panels; upper panel scale bar 10 μm; lower panel scale bar 50 μm). All tumor types show staining of CD99 in the tumor vasculature (in hepatic cancer and EWS indicated by arrow heads). **(B)** Illustration of the vaccination strategy required for breaking self-tolerance. (1) The fusion protein (TRXtr-mCD99$_{extracellular}$) mixed with a potent adjuvant is injected s.c. or i.m. (2) Antigen presenting cells (pink) will take up the fusion protein, digest it into self (mCD99) and foreign (TRXtr) peptides and present these peptides on their MHC class 2. (3) Foreign peptides are recognized by T-helper cells (Th, green) and these become activated. The presented self-peptides will not be recognized by the Th cells, since it is believed that all self-reactive T-cells are deleted in the thymus during development. (4) Auto-reactive B-cells (blue), existing in the circulation, recognize the self-part of the fusion protein via their B-cell receptor, internalize the fusion protein, and present self- and foreign peptides via MHC class II. The by the foreign peptides activated T-helper cells will now activate the auto-reactive B-cells, since they present the same foreign peptides. (4) The activated B-cells undergo clonal expansion and produce anti-self (mCD99) antibodies. By this means a polyclonal antibody response against the mCD99 is induced. **(C)** Schematic representation of the human CD99 protein: signal peptide (amino acids (aa) 1–22 (signal; white); extracellular domain aa 23–122 (extracellular; green); transmembrane region (TMR; pink) aa 123–147; cytoplasmic domain aa 148–185 (Cyto; orange). Retrieved from the uniport data base (UniProtKB—P14209 (CD99_human). **(D)** Illustration of the pET21a expression vector encoding TRXtr-mCD99. The TRXtr-mCD99$_{extracellular}$ DNA sequence was

inserted between the restriction sites *NdeI* and *XhoI* into the multiple cloning site (MSC). Protein expression is under the control of the IPTG-inducible T7*lac* promoter. Amp, *Ampicillin resistance gene*.

Supplementary Figure 2 | Additional data osteosarcoma study I and II, CT26 study and long-term follow-up study. **(A)** Antibody titers of anti-CD99 antibodies in the sera of TRXtr ($n = 5$; left panel) and TRXtr-mCD99 ($n = 10$; CD99; middle and right panel) vaccinated mice at time point 9 weeks of study I Os-P0107 (C3H mice). TRXtr vaccinated mice are devoid of anti-CD99 antibodies. **(B)** Anti-mCD99 antibody levels in the sera of the C3H mice (Os-P0107 model) at different time points (weeks) of study II ($n = 5$ mice per group). **(C)** Body weight of CD99 vaccinated (CD99; red) and control vaccinated mice (TRXtr; blue) of the osteosarcoma study I and II (left and middle panel) and the CT26 study (right panel). No difference in body weight between the treatment groups was observed in all three different studies. Values are depicted as mean ± SEM. [study I: TRXtr ($n = 5$); CD99 ($n = 10$); study II: TRXtr and CD99 ($n = 5$); CT26: TRXtr and CD99 ($n = 4$)] **(D)** Kidneys stained for CD31 (brown-reddish staining) of TRXtr-mCD99 ($n = 5$; CD99) and control vaccinated ($n = 5$; TRXtr) mice from the long-term follow-up study (time point 45 weeks). Tissues were counter stained with Mayer's hematoxylin (blue) (scale bar 50 μm). No difference in tissue morphology was found between TRXtr-mCD99 vaccinated and control vaccinated mice.

Supplementary Figure 3 | Morphology of normal organs of TRXtr-mCD99 and TRXtr vaccinated mice of the long-term follow-up study. **(A)** Hematoxylin eosin staining of organs (heart, lung, kidney, liver) of TRXtr-mCD99 ($n = 5$; CD99) and control vaccinated ($n = 5$; TRXtr) mice from the long-term follow-up study (time point 45 weeks) (scale bar 35 μm). No difference in tissue morphology was found between TRXtr-mCD99 vaccinated and control vaccinated mice.

Supplementary Figure 4 | Anti-mCD99 antibodies induced by the TRXtr-mCD99 vaccine recognize native CD99 in tumor tissue. **(A)** Os-P0107 tumor tissues from control vaccinated mice were stained with either serum derived from TRXtr-vaccinated mice (TRXtr, left panels) or TRXtr-CD99 vaccinated mice (CD99, right panels). The upper right panel shows specific staining of CD99 as indicated by the arrows. In the lower right panel specific staining for CD99 is indicated by the arrow heads. All sections show high background, because mouse serum was used on mouse tissue (upper panels, scale bars 35 μm; lower panels, scale bars 50 μm). **(B)** Relative expression (2^{-dCt}) of human CD99 variants in peripheral blood mononuclear cells (PBMC) ($n = 3$; three different healthy donors). Only low levels of CD99 are present on mRNA level in PBMC (k + l primer pair). The main variants detected in PBMC are variant 1, variant 5, variant 7, and variant 4 (var 1, var 5, var 7, var 4) identified by primer pair a + b.

Supplementary Figure 5 | Human CD99 splice variants. **(A)** Human CD99 variants described in the NCBI database Gene ID: 4267. **(B)** Human CD99 variants described in the Ensembl database Gene: CD99 ENSG00000002586. **(C)** Alignment of the protein sequences of the different human CD99 splice variants.

REFERENCES

1. Dejana E. Endothelial cell-cell junctions: happy together. *Nat Rev Mol Cell Biol.* (2004) 5:261–70. doi: 10.1038/nrm1357
2. Bixel MG, Li H, Petri B, Khandoga AG, Khandoga A, Zarbock A, et al. CD99 and CD99L2 act at the same site as, but independently of, PECAM-1 during leukocyte diapedesis. *Blood.* (2010) 116:1172–84. doi: 10.1182/blood-2009-12-256388
3. Schenkel AR, Mamdouh Z, Chen X, Liebman RM, Muller WA. CD99 plays a major role in the migration of monocytes through endothelial junctions. *Nat Immunol.* (2002) 3:143–50. doi: 10.1038/ni749
4. Watson RL, Buck J, Levin LR, Winger RC, Wang J, Arase H, et al. Endothelial CD99 signals through soluble adenylyl cyclase and PKA to regulate leukocyte transendothelial migration. *J Exp Med.* (2015) 212:1021–41. doi: 10.1084/jem.20150354
5. Lou O, Alcaide P, Luscinskas FW, Muller WA. CD99 is a key mediator of the transendothelial migration of neutrophils. *J Immunol.* (2007) 178:1136–43. doi: 10.4049/jimmunol.178.2.1136
6. Imbert AM, Belaaloui G, Bardin F, Tonnelle C, Lopez M, Chabannon C. CD99 expressed on human mobilized peripheral blood CD34+ cells is involved in transendothelial migration. *Blood.* (2006) 108:2578–86. doi: 10.1182/blood-2005-12-010827
7. Riggi N, Stamenkovic I. The biology of Ewing sarcoma. *Cancer Lett.* (2007) 254:1–10. doi: 10.1016/j.canlet.2006.12.009
8. Balamuth NJ, Womer RB. Ewing's sarcoma. *Lancet Oncol.* (2010) 11:184–92. doi: 10.1016/S1470-2045(09)70286-4
9. Hu-Lieskovan S, Zhang J, Wu L, Shimada H, Schofield DE, Triche TJ. EWS-FLI1 fusion protein up-regulates critical genes in neural crest development and is responsible for the observed phenotype of Ewing's family of tumors. *Cancer Res.* (2005) 65:4633–44. doi: 10.1158/0008-5472.CAN-04-2857
10. Miyagawa Y, Okita H, Nakaijima H, Horiuchi Y, Sato B, Taguchi T, et al. Inducible expression of chimeric EWS/ETS proteins confers Ewing's family tumor-like phenotypes to human mesenchymal progenitor cells. *Mol Cell Biol.* (2008) 28:2125–37. doi: 10.1128/MCB.00740-07
11. Amaral AT, Manara MC, Berghuis D, Ordó-ez JL, Biscuola M, Lopez-García MA, et al. Characterization of human mesenchymal stem cells from ewing sarcoma patients. Pathogenetic implications. *PLoS ONE.* (2014) 9:e85814. doi: 10.1371/journal.pone.0085814
12. Rocchi A, Manara MC, Sciandra M, Zambelli D, Nardi F, Nicoletti G, et al. CD99 inhibits neural differentiation of human Ewing sarcoma cells and thereby contributes to oncogenesis. *J Clin Invest.* (2010) 120:668–80. doi: 10.1172/JCI36667
13. Franzetti GA, Laud-Duval K, Bellanger D, Stern MH, Sastre-Garau X, Delattre O. MiR-30a-5p connects EWS-FLI1 and CD99, two major therapeutic targets in Ewing tumor. *Oncogene.* (2013) 32:3915–21. doi: 10.1038/onc.2012.403
14. Kreppel M, Aryee DN, Schaefer KL, Amann G, Kofler R, Poremba C, et al. Suppression of KCMF1 by constitutive high CD99 expression is involved in the migratory ability of Ewing's sarcoma cells. *Oncogene.* (2006) 25:2795–800. doi: 10.1038/sj.onc.1209300
15. Seol HJ, Chang JH, Yamamoto J, Romagnuolo R, Suh Y, Weeks A, et al. Overexpression of CD99 increases the migration and invasiveness of human malignant glioma cells. *Genes Cancer.* (2012) 3:535–49. doi: 10.1177/1947601912473603
16. Guerzoni C, Fiori V, Terracciano M, Manara MC, Moricoli D, Pasello M, et al. CD99 triggering in Ewing sarcoma delivers a lethal signal through p53 pathway reactivation and cooperates with doxorubicin. *Clin Cancer Res.* (2015) 21:146–56. doi: 10.1158/1078-0432.CCR-14-0492
17. Scotlandi K, Perdichizzi S, Bernard G, Nicoletti G, Nanni P, Lollini P, et al. Targeting CD99 in association with doxorubicin: an effective combined treatment for Ewing's sarcoma. *Eur J Cancer.* (2006) 42:91–6. doi: 10.1016/j.ejca.2005.09.015
18. O'Neill AF, Dearling JL, Wang Y, Tupper T, Sun Y, Aster JC, et al. Targeted imaging of Ewing sarcoma in preclinical models using a 64Cu-labeled anti-CD99 antibody. *Clin Cancer Res.* (2014) 20:678–87. doi: 10.1158/1078-0432.CCR-13-1660
19. Dworzak MN, Fröschl G, Printz D, Zen LD, Gaipa G, Ratei R, et al. CD99 expression in T-lineage ALL: implications for flow cytometric detection of minimal residual disease. *Leukemia.* (2004) 18:703–8. doi: 10.1038/sj.leu.2403303
20. Chung SS, Eng WS, Hu W, Khalaj M, Garrett-Bakelman FE, Tavakkoli M, et al. CD99 is a therapeutic target on disease stem cells in myeloid malignancies. *Sci Transl Med.* (2017) 9: eaaj2025. doi: 10.1126/scitranslmed.aaj2025
21. Vaikari VP, Jang M, Akhtari M, Alachkar H. CD99 is highly expressed in Acute Myeloid Leukemia (AML) and presents a viable therapeutic target. *Blood.* (2016) 128:1540
22. van Wanrooij EJ, de Vos P, Bixel MG, Vestweber D, van Berkel TJ, Kuiper J. Vaccination against CD99 inhibits atherogenesis in low-density lipoprotein receptor-deficient mice. *Cardiovasc Res.* (2008) 78:590–6. doi: 10.1093/cvr/cvn025
23. Huijbers EJ, Ringvall M, Femel J, Kalamajski S, Lukinius A, Abrink M, et al. Vaccination against the extra domain-B of fibronectin as a novel tumor therapy. *FASEB J.* (2010) 24:4535–44. doi: 10.1096/fj.10-163022

24. Femel J, Huijbers EJ, Saupe F, Cedervall J, Zhang L, RoswallP, et al. Therapeutic vaccination against fibronectin ED-A attenuates progression of metastatic breast cancer. *Oncotarget.* (2014) 5:12418–27. doi: 10.18632/oncotarget.2628
25. Huijbers EJM, Griffioen AW. The revival of cancer vaccines - the eminent need to activate humoral immunity. *Hum Vaccin Immunother.* (2017) 13:1112–4. doi: 10.1080/21645515.2016.1276140
26. Huijbers EJM, van Beijnum JR, Lê CT, Langman S, Nowak-Sliwinska P, Mayo KH, et al. An improved conjugate vaccine technology; induction of antibody responses to the tumor vasculature. *Vaccine.* (2018) 36:3054–60. doi: 10.1016/j.vaccine.2018.03.064
27. Hahn JH, Kim MK, Choi EY, Kim SH, Sohn HW, Ham DI, et al. CD99 (MIC2) regulates the LFA-1/ICAM-1-mediated adhesion of lymphocytes, and its gene encodes both positive and negative regulators of cellular adhesion. *J Immunol.* (1997) 159:2250–8.
28. Park SH, Shin YK, Suh YH, Park WS, Ban YL, Choi HS, et al. Rapid divergency of rodent CD99 orthologs: implications for the evolution of the pseudoautosomal region. *Gene.* (2005) 353:177–88. doi: 10.1016/j.gene.2005.04.023
29. Pasello M, Manara MC, Scotlandi K. CD99 at the crossroads of physiology and pathology. *J Cell Commun Signal.* (2018) 12:55–68. doi: 10.1007/s12079-017-0445-z
30. Gene NCBI-d. *CD99 CD99 Molecule (Xg Blood Group) [Homo sapiens (Human)] Gene ID:4267*. (2018). Available online at: https://www.ncbi.nlm.nih.gov/gene/4267 (Accessed 2018).
31. Huang P, McKee TD, Jain RK, Fukumura D. Green fluorescent protein (GFP)-expressing tumor model derived from a spontaneous osteosarcoma in a vascular endothelial growth factor (VEGF)-GFP transgenic mouse. *Comp Med.* (2005) 55:236–43.
32. Uhlén M, Fagerberg L, Hallström BM, Lindskog C, Oksvold P, Mardinoglu A, et al. Tissue-based map of the human proteome. *Science.* (2015). 347:1260419. doi: 10.1126/science.1260419
33. Pontén F, Jirström K, Uhlen M. The human protein atlas-a tool for pathology. *J Pathol.* (2008) 216:387–93. doi: 10.1002/path.2440
34. Nowak-Sliwinska P, Alitalo K, Allen E, Anisimov A, Aplin AC, Auerbach R, et al. Consensus guidelines for the use and interpretation of angiogenesis assays. *Angiogenesis.* (2018) 21:425–532. doi: 10.1007/s10456-018-9613-x
35. Thijssen VL, Brandwijk RJ, Dings RP, Griffioen AW. Angiogenesis gene expression profiling in xenograft models to study cellular interactions. *Exp Cell Res.* (2004) 299:286–93. doi: 10.1016/j.yexcr.2004.06.014
36. Bixel G, Kloep S, Butz S, Petri B, Engelhardt B, Vestweber D. Mouse CD99 participates in T-cell recruitment into inflamed skin. *Blood.* (2004) 104:3205–13. doi: 10.1182/blood-2004-03-1184
37. Vernersson M, Ledin A, Johansson J, Hellman L. Generation of therapeutic antibody responses against IgE through vaccination. *FASEB J.* (2002) 16:875–7. doi: 10.1096/fj.01-0879fje
38. Lipman NS, Jackson LR, Trudel LJ, Weis-Garcia F. Monoclonal versus polyclonal antibodies: distinguishing characteristics, applications, and information resources. *ILAR J.* (2005) 46:258–68. doi: 10.1093/ilar.46.3.258
39. Wold ED, Smider VV, Felding B H. Antibody therapeutics in oncology. *Immunotherapy.* (2016) 2:27081677 doi: 10.4172/2471-9552.1000108
40. Scott AM, Allison JP, Wolchok JD. Monoclonal antibodies in cancer therapy. *Cancer Immun.* (2012) 12:14.
41. Jain RK. Normalization of tumor vasculature: an emerging concept in antiangiogenic therapy. *Science.* (2005) 307:58–62. doi: 10.1126/science.1104819
42. Griffioen AW, Mans LA, de Graaf AMA, Nowak-Sliwinska P, de Hoog CLMM, de Jong TAM, et al. Rapid angiogenesis onset after discontinuation of sunitinib treatment of renal cell carcinoma patients. *Clin Cancer Res.* (2012) 18:3961–71. doi: 10.1158/1078-0432.CCR-12-0002
43. Griffioen AW, Molema G. Angiogenesis: potentials for pharmacologic intervention in the treatment of cancer, cardiovascular diseases, and chronic inflammation. *Pharmacol Rev.* (2000) 52:237–68.
44. Huijbers EJ, van Beijnum JR, Thijssen VL, Sabrkhany S, Nowak-Sliwinska P, Griffioen AW. Role of the tumor stroma in resistance to anti-angiogenic therapy. *Drug Resist Update.* (2016) 25:26–37. doi: 10.1016/j.drup.2016.02.002
45. van Beijnum JR, Nowak-Sliwinska P, Huijbers EJ, Thijssen VL, Griffioen AW. The great escape; the hallmarks of resistance to antiangiogenic therapy. *Pharmacol Rev.* (2015) 67:441–61. doi: 10.1124/pr.114.010215
46. Gerhard DS, Wagner L, Feingold EA, Shenmen CM, Grouse LH, Schuler G, et al. The status, quality, and expansion of the NIH full-length cDNA project: the Mammalian Gene Collection (MGC). *Genome Res.* (2004) 14:2121–7. doi: 10.1101/gr.2596504
47. Aubrit F, Gelin C, Pham D, Raynal B, Bernard A. The biochemical characterization of E2, a T cell surface molecule involved in rosettes. *Eur J Immunol.* (1989) 19:1431–6. doi: 10.1002/eji.1830190813
48. Al-Rubeai M. (ed). *Animal Cell Culture (Cell Engineering Series).* Cham: Springer International Publishing (2014). 9. doi: 10.1007/978-3-319-10320-4_2

Conflict of Interest Statement: The authors declare that the research was conducted in the absence of any commercial or financial relationships that could be construed as a potential conflict of interest.

frontiers in Immunology

MINI REVIEW
published: 09 May 2019
doi: 10.3389/fimmu.2019.01023

Exploring the Immunological Mechanisms Underlying the Anti-vascular Endothelial Growth Factor Activity in Tumors

Rodrigo Barbosa de Aguiar and Jane Zveiter de Moraes*

Department of Biophysics, Universidade Federal de São Paulo, São Paulo, Brazil

Several studies report the key role of the vascular endothelial growth factor (VEGF) signaling on angiogenesis and on tumor growth. This has led to the development of a number of VEGF-targeted agents to treat cancer patients by disrupting the tumor blood vessel supply. Of them, bevacizumab, an FDA-approved humanized monoclonal antibody against VEGF, is the most promising. Although the use of antibodies targeting the VEGF pathway has shown clinical benefits associated with a reduction in the tumor blood vessel density, the inhibition of VEGF-driven vascular effects is only part of the functional mechanism of these therapeutic agents in the tumor ecosystem. Compelling reports have demonstrated that VEGF confers, in addition to the activation of angiogenesis-related processes, immunosuppressive properties in tumors. It is also known that structural remodeling of the tumor blood vessel bed by anti-VEGF approaches affect the influx and activation of immune cells into tumors, which might influence the therapeutic results. Besides that, part of the therapeutic effects of antiangiogenic antibodies, including their role in the tumor vascular network, might be triggered by Fc receptors in an antigen-independent manner. In this mini-review, we explore the role of VEGF inhibitors in the tumor microenvironment with focus on the immune system, discussing around the functional contribution of both bevacizumab's Fab and Fc domains to the therapeutic results and the combination of bevacizumab therapy with other immune-stimulatory settings, including adjuvant-based vaccine approaches.

Keywords: vascular endothelial growth factor, bevacizumab, angiogenesis, Fc receptors, immune-modulation, immunity

OPEN ACCESS

Edited by:
Vijaya Iragavarapu-Charyulu, Florida Atlantic University, United States

Reviewed by:
Lorenzo Mortara, University of Insubria, Italy
Theresa L. Whiteside, University of Pittsburgh, United States

****Correspondence:***
Rodrigo Barbosa de Aguiar
rodrigo.aguiar@live.com

Specialty section:
This article was submitted to Vaccines and Molecular Therapeutics, a section of the journal Frontiers in Immunology

Received: *31 December 2018*
Accepted: *23 April 2019*
Published: *09 May 2019*

Citation:
Aguiar RB and Moraes JZ (2019) Exploring the Immunological Mechanisms Underlying the Anti-vascular Endothelial Growth Factor Activity in Tumors. Front. Immunol. 10:1023. doi: 10.3389/fimmu.2019.01023

INTRODUCTION

The role of VEGF in driving tumor angiogenesis has made it an attractive target for therapeutic interventions, being bevacizumab, an FDA-approved humanized monoclonal antibody against VEGF, the most promising of them (1). Although these therapeutics were originally designed to control blood-vessel formation, increasing evidences point to their additional immunoregulatory role. In this mini-review, we uncover a more complete picture of the immunological changes induced by VEGF-targeting agents, specifically bevacizumab, in the tumor microenvironment (TME).

We discuss the functional contribution of bevacizumab's Fab and Fc domains to the tumor immune landscape and outline the therapeutic potential of combining bevacizumab with other immune-stimulatory agents.

THE IMMUNOTHERAPEUTIC ROLE OF AN ANGIOGENESIS TARGETED AGENT

The vascular endothelium represents a barrier that lines the vessel compartment and regulates the access of blood components to the surrounding tissue. In tumors, however, this barrier is found corrupted. It determines a tortuous and disorganized vessel network with low pericyte coverage and high vascular permeability, contributing to install an immunosuppressive milieu (2, 3).

VEGF inhibitors, particularly bevacizumab, have been found to restore tumor blood vessel structure to normal, a process called vessel normalization (4). The "normalized" tumor vasculature results in increased tumor blood perfusion, higher pericyte coverage and reduced areas with sluggish blood flow, leading to enhanced influx of leukocytes into tumor parenchyma (5). On this topic, strong correlations were found between increased tumor-infiltrating lymphocytes—such as $CD4^+$ and $CD8^+$ T cells—and the vascular normalization imposed by VEGF pathway inhibitors (6, 7). The higher hydrodynamic force applied to endothelial wall may have a role on that, having in mind that a minimum level (above 0.5 dyn/cm^2) of wall shear stress—that is, the parallel pressure exerted by the blood flow in the endothelial cell lining (5)—is required for enhanced endothelial cell expression of selectin family members, cell-surface molecules involved in leukocyte rolling in vessel wall (5, 8). On the other hand, the adhesion molecule content on the tumor blood vessel wall is also regulated by the local VEGF activity. Endothelial cell exposure to VEGF was found to hamper the expression of ICAM-1/2, VCAM-1, and CD34 molecules, all of them related to trans-endothelial cell migration and influx of leukocytes into the tumor parenchyma (9, 10).

Combined, these are structural and molecular characteristics of the TME, whose regulation affects the tumor vascular network and potentially participates in the bevacizumab-induced tumor recruitment of immune cells. Using a metaphor, the break imposed by VEGF inhibitors in the endothelial physicochemical barrier allows combat troops—here represented by the immune cells—access more easily the enemy territory—the tumor.

But the relationship between bevacizumab and the immune system is not only summarized by such indirect effects. In fact, the inhibition of VEGF also interferes directly in the activation and modulation of the immune response within the TME. In addition to vascular normalization, the pharmacological blockade of the VEGF/VEGFR axis can enhance the recruitment, trafficking and activation of $CD8^+$ T-cell response in solid tumor models (9, 11, 12). Similarly, the expression levels of VEGF were found associated with decreased activation of $CD8^+$ T and T_H1 cell response on colorectal tumors (13), and the VEGF-enhanced expression of inhibitory checkpoints on $CD8^+$ T cells can be reverted by VEGF- and VEGFR-targeted agents (14).

Beyond the effects on T cells, VEGF signaling also mediates tumor-associated immunodeficiency by expanding inhibitory immune cell subsets, such as $FoxP3^+$ regulatory T lymphocytes (Tregs) and myeloid-derived suppressor cells (MDSCs). Tada and colleagues reported recently that the treatment of advanced gastric cancer patients with ramucirumab–a fully humanized IgG monoclonal anti-VEGF receptor 2 (VEGFR2) antibody–not only increased $CD8^+$ T-cell tumor infiltration, but also significantly reduced the frequency of $CD45RA^-$ $FOXP3^{high}$ $CD4^+$ cells (effector regulatory T cells [eTreg]) in tumors. Ramucirumab was also found to overcome VEGF-induced eTreg proliferation *in vitro* (15). These findings are in line with experimental data showing that VEGF directly enhances Treg proliferation in tumor-bearing mice. Moreover, bevacizumab significantly reduces the percentage of Tregs in peripheral blood from cancer patients and inhibits *in vitro* tumor cell-increased Treg proportion in PBMC (16, 17). In regard to MDSCs, it was found that VEGF promotes the expansion of these cells, being the $CD11b^+$ $VEGFR1^+$ MDSC population decreased in the peripheral blood of renal cell cancer patients treated with bevacizumab (18). Tumor-infiltrating MDSCs are known to contribute to the local immune suppression by inhibiting T cell activity and inducing Treg expansion (19).

Dendritic cells (DCs) and tumor-associated macrophages (TAMs) are other major components of the immune system that may be impaired by VEGF-targeting therapies. DCs are antigen-presenting units that act as messengers between the innate and adaptive immune systems. VEGF inhibits the DC precursor differentiation and maturation into functional cells capable of presenting tumor antigens and stimulating an allogeneic T-cell response. DCs were found inversely correlated with VEGF serum levels (20). Also, experimental data showed that the VEGF-induced DC dysfunction is recovered by both anti-VEGF and anti-VEGFR2 antibodies (20–25). When looking at TAMs, known as prominent players of the cell repertoire that populates tumors, we face again with a chemoattractant role of VEGF. The signal conferred by this growth factor contributes to increase the number of TAMs within the tumor bed and, as expected, VEGF inhibitors impair that (26–28). Also, VEGF-exposed macrophages were described to express endothelial cell markers and to contribute to vascular mimicry (29).

The role of macrophages in tumors varies depending on the environment. Based on their distinct regulatory and effector functions within the tissue microenvironment, TAMs are often classified on two major categories: (i) M1, designating classically activated macrophages that arose in response to IFN-γ, a T_H1 signature cytokine; and (ii) M2, referring to "alternatively" activated macrophages induced by T_H2-type

Abbreviations: VEGF, vascular endothelial growth factor; TME, tumor microenvironment; Treg, regulatory T cells; MDSC, myeloid-derived suppressor cell; PBMC, peripheral blood mononuclear cell; DC, dendritic cell; TAM, tumor-associated macrophage; VEGFR, VEGF receptor; IFN-γ, interferon-γ; IL, interleukin; IgG, immunoglobulin G; FcγR, Fc-specific transmembrane receptor for IgG; ADCC, antibody-dependent cell-mediated cytotoxicity; ADCP, antibody-dependent cellular phagocytosis; CDC, complement-dependent cytotoxicity; TGF-β; transforming growth factor-β; CTLA, cytotoxic T-lymphocyte-associated protein-4; PD-L1, programed cell death ligand 1; CSF1R, colony-stimulating factor 1 receptor kinase; MIF, migration inhibition factor.

cytokines (specifically IL-4 and IL-13), although we currently know that such yin-yang nomenclature does not recapitulate the whole spectrum of macrophage phenotypes (30, 31). From a tumor perspective, this classification not only reflects the T_H1-T_H2 polarization of T cell's response (32, 33), but also the TAM phenotype within the tumor landscape: while M1 macrophages exert antitumor functions, the M2-polarized ones are oriented toward promoting tumor growth, angiogenesis and tissue remodeling. Most TAMs acquire M2-skewed functions in the TME (34, 35), which means that the increased tumor macrophage content imposed by VEGF stimulation may contribute, together with the previously mentioned cellular effects, to establish an immunologically permissive environment for tumor growth. Although these data reveal that anti-VEGF settings decrease the frequency of TAMs in tumors, the VEGF-macrophage relationship goes further. Accumulation of M2-polarized macrophages within the TME was found as an indicator of tumor resistance to anti-VEGF therapy (36, 37), being possible targets to be explored in therapeutic approaches aiming to surpass such resistance. The vascular mimicry is among the M2 macrophage's contributions to the tumor refractoriness to anti-VEGF therapy (38).

EXPLORING THE OTHER SIDE OF VEGF-TARGETED IgG ANTIBODIES

Reducing the bioavailability of VEGF with full-length IgG antibodies compromises not only the tumor vasculature, but also the frequency and phenotype of immune infiltrative cells in tumors, changing the local ecosystem. But that is only the antibody's Fab side of the story.

The structure arrangement of bevacizumab, as of all other full-length IgG antibodies, comprises three functional domains, identified based on the product of the immunoglobulin digestion by papain: two Fab arms, and a single Fc domain (39). While the Fab arms have the variable amino acid sequence responsible for the antibody binding to the target antigen—which is, in that case, VEGF–, the significance of the Fc portion of IgGs lies on its ability to mediate cellular responses through a Fc-specific transmembrane receptor for IgGs (FcγR).

FcγRs are present on the surface of most cells from the immune system (39, 40). The binding of Fc domain of IgG to those specialized receptors initiates downstream effector functions, which englobes the antibody-dependent cell-mediated cytotoxicity (ADCC), antibody-dependent cellular phagocytosis (ADCP), and complement-dependent cytotoxicity (CDC). And that list goes further.

Data published so far reveal that FcγRs, when activated, signal a number of functional cellular changes in the tissue ecosystem, which is not limited to the immune repertoire. Functional FcγRs detected on endothelial and tumor cells contribute to pathway activations, cell proliferation and adhesion (41–46). Moreover, the signaling transduced by these receptors can even interfere in the tumor vascular network, an effect experimentally demonstrated by Bogdanovich et al. Bevacizumab was found to inhibit angiogenesis via Fc-mediated signaling through FcγR in a VEGF-independent manner (47). Such angioinhibition does not depend on ADCC, APCD, or CDC, suggesting the role of other FcγR-triggered effector responses induced by the antibody. It has also been reported that infusion of IgGs in both mice and humans inhibits angiogenesis (48) and that bevacizumab is more effective than its Fab fragment version—available commercially as ranibizumab—for the control of vessel formation (49). It is noteworthy that Fc-mediated effects were found to be required for achieving the maximum therapeutic effect of neutralizing antibodies (50, 51).

With our current knowledge, we cannot summarize all the effects triggered by bevacizumab-FcγR complexes. However, it should be kept in mind that the effects are not limited to what has been described above. To note, the IgG-FcγR interaction potentially provides critical scaffolding to trigger adaptive immunity. Experimental and clinical data revealed that passively administered IgG antibodies engage Fc receptors on DCs to stimulate a long-lasting anti-tumor cellular immune response (51), what is termed as "vaccinal effect." Upon IgG immune complex binding, DCs undergo maturation and enhance $CD8^+$ T-cell adaptive immunity through their antigen presentation function, as well as prime a T_H1 $CD4^+$ T-cell response (51, 52). Although most of these data were found for rituximab, the "vaccinal effect" potentially contributes to the Fc moiety of bevacizumab in mediating an immune response targeting VEGF found on TME cells. This is a point that deserves to be explored. Also, it should be considered that the expression of Fc receptors in TME cells is not fixed, being subjected to local changes that occur throughout treatment regimens. An example is FcγRIIb, a Fcγ receptor family member whose expression can be upregulated by T_H2-type cytokines, such as IL-10, IL-4, and TGF-β, and downregulated by T_H1-type cytokines, such as IFN-γ (53).

Taken together, these data highlight the diversity and complexity of the effects triggered by Fc domain-FcγR complexes within the TME profile, which certainly affect the tumor outcome. The understanding of the FcγR-mediated immunomodulatory pathways in different environments and cell subsets within the tumor ecosystem may be essential to improve the therapeutic benefits of bevacizumab.

COMBINING BEVACIZUMAB WITH IMMUNE MODULATORS TO ENHANCE ANTI-TUMOR RESPONSE

The dual effect of bevacizumab on remodeling both vasculature and immune components of tumors opens up an opportunity for exploring combinatorial therapies aiming to enhance T_H1 immune response against tumors. And some of the initiatives in this way seem promising.

Hodi et al. investigated the combination of bevacizumab and ipilimumab, an anti-CTLA-4 neutralizing mAb, in patients with metastatic melanoma. The blockade of CTLA-4, a negative regulator of T-cell responses, by ipilimumab may augment the endogenous anti-tumor cellular immune response, leading to tumor cell death. Results revealed an increased infiltration of

$CD8^+$ and $CD163^+$ cells in tumors from patients receiving both mAbs, compared to the observed in tumor samples from the ipilimumab-only group (54). This was accompanied by the concentrated CD31 staining detected at interendothelial junctions of tumor vessels from the bevacizumab-treated group (54), which evidences the vascular changes occurring during VEGF blockade. CD31 is a vascular adhesion glycoprotein known to influence lymphocyte extravasation (54, 55), and whose expression and distribution pattern may have contributed to the detected intratumoral leukocyte content. These results are compatible with the obtained in further studies from the same research group (56).

The functional significance of the increased $CD163^+$ cell population found under bevacizumab-containing regimen is not clear. CD163 is identified as a scavenger receptor for hemoglobin-haptoglobin complexes (57), but also as marker for M2 macrophages (58). Perhaps the increased $CD163^+$ cell infiltration is an indicative of an evasive mechanism, mediated by M2 macrophages, to the anti-VEGF therapy. Besides that, few studies have investigated the functions of CD163, whose expression is also detected in subsets of classical and monocyte-derived DCs (59, 60). It is not even possible to discard that the expression of CD163 is an immune response to the extravascular hemoglobin content, secondary to necrosis index, eventually increased in tumors from patients receiving the combinatory treatment. Extravascular hemoglobin is a known endogenous danger signal that induces M2-skewed macrophage influx and CD163-macrophage polarization (61, 62). Clinically, $CD163^+$ cell infiltration has been associated to both good (63) and bad (64–68) prognosis.

Similar benefits have been found under therapeutic interventions targeting programed cell death ligand 1 (PD-L1; a suppressor of the immune system). It was recently demonstrated that anti-VEGF and anti-PD-L1 combination therapy increases $CD4^+$ and $CD8^+$ cell infiltration in tumors and synergistically improves treatment outcome, compared to the obtained with each monotherapy (69). An ongoing clinical trial (ClinicalTrials.gov, trial identifier NCT01633970) is also investigating that. Moreover, even initiatives aiming to reprogram the M2 TAM-dominated TME have been put on the table, considering the described relationship between tumor M2 macrophages and bevacizumab resistance. Experimental study showed that combinatory treatment with a colony-stimulating factor 1 receptor kinase (CSF1R) inhibitor reduces the M2 macrophage content within tumors and aids in overcoming adaptive resistance to the herein explored anti-VEGF antibody performance (70).

Another approach with potential to be considered is the combination of bevacizumab therapy with adjuvant-based vaccines that stimulate a T_H1 response against tumors. Vaccine adjuvants represent an attractive tool to modulate the immune cell effector function, with some of them being classified as inducers of T_H1 T-cell immunity. That is the case of toll-like receptor agonists, such as dextran-conjugated CpG oligodeoxynucleotides (71) and double-stranded RNAs (72, 73), whose application in vaccine formulations enhances tumor-specific T_H1-polarized $CD4^+$ T cells and CTL responses. Although combining bevacizumab with vaccination settings seems to be a promising way to enhance the anti-tumor effect, there is no report on that up to now, with the few works in this direction limited to the use of T_H1-inducer adjuvants in anti-VEGF vaccines (74, 75). And even in these cases, the results are restricted to the detection of specific cellular immune responses, remaining the clinical benefits yet to be demonstrated. In fact, all the herein exposed combination initiatives are in their first steps and further works are needed to clarify the effects in the TME and to achieve an optimized therapeutic protocol.

A MATTER OF ANTIGEN SPECIFICITY: BEVACIZUMAB RECOGNIZES ANOTHER BIOMOLECULE BEYOND VEGF

It is becoming increasingly evident that both Fab and Fc IgG domains—the two sides of the same coin—play a role in changing the vascular and immune components of solid tumors. As outlined above, a wide array of regulatory functions within TME are driven by the bevacizumab's constant region (Fc), which was not initially expected when this antibody was first employed in therapeutic settings. Likewise, it was not expected that bevacizumab's Fab domain recognizes other biomolecules in addition to the one it is known to identify.

Muller and coworkers demonstrated that bevacizumab directly binds to and sequesters the macrophage migration inhibition factor (MIF) from the TME. This may be due to certain similarities detected between amino acid sequences 48–76 of MIF and 29–51 of VEGF, the latter of which covers residues implicated in the bevacizumab binding (76).

MIF is described as an important regulator of immune responses (77). Experimental data showed that MIF downregulation led to increased intratumoral IFN-γ-producing $CD4^+$ and $CD8^+$ T cells, higher number of activated DCs, and reduced prevalence of MDSC and Tregs within tumors (36, 78–80), just as detected following VEGF inhibition. In the same direction, the interference with the MIF signaling was reported to decrease M2 macrophage shift in melanoma (81) and in multiple myeloma (82) models. Similar polarization effect was also found in microglial cells under MIF inhibition (83). Despite these findings, MIF is not always described as a M2 phenotype inducer. Lower levels of MIF at the tumor edge of glioblastomas were showed both to increase the local macrophage population, mainly from bone marrow-derived cells, and to polarize these cells to a M2 phenotype (36), which suggests that different microenvironmental contexts may imply in different MIF effects on tumor-infiltrating immune cells.

Overall, the functional significance of bevacizumab's Fab domain includes the inhibition of MIF. However, it is important to note that the direct binding to MIF is just one of the demonstrated mechanisms by which bevacizumab inhibits the MIF's function. MIF expression is transcriptionally regulated by VEGF (36), then subjected to the reduced local VEGF bioavailability imposed by bevacizumab therapy.

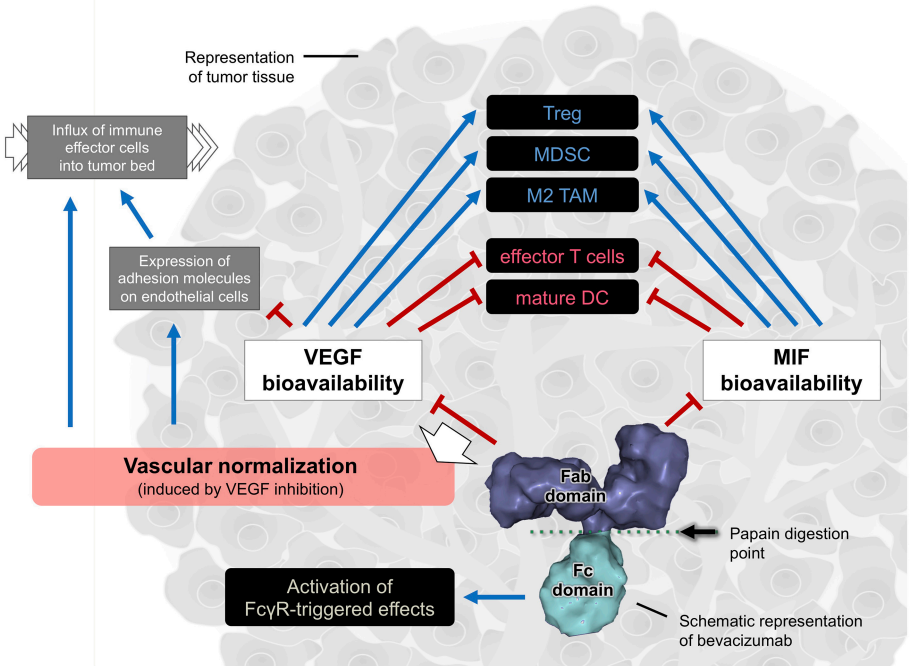

FIGURE 1 | Cartoon summarizing the effects mediated by the bevacizumab's Fab and Fc domains in the tumor immune landscape. The vascular normalization, due to the blockade of excessive VEGF signaling in tumors, is one possible implication of bevacizumab therapy in tumors. The solid blue arrow lines indicate activation while the solid red hammer lines indicate inhibition. The black dashed line indicates inconclusive association (both activation and inhibition were reported). Surface model of an IgG (PDB entry: 1IGT) was used to represent bevacizumab. Image without scale.

GENERAL OVERVIEW

Rather than just inhibiting angiogenesis, VEGF inhibitors have proved to regulate the immune response in tumors. The anti-VEGF antibody bevacizumab interferes in the composition and function of several immune cells within the TME, including T cells, TAMs, Tregs, MDSCs, and DCs. Bevacizumab was also found to trigger FcγR-mediated responses and to inhibit another immunoregulatory biomolecule beyond VEGF, which points out to the diversity of actions of this antibody in the tumor immune landscape. The herein described bevacizumab's immune-modulating effects are summarized on **Figure 1**. Overall, these data evidence that the therapeutic effects of anti-VEGF immunoglobulins reflect their multiple interactions with different elements that compose the tumor tissue. Understanding these effects is crucial to improve therapeutic effectiveness. That is a perspective beyond VEGF inhibition.

AUTHOR CONTRIBUTIONS

RA conceived and outlined the review. RA and JM contributed critically to the manuscript preparation.

ACKNOWLEDGMENTS

The authors thank support from Brazilian National Research Council (CNPq; #150161/2017-4) and São Paulo Research Foundation (FAPESP, #09/18631-1).

REFERENCES

1. Ferrara N, Hillan KJ, Gerber HP, Novotny W. Discovery and development of bevacizumab, an anti-VEGF antibody for treating cancer. *Nat Rev Drug Discov*. (2004) 3:391–400. doi: 10.1038/nrd1381
2. Hamzah J, Jugold M, Kiessling F, Rigby P, Manzur M, Marti HH, et al. Vascular normalization in Rgs5-deficient tumours promotes immune destruction. *Nature*. (2008) 453:410–4. doi: 10.1038/nature06868
3. Tian L, Goldstein A, Wang H, Ching Lo H, Sun Kim I, Welte T, et al. Mutual regulation of tumour vessel normalization and immunostimulatory reprogramming. *Nature*. (2017) 544:250–4. doi: 10.1038/nature21724
4. Jain RK. Normalization of tumor vasculature: an emerging concept in antiangiogenic therapy. *Science*. (2005) 307:58–62. doi: 10.1126/science.1104819
5. Hendry SA, Farnsworth RH, Solomon B, Achen MG, Stacker SA, Fox SB. The role of the tumor vasculature in the host immune response: implications for therapeutic strategies targeting the tumor microenvironment. *Front Immunol*. (2016) 7:621. doi: 10.3389/fimmu.2016.00621
6. Shrimali RK, Yu Z, Theoret MR, Chinnasamy D, Restifo NP, Rosenberg SA. Antiangiogenic agents can increase lymphocyte infiltration into tumor and enhance the effectiveness of adoptive immunotherapy of cancer. *Cancer Res*. (2010) 70:6171–80. doi: 10.1158/0008-5472.CAN-10-0153
7. Huang Y, Yuan J, Righi E, Kamoun WS, Ancukiewicz M, Nezivar J, et al. Vascular normalizing doses of antiangiogenic treatment reprogram the immunosuppressive tumor microenvironment and enhance immunotherapy. *Proc Natl Acad Sci USA*. (2012) 109:17561–66. doi: 10.1073/pnas.1215397109
8. Lawrence MB, Kansas GS, Kunkel EJ, Ley K. Threshold levels of fluid shear promote leukocyte adhesion through selectins (CD62L,P,E). *J Cell Biol*. (1997) 136:717–27.

9. Huang H, Langenkamp E, Georganaki M, Loskog A, Fuchs PF, Dieterich LC, et al. VEGF suppresses T-lymphocyte infiltration in the tumor microenvironment through inhibition of NF-κB-induced endothelial activation. *FASEB J*. (2015) 29:227–38. doi: 10.1096/fj.14-250985
10. Griffioen AW, Damen CA, Mayo KH, Barendsz-Janson AF, Martinotti S, Blijham GH, et al. Angiogenesis inhibitors overcome tumor induced endothelial cell anergy. *Int J Cancer*. (1999) 80:315–9. doi: 10.1002/(SICI)1097-0215(19990118)80:2<315::AID-IJC23>3.0.CO;2-L
11. Griffioen AW, Damen CA, Blijham GH, Groenewegen G. Tumor angiogenesis is accompanied by a decreased inflammatory response of tumor-associated endothelium. *Blood*. (1996) 88:667–73.
12. Malo CS, Khadka RH, Ayasoufi K, Jin F, AbouChehade JE, Hansen MJ, et al. Immunomodulation mediated by anti-angiogenic therapy improves CD8 T cell immunity against experimental glioma. *Front Oncol*. (2018) 8:320. doi: 10.3389/fonc.2018.00320
13. Zhang L, Zhao Y, Dai Y, Cheng JN, Gong Z, Feng Y, et al. Immune landscape of colorectal cancer tumor microenvironment from different primary tumor location. *Front Immunol*. (2018) 9:1578. doi: 10.3389/fimmu.2018.01578
14. Voron T, Colussi O, Marcheteau E, Pernot S, Nizard M, Pointet AL, et al. VEGF-A modulates expression of inhibitory checkpoints on CD8+ T cells in tumors. *J Exp Med*. (2015) 212:139–48. doi: 10.1084/jem.20140559
15. Tada Y, Togashi Y, Kotani D, Kuwata T, Sato E, Kawazoe A, et al. Targeting VEGFR2 with Ramucirumab strongly impacts effector/ activated regulatory T cells and CD8+ T cells in the tumor microenvironment. *J Immunother Cancer*. (2018) 6:106. doi: 10.1186/s40425-018-0403-1
16. Wada J, Suzuki H, Fuchino R, Yamasaki A, Nagai S, Yanai K, et al. The contribution of vascular endothelial growth factor to the induction of regulatory T-cells in malignant effusions. *Anticancer Res*. (2009) 29:881–8.
17. Terme M, Pernot S, Marcheteau E, Sandoval F, Benhamouda N, Colussi O, et al. VEGFA-VEGFR pathway blockade inhibits tumor-induced regulatory T- cell proliferation in colorectal cancer. *Cancer Res*. (2013) 73:539–49. doi: 10.1158/0008-5472.CAN-12-2325
18. Gabrilovich D, Ishida T, Oyama T, Ran S, Kravtsov V, Nadaf S, et al. Vascular endothelial growth factor inhibits the development of dendritic cells and dramatically affects the differentiation of multiple hematopoietic lineages *in vivo*. *Blood*. (1998) 92:4150–66.
19. Chen J, Ye Y, Liu P, Yu W, Wei F, Li H, et al. Suppression of T cells by myeloid-derived suppressor cells in cancer. *Hum Immunol*. (2017) 78:113–9. doi: 10.1016/j.humimm.2016.12.001
20. Della Porta M, Danova M, Rigolin GM, Brugnatelli S, Rovati B, Tronconi C, et al. Dendritic cells and vascular endothelial growth factor in colorectal cancer: correlations with clinicobiological findings. *Oncology*. (2005) 68:276–84. doi: 10.1159/000086784
21. Oyama T, Ran S, Ishida T, Nadaf S, Kerr L, Carbone DP, et al. Vascular endothelial growth factor affects dendritic cell maturation through the inhibition of nuclear factor-kappa B activation in hemopoietic progenitor cells. *J Immunol*. (1998) 160:1224–32.
22. Dikov MM, Ohm JE, Ray N, Tchekneva EE, Burlison J, Moghanaki D, et al. Differential roles of vascular endothelial growth factor receptors 1 and 2 in dendritic cell differentiation. *J Immunol*. (2005) 174:215–22. doi: 10.4049/jimmunol.174.1.215
23. Mimura K, Kono K, Takahashi A, Kawaguchi Y, Fujii H. Vascular endothelial growth factor inhibits the function of human mature dendritic cells mediated by VEGF receptor-2. *Cancer Immunol Immunother*. (2007) 56:761–70. doi: 10.1007/s00262-006-0234-7
24. Osada T, Chong G, Tansik R, Hong T, Spector N, Kumar R, et al. The effect of anti-VEGF therapy on immature myeloid cell and dendritic cells in cancer patients. *Cancer Immunol Immunother*. (2008) 57:1115–24. doi: 10.1007/s00262-007-0441-x
25. Yang DH, Park JS, Jin CJ, Kang HK, Nam JH, Rhee JH, et al. The dysfunction and abnormal signaling pathway of dendritic cells loaded by tumor antigen can be overcome by neutralizing VEGF in multiple myeloma. *Leuk Res*. (2009) 33:665–70. doi: 10.1016/j.leukres.2008.09.006
26. Muramatsu M, Yamamoto S, Osawa T, Shibuya M. Vascular endothelial growth factor receptor-1 signaling promotes mobilization of macrophage lineage cells from bone marrow and stimulates solid tumor growth. *Cancer Res*. (2010) 70:8211–21. doi: 10.1158/0008-5472.CAN-10-0202
27. Linde N, Lederle W, Depner S, van Rooijen N, Gutschalk CM, Mueller MM. Vascular endothelial growth factor-induced skin carcinogenesis depends on recruitment and alternative activation of macrophages. *J Pathol*. (2012) 227:17–28. doi: 10.1002/path.3989
28. Lee HW, Choi HJ, Ha SJ, Lee KT, Kwon YG. Recruitment of monocytes/macrophages in different tumor microenvironments. *Biochim Biophys Acta*. (2013) 1835:170–9. doi: 10.1016/j.bbcan.2012.12.007
29. Scavelli C, Nico B, Cirulli T, Ria R, Di Pietro G, Mangieri D, et al. Vasculogenic mimicry by bone marrow macrophages in patients with multiple myeloma. *Oncogene*. (2008) 27:663–74. doi: 10.1038/sj.onc.1210691
30. Mosser DM, Edwards JP. Exploring the full spectrum of macrophage activation. *Nat Rev Immunol*. (2008) 8:958–69. doi: 10.1038/nri2448
31. Murray PJ, Allen JE, Biswas SK, Fisher EA, Gilroy DW, Goerdt S, et al. Macrophage activation and polarization: nomenclature and experimental guidelines. *Immunity*. (2014) 41:14–20. doi: 10.1016/j.immuni.2014.06.008
32. Mills CD, Kincaid K, Alt JM, Heilman MJ, Hill AM. M-1/M-2 macrophages and the Th1/Th2 paradigm. *J Immunol*. (2000) 164:6166–73. doi: 10.4049/jimmunol.164.12.6166
33. Parisi L, Gini E, Baci D, Tremolati M, Fanuli M, Bassani B, et al. Macrophage polarization in chronic inflammatory diseases: killers or builders? *J Immunol Res*. (2018) 2018:8917804. doi: 10.1155/2018/8917804
34. Mantovani A, Allavena P, Sica A, Balkwill F. Cancer-related inflammation. *Nature*. (2008) 454:436–44. doi: 10.1038/nature07205
35. Mantovani A, Marchesi F, Malesci A, Laghi L, Allavena P. Tumour-associated macrophages as treatment targets in oncology. *Nat Rev Clin Oncol*. (2017) 14:399–416. doi: 10.1038/nrclinonc.2016.217
36. Castro BA, Flanigan P, Jahangiri A, Hoffman D, Chen W, Kuang R, et al. Macrophage migration inhibitory factor downregulation: a novel mechanism of resistance to anti-angiogenic therapy. *Oncogene*. (2017) 36:3749–59. doi: 10.1038/onc.2017.1
37. Dalton HJ, Pradeep S, McGuire M, Hailemichael Y, Ma S, Lyons Y, et al. Macrophages facilitate resistance to Anti-VEGF therapy by altered VEGFR expression. *Clin Cancer Res*. (2017) 23:7034–46. doi: 10.1158/1078-0432.CCR-17-0647
38. Rong X, Huang B, Qiu S, Li X, He L, Peng Y. Tumor-associated macrophages induce vasculogenic mimicry of glioblastoma multiforme through cyclooxygenase-2 activation. *Oncotarget*. (2016) 7:83976–86. doi: 10.18632/oncotarget.6930
39. Nimmerjahn F, Ravetch JV. FcγRs in health and disease. *Curr Top Microbiol Immunol*. (2011) 350:105–25. doi: 10.1007/82_2010_86
40. Ravetch JV, Bolland S. IgG Fc receptors. *Annu Rev Immunol*. (2001) 19:275–90. doi: 10.1146/annurev.immunol.19.1.275
41. Gorini G, Ciotti MT, Starace G, Vigneti E, Raschellà G. Fc gamma receptors are expressed on human neuroblastoma cell lines: lack of correlation with N-myc oncogene activity. *Int J Neurosci*. (1992) 62:287–97.
42. Pan L, Kreisle RA, Shi Y. Expression of endothelial cell IgG Fc receptors and markers on various cultures. *Chin Med J*. (1999) 112:157–61.
43. Cassard L, Dragon-Durey MA, Ralli A, Tartour E, Salamero J, Fridman WH, et al. Expression of low- affinity Fc gamma receptor by a human metastatic melanoma line. *Immunol Lett*. (2000) 75:1–8. doi: 10.1016/S0165-2478(00)00286-8
44. Nelson MB, Nyhus JK, Oravecz-Wilson KI, Barbera-Guillem E. Tumor cells express FcgammaRI which contributes to tumor cell growth and a metastatic phenotype. *Neoplasia*. (2001) 3:115–24. doi: 10.1038/sj/neo/7900140
45. Devaraj S, Davis B, Simon SI, Jialal I. CRP promotes monocyte-endothelial cell adhesion via Fcgamma receptors in human aortic endothelial cells under static and shear flow conditions. *Am J Physiol Heart Circ Physiol*. (2006) 291:H1170–6. doi: 10.1152/ajpheart.00150.2006
46. Cassard L, Cohen-Solal JF, Fournier EM, Camilleri-Broët S, Spatz A, Chouaïb S, et al. Selective expression of inhibitory Fcgamma receptor by metastatic melanoma impairs tumor susceptibility to IgG-dependent cellular response. *Int J Cancer*. (2008) 123:2832–9. doi: 10.1002/ijc.23870
47. Bogdanovich S, Kim Y, Mizutani T, Yasuma R, Tudisco L, Cicatiello V, et al. Human IgG1 antibodies suppress angiogenesis in a target-independent manner. *Signal Transduct Target Ther*. (2016) 1:15001. doi: 10.1038/sigtrans.2015.1
48. Yasuma R, Cicatiello V, Mizutani T, Tudisco L, Kim Y, Tarallo V, et al. Intravenous immune globulin suppresses angiogenesis in mice and humans. *Signal Transduct Target Ther*. (2016) 1:15002. doi: 10.1038/sigtrans.2015.2
49. Kim JH, Seo HW, Han HC, Lee JH, Choi SK, Lee D. The effect of bevacizumab versus ranibizumab in the treatment of corneal

neovascularization: a preliminary study. *Korean J Ophthalmol*. (2013) 27:235–42. doi: 10.3341/kjo.2013.27.4.235
50. Bournazos S, Klein F, Pietzsch J, Seaman MS, Nussenzweig MC, Ravetch JV. Broadly neutralizing anti-HIV-1 antibodies require Fc effector functions for *in vivo* activity. *Cell*. (2014) 158:1243–53. doi: 10.1016/j.cell.2014.08.023
51. DiLillo DJ, Ravetch JV. Differential Fc-receptor engagement drives an anti-tumor vaccinal effect. *Cell*. (2015) 161:1035–45. doi: 10.1016/j.cell.2015.04.016
52. Nimmerjahn F, Ravetch JV. Fcgamma receptors as regulators of immune responses. *Nat Rev Immunol*. (2008) 8:34–47. doi: 10.1038/nri2206
53. Rosales C. Fcγ receptor heterogeneity in leukocyte functional responses. *Front Immunol*. (2017) 8:280. doi: 10.3389/fimmu.2017.00280
54. Hodi FS, Lawrence D, Lezcano C, Wu X, Zhou J, Sasada T, et al. Bevacizumab plus ipilimumab in patients with metastatic melanoma. *Cancer Immunol Res*. (2014) 2:632–42. doi: 10.1158/2326-6066.CIR-14-0053
55. Muller WA. The role of PECAM-1 (CD31) in leukocyte emigration: studies *in vitro* and *in vivo*. *J Leukoc Biol*. (1995) 57:523–8. doi: 10.1002/jlb.57.4.523
56. Wu X, Giobbie-Hurder A, Liao X, Lawrence D, McDermott D, Zhou J, et al. VEGF neutralization plus CTLA-4 blockade alters soluble and cellular factors associated with enhancing lymphocyte infiltration and humoral recognition in melanoma. *Cancer Immunol Res*. (2016) 4:858–68. doi: 10.1158/2326-6066.CIR-16-0084
57. Kristiansen M, Graversen JH, Jacobsen C, Sonne O, Hoffman HJ, Law SK, et al. Identification of the haemoglobin scavenger receptor. *Nature*. (2001) 409:198–201. doi: 10.1038/35051594
58. Shiraishi D, Fujiwara Y, Horlad H, Saito Y, Iriki T, Tsuboki J, et al. CD163 is required for protumoral activation of macrophages in human and murine sarcoma. *Cancer Res*. (2018) 78:3255–66. doi: 10.1158/0008-5472.CAN-17-2011
59. Alcántara-Hernández M, Leylek R, Wagar LE, Engleman EG, Keler T, Marinkovich MP, et al. High-dimensional phenotypic mapping of human dendritic cells reveals interindividual variation and tissue specialization. *Immunity*. (2017) 47:1037–50.e6. doi: 10.1016/j.immuni.2017.11.001
60. Maniecki MB, Møller HJ, Moestrup SK, Møller BK. CD163 positive subsets of blood dendritic cells: the scavenging macrophage receptors CD163 and CD91 are coexpressed on human dendritic cells and monocytes. *Immunobiology*. (2006) 211:407–17. doi: 10.1016/j.imbio.2006.05.019
61. Rubio-Navarro A, Amaro Villalobos JM, Lindholt JS, Buendía I, Egido J, Blanco-Colio LM, et al. Hemoglobin induces monocyte recruitment and CD163-macrophage polarization in abdominal aortic aneurysm. *Int J Cardiol*. (2015) 201:66–78. doi: 10.1016/j.ijcard.2015.08.05
62. Yin T, He S, Liu X, Jiang W, Ye T, Lin Z, et al. Extravascular red blood cells and hemoglobin promote tumor growth and therapeutic resistance as endogenous danger signals. *J Immunol*. (2015) 194:429–37. doi: 10.4049/jimmunol.1400643
63. Nagorsen D, Voigt S, Berg E, Stein H, Thiel E, Loddenkemper C. Tumor-infiltrating macrophages and dendritic cells in human colorectal cancer: relation to local regulatory T cells, systemic T-cell response against tumor-associated antigens and survival. *J Transl Med*. (2007) 5:62. doi: 10.1186/1479-5876-5-62
64. Fujita Y, Okamoto M, Goda H, Tano T, Nakashiro K, Sugita A, et al. Prognostic significance of interleukin-8 and CD163-positive cell-infiltration in tumor tissues in patients with oral squamous cell carcinoma. *PLoS ONE*. (2014) 9:e110378. doi: 10.1371/journal.pone.0110378
65. Koh YW, Park CS, Yoon DH, Suh C, Huh J. CD163 expression was associated with angiogenesis and shortened survival in patients with uniformly treated classical Hodgkin lymphoma. *PLoS ONE*. (2014) 9:e87066. doi: 10.1371/journal.pone.0087066
66. Sugimura K, Miyata H, Tanaka K, Takahashi T, Kurokawa Y, Yamasaki M, et al. High infiltration of tumor-associated macrophages is associated with a poor response to chemotherapy and poor prognosis of patients undergoing neoadjuvant chemotherapy for esophageal cancer. *J Surg Oncol*. (2015) 111:752–9. doi: 10.1002/jso.23881
67. Han Q, Shi H, Liu F. CD163(+) M2-type tumor-associated macrophage support the suppression of tumor-infiltrating T cells in osteosarcoma. *Int Immunopharmacol*. (2016) 34:101–6. doi: 10.1016/j.intimp.2016.01.023
68. Hu JM, Liu K, Liu JH, Jiang XL, Wang XL, Chen YZ, et al. CD163 as a marker of M2 macrophage, contribute to predicte aggressiveness and prognosis of Kazakh esophageal squamous cell carcinoma. *Oncotarget*. (2017) 8:21526–38. doi: 10.18632/oncotarget.15630
69. Meder L, Schuldt P, Thelen M, Schmitt A, Dietlein F, Klein S, et al. Combined VEGF and PD-L1 blockade displays synergistic treatment effects in an autochthonous mouse model of small cell lung cancer. *Cancer Res*. (2018) 78:4270–81. doi: 10.1158/0008-5472.CAN-17-2176
70. Lyons YA, Pradeep S, Wu SY, Haemmerle M, Hansen JM, Wagner MJ, et al. Macrophage depletion through colony stimulating factor 1 receptor pathway blockade overcomes adaptive resistance to anti-VEGF therapy. *Oncotarget*. (2017) 8:96496–505. doi: 10.18632/oncotarget.20410
71. Xu X, Jin Z, Liu Y, Gong H, Sun Q, Zhang W, et al. Th1 and CD8+ T-cell responses and reduce the immunosuppressive activity of MDSCs. *Cancer Lett*. (2019) 440–441:94–105. doi: 10.1016/j.canlet.2018.10.013
72. Matsumoto M, Seya T. TLR3: interferon induction by double-stranded RNA including poly(I:C). *Adv Drug Deliv Rev*. (2008) 60:805–12. doi: 10.1016/j.addr.2007.11.005
73. Matsumoto M, Takeda Y, Tatematsu M, Seya T. Toll-like receptor 3 signal in dendritic cells benefits cancer immunotherapy. *Front Immunol*. (2017) 8:1897. doi: 10.3389/fimmu.2017.01897
74. Gavilondo JV, Hernández-Bernal F, Ayala-Ávila M, de la Torre AV, de la Torre J, Morera-Díaz Y, et al. Specific active immunotherapy with a VEGF vaccine in patients with advanced solid tumors. Results of the CENTAURO antigen dose escalation phase I clinical trial. *Vaccine*. (2014) 32:2241–50. doi: 10.1016/j.vaccine.2013.11.102
75. Morera Y, Sánchez J, Bequet-Romero M, Selman-Housein KH, de la Torre A, Hernández-Bernal F, et al. Specific humoral and cellular immune responses in cancer patients undergoing chronic immunization with a VEGF-based therapeutic vaccine. *Vaccine*. (2017) 35:3582–90. doi: 10.1016/j.vaccine.2017.05.020
76. Muller YA, Chen Y, Christinger HW, Li B, Cunningham BC, Lowman HB, et al. VEGF and the Fab fragment of a humanized neutralizing antibody: crystal structure of the complex at 2.4 A resolution and mutational analysis of the interface. *Structure*. (1998) 6:1153–67. doi: 10.1016/S0969-2126(98)00116-6
77. Calandra T, Roger T. Macrophage migration inhibitory factor: a regulator of innate immunity. *Nat Rev Immunol*. (2003) 3:791–800. doi: 10.1038/nri1200
78. Choi S, Kim HR, Leng L, Kang I, Jorgensen WL, Cho CS, et al. Role of macrophage migration inhibitory factor in the regulatory T cell response of tumor-bearing mice. *J Immunol*. (2012) 189:3905–13. doi: 10.4049/jimmunol.1102152
79. Simpson KD, Templeton DJ, Cross JV. Macrophage migration inhibitory factor promotes tumor growth and metastasis by inducing myeloid-derived suppressor cells in the tumor microenvironment. *J Immunol*. (2012) 189:5533–40. doi: 10.4049/jimmunol.1201161
80. Balogh KN, Templeton DJ, Cross JV. Macrophage migration inhibitory factor protects cancer cells from immunogenic cell death and impairs anti-tumor immune responses. *PLoS ONE*. (2018) 13:e0197702. doi: 10.1371/journal.pone.0197702
81. Yaddanapudi K, Putty K, Rendon BE, Lamont GJ, Faughn JD, Satoskar A, et al. Control of tumor-associated macrophage alternative activation by macrophage migration inhibitory factor. *J Immunol*. (2013) 190:2984–93. doi: 10.4049/jimmunol.1201650
82. Gutiérrez-González A, Martínez-Moreno M, Samaniego R, Arellano-Sánchez N, Salinas-Muñoz L, Relloso M, et al. Evaluation of the potential therapeutic benefits of macrophage reprogramming in multiple myeloma. *Blood*. (2016) 128:2241–52. doi: 10.1182/blood-2016-01-695395
83. Ghoochani A, Schwarz MA, Yakubov E, Engelhorn T, Doerfler A, Buchfelder M, et al. MIF-CD74 signaling impedes microglial M1 polarization and facilitates brain tumorigenesis. *Oncogene*. (2016) 35:6246–61. doi: 10.1038/onc.2016.160

Conflict of Interest Statement: The authors declare that the research was conducted in the absence of any commercial or financial relationships that could be construed as a potential conflict of interest.

frontiers in Immunology

MINI REVIEW
published: 04 June 2019
doi: 10.3389/fimmu.2019.01278

Mechanisms of Action of Novel Drugs Targeting Angiogenesis-Promoting Matrix Metalloproteinases

Gregg B. Fields [1,2]*

[1] Department of Chemistry and Biochemistry, Florida Atlantic University, Jupiter, FL, United States, [2] Department of Chemistry, The Scripps Research Institute/Scripps Florida, Jupiter, FL, United States

Angiogenesis is facilitated by the proteolytic activities of members of the matrix metalloproteinase (MMP) family. More specifically, MMP-9 and MT1-MMP directly regulate angiogenesis, while several studies indicate a role for MMP-2 as well. The correlation of MMP activity to tumor angiogenesis has instigated numerous drug development programs. However, broad-based and Zn^{2+}-chelating MMP inhibitors have fared poorly in the clinic. Selective MMP inhibition by antibodies, biologicals, and small molecules has utilized unique modes of action, such as (a) binding to protease secondary binding sites (exosites), (b) allosterically blocking the protease active site, or (c) preventing proMMP activation. Clinical trials have been undertaken with several of these inhibitors, while others are in advanced pre-clinical stages. The mechanistically non-traditional MMP inhibitors offer treatment strategies for tumor angiogenesis that avoid the off-target toxicities and lack of specificity that plagued Zn^{2+}-chelating inhibitors.

Keywords: protease inhibitor, clinical trial, metalloproteinase, cancer, angiogenesis, antibody, exosite

OPEN ACCESS

Edited by:
Julia Kzhyshkowska, Universität Heidelberg, Germany

Reviewed by:
Lasse Dahl Ejby Jensen, Linköping University, Sweden
Domenico Ribatti, University of Bari Aldo Moro, Italy

***Correspondence:**
Gregg B. Fields
fieldsg@fau.edu

Specialty section:
This article was submitted to Vaccines and Molecular Therapeutics, a section of the journal Frontiers in Immunology

Received: *11 December 2018*
Accepted: *20 May 2019*
Published: *04 June 2019*

Citation:
Fields GB (2019) Mechanisms of Action of Novel Drugs Targeting Angiogenesis-Promoting Matrix Metalloproteinases. Front. Immunol. 10:1278. doi: 10.3389/fimmu.2019.01278

INTRODUCTION

During the process of angiogenesis (the development of new blood vessels), the extracellular matrix (ECM) is degraded by matrix metalloproteinases (MMPs), facilitating endothelial cell invasion and leading to sprouting of new vessels (1–3). The MMP family (**Figure 1**) has fairly conserved sequences between species, indicating that they are part of essential biological processes. The domain organization of MMPs is also fairly conserved, as all contain a signal peptide, a pro-domain, and a catalytic (CAT) domain with a Zn^{2+} binding His-Glu-X-X-His-X-X-Gly-X-X-His motif (**Figure 1**). Most MMPs contain a linker region and a hemopexin-like (HPX) domain (**Figure 1**). In addition, some harbor specific features such as a furin activation domain (MMP-14/MT1-MMP, MMP-15/MT2-MMP, MMP-16/MT3-MMP, MMP-21, MMP-24/MT5-MMP, MMP-23, and MMP-28), fibronectin type II middle inserts (MMP-2 and MMP-9), and/or a transmembrane domain (MMP-14/MT1-MMP, MMP-15/MT2-MMP, MMP-16/MT3-MMP, and MMP-24/MT5-MMP) (**Figure 1**).

MMP-9 and MT1-MMP directly regulate angiogenesis, while some studies indicate a role for MMP-2 as well (1, 4). Tumor angiogenesis and growth is reduced in MMP-2 knockout mice (1). MMP-9 has been well-documented as a key contributor to the "angiogenic switch" in cancer progression (5–8). The roles of MMP-9 in angiogenesis include the release of vascular endothelial growth factor (VEGF) and/or basic fibroblast growth factor (FGF-2) (5, 7). Tumor-associated macrophages, once polarized into the M2 phenotype, release VEGF and MMP-9 (9). MT1-MMP contributes to blood vessel invasion, FGF-2-induced corneal angiogenesis, endothelial cell

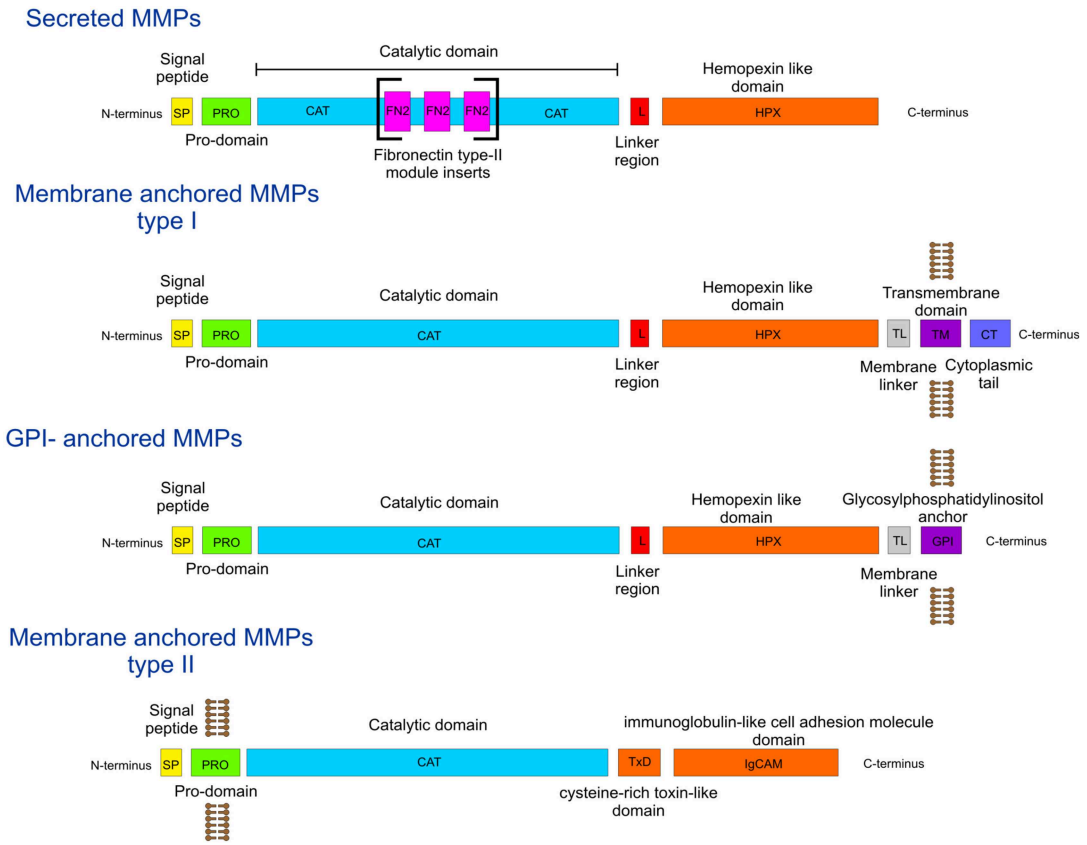

FIGURE 1 | Diagrammatic representation of MMP domain organization.

migration and tubulogenesis in three-dimensional collagen matrices, and vascular lumen formation (10–15).

Inhibiting enzymes involved in tumor-driven angiogenesis has been recognized as a potential anticancer therapy (16). Broad spectrum and moderately selective MMP inhibitors have been recognized as possessing antiangiogenic activity (17–19). The majority of MMP inhibitors contain a hydroxamic acid group which chelates the active site Zn^{2+} (20–24). Problems with hydroxamic acid-based metalloprotease inhibitors include the tendency of hydroxamic acids to chelate zinc in a non-selective fashion (25). An often observed side effect of hydroxamic acid-based MMP inhibitors has been musculoskeletal syndrome (MSS). MSS has been attributed to combined inhibition of MMP-1 and a disintegrin and metalloproteinase 17 (ADAM17) (26). A pyrimidine-2,4,6-trione derivative that selectively inhibits MT1-MMP, MMP-2, and MMP-9 is not associated with MSS (27).

Abbreviations: Abs, antibodies; ADAM, a disintegrin and metalloproteinase; CAT, catalytic; ClC-3, chloride channel-3; ClTx, chlorotoxin; ECM, extracellular matrix; EGFR, epidermal growth factor receptor; FGF-2, basic fibroblast growth factor 2; Flp, (2*S*,4*R*)-4-fluoroproline; HPX, hemopexin-like; mep, (2*S*,4*R*)-4-methylproline; MMP, matrix metalloproteinase; MSS, musculoskeletal syndrome; PDAC, pancreatic ductal adenocarcinoma; scFv, single chain variable fragment; THP, triple-helical peptide; THPI, triple-helical peptide inhibitor; TIMP, tissue inhibitor of metalloproteinase; UC, ulcerative colitis; VEGF, vascular endothelial growth factor.

Recent advances in the development of selective MMP inhibitors have included unique modes of action for inhibiting MMPs implicated in angiogenesis (MMP-2, MMP-9, and MT1-MMP).

MMP-2/MMP-9 INHIBITORS

Mechanism-based inhibitors selective for MMP-2 and MMP-9 were developed based on the thiirane moiety (**Figure 2A**) (28). Although it was initially proposed that the thiirane would be activated via coordination with the active site Zn^{2+}, allowing for covalent modification by an active site nucleophile (28), subsequent studies revealed a mechanism by which deprotonation at the methylene adjacent to the sulfone occurred, initiating ring opening of the thiirane and formation of a stable Zn^{2+}-thiolate complex (31). The thiirane-based inhibitor SB-3CT (**Figure 2A**) exhibited antiangiogenic and antimetastatic behaviors (32, 33). *In vivo*, SB-3CT was found to be metabolized by several routes, including *p*-hydroxylation, hydroxylation at the methylene adjacent to the sulfone leading to sulfinic acid formation, and glutathione-based Cys conjugation of the thiirane ring (34). α-Methyl variants of SB-3CT had improved metabolic profiles, as only oxidation of the thiirane sulfur was observed (35). Unfortunately, SB-3CT was poorly water soluble. Thiirane-based inhibitors with improved water solubility were subsequently developed (36). ND-322 (which was selective for

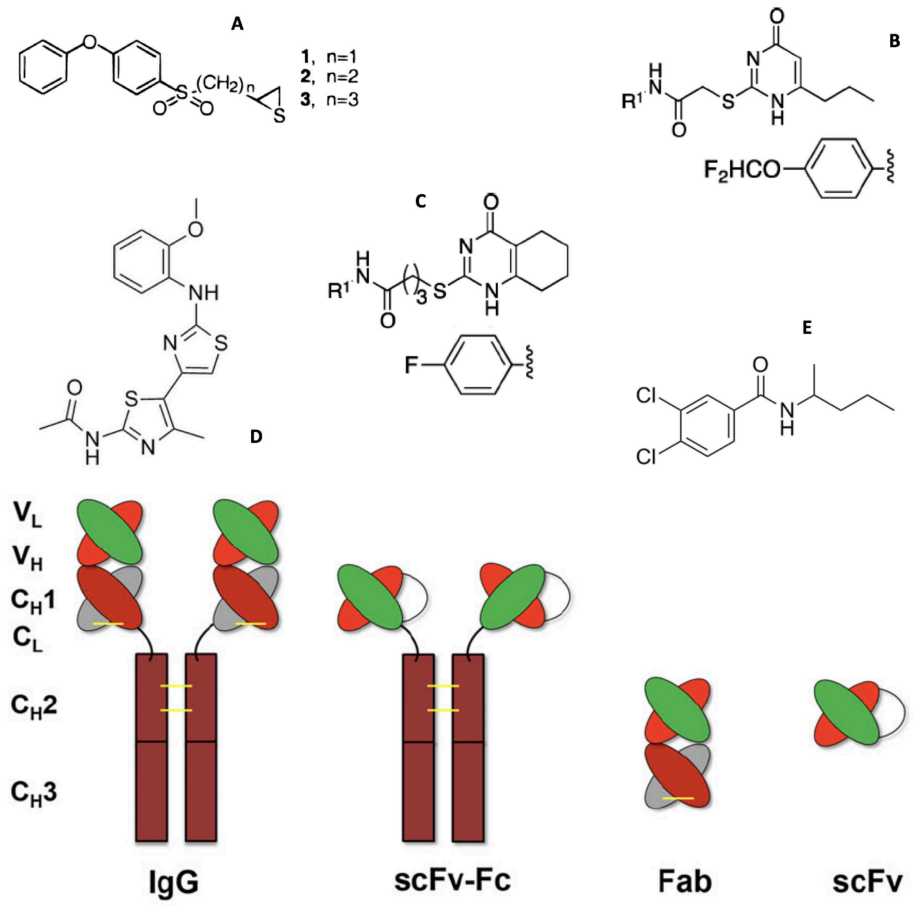

FIGURE 2 | Structures of MMP small molecule inhibitors **(A)** thiiranes (where n = 1 for SB-3CT), **(B)** *N*-[4-(difluoromethoxy)phenyl]-2-[(4-oxo-6-propyl-1 *H*-pyrimidin-2-yl)sulfanyl]-acetamide, **(C)** *N*-(4-fluorophenyl)-4-(4-oxo-3,4,5,6,7,8-hexahydroquinazolin-2-ylthio)butanamide, **(D)** JNJ0966 [*N*-(2-((2-methoxyphenyl) amino)-4′-methyl-[4,5′-bithiazol]-2′-yl)acetamide], and **(E)** NSC405020 [3,4-dichloro-*N*-(1-methylbutyl)benzamide], and (bottom) MMP inhibitory antibodies (IgG) and antibody fragments. Illustrations reprinted with permission from Brown et al. (28), Alford et al. (29), and Santamaria and de Groot (30). Copyright 2000 and 2017 American Chemical Society and 2018 John Wiley and Sons.

MMP-2 and MT1-MMP) was found to have antimetastatic activity (37), while the *O*-phosphate prodrug form of SB-3CT crossed the blood-brain barrier (38).

Targeting antibodies (Abs) (**Figure 2**, bottom) directly to the Zn^{2+} complex in the MMP active site (designated metallobodies) could have superior properties over classical Abs by mimicking the molecular recognition offered by the endogenous inhibitors of MMPs, tissue inhibitor of metalloproteinases (TIMPs), while providing better selectivity (39). Mice were immunized with synthetic organic ligands bound to a metal ion (Zinc-Tripod), which mimicked the MMP catalytic Zn^{2+} complex. This was followed by immunization with the full-length MMP. The immunization procedure yielded function blocking metallobodies (SDS3 and SDS4) directed at the catalytic Zn^{2+} and enzyme surface epitopes in activated MMP-9 (39). Metallobodies SDS3 and SDS4 bound and inhibited MMP-9 with $K_D = 200$ and 20 nM, respectively, and $K_i = 1\,\mu M$ and 54 nM, respectively. SDS3 and SDS4 also effectively inhibited MMP-2, but had no inhibitory activity toward MMP-1, MMP-7, MMP-12, or ADAM17, and more than an order of magnitude lower activity toward MT1-MMP. SDS3 was shown, in both prophylactic and therapeutic applications, to protect mice from dextran sodium sulfate-induced colitis (39).

In general, metalloproteinases use the nucleophilic attack of a water molecule as one of the steps of amide bond hydrolysis (40). Water addition to the amide carbonyl results in a tetrahedral transition state. Phosphinic peptides [$\Psi\{PO_2H\text{-}CH_2\}$] are analogs of this transition state and behave as inhibitors of MMPs (41). Phosphinate triple-helical (collagen mimic) MMP inhibitors allow incorporation of specificity elements for both the S and S' subsites of the enzyme. Although binding to the non-primed region of the active site is generally weaker than the primed site to prevent product inhibition (40), it does add sequence diversity and potential selectivity. Triple-helical structure allows for interaction with both the active site and secondary binding sites (exosites) of collagenolytic MMPs (42–44), which include MMP-2, MMP-9, and MT1-MMP (45).

Our laboratory produced a series of triple-helical peptide inhibitors (THPIs) based on GlyΨ{PO_2H-CH_2}Leu, GlyΨ{PO_2H-CH_2}Val, and GlyΨ{PO_2H-CH_2}Ile transition state analogs (42, 46–51). The α1(V)GlyΨ{PO_2H-CH_2}Val THPI [C_6-(Gly-Pro-Hyp)$_4$-Gly-Pro-Pro-GlyΨ{PO_2H-CH_2}(*R*,*S*)Val-Val-Gly-Glu-Gln-Gly-Glu-Gln-Gly-Pro-Pro-(Gly-Pro-Hyp)$_4$-NH_2], based on the cleavage site in type V collagen by MMP-9 (52), was a selective inhibitor for MMP-2 and MMP-9 (46). The thermal stability of the α1(V)GlyΨ{PO_2H-CH_2}Val THPI was greatly reduced compared to the parent substrate (46, 53). We synthesized a stabilized version of the α1(V)GlyΨ{PO_2H-CH_2}Val THPI, designated α1(V)GlyΨ{PO_2H-CH_2}Val [mep$_{14,32}$,Flp$_{15,33}$] THPI, where mep was (2*S*,4*R*)-4-methylproline and Flp was (2*S*,4*R*)-4-fluoroproline (51). α1(V)GlyΨ{PO_2H-CH_2}Val [mep$_{14,32}$,Flp$_{15,33}$] THPI had a melting point (T_m value) 18 °C higher than α1(V)GlyΨ{PO_2H-CH_2}Val THPI (51). α1(V)GlyΨ{PO_2H-CH_2}Val [mep$_{14,32}$,Flp$_{15,33}$] THPI exhibited K_i values against MMP-2 and MMP-9 of 189.1 and 90.6 nM, respectively, at 25°C, and 2.24 and 0.98 nM, respectively, at 37°C (51).

Triple-helical peptides (THPs) have been found to be reasonably stable to general proteolysis, as observed *in vitro* in mouse, rat, and human serum and/or plasma and *in vivo* in rats (54–58). The stability of THPs has allowed for their administration orally (59). The α1(V)GlyΨ{PO_2H-CH_2}Val [mep$_{14,32}$,Flp$_{15,33}$] THPI was effective *in vivo* in a mouse model of multiple sclerosis, reducing clinical severity and weight loss (51).

MMP-2 SELECTIVE INHIBITORS

Chlorotoxin (ClTx) is 36-residue peptide isolated from the venom of the Israeli Yellow scorpion *Leiurus quinquestriatus* (60). ClTx preferentially binds neuroectodermal tumors and exhibits antiangiogenic and anti-invasion activity (61–65). ClTx selectively inhibits MMP-2 in a dose-dependent manner ($K_D \sim$ 115 nM) (62). The ClTx interaction with a membrane complex of chloride channel-3 (ClC-3) and MMP-2 (66) has been used to create numerous cancer imaging agents (63, 65, 67–69). ClTx can pass through the blood-brain barrier (65), and has yielded promising preclinical and clinical results in the treatment of glioblastoma (64, 68).

MMP-9 SELECTIVE INHIBITORS

Mouse mAb REGA-3G12, a selective inhibitor of MMP-9, was prepared using MMP-9 as antigen (70). REGA-3G12 recognized the MMP-9 Trp116 to Lys214 region, located in the CAT domain but not part of the Zn^{2+} binding site (71). REGA-3G12 bound to MMP-9 with K_D = 2.1 nM (70). REGA-3G12 prevented interleukin-8-induced mobilization of hematopoietic progenitor cells in rhesus monkeys (72). A single chain variable fragment (scFv) (**Figure 2**, bottom) derived from REGA-3G12 selectively inhibited MMP-9 compared to MMP-2 (73). Gelatin hydrolysis was inhibited 44% at a scFv concentration of 5 μM (73).

Two monoclonal anti-MMP-9 antibodies, AB0041 and AB0046, were shown to inhibit tumor growth and metastasis in a surgical orthotopic xenograft model of colorectal carcinoma (74). AB0046 improved immune responses to tumors, as the inhibition of MMP-9 reversed MMP-9 inactivation of T-cell chemoattractant CXCR3 ligands (CXCL9, CXCL10, and CXCL11) (75). A humanized version of AB0041, GS-5745 (Andecaliximab), was generated for use in clinical trials (74). GS-5745 was found to bind to MMP-9 near the junction between the pro-domain and CAT domain, distal to the active site, and (a) inhibited proMMP-9 activation and (b) non-competitively inhibited MMP-9 activity (76). GS-5745 bound to MMP-9 with ∼150-400-fold weaker affinity compared with proMMP-9 (K_D = 2.0–6.6 vs. 0.008–0.043 nM) (76). GS-5745/Andecaliximab has been evaluated under several clinical trials. A randomized placebo controlled phase 1b single and multiple ascending dose-ranging clinical trial on 72 patients diagnosed with moderately to severely active ulcerative colitis (UC) showed that GS-5745 was safe, well-tolerated, and could be used as a potential therapeutic agent for UC (77). A phase 2/3 UC study with 165 patients treated over 8 weeks further indicated that GS-5745 was well-tolerated (78). A phase 1b trial investigating the safety, pharmacokinetics, and disease-related outcomes for 15 rheumatoid arthritis patients (ClinicalTrials.gov Identifier NCT02176876) demonstrated that GS-5745 was safe, with adverse events that were only grade 1 or 2 in severity and no indication of MSS (79).

Several non-active site small molecule MMP-9 inhibitors have been described. *N*-[4-(difluoromethoxy)phenyl]-2-[(4-oxo-6-propyl-1*H*-pyrimidin-2-yl)sulfanyl]-acetamide (**Figure 2B**) bound selectively to the MMP-9 HPX domain with K_D = 2.1 μM and inhibited tumor growth and lung metastasis in MDA-MB-435 mouse models (80). Based on this lead compound a library of analogs was generated, and *N*-(4-fluorophenyl)-4-(4-oxo-3,4,5,6,7,8-hexahydroquinazolin-2-ylthio)butanamide (**Figure 2C**) emerged as a more potent inhibitor (K_D = 320 nM) (29). This compound prevented association of proMMP-9 with the α4β1 integrin and CD44, resulting in the dissociation of epidermal growth factor receptor (EGFR) from the β1 integrin subunit and CD44 (29). High-throughput screening led to the identification of compound JNJ0966 [*N*-(2-((2-methoxyphenyl)amino)-4′-methyl-[4,5′-bithiazol]-2′-yl)acetamide] (**Figure 2D**), which bound selectively to proMMP-9 with K_D = 5.0 μM (81). JNJ0966 inhibited the activation of proMMP-9 and the migration of HT1080 cells, and was able to penetrate the blood-brain barrier (81).

MT1-MMP SELECTIVE INHIBITORS

Several selective MT1-MMP inhibitory antibodies and antibody fragments have been described (27, 30, 82–84). Screening a human Fab display phage library resulted in the development of DX-2400, a selective, fully human MT1-MMP inhibitory antibody (K_i = 0.8 nM) (27, 85). DX-2400 was a competitive inhibitor of MT1-MMP (85). DX-2400 inhibited tumor MT1-MMP activity, resulting in the inhibition of MDA-MB-231 primary tumor growth but not MCF-7 tumor growth in xenograft

mouse models (85). DX-2400 also inhibited metastasis (85), and enhanced tumor response to radiation therapy (86).

Recombinant human scFv antibodies (**Figure 2**, bottom) were generated against the MT1-MMP HPX domain (87). Two scFv antibodies, CHA and CHL (K_D = 10.7 and 169 nM, respectively), were found to have differing activities. CHL inhibited MT1-MMP binding to collagen, while CHA had the opposite effect, yet both scFv antibodies inhibited HT1080 invasion of type I collagen. CHA inhibited CD44 shedding and endothelial cell sprouting from endothelial cell/fibroblast co-cultures in type I collagen, while CHL had no effect on either activity (87).

Monoclonal antibody (mAb) 9E8 (K_D = 0.6 nM) inhibited MT1-MMP activation of proMMP-2, but not other MT1-MMP catalytic activities (88). mAb 9E8 bound to the Pro163 to Gln174 loop in the MT1-MMP CAT domain (89). This loop region is present in the CAT domain of MT1-MT6-MMPs, but is not found in all other MMPs. mAb 9E8 prevented formation of the MT1-MMP•TIMP-2•proMMP-2 complex required for proMMP-2 activation by interfering with TIMP-2 binding (89). Another antibody raised against the loop region, $LOOP_{Ab}$, also inhibited MT1-MMP activation of proMMP-2, but not MT1-MMP collagenolysis (90).

The LEM-2/15 antibody was generated using a cyclic peptide mimicking the MT1-MMP CAT domain V-B loop (residues 218-233) (91). A minimized Fab fragment (**Figure 2**, bottom) of LEM-2/15 was designed, and possessed a reasonable binding affinity compared to the intact antibody (K_D = 2.3 vs. 0.4 nM, respectively) (92). The Fab fragment was a non-competitive inhibitor of MT1-MMP activities, including collagenolysis (92). The Fab fragment of LEM-2/15 induced a conformational change in MT1-MMP by destabilizing the exposed region of the V-B loop, ultimately narrowing the substrate binding cleft (30, 84, 92). Treatment with the Fab fragment of LEM-2/15 significantly increased the ability of virally infected mice to fight off secondary *Strep. pneumoniae* bacterial infection (93). Treatment with the Fab fragment of LEM-2/15, before or after infection, helped to maintain tissue integrity (93).

Human scFv-Fc (**Figure 2**, bottom) antibody E3 bound to the MT1-MMP CAT domain and inhibited type I collagen binding (94). A second generation E3 clone (E2_C6, K_D = 0.11 nM) inhibited tumor growth and metastasis (94).

Human antibody Fab libraries were synthesized where the Peptide G sequence (Phe-Ser-Ile-Ala-His-Glu) (95) was incorporated into complementarity determining region (CDR)-H3 (96). Fab 1F8 exhibited EC_{50} = 8.3 nM against the MT1-MMP CAT domain, and inhibited MT1-MMP CAT domain activity with K_i = 110 nM (96).

Screening of a phage displayed synthetic humanized Fab library led to the identification of Fab 3369 (97). Fab 3369 inhibited the activity of the MT1-MMP CAT domain with IC_{50} = 62 nM (97). IgG 3369 treatment of MDA-MB-231 mammary orthotopic xenograft mice reduced lung metastases, collagen processing, and tumor density of $CD31^+$ blood vessels (97).

It has been noted that antibody antigen binding sites are not complimentary to the concave shape of catalytic clefts, as antigen binding sites are planar or concave (84). To overcome this, the convex-shaped paratope of camelid antibodies was incorporated into the human antibody scaffold (98). Fab 3A2 bound selectively to MT1-MMP CAT domain outside of the active site cavity with K_D = 4.8 nM, and was a competitive inhibitor with K_i = 9.7 nM (98, 99). Fab 3A2 inhibited MT1-MMP collagenolysis and reduced metastasis in a melanoma mouse model (99).

Virtual ligand screening of the NCI/NIH Developmental Therapeutics Program ∼275,000 compound library resulted in the identification of compound NSC405020 [3,4-dichloro-*N*-(1-methylbutyl)benzamide] (**Figure 2E**), a small molecule MT1-MMP HPX domain inhibitor (100). NSC405020 inhibited MT1-MMP homodimerization but not proMMP-2 activation or catalytic activity toward a peptide substrate. NSC405020 reduced the collagenolytic activity of MCF7-β3/MT1-MMP cells and was effective *in vivo*, as intratumoral injections reduced tumor size significantly (100).

CRITICAL OVERVIEW

Tumor growth is limited without the ability of the tumor to create its own blood supply (101). The use of antiangiogenic therapeutic agents is viewed as beneficial due to (a) the prevention of new blood vessel formation and/or (b) the normalization of tumor-associated vasculature (102). Normalizing the tumor-associated vasculature can enhance the penetration of therapeutic agents (102, 103). Clinically utilized antiangiogenic agents typically target VEGF or the VEGF receptor (VEGFR), or are multikinase inhibitors (102). Significant improvement in overall survival and prolonged progression-free survival was observed when angiogenesis inhibitors were applied in gastric cancer (104). Anti-VEGFR-2 and multikinase inhibitor treatments were more efficacious than anti-VEGF treatment (104). This was suggested to be due to blocking only VEGF-A in the latter treatment (104). Thus, angiogenesis targeting via MMP inhibition could be very efficacious based on the potential broader impact than just VEGF-A inhibition (as discussed in the Introduction). The ability of the combination of angiogenesis inhibition and chemotherapy to prolong progression-free survival in patients with gastric cancer was dependent upon the antiangiogenic agent used (104).

Antiangiogenic therapies can have serious side effects, such as bleeding, venous or arterial thromboembolisms, proteinuria, and hypertension, and can also increase drug resistance, cancer invasion, and metastasis (102, 104–106). An obvious concern is that antiangiogenic approaches can negatively impact capillaries and blood flow in healthy tissues (104). Additionally, targeting VEGF can lead to upregulation of other pro-angiogenic factors (107, 108). All in all, side effects from the use of angiogenesis inhibitors are often viewed as manageable (104, 105, 109).

Unique modes of action have been used to develop antibody-based, triple-helical peptide, and small molecule inhibitors of MMPs implicated in angiogenesis. The selective, small molecule MMP-9 and MT1-MMP inhibitors do not yet have preferred affinities, but represent a promising start based on their novel mechanisms of inhibition. Clinical trials utilizing antibodies have provided evidence that selective MMP inhibitors do not induce MSS. Unfortunately, antibodies are subject to proteolysis, may be removed from circulation rapidly, and are costly.

Nonetheless, antibodies have provided truly selective, high affinity MMP inhibitors. Selective, high affinity inhibitors can be developed for MMPs based on triple-helical structure. THPIs have excellent pharmacokinetic properties compared with other peptide-based therapeutics. The mechanistically non-traditional MMP inhibitors offer treatment strategies for tumor angiogenesis that avoid the off-target toxicities and lack of specificity that plagued Zn^{2+}-chelating inhibitors.

One must consider that when applied as antiangiogenic agents, MMP inhibitors may have the undesired effect of (a) limiting turnover of already existing tumor vessels and (b) disrupting vascular homoeostatis, where normal vessel turnover and other related activities are needed. This would be dependent upon which MMP was targeted. For example, MT1-MMP has been shown to contribute to both angiogenesis and vascular regression in an aortic ring model (110). Inhibition of MT1-MMP catalytic activity following the vessel growth phase resulted in reduced vascular regression due to inhibition of collagenolysis (110). Vessels are destabilized by MT1-MMP shedding of Tie-2 from endothelial cells (111), and thus enzyme inhibition could stabilize tumor vessels (103). In similar fashion, TIMP-2 and TIMP-3 were found to stabilize newly formed vascular networks by (a) inhibiting regression and (b) preventing further endothelial cell tube morphogenesis (112). The action of TIMP-2 and TIMP-3 was correlated to MT1-MMP activity, and thus inhibition of MT1-MMP could stabilize vascular networks (112). Deletion of MT1-MMP or inhibition of MT1-MMP activity resulted in increased vascular leakage (103). In this latter case, MT1-MMP was proposed to modulate TGFβ availability, with decreased TGFβ levels impacting vascular homoeostatsis (103). MT1-MMP shedding of endoglin (CD105) results in the release of sEndoglin, which inhibits angiogenesis (113). MMP-9 contributes to edema prevention, which is a component of vascular homoeostasis (103). MMP-2 cleavage of ECM biomolecules leads to disruption of endothelial cell β1 integrin binding and subsequent signaling (114, 115). In turn, disruption of signaling leads to a decrease in MT1-MMP production (114).

Another consideration for MMP inhibition is the effect on the production of antiangiogenic agents, such as angiostatin (from plasminogen), endostatin (from type XVIII collagen), arresten (from the α1(IV) collagen chain), canstatin (from the α2(IV) collagen chain), and tumstatin (from the α3(IV) collagen chain). MMP-9 is capable of generating angiostatin (116, 117), endostatin (118, 119), arresten (120), canstatin (120), and tumstatin (120, 121). However, the redundancy of proteases capable of generating these agents (116, 118, 120) suggests that inhibiting one (such as MMP-9) may have little effect on these particular antiangiogenic activities.

While selective MMP inhibitors are greatly needed, often overlooked is that the timing of MMP inhibitor application is also critical (see above). Application of a broad spectrum MMP inhibitor (marimostat) in combination with gemcitabine significantly improved survival in pancreatic cancer patients with disease confined to the pancreas (122). Presurgical treatment with an oral MMP inhibitor improved survival from 67 to 92% in a mouse breast cancer model (123). As discussed earlier, MMP-9 is a key contributor to the angiogenic switch during carcinogenesis of pancreatic islets (5). However, MMP-9 deficiency in pancreatic ductal adenocarcinoma (PDAC) mouse models resulted in more invasive tumors and an increase in desmoplastic stroma (124). The absence of MMP-9 led to increased interleukin 6 levels in the bone marrow, which activated tumor cell STAT3 signaling and promoted PDAC invasion and metastasis (124). Thus, MMP-9 represents an anti-target in the later stage of pancreatic cancer. The "window of opportunity" for MMP inhibitor application is often in premetastatic disease (125).

AUTHOR CONTRIBUTIONS

The author confirms being the sole contributor of this work and has approved it for publication.

FUNDING

Work on MMP inhibitors in my laboratory has been supported by the National Institutes of Health (CA098799, AR063795, CA239214, and NHLBI contract 268201000036C), the James and Esther King Biomedical Research Program, the US-Israel Binational Science Foundation (BSF), the Center for Molecular Biology and Biotechnology at Florida Atlantic University, and the State of Florida, Executive Office of the Governor's Department of Economic Opportunity.

REFERENCES

1. Egeblad M, Werb Z. New functions for the matrix metalloproteinases in cancer progression. *Nat Rev Cancer.* (2002) 2:161–74. doi: 10.1038/nrc745
2. Senger DR, Davis GE. Angiogenesis. *Cold Spring Harb Perspect Biol.* (2011) 3:1–19. doi: 10.1101/cshperspect.a005090
3. Kang H, Hong Z, Zhong M, Klomp J, Bayless KJ, Mehta D, et al. Piezo1 mediates angiogenesis through activation of MT1-MMP signaling. *Am J Physiol Cell Physiol.* (2019) 316:C92–C103. doi: 10.1152/ajpcell.00346.2018
4. Deryugina EI, Quigley JP. Pleiotropic roles of matrix metalloproteinases in tumor angiogenesis: Contrasting, overlapping and compensatory functions. *Biochim Biophys Acta.* (2010) 1803:103–20. doi: 10.1016/j.bbamcr.2009.09.017
5. Bergers G, Brekken RA, McMahon G, Vu TH, Itoh T, Tamaki K, et al. Matrix metalloproteinase-9 triggers the angiogenic switch during carcinogenesis. *Nat Cell Biol.* (2000) 2:737–44. doi: 10.1038/35036374
6. Ardi VC, Kupriyanova TA, Deryugina EI, Quigley JP. Human neutrophils uniquely release TIMP-free MMP-9 to provide a potent catalytic stimulator of angiogenesis. *Proc Natl Acad Sci USA.* (2007) 104:20262–7. doi: 10.1073/pnas.0706438104
7. Ardi VC, Van den Steen PE, Opdenakker G, Schweighofer B, Deryugina EI, Quigley JP. Neutrophil MMP-9 proenzyme, unencumbered by TIMP-1, undergoes efficient activation *in vivo* and catalytically induces angiogenesis via a basic fibroblast growth factor (FGF-2)/FGFR-2 pathway. *J Biol Chem.* (2009) 284:25854–66. doi: 10.1074/jbc.M109.033472

8. Bekes EM, Schweighofer B, Kupriyanova TA, Zajac E, Ardi VC, Quigley JP, et al. Tumor-recruited neutrophils and neutrophil TIMP-free MMP-9 regulate coordinately the levels of tumor angiogenesis and efficiency of malignant cell intravasation. *Am J Pathol.* (2011) 179:1455–70. doi: 10.1016/j.ajpath.2011.05.031
9. Riabov V, Gudima A, Wang N, Mickley A, Orekhov A, Kzhyshkowska J. Role of tumor associated macrophages in tumor angiogenesis and lymphangiogenesis. *Front Physiol.* (2014) 5:75. doi: 10.3389/fphys.2014.00075
10. Zhou Z, Apte SS, Soininen R, Cao R, Baaklini GY, Rauser RW, et al. Impaired endochondral ossification and angiogenesis in mice deficient in membrane-type matrix metalloproteinase 1. *Proc Natl Acad Sci USA.* (2000) 97:4052–7. doi: 10.1073/pnas.060037197
11. Koike T, Vernon RB, Hamner MA, Sadoun E, Reed MJ. MT1-MMP, but not secreted MMPs, influences the migration of human microvascular endothelial cells in 3-dimensional collagen gels. *J Cell Biochem.* (2002) 86:748–58. doi: 10.1002/jcb.10257
12. Chun T-H, Sabeh F, Ota I, Murphy H, McDonagh KT, Holmbeck K, et al. MT1-MMP-dependent neovessel formation within the confines of the three-dimensional extracellular matrix. *J Cell Biol.* (2004) 167:757–67. doi: 10.1083/jcb.200405001
13. Genís L, Gálvez BG, Gonzalo P, Arroyo AG. MT1-MMP: universal or particular player in angiogenesis? *Cancer Metastasis Rev.* (2006) 25:77–86. doi: 10.1007/s10555-006-7891-z
14. Stratman AN, Saunders WB, Sacharidou A, Koh W, Fisher KE, Zawieja DC, et al. Endothelial cell lumen and vascular guidance tunnel formatinon requires MT1-MMP-dependent proteolysis in 3-dimensional collagen matrices. *Blood.* (2009) 114:237–47. doi: 10.1182/blood-2008-12-196451
15. Sacharidou A, Koh W, Stratman AN, Mayo AM, Fisher KE, Davis GE. Endothelial lumen signaling complexes control 3D matrix-specific tubulogenesis through interdependent Cdc42- and MT1-MMP-mediated events. *Blood.* (2010) 115:5259–69. doi: 10.1182/blood-2009-11-252692
16. Ricciuti B, Foglietta J, Bianconi V, Sahebkar A, Pirro M. Enzymes involved in tumor-driven angiogenesis: A valuable target for anticancer therapy. *Semin Cancer Biol.* (2017). doi: 10.1016/j.semcancer.2017.11.005. [Epub ahead of print].
17. Gatto C, Rieppi M, Borsotti P, Innocenti S, Ceruti R, Drudis T, et al. BAY 12-9566, a novel inhibitor of matrix metalloproteinases with antiangiogenic activity. *Clin Cancer Res.* (1999) 5:3603–7.
18. Shalinsky DR, Brekken J, Zou H, McDermott CD, Forsyth P, Edwards D, et al. Broad antitumor and antiangiogenic activities of AG3340, a potent and selective MMP inhibitor undergoing advanced oncology clinical trials. *Ann N Y Acad Sci.* (1999) 878:236–70. doi: 10.1111/j.1749-6632.1999.tb07689.x
19. Lockhart AC, Braun RD, Yu D, Ross JR, Dewhirst MW, Humphrey JS, et al. Reduction of wound angiogenesis in patients treated with BMS-275291, a broad spectrum matrix metalloproteinase inhibitor. *Clin Cancer Res.* (2003) 9:586–93.
20. Beckett RP. Recent advances in the field of matrix metalloproteinase inhibitors. *Exp Opin Ther Patents.* (1996) 6:1305–15. doi: 10.1517/13543776.6.12.1305
21. Beckett RP, Whittaker M. Matrix metalloproteinase inhibitors 1998. *Exp Opin Ther Patents.* (1998) 8:259–82. doi: 10.1517/13543776.8.3.259
22. Whittaker M, Floyd CD, Brown P, Gearing AJH. Design and therapeutic application of matrix metalloproteinase inhibitors. *Chem Rev.* (1999) 99:2735–76. doi: 10.1021/cr9804543
23. Lauer-Fields JL, Fields GB. Matrix metalloproteinase inhibitors and cancer. *Exp Opin Ther Patents.* (2000) 10:1873–84. doi: 10.1517/13543776.10.12.1873
24. Rao BG. Recent developments in the design of specific matrix metalloproteinase inhibitors aided by structural and computational studies. *Curr Pharm Design.* (2005) 11:295–322. doi: 10.2174/1381612053382115
25. Saghatelian A, Jessani N, Joseph A, Humphrey M, Cravatt BF. Activity-based probes for the proteomic profiling of metalloproteases. *Proc Natl Acad Sci USA.* (2004) 101:10000–5. doi: 10.1073/pnas.0402784101
26. Becker DP, Barta TE, Bedell LJ, Boehm TL, Bond BR, Carroll J, et al. Orally active MMP-1 sparing α-tetrahydropyranyl and α-piperidinyl sulfone matrix metalloproteinase (MMP) inhibitors with efficacy in cancer, arthritis, and cardiovascular disease. *J Med Chem.* (2010) 53:6653–80. doi: 10.1021/jm100669j
27. Devy L, Dransfield DT. New strategies for the next generation of matrix-metalloproteinase inhibitors: selectively targeting membrane-anchored MMPs with therapeutic antibodies. *Biochem Res Int.* (2011) 2011:191670. doi: 10.1155/2011/191670
28. Brown S, Bernardo MM, Li Z-H, Kotra LP, Tanaka Y, Fridman R, et al. Potent and selective mechanism-based inhibition of gelatinases. *J Am Chem Soc.* (2000) 122:6799–800. doi: 10.1021/ja001461n
29. Alford VM, Kamath A, Ren X, Kumar K, Gan Q, Awwa M, et al. Targeting the hemopexin-like domain of latent matrix metalloproteinase-9 (proMMP-9) with a small molecule inhibitor prevents the formation of focal adhesion junctions. *ACS Chem Biol.* (2017) 12:2788–803. doi: 10.1021/acschembio.7b00758
30. Santamaria S, de Groot R. Monoclonal antibodies against metzincin targets. *Br J Pharmacol.* (2019) 176:52–66. doi: 10.1111/bph.14186
31. Forbes C, Shi Q, Fisher JF, Lee M, Hesek D, Llarrull LI, et al. Active site ring-opening of a thiirane moiety and picomolar inhibition of gelatinases. *Chem Biol Drug Des.* (2009) 74:527–34. doi: 10.1111/j.1747-0285.2009.00881.x
32. Krüger A, Arlt MJE, Gerg M, Kopitz C, Bernardo MM, Chang M, et al. Antimetastatic activity of a novel mechanism-based gelatinase inhibitor. *Cancer Res.* (2005) 65:3523–6. doi: 10.1158/0008-5472.CAN-04-3570
33. Bonfil RD, Sabbota A, Nabha S, Bernardo MM, Dong Z, Meng H, et al. Inhibition of human prostate cancer growth, osteolysis and angiogenesis in a bone metastasis model by a novel mechanism-based selective gelatinase inhibitor. *Int J Cancer.* (2006) 118:2721–6. doi: 10.1002/ijc.21645
34. Celenza G, Villegas-Estrada A, Lee M, Boggess B, Forbes C, Wolter WR, et al. Metabolism of (4-phenoxyphenylsulfonyl) methylthiirane, a selective gelatinase inhibitor. *Chem Biol Drug Des.* (2008) 71:187–96. doi: 10.1111/j.1747-0285.2008.00632.x
35. Gooyit M, Lee M, Hesek D, Boggess B, Oliver AG, Fridman R, et al. Synthesis, kinetic characterization and metabolism of diastereomeric 2-(1-(4-phenoxyphenylsulfonyl)ethyl)thiiranes as potent gelatinase and MT1-MMP inhibitors. *Chem Biol Drug Des.* (2009) 74:535–46. doi: 10.1111/j.1747-0285.2009.00898.x
36. Gooyit M, Lee M, Schroeder VA, Ikejiri M, Suckow MA, Mobashery S, et al. Selective water-soluble gelatinase inhibitor prodrugs. *J Med Chem.* (2011) 54:6676–90. doi: 10.1021/jm200566e
37. Marusak C, Bayles I, Ma J, Gooyit M, Gao M, Chang M, et al. The thiirane-based selective MT1-MMP/MMP2 inhibitor ND-322 reduces melanoma tumor growth and delays metastatic dissemination. *Pharmacol Res.* (2016) 113:515–20. doi: 10.1016/j.phrs.2016.09.033
38. Lee M, Chen Z, Tomlinson BN, Gooyit M, Hesek D, Juárez MR, et al. Water-soluble MMP-9 inhibitor reduces lesion volume after severe traumatic brain injury. *ACS Chem Neurosci.* (2015) 6:1658–64. doi: 10.1021/acschemneuro.5b00140
39. Sela-Passwell N, Kikkeri R, Dym O, Rozenberg H, Margalit R, Arad-Yellin R, et al. Antibodies targeting the catalytic zinc complex of activated matrix metalloproteinases show therapeutic potential. *Nat Med.* (2011) 18:143–7. doi: 10.1038/nm.2582
40. Babine RE, Bender SL. Molecular recognition of protein-ligand complexes: applications to drug design. *Chem Rev.* (1997) 97:1359–472. doi: 10.1021/cr960370z
41. Gall AL, Ruff M, Kannan R, Cuniasse P, Yiotakis A, Dive V, et al. Crystal structure of the stromelysin-3 (MMP-11) catalytic domain complexed with a phosphinic inhibitor mimicking the transition-state. *J Mol Biol.* (2001) 307:577–86. doi: 10.1006/jmbi.2001.4493
42. Lauer-Fields JL, Chalmers MJ, Busby SA, Minond D, Griffin PR, Fields GB. Identification of specific hemopexin-like domain residues that facilitate matrix metalloproteinase collagenolytic activity. *J Biol Chem.* (2009) 284:24017–24. doi: 10.1074/jbc.M109.016873
43. Bertini I, Fragai F, Luchinat C, Melikian M, Toccafondi M, Lauer JL, et al. Structural basis for matrix metalloproteinase 1 catalyzed collagenolysis. *J Am Chem Soc.* (2012) 134:2100–10. doi: 10.1021/ja208338j
44. Manka SW, Carafoli F, Visse R, Bihan D, Raynal N, Farndale RW, et al. Structural insights into triple-helical collagen cleavage by matrix metalloproteinase 1. *Proc Natl Acad Sci USA.* (2012) 109:12461–6. doi: 10.1073/pnas.1204991109

45. Amar S, Smith L, Fields GB. Matrix metalloproteinase collagenolysis in health and disease. *Biochim Biophys Acta Mol Cell Res.* (2017) 1864:1940–51. doi: 10.1016/j.bbamcr.2017.04.015
46. Lauer-Fields JL, Brew K, Whitehead JK, Li S, Hammer RP, Fields GB. Triple-helical transition-state analogs: a new class of selective matrix metalloproteinase inhibitors. *J Am Chem Soc.* (2007) 129:10408–17. doi: 10.1021/ja0715849
47. Lauer-Fields JL, Whitehead JK, Li S, Hammer RP, Brew K, Fields GB. Selective modulation of matrix metalloproteinase 9 (MMP-9) functions via exosite inhibition. *J Biol Chem.* (2008) 283:20087–95. doi: 10.1074/jbc.M801438200
48. Bhowmick M, Sappidi RR, Fields GB, Lepore SD. Efficient synthesis of fmoc-protected phosphinic pseuedodipeptides: building blocks for the synthesis of matrix metalloproteinase inhibitors (MMPIs). *Biopolymers.* (2011) 96:1–3. doi: 10.1002/bip.21425
49. Bhowmick M, Fields GB. Synthesis of Fmoc-Gly-Ile phosphinic pseudodipeptide: residue specific conditions for construction of matrix metalloproteinase inhibitor building blocks. *Int J Pept Res Ther.* (2012) 18:335–9. doi: 10.1007/s10989-012-9307-y
50. Bhowmick M, Stawikowska R, Tokmina-Roszyk D, Fields GB. Matrix metalloproteinase inhibition by heterotrimeric triple-helical peptide transition state analogs. *ChemBioChem.* (2015) 16:1084–92. doi: 10.1002/cbic.201402716
51. Bhowmick M, Tokmina-Roszyk D, Onwuha-Ekpete L, Harmon K, Robichaud T, Fuerst R, et al. Second generation triple-helical peptide transition state analog matrix metalloproteinase inhibitors. *J Med Chem.* (2017) 60:3814–27. doi: 10.1021/acs.jmedchem.7b00018
52. Niyibizi C, Chan R, Wu J-J, Eyre D. A 92 kDa gelatinase (MMP-9) cleavage site in native type V collagen. *Biochem Biophys Res Commun.* (1994) 202:328–33. doi: 10.1006/bbrc.1994.1931
53. Lauer-Fields JL, Sritharan T, Stack MS, Nagase H, Fields GB. Selective hydrolysis of triple-helical substrates by matrix metalloproteinase-2 and−9. *J Biol Chem.* (2003) 278:18140–5. doi: 10.1074/jbc.M211330200
54. Fan C-Y, Huang C-C, Chiu W-C, Lai C-C, Liou G-G, Li H-C, et al. Production of multivalent protein binders using a self-trimerizing collagen-like peptide scaffold. *FASEB J.* (2008) 22:3795–804. doi: 10.1096/fj.08-111484
55. Ndinguri MW, Zheleznyak A, Lauer JL, Anderson CJ, Fields GB. Application of collagen-model triple-helical peptide-amphiphiles for CD44 targeted drug delivery systems. *J. Drug Deliv.* (2012). 2012:592602. doi: 10.1155/2012/592602
56. Yamazaki CM, Nakase I, Endo H, Kishimoto S, Mashiyama Y, Masuda R, et al. Collagen-like cell-penetrating peptides. *Angew Chem Int Ed Engl.* (2013) 52:5497–500. doi: 10.1002/anie.201301266
57. Yasui H, Yamazaki CM, Nose H, Awada C, Takao T, Koide T. Potential of collagen-like triple helical peptides as drug carriers: their *in vivo* distribution, metabolism, and excretion profiles in rodents. *Biopolymers.* (2013) 100:705–13. doi: 10.1002/bip.22234
58. Shinde A, Feher KM, Hu C, Slowinska K. Peptide internalization enabled by folding: triple-helical cell-penetrating peptides. *J Pept Sci.* (2015) 21:77–84. doi: 10.1002/psc.2725
59. Koide T, Yamamoto N, Taira KB, Yasui H. Fecal excretion of orally administered collagen-like peptides in rats: contribution of the triple-helical conformation to their stability. *Biol Pharm Bull.* (2016) 39:135–7. doi: 10.1248/bpb.b15-00561
60. DeBin JA, Strichartz GR. Chloride channel inhibition by the venom of the scorpion Leiurus quinquestriatus. *Toxicon.* (1991) 29:1403–8. doi: 10.1016/0041-0101(91)90128-E
61. Soroceanu L, Gillespie Y, Khazaeli MB, Sontheimer H. Use of chlorotoxin for targeting of primary brain tumors. *Cancer Res.* (1998) 58:4871–9.
62. Deshane J, Garner CC, Sontheimer H. Chlorotoxin inhibits glioma cell invasion via matrix metalloproteinase-2. *J Biol Chem.* (2003) 278:4135–44. doi: 10.1074/jbc.M205662200
63. Mamelak AN. Targeted antitumor therapy with the scorpion venom chlorotoxin. *Drugs Future.* (2011) 36:615–25. doi: 10.1358/dof.2011.36.8.1656504
64. Cohen-Inbar O, Zaaroor M. Glioblastoma multiforme targeted therapy: the chlorotoxin story. *J Clin Neurosci.* (2016) 33:52–8. doi: 10.1016/j.jocn.2016.04.012
65. Cohen G, Burks SR, Frank JA. Chlorotoxin-A multimodal imaging platform for targeting glioma tumors. *Toxins.* (2018) 10:E496. doi: 10.3390/toxins10120496
66. Qin C, He B, Dai W, Lin Z, Zhang H, Wang X, et al. The impact of a chlorotoxin-modified liposome system on receptor MMP-2 and the receptor-associated protein ClC-3. *Biomaterials.* (2014) 35:5908–20. doi: 10.1016/j.biomaterials.2014.03.077
67. Veiseh M, Gabikian P, Bahrami SB, Veiseh O, Zhang M, Hackman RC, et al. Tumor paint: a chlorotoxin:Cy5.5 bioconjugate for intraoperative visualization of cancer foci. *Cancer Res.* (2007) 67:6882–8. doi: 10.1158/0008-5472.CAN-06-3948
68. Staderini M, Megia-Fernandez A, Dhaliwal K, Bradley M. Peptides for optical medical imaging and steps towards therapy. *Bioorg Med Chem.* (2018) 26:2816–26. doi: 10.1016/j.bmc.2017.09.039
69. Zhao J, Wang YL, Li XB, Gao SY, Liu SY, Song YK, et al. Radiosynthesis and preliminary biological evaluation of 18F-fluoropropionyl-chlorotoxin as a potential PET tracer for glioma imaging. *Contrast Media Mol Imag.* (2018) 2018:8439162. doi: 10.1155/2018/8439162
70. Paemen L, Martens E, Masure S, Opdenakker G. Monoclonal antibodies specific for natural human neutrophil gelatinase B used for affinity purification, quantitation by two-site ELISA and inhibition of enzymatic activity. *Eur J Biochem.* (1995) 234:759–65. doi: 10.1111/j.1432-1033.1995.759_a.x
71. Martens E, Leyssen A, Van Aelst I, Fiten P, Piccard H, Hu J, et al. A monoclonal antibody inhibits gelatinase B/MMP-9 by selective binding to part of the catalytic domain and not to the fibronectin or zinc binding domains. *Biochim Biophys Acta.* (2007) 1770:178–86. doi: 10.1016/j.bbagen.2006.10.012
72. Pruijt JF, Fibbe WE, Laterveer L, Pieters RA, Lindley IJ, Paemen L, et al. Prevention of interleukin-8-induced mobilization of hematopoietic progenitor cells in rhesus monkeys by inhibitory antibodies against the metalloproteinase gelatinase B (MMP-9). *Proc Natl Acad Sci USA.* (1999) 96:10863–8. doi: 10.1073/pnas.96.19.10863
73. Hu J, Van den Steen PE, Houde M, Ilenchuk TT, Opdenakker G. Inhibitors of gelatinase B/matrix metalloproteinase-9 activity comparison of a peptidomimetic and polyhistidine with single-chain derivatives of a neutralizing monoclonal antibody. *Biochem Pharmacol.* (2004) 67:1001–9. doi: 10.1016/j.bcp.2003.10.030
74. Marshall DC, Lyman SK, McCauley S, Kovalenko M, Spangler R, Liu C, et al. Selective allosteric inhibition of MMP9 is efficacious in preclinical models of ulcerative colitis and colorectal cancer. *PLoS ONE.* (2015) 10:e0127063. doi: 10.1371/journal.pone.0127063
75. Juric V, O'Sullivan C, Stefanutti E, Kovalenko M, Greenstein A, Barry-Hamilton V, et al. MMP-9 inhibition promotes anti-tumor immunity through disruption of biochemical and physical barriers to T-cell trafficking to tumors. *PLoS ONE.* (2018) 13:e0207255. doi: 10.1371/journal.pone.0207255
76. Appleby TC, Greenstein AE, Hung M, Liclican A, Velasquez M, Villaseñor AG, et al. Biochemical characterization and structure determination of a potent, selective antibody inhibitor of human MMP9. *J Biol Chem.* (2017) 292:6810–20. doi: 10.1074/jbc.M116.760579
77. Sandborn WJ, Bhandari BR, Fogel R, Onken J, Yen E, Zhao X, et al. Randomised clinical trial: a phase 1, dose-ranging study of the anti-matrix metalloproteinase-9 monoclonal antibody GS-5745 versus placebo for ulcerative colitis. *Aliment Pharmacol Ther.* (2016) 44:157–69. doi: 10.1111/apt.13653
78. Sandborn WJ, Bhandari BR, Randall C, Younes ZH, Romanczyk T, Xin Y, et al. Andecaliximab [anti-matrix metalloproteinase-9] induction therapy for ulcerative colitis: a randomised, double-blind, placebo-controlled, phase 2/3 study in patients with moderate to severe disease. *J Crohns Colitis.* (2018) 12:1021–9. doi: 10.1093/ecco-jcc/jjy049
79. Gossage DL, Cieslarová B, Ap S, Zheng H, Xin Y, Lal P, et al. Phase 1b Study of the safety, pharmacokinetics, and disease-related outcomes of the matrix metalloproteinase-9 inhibitor andecaliximab in patients with rheumatoid arthritis. *Clin. Ther.* (2018) 40:156–65.e155. doi: 10.1016/j.clinthera.2017.11.011

80. Dufour A, Sampson NS, Li J, Kuscu C, Rizzo RC, DeLeon JL, et al. Small molecule anti-cancer compounds selectively target the hemopexin domain of matrix metalloproteinase-9 (MMP-9). *Cancer Res.* (2011) 71:4977–88. doi: 10.1158/0008-5472.CAN-10-4552
81. Scannevin RH, Alexander R, Haarlander TM, Burke SL, Singer M, Huo C, et al. Discovery of a highly selective chemical inhibitor of matrix metalloproteinase-9 (MMP-9) that allosterically inhibits zymogen activation. *J Biol Chem.* (2017) 292:17963–74. doi: 10.1074/jbc.M117.806075
82. Zucker S, Cao J. Selective matrix metalloproteinase (MMP) inhibitors in cancer therapy: ready for prime time? *Cancer Biol Ther.* (2009) 8:1–3. doi: 10.4161/cbt.8.24.10353
83. Sela-Passwell N, Rosenblum G, Shoham T, Sagi I. Structural and functional bases for allosteric control of MMP activities: can it pave the path for selective inhibition? *Biochim Biophys Acta.* (2010) 1803:29–38. doi: 10.1016/j.bbamcr.2009.04.010
84. Levin M, Udi Y, Solomonov I, Sagi I. Next generation matrix metalloproteinase inhibitors - Novel strategies bring new prospects. *Biochim Biophys Acta.* (2017) 1864:1927–39. doi: 10.1016/j.bbamcr.2017.06.009
85. Devy L, Huang L, Naa L, Yanamandra N, Pieters H, Frans N, et al. Selective inhibition of matrix metalloproteinase-14 blocks tumor growth, invasion, and angiogenesis. *Cancer Res.* (2009) 69:1517–26. doi: 10.1158/0008-5472.CAN-08-3255
86. Ager EI, Kozin SV, Kirkpatrick ND, Seano G, Kodack DP, Askoxylakis V, et al. Blockade of MMP14 activity in murine breast carcinomas: implications for macrophages, vessels, and radiotherapy. *J Natl Cancer Inst.* (2015)107:djv017. doi: 10.1093/jnci/djv017
87. Basu B, Correa de Sampaio P, Mohammed H, Fogarasi M, Corrie P, Watkins NA, et al. Inhibition of MT1-MMP activity using functional antibody fragments selected against its hemopexin domain. *Int J Biochem Cell Biol.* (2012) 44:393–403. doi: 10.1016/j.biocel.2011.11.015
88. Ingvarsen S, Porse A, Erpicum C, Maertens L, Jürgensen HJ, Madsen DH, et al. Targeting a single function of the multifunctional matrix metalloproteinase MT1-MMP: impact on lymphangiogenesis. *J Biol Chem.* (2013) 288:10195–204. doi: 10.1074/jbc.M112.447169
89. Shiryaev SA, Remacle AG, Golubkov VS, Ingvarsen S, Porse A, Behrendt N, et al. A monoclonal antibody interferes with TIMP-2 binding and incapacitates the MMP-2-activating function of multifunctional, pro-tumorigenic MMP-14/MT1-MMP. *Oncogenesis.* (2013) 2:e80. doi: 10.1038/oncsis.2013.44
90. Woskowicz AM, Weaver SA, Shitomi Y, Ito N, Itoh Y. MT-LOOP-dependent localization of membrane type I matrix metalloproteinase (MT1-MMP) to the cell adhesion complexes promotes cancer cell invasion. *J Biol Chem.* (2013) 288:35126–37. doi: 10.1074/jbc.M113.496067
91. Gálvez BG, Matías-Román S, Albar JP, Sánchez-Madrid F, Arroyo AG. Membrane type 1-matrix metalloproteinase is activated during migration of human endothelial cells and modulates endothelial motility and matrix remodeling. *J Biol Chem.* (2001) 276:37491–500. doi: 10.1074/jbc.M104094200
92. Udi Y, Grossman M, Solomonov I, Dym O, Rozenberg H, Moreno V, et al. Inhibition mechanism of membrane metalloprotease by an exosite-swiveling conformational antibody. *Structure.* (2015) 23:104–15. doi: 10.1016/j.str.2014.10.012
93. Talmi-Frank D, Altboum Z, Solomonov I, Udi Y, Jaitin DA, Klepfish M, et al. Extracellular matrix proteolysis by MT1-MMP contributes to influenza-related tissue damage and mortality. *Cell Host Microbe.* (2016) 20:458–70. doi: 10.1016/j.chom.2016.09.005
94. Botkjaer KA, Kwok HF, Terp MG, Karatt-Vellatt A, Santamaria S, McCafferty J, et al. Development of a specific affinity-matured exosite inhibitor to MT1-MMP that efficiently inhibits tumor cell invasion *in vitro* and metastasis *in vivo*. *Oncotarget.* (2016) 7:16773–92. doi: 10.18632/oncotarget.7780
95. Suojanen J, Salo T, Koivunen E, Sorsa T, Pirilä E. A novel and selective membrane type-1 matrix metalloproteinase (MT1-MMP) inhibitor reduces cancer cell motility and tumor growth. *Cancer Biol Ther.* (2009) 8:2362–70. doi: 10.4161/cbt.8.24.10139
96. Nam DH, Rodriguez C, Remacle AG, Strongin AY, Ge X. Active-site MMP-selective antibody inhibitors discovered from convex paratope synthetic libraries. *Proc Natl Acad Sci USA.* (2016) 113:14970–5. doi: 10.1073/pnas.1609375114
97. Ling B, Watt K, Banerjee S, Newsted D, Truesdell P, Adams J, et al. A novel immunotherapy targeting MMP-14 limits hypoxia, immune suppression and metastasis in triple-negative breast cancer models. *Oncotarget.* (2017) 8:58372–85. doi: 10.18632/oncotarget.17702
98. Nam DH, Fang K, Rodriguez C, Lopez T, Ge X. Generation of inhibitory monoclonal antibodies targeting matrix metalloproteinase-14 by motif grafting and CDR optimization. *Protein Eng Des Sel.* (2017) 30:113–8. doi: 10.1093/protein/gzw070
99. Remacle AG, Cieplak P, Nam DH, Shiryaev SA, Ge X, Strongin AY. Selective function-blocking monoclonal human antibody highlights the important role of membrane type-1 matrix metalloproteinase (MT1-MMP) in metastasis. *Oncotarget.* (2017) 8:2781–99. doi: 10.18632/oncotarget.13157
100. Remacle AG, Golubkov VS, Shiryaev SA, Dahl R, Stebbins JL, Chernov AV, et al. Novel MT1-MMP small-molecule inhibitors based on insights into hemopexin domain function in tumor growth. *Cancer Res.* (2012) 72:2339–49. doi: 10.1158/0008-5472.CAN-11-4149
101. Folkman J. Tumour Angiogenesis. In: Mendelsohn J, Howley PM, Israel MA, Liotta LA. *The Molecular Basis of Cancer.* Philadelphia, PA: WB Saunders (1995). p. 206–32.
102. Abdalla AME, Xiao L, Ullah MW, Yu M, Ouyang C, Yang G. Current challenges of cancer anti-angiogenic therapy and the promise of nanotherapeutics. *Theranostics.* (2018) 8:533–48. doi: 10.7150/thno.21674
103. Sounni NE, Paye A, Host L, Noël A. MT-MMPs as regulators of vessel stability associated with angiogenesis. *Front Pharmacol.* (2011) 2:111. doi: 10.3389/fphar.2011.00111
104. Yu J, Zhang Y, Leung LH, Liu L, Yang F, Yao X. Efficacy and safety of angiogenesis inhibitors in advanced gastric cancer: a systematic review and meta-analysis. *J Hematol Oncol.* (2016) 9:111. doi: 10.1186/s13045-016-0340-8
105. Kamba T, McDonald DM. Mechanisms of adverse effects of anti-VEGF therapy for cancer. *Br J Cancer.* (2007) 96:1788–95. doi: 10.1038/sj.bjc.6603813
106. Ebos JM, Lee CR, Kerbel RS. Tumor and host-mediated pathways of resistance and disease progression in response to antiangiogenic therapy. *Clin Cancer Res.* (2009) 15:5020–5. doi: 10.1158/1078-0432.CCR-09-0095
107. Kopetz S, Hoff PM, Morris JS, Wolff RA, Eng C, Glover KY, et al. Phase II trial of infusional fluorouracil, irinotecan, and bevacizumab for metastatic colorectal cancer: efficacy and circulating angiogenic biomarkers associated with therapeutic resistance. *J Clin Oncol.* (2010) 28:453–9. doi: 10.1200/JCO.2009.24.8252
108. Gyanchandani R, Ortega Alves MV, Myers JN, Kim S. A proangiogenic signature is revealed in FGF-mediated bevacizumab-resistant head and neck squamous cell carcinoma. *Mol Cancer Res.* (2013) 11:1585–96. doi: 10.1158/1541-7786.MCR-13-0358
109. Li J, Zhao X, Chen L, Guo H, Lv F, Jia K, et al. Safety and pharmacokinetics of novel selective vascular endothelial growth factor receptor-2 inhibitor YN968D1 in patients with advanced malignancies. *BMC Cancer.* (2010) 10:529. doi: 10.1186/1471-2407-10-529
110. Aplin AC, Zhu WH, Fogel E, Nicosia RF. Vascular regression and survival are differentially regulated by MT1-MMP and TIMPs in the aortic ring model of angiogenesis. *Am J Physiol Cell Physiol.* (2009) 297:C471–C480. doi: 10.1152/ajpcell.00019.2009
111. Onimaru M, Yonemitsu Y, Suzuki H, Fujii T, Sueishi K. An autocrine linkage between matrix metalloproteinase-14 and Tie-2 via ectodomain shedding modulates angiopoietin-1-dependent function in endothelial cells. *Arterioscler Thromb Vasc Biol.* (2010) 30:818–26. doi: 10.1161/ATVBAHA.109.201111
112. Saunders WB, Bohnsack BL, Faske JB, Anthis NJ, Bayless KJ, Hirschi KK, et al. Coregulation of vascular tube stabilization by endothelial cell TIMP-2 and pericyte TIMP-3. *J Cell Biol.* (2006) 175:179–91. doi: 10.1083/jcb.200603176
113. Hawinkels LJAC, Kuiper P, Wiercinska E, Verspaget HW, Liu Z, Pardali E, et al. Matrix metalloproteinase-14 (MT1-MMP)-mediated endoglin shedding inhibits tumor angiogenesis. *Cancer Res.* (2010) 70:4141–50. doi: 10.1158/0008-5472.CAN-09-4466
114. Yan L, Moses MA, Huang S, Ingber DE. Adhesion-dependent control of matrix metalloproteinase-2 activation in human capillary endothelial cells. *J Cell Sci.* (2000) 113:3979–87.

115. Miki T, Shamma A, Kitajima S, Takegami Y, Noda M, Nakashima Y, et al. The beta1-integrin-dependent function of RECK in physiologic and tumor angiogenesis. *Mol Cancer Res.* (2010) 8:665–76. doi: 10.1158/1541-7786.MCR-09-0351
116. Cornelius LA, Nehring LC, Harding E, Bolanowski M, Welgus HG, Kobayashi DK, et al. Matrix metalloproteinases generate angiostatin: effects on neovascularization. *J Immunol.* (1998) 161:6845–52.
117. O'Reilly MS, Wiederschain D, Stetler-Stevenson WG, Folkman J, Moses MA. Regulation of angiostatin production by matrix metalloproteinase-2 in a model of concomitant resistance. *J Biol Chem.* (1999) 274:29568–71. doi: 10.1074/jbc.274.41.29568
118. Heljasvaara R, Nyberg P, Luostarinen J, Parikka M, Heikkilä P, Rehn M, et al. Generation of biologically active endostatin fragments from human collagen XVIII by distinct matrix metalloproteases. *Exp Cell Res.* (2005) 307:292–304. doi: 10.1016/j.yexcr.2005.03.021
119. Bendrik C, Robertson J, Gauldie J, Dabrosin C. Gene transfer of matrix metalloproteinase-9 induces tumor regression of breast cancer *in vivo*. *Cancer Res.* (2008) 68:3405–12. doi: 10.1158/0008-5472.CAN-08-0295
120. Ghajar CM, George SC, Putnam AJ. Matrix metalloproteinase control of capillary morphogenesis. *Crit Rev Eukaryot Gene Expr.* (2008) 18:251–78. doi: 10.1615/CritRevEukarGeneExpr.v18.i3.30
121. Hamano Y, Zeisberg M, Sugimoto H, Lively JC, Maeshima Y, Yang C, et al. Physiological levels of tumstatin, a fragment of collagen IV alpha3 chain, are generated by MMP-9 proteolysis and suppress angiogenesis via alphaV beta3 integrin. *Cancer Cell.* (2003) 3:589–601. doi: 10.1016/S1535-6108(03)00133-8
122. Bramhall SR, Schulz J, Nemunaitis J, Brown PD, Baillet M, Buckels JA. A double-blind placebo-controlled, randomised study comparing gemcitabine and marimastat with gemcitabine and placebo as first line therapy in patients with advanced pancreatic cancer. *Br J Cancer.* (2002) 87:161–7. doi: 10.1038/sj.bjc.6600446
123. Winer A, Janosky M, Harrison B, Zhong J, Moussai D, Siyah P, et al. Inhibition of breast cancer metastasis by presurgical treatment with an oral matrix metalloproteinase inhibitor: a preclinical proof-of-principle study. *Mol Cancer Ther.* (2016) 15:2370–7. doi: 10.1158/1535-7163.MCT-16-0194
124. Grünwald B, Vandooren J, Gerg M, Ahomaa K, Hunger A, Berchtold S, et al. Systemic ablation of MMP-9 triggers invasive growth and metastasis of pancreatic cancer via Deregulation of IL6 expression in the bone marrow. *Mol Cancer Res.* (2016) 14:1147–58. doi: 10.1158/1541-7786.MCR-16-0180
125. Bloomston M, Zervos EE, Rosemurgy, ASII. Matrix metalloproteinases and their role in pancreatic cancer: a review of preclinical studies and clinical trials. *Ann Surg Oncol.* (2002) 9:668–74. doi: 10.1007/BF02574483

Conflict of Interest Statement: The author declares that the research was conducted in the absence of any commercial or financial relationships that could be construed as a potential conflict of interest.

frontiers in Immunology

REVIEW
published: 08 August 2019
doi: 10.3389/fimmu.2019.01924

Targeting Angiogenesis With Peptide Vaccines

Michal A. Rahat [1,2]*

[1] Immunotherapy Laboratory, Carmel Medical Center, Haifa, Israel, [2] The Ruth and Bruce Rappaport Faculty of Medicine, Technion-Israel Institute of Technology, Haifa, Israel

Most cancer peptide vaccinations tested so far are capable of eliciting a strong immune response, but demonstrate poor clinical benefits. Since peptide vaccination is safe and well-tolerated, and several indications suggest that it has clear potential advantages over other modalities of treatment, it is important to investigate the reasons for these clinical failures. In this review, the current state of the art in targeting angiogenic proteins via peptide vaccines is presented, and the underlying reasons for both the successes and the failures are analyzed. The review highlights a number of areas critical for future success, including choice of target antigens, types of peptides used, delivery methods and use of proper adjuvants, and suggests ways to achieve better clinical results in the future.

Keywords: angiogenesis, peptide vaccines, adjuvant, cancer, VEGF, EMMPRIN

OPEN ACCESS

Edited by:
Nurit Hollander,
Tel Aviv University, Israel

Reviewed by:
Cristina Maccalli,
Sidra Medical and Research Center, Qatar
Lorenzo Mortara,
University of Insubria, Italy

***Correspondence:**
Michal A. Rahat
mrahat@netvision.net.il;
rahat_miki@clalit.org.il

Specialty section:
This article was submitted to Cancer Immunity and Immunotherapy, a section of the journal Frontiers in Immunology

Received: *06 June 2019*
Accepted: *30 July 2019*
Published: *08 August 2019*

Citation:
Rahat MA (2019) Targeting Angiogenesis With Peptide Vaccines. Front. Immunol. 10:1924. doi: 10.3389/fimmu.2019.01924

INTRODUCTION—WHY TARGET ANGIOGENESIS?

The unprecedented success of checkpoint inhibitors in the therapy of solid tumors has ignited renewed interest in immunotherapy as a strategy to eradicate tumor cells and prevent metastasis. However, even recent interventions such as the checkpoint inhibitors anti-CTLA4 and anti-PD-1 that "release the brakes" and mobilize effector T cells into the tumors so they can eradicate tumor cells, show limited clinical success, with only about 20–40% of the patients responding to checkpoint inhibitors as monotherapy (1). Patients treated with monoclonal antibodies that attack tumor antigens and patients treated with tyrosine kinase inhibitors (TKIs) that inhibit receptor signaling pathways, are still experiencing tumor recurrence and progression, and suffer from high mortality rates (2). Therefore, the search for an adjuvant therapy that improves survival rates is expanding, with targets other than tumor cell proteins being considered.

Tumor cells depend on angiogenesis, the process of generating new capillaries from pre-existing blood vessels, to supply them with oxygen and nutrients, remove waste products, and support tumor survival, progression, invasion and metastasis. Therefore, it has been suggested to target proteins that mediate this process. In normal physiological conditions, angiogenesis occurs during development, menstrual cycle, or wound healing, and depends on the balance between pro- and anti-angiogenic factors. However, when this balance is disrupted and pro-angiogenic factors begin to accumulate, an "angiogenic switch" occurs to initiate pathological angiogenesis, associated with many types of chronic inflammatory diseases, including cancer (3). This causes the activation, proliferation and migration of endothelial cells (ECs) through the basement membrane and extracellular matrix (ECM), using matrix metalloproteinases (MMPs) to degrade them. The migrated ECs then spatially reorganize to form tube-like structures that may mature into functional vessels. In cancer, these vessels are typically leaky due to increased permeability and lack of sufficient stabilization and maturation via attachment of pericytes (3), and are usually more complex, dilated, tortuous, and in a state of chronic inflammation (3, 4).

Targeting angiogenesis and EC mobility as an anti-tumor strategy, as was first suggested by Judah Folkman (5), may offer additional benefits. First, ECs play an important role in establishing the immunosuppressive tumor microenvironment (TME). The heterogeneous vessel density produces irregular blood flow that generates hypoxia in some regions, which is the driving force of the angiogenic switch and tumor cell metabolism via activation of the transcription factor hypoxia-induced factor-α (HIF-1α) (3, 6–9). Thus, targeting ECs may indirectly affect tumor metabolism. Second, the chronic production of angiogenic factors suppresses adhesion molecules (e.g., ICAM-1, E-selectin, CD34), thus making the infiltration and adhesion of T cells into the tumor more difficult, increasing immune suppression (10, 11). Third, tumor ECs may also actively assist in the killing of Fas-expressing effector T cells, but not T regulatory cells (Tregs), by expressing Fas ligand (FasL) (12). Fourth, tumor cells utilize several strategies to escape immune recognition, including the alteration or loss of MHC/HLA class I molecules, leading to the inability of $CD8^+$ cytotoxic T cells (CTLs) to attack them (13). As ECs are genetically stable, they express class I molecules, present angiogenic targets, and allow CTLs to attack them thus causing vasculature damage (14). Thus, attacking the tumor vasculature indirectly leads to tumor cell death, as the latter are deprived of their oxygen and nutrients.

The most potent pro-angiogenic factor is vascular endothelial growth factor (VEGF), and VEGF itself or its signaling pathway have been targeted by monoclonal antibodies or their fragments (e.g., bevacizumab/Avastin, Ranibizumab/Lucentis), soluble receptors (e.g., ziv-aflibercep/Zaltrap, ramucirumab) and small molecules receptor TKIs (e.g., sorafenib, sunitinib, and others). However, these agents were proven insufficient, as their effect was transitory and moderate, they exhibited off-target toxicities and reduced delivery of chemotherapeutic agents (15–17). More importantly, upon withdrawal of treatment tumors demonstrated a more aggressive phenotype of enhanced growth, invasion and metastasis, known as the "rebound effect" (18, 19), probably because of compensatory pathways activated by other VEGF family members, pro-angiogenic factors and cytokines (4, 20). Alternatively, other, more immediate mechanisms may compensate for reduced angiogenesis, such as vessel cooption, vessel intussusception, or vasculogenic mimicry to sustain tumor blood flow and bypass the effect of the angiogenesis inhibitors (4, 20). Thus, a different approach to the targeting of angiogenesis that yields long-lasting effects is needed.

Several vaccination strategies and delivery systems have already been tried, including recombinant proteins, fusion proteins, DNA vaccines, pulsed dendritic cells and whole endothelial cell vaccines (11). However, in this review I focus only on the progress made in peptide vaccination that elicits an immune response against angiogenic targets, and I do not discuss other forms of vaccination or other mechanisms of action used by peptides (e.g., inhibition, competition), which have already been addressed by other reviews (20–23).

PRINCIPLES OF PEPTIDE VACCINATION

Tumor cells are in constant interaction with immune cells, especially macrophages, as explained by the concept of immunoediting (24). The contributions of immune cells to the killing of tumors in early stages, to the shaping of the tumor during the equilibrium stage, and to the support of tumor growth in later stages [by secreting immunosuppressive and pro-angiogenic factors to the tumor microenvironment (TME)], suggests an intricate relationship between the cell types. However, although suppressed, the potential to recognize and eliminate tumor cells inherently exists even in late stages of tumor escape, as suggested by the presence of autoantibodies found in many cancer patients (25), and by the release of pre-existing CTLs from immune suppression by checkpoint inhibitors (26). Thus, the goal of any form of immunotherapy is to restore the ability of adaptive immune effector cells to attack and eradicate the tumor.

Most current immunotherapeutic approaches rely on passive immunization by introducing monoclonal antibodies directed against tumor antigens or against checkpoint co-inhibitory molecules. The advantages of monoclonal antibodies are their high specificity and affinity to tumor antigens, thus avoiding off-target toxicity. However, antibodies are very costly to develop and to produce, and they must be provided in repeated injections of high doses. In addition to the rebound effect known to arise especially in antibodies and TKIs directed against angiogenic targets (15), antibodies might also lose their effectiveness over time, as anti-drug antibody (ADA) response develops against the antigen-binding site of the therapeutic antibody and confers resistance to treatment (27, 28).

In contrast, peptide vaccination depends on active vaccination that elicits a strong immune response with memory, which may be critical to prevent tumor recurrence. This strategy is generally considered a simpler approach, with high specificity, reduced costs, easy synthesis, which is safe and well-tolerated, as detailed below. Nonetheless, despite their ability to elicit a strong immune response, cancer peptide vaccines have so far yielded only limited clinical benefits. This is mostly explained by central and peripheral tolerance mechanisms, which limit the T cell repertoire able to recognize self-antigens only to low-affinity T cells, and by the immunosuppressive TME (29, 30). Additional strategies that the tumor may employ to escape immune recognition, such as reduced MHC class I expression (30, 31) or loss of IFNAR expression (32), may also take a part in this general failure to use cancer peptide vaccination effectively.

Choice of Antigens

The choice of the target antigen is critical to the success of the vaccination. Ideally, the target should be highly expressed only on tumor cells, to ensure that even low-affinity effector T and B cells could recognize it and mount an effective immune response. Tumor antigens are classified as tumor-specific antigens (TSAs) and tumor-associated antigens (TAAs). Viral antigens are a class of TSAs unique to tumors that originate from viral transformation, such as in the case of HPV or EBV. However, most tumors arise due to genetic

instability, and different mutations (translocations, frame-shift mutations or point mutations) may generate a new protein, a truncated protein, or expose a previously hidden (crypt) epitope that are different from the normal self-protein. Therefore, such mutations that generate neoantigens could potentially be recognized by the immune system. A correlation was found between high tumor mutation load and anti-tumoral response, positive clinical response, survival, and response to checkpoint inhibitors therapy, which strengthens this premise (33). The idea to elicit an immune response against neoantigens is a promising "personalized medicine" approach, but its clinical translation may be challenging and require a multistep process (22). This process includes mapping the tumor exome, assessing the immunogenicity of specific mutations *in silico,* selecting peptide(s) that are predicted to match to the patients HLA class I and II molecules, synthesizing the selected peptide(s) under Good Manufacturing Practice (GMP) conditions and injecting them to the patient (34). Thus, tailoring the vaccine to each patient may increase the response rates, but this approach is time consuming, labor-intensive and still costly.

In contrast to TSAs, TAAs are self-antigens that are aberrantly overexpressed on cancer cells but physiologically expressed on some normal cells. For example, cancer-testis (CT) antigens are expressed on male gametes, silenced in normal adult tissues and reactivated in tumor cells (e.g., MAGE-A, NY-ESO-1, and SSX-2). Differentiation antigens are specific to a cell lineage or a tissue (e.g., Melan-A/MART-1, gp100, tyrosinase). If overexpressed in the tumor, these antigens may become immunogenic when their expression exceeds the threshold required for TCR recognition and $CD4^+$ T helper activation. Antibodies directed against TAAs found in the serum of cancer patients suggest that such recognition occurs, even without treatment (25). Most peptide vaccination approaches to date were designed to target TAAs such as the CT antigen 1B (CTAG1B), MAGE family member 3 (MAGE-3), TTK protein kinase (TTK), Wilms tumor 1 (WT1), survivin (BIRC5), EGFR, erb2/Her2, indoleamine 2,3-dioxygenase (IDO1), and others (30). However, such antigens are not necessarily critical for tumor survival, and may be suppressed when attacked.

Another approach would be that of targeting proteins that regulate angiogenesis or regulate the interactions between stroma and tumor cells that promote pathological angiogenesis. This may provide universal targets to indirectly attack tumor cells, especially in combination with other treatment modalities, and reduce vaccination costs (22).

Types of Peptides Used for Vaccination

Two types of peptides are typically used for peptide vaccination. Short peptides (<15 amino acids long, usually 9–10 amino acids) have a short half-life and are rapidly degraded in the serum. These peptides can be loaded onto the HLA class I groove from the outside of the nucleated cell, even without prior processing in professional antigen presenting cells (APCs). This may lead to tolerance or to a short-term induction of $CD8^+$ T cells, without parallel induction of $CD4^+$ T cells and without induction of memory (35, 36). Therefore, they are often conjugated to a carrier protein, to allow uptake and processing by APCs and to elicit an effective immune response. In contrast, synthetic long peptides (SLPs) (>20 amino acids), are more stable and immunogenic. Since they are efficiently taken-up and processed by dendritic cells (DCs), they can present the epitope in the context of both class I and class II molecules, resulting in a strong, long-lasting, and balanced anti-tumoral immune response that involves $CD4^+$ T cells, $CD8^+$ T cells and antibody production by B cells (35, 36). Some studies use the multiple epitope approach, where several epitope peptides are mixed and injected together, or where a single long peptide that contains several epitopes is injected. Targeting several epitopes derived from different antigens simultaneously may circumvent the ability of the tumor cell to evade immune recognition by losing an antigen.

The magnitude and strength of the immune response depends on the interaction of the peptide with the presenting MHC/HLA molecule, and even small changes in the peptide sequence may affect this interaction. Therefore, several modifications of the peptide sequence were investigated. Some studies substituted a single amino acid in the peptide sequence to better anchor the peptide to the MHC groove and enhance the T cell response (35, 37). Other modified peptides, called mimotopes or altered peptide ligands (APL), mimic the spatial structure of the presented epitope, and not necessarily its sequence. However, although mimotopes/APL elicited a better expansion of T cells than the unchanged peptide, these T cells did not efficiently cross-react with the native antigen or presented a reduced affinity relative to the native epitope (37), requiring additional boost vaccination with the native tumor antigen to improve anti-tumor immunity (38). Yet, although this approach increased the *ex vivo* $CD8^+$ T cells responses in melanoma patients, it did not extend the patients' overall survival (39). This could be due to the limited number of MHC-peptide complexes exhibited by tumor cells and the lack of expression of co-stimulatory molecules (37). Multiple antigenic peptide (MAP) represents a different approach to peptide modification. Here, the peptide epitope is conjugated four or eight times onto a core of lysine residues, generating a branched peptide tree with a molecular weight of a small protein (40). This structure endows the peptide with high stability (41, 42) and increases its immunogenicity due to the increased concentrations of the repeated peptide sequence and the changes in the three-dimensional structure (43).

Peptide Delivery and the Role of Adjuvants

Peptides can be delivered by direct subcutaneous injections in the presence of an adjuvant, or by re-infusing DCs that have first been isolated from peripheral blood, matured and expanded *ex vivo*, and then pulsed with the peptide. Both approaches yield comparable results in terms of eliciting immune responses and clinical responses (44). Novel delivery systems that were used to enhance the efficiency of vaccination include liposomes, virus-like particles that do not include the viral genome, and caged proteins nanoparticles that are self-assembled protein structures, that can be delivered with or without adjuvants (45). The different forms of nanoparticles show improved uptake by DCs, and may enhance antigen presentation on these cells (46).

Adjuvants are necessary to protect peptides from fast degradation, to prolong the release of the peptide (the depot

effect) and therefore the duration of the immune response, and to recruit and stimulate APCs to process and present the peptides to B and T cells (47). The most used adjuvant for human subjects in pathogen vaccination are aluminum salts (Alum), but as these promote Th2 responses, they are not compatible with cancer vaccines (47). Thus, in human cancer patients, the most used adjuvant is Incomplete Freund's adjuvant (IFA) or Montanide ISA-51, water-in-oil emulsions of the antigen that form a depot that slowly releases the antigen. However, in some cases, the slow release of short peptide vaccines promotes secretion of pro-inflammatory cytokines (e.g., IFNγ), which in turn, enhance Fas ligand (FasL) expression on tissue cells and T cell apoptosis, exhaustion and reduced memory formation (48). This leads to persistence of T cells in the vaccination site, inhibiting their movement to the tumor, and therefore, sufficient anti-tumoral responses are not mediated (36, 49). Thus, the commonly used adjuvants could be contributing to the limited clinical success observed with peptide vaccination so far, despite the presence of peptide-specific $CD8^+$ T cells in the circulation.

Alternative adjuvants that could first recruit leukocytes to the vaccination site, support T cell expansion and activation, and promote their migration to the lymph nodes and tumor site, could potentially include bacterial or synthetic TLR ligands, cytokines and growth factors, or nanoparticles that deliver the antigen (50, 51). Currently, TLR ligands, such as unmethylated CpG motifs that activate TLR9, or polyI:C that binds to TLR3, show improved immune responses to peptide vaccinations alone or with Montanide ISA-51, increased Th1 polarization and CTL responses (51). Inclusion in the adjuvant formulation of cytokines, such as GM-CSF that enhances DCs and macrophage proliferation, or IL-12 that enhances IFNγ production in T cells and NK cells, improved immune responses to peptide vaccination (51, 52). However, in most cases GM-CSF provided only weak adjuvant properties (47), and since it can potentially expand the MDSCs population and increase immunosuppression in high doses, it is recommended to use it in in low and repeated doses (51, 52).

ANGIOGENIC TARGETS FOR PEPTIDE VACCINATION

As mentioned before, most cancer peptide vaccines used so far were directed against TAAs, and only a few angiogenic proteins were targeted. In contrast to neoantigens, these targets are shared between many types of tumors, they are not subject to genetic variations, and they are expressed on stroma cells, such as ECs. VEGF and its receptors stand out as the main targets of this class of proteins, but other potential targets were also tested, especially in preclinical studies (summarized in **Table 1**).

Pre-clinical Studies

VEGF itself or its receptors can be obvious angiogenic targets. In a pre-clinical study, Wentick et al. (10) used a 79 amino acid long peptide that includes critical areas in the VEGF molecule, including the typical cysteine-knot fold. This sequence reconstitutes the complete conformation of the discontinuous binding site of bevacizumab to $VEGF_{165}$. Furthermore, to prevent oxidative folding of the peptide, two cysteine residues were substituted for alanine, thus modifying the peptide. Vaccination with this peptide produced antibodies that were cross-reactive with VEGF and comparable to bevacizumab, and inhibited tumor growth in two mouse models (10). A similar approach included engineering a conformational shorter peptide of 23 amino acids that correctly mimics the VEGF binding site to VEGFR2 and includes an insertion of two cysteine residues to allow cyclization of the peptide. This peptide (VEGF-P3-CYC) inhibited the proliferation, migration and tube formation, as well as VEGFR2 phosphorylation in human umbilical vein endothelial cell (HUVEC) *in vitro*, and when injected to the transgenic $VEGF^{+/-}Neu2\text{-}5^{+/-}$ mouse model, the peptide significantly delayed tumor growth (60). In a follow-up study, the authors vaccinated mice with a Her2 peptide, and after tumor implantation, VEGF mimic peptides (the VEGF-P3-CYC and the same sequence synthesized in reverse with D-amino acids-RI-VEGF-P4-CYC) were weakly intravenously injected to the tumor-bearing mice. The combination of these two peptides resulted in a marked inhibition of tumor growth relative to each single treatment or to the controls, as well as inhibition of cell proliferation and reduction of microvascular density in the tumors (61). However, in both studies, the VEGF mimic peptides were injected to the tail vein in PBS and in the absence of adjuvant. Thus, only their anti-angiogenic functions, including inhibition of proliferation, VE-cadherin expression and angiogenesis in an aortic ring assay were measured, whereas the ability to elicit an immune response with both humoral and cellular responses was not checked.

Another approach to target VEGF was demonstrated by developing a VEGF mimotope that was identified by using a phage display technology followed by screening the library with bevacizumab/Avastin (62). Although the peptide sequence was not identical to VEGF, it mimicked the spatial organization of the epitope, suggesting that Avastin recognizes a discontinuous conformational epitope on VEGF. The resulting 12 amino acid peptide was conjugated to KLA and used to immunize mice who developed high titer of VEGF-specific antibodies that blocked VEGF binding to VEGFR2. The purified Ab inhibited the proliferation of HUVEC cells, their ability to migrate and to form tubes (62).

Kim et al. report on inhibition of VEGF using an antagonizing branched dimeric peptide with two repetitions of the six amino acids peptide sequence RRKRRR (RK6) synthesized as D-amino acids (MAP2-dRK6). This modified MAP peptide had increased stability to serum proteolysis and inhibited the binding of VEGF to its receptors expressed on HUVECs, more than the L-amino acid counterpart or the unmodified linear peptides. MAP2-dRK6 inhibited VEGF-induced, but not bFGF-induced, proliferation and signaling in HUVECs, as well as their ability to form tube-like structures *in vitro*. In a model of SW480 human colorectal cancer cells implanted in nude mice, MAP2-dRK6 could inhibit tumor growth by 65%, and reduce the microvessel density, suggesting that it effectively blocked angiogenesis (53). However, as MAP2-dRK6 was injected *s.c.* daily for 14 days without the presence of adjuvant, and tumors were monitored for only 20

TABLE 1 | Preclinical trials for pro-angiogenic peptide vaccines.

Antigen	Type of peptide	Cancer type	Adjuvant used	Timing	Result	References
VEGF	Long peptide (79 aa), two cysteine residues replace with alanine	Melanoma	Raffinose fatty acid sulfate ester (RFASE)	Prophylactic[a] vaccination	Inhibition of tumor growth by ∼50%	(10)
VEGF	MAP2-dRK6	Colorectal	None	Therapeutic vaccination	Inhibition of tumor growth by ∼65%	(53)
VEGFR2	Epitope screening of 38 short peptides (9–10 aa each)	A2/K2 transgenic mice implanted with different mouse tumor cells	IFA	Therapeutic vaccination	Inhibition of tumor growth by ∼5-fold	(14)
VEGFR1	Epitope screening of 40 short peptides (9–10 aa each)	A2/K2 transgenic mice implanted with different mouse tumor cells	IFA	Therapeutic vaccination	Inhibition of tumor growth by ∼2-fold	(54)
Fibronectin, ED-A fragment	Recombinant fusion peptide (<100 aa) conjugated to bacterial thioredoxin	metastatic mammary adenocarcinoma (MMTV-PyMT)	Montanide ISA-720 with GpC oligo	Therapeutic vaccination	Inhibition of tumor growth by ∼40%	(55)
Heparanase	Octa-branched MAP with a 15 aa peptide	Hepatocarcinoma (HCC-97H cells)	CFA/IFA	Therapeutic passive vaccination	Reduced tumor volume by ∼3-fold; Reduced pulmonary metastasis by 10-fold	(56, 57)
FGF-2	Heparin binding domain of FGF-2 (44 aa peptide)	B16BL6 and experimental lung metastasis models	Liposomes and lipid A	Prophylactic vaccination	Inhibition of 96% of macroscopic metastases	(58)
EMMPRIN/CD147	Octa-branched MAP with a 9 aa peptide	A498 renal, CT26 colon and TRAMP-C2 prostate carcinomas	CFA/IFA	Prophylactic and Therapeutic vaccination	Inhibition of tumor growth by 72% and 94%.	(59)

[a]*Prophylactic, vaccination was carried out before injection of tumor cells; Therapeutic, vaccination was carried out after injection of tumor cells.*

days, this study did not examine a possible activation of the immune system.

In an attempt to identify the best peptide sequences to target in human VEGFR2 or VEGFR1, a library of peptides of 9–10 aa long was synthesized according to their predicted binding affinities to HLA-A0201 or HLA-A2402. Peptide-specific cytotoxic T cells (CTLs) were identified by their ability to kill HLA-restricted target cells that were pulsed with each peptide. Leading peptides for each receptor matched to the specific HLA molecule were also identified by the ability to drive cytotoxicity and IFNγ production of peptide-pulsed target cells incubated with spleen cells derived from peptide-vaccinated A2/k2 transgenic mice that express HLA-A0201 (14, 54). Lastly, the selected HLA-A0201-restricted peptides were used to vaccinate A2/Kb transgenic mice implanted with several tumor cell lines (that do not express HLA and are therefore not targeted themselves) to demonstrate *in vivo* efficacy. Inhibition of tumor growth suggests that targeting angiogenesis *in vivo* could be a feasible strategy (14, 54). These experiments helped identify the VEGFR1-1084 and VEGFR2-169 peptides that were subsequently used in clinical trials.

FGF-2 (or bFGF) is a potent pro-angiogenic factor that promotes ECs proliferation by binding either to the FGF receptor or to heparin sulfate proteoglycan on the cell surface. Vaccinating mice with an FGF-2-derived peptide (44 aa long) directed to the heparin binding site domain, but not with a peptide (22 aa long) directed to the receptor binding site domain, administered in liposomes containing lipid A, resulted in generation of high titer of FGF-2 specific antibodies. Moreover, the heparin domain peptide inhibited neovascularization in an angiogenesis sponge model, and reduced metastatic foci by 96% in the lungs of vaccinated mice (58).

Fibronectin (FN) is a complex ECM protein that has many isoforms due to alternative splicing. Interestingly, the specific FN type III extracellular domains A and B (ED-A, ED-B) are only expressed during vasculogenesis in the embryo and are spliced out in adult normal tissue. However, they are expressed again in high levels in tumors, especially near angiogenic vasculature (55). Here, Femel et al. therapeutically vaccinated the transgenic MMTV-PyMT mice model of metastatic mammary adenocarcinoma with a construct consisting of the ED-A fragment (<90 aa) conjugated to bacterial thioredoxin (TRX). They demonstrate a significant 40% reduction in primary tumor weight and reduction in metastases relative to control mice, with increased infiltration of macrophages into the tumors. While CD31-stained blood vessels were not reduced in number, their functionality was compromised by the vaccination, as more fibrinogen leaked out of the vessels and less FITC-labeled lectin was perfused (55). Surprisingly, although the titer of anti-ED-A antibodies was significantly elevated, the authors do not mention any attempt to examine a $CD8^+$ T cell response as well.

Heparanase is the only endoglycosidase found that specifically degrades and removes heparan sulfate (HS) side chains from heparan sulfate proteoglycans, thus releasing heparin-binding proteins to the TME. It is expressed by tumor- and activated stroma-cells including ECs, activated only in acidic conditions that are typical to the tumor TME, and in addition to regulating ECM remodeling it has a role in activating signaling pathways that increase transcription of pro-angiogenic factors,

such as VEGF (63, 64). Testing of the passive vaccination against heparanase was reported in two papers, where rabbits were immunized with a 15-amino acids sequence derived from human heparanase that was synthesized as octa-branched MAP. The resulting polyclonal antibodies were then purified from rabbit serum and injected to mice bearing the HCC-97H hepatocarcinoma tumor in different doses. The antibodies reduced the serum levels of VEGF and FGF and decreased MVD, tumor volumes and the number of pulmonary metastasis (56, 57).

EMMPRIN is a multifunctional protein, which is moderately expressed on stroma cells, and overexpressed on many types of tumor cells. Among its many functions, EMMPRIN can induce the expression of VEGF and several types of MMPs. We have previously identified a specific short epitope as being responsible for the induction of VEGF and MMPs (65), and synthesized this epitope as an octa-branched MAP and vaccinated tumor-bearing mice with it (59). We show in three different implanted models and in two experimental metastasis models that the vaccination reduced angiogenesis by reducing MVD, VEGF, and MMP-9 concentrations. Additionally, the vaccination reduced tumor cell proliferation, increased macrophages and CTL infiltration into the tumor, and shifted the TME to allow more cytotoxicity toward the tumor cells, thereby reducing tumor size and the number of metastatic lung foci (59). In a DSS-induced colitis model that simulates the human autoimmune disease ulcerative colitis, we show that a similar effect occurs, where angiogenesis is reduced and infiltration of macrophages and CTLs to the colon tissue is increased, ultimately leading to improvement in the clinical score of the vaccinated mice relative to their controls (66).

Clinical Studies

Currently, most clinical studies are at phase I or II, designed to test safety of peptide vaccination, toxicity, required dose, and induction of immune responses by the vaccine (immunogenicity), and not to estimate the efficacy of the vaccination. In some studies, a monotherapy approach was taken, vaccinating patients with single or multiple peptides, whereas in others a combination with chemotherapy was tested. These experiments are summarized in **Table 2**.

Targeting VEGFR2, Miyazawa et al. (67) have vaccinated pancreatic cancer patients with a VEGFR2-derived peptide (VEGF-169, HLA-A2402 restricted) and vaccinated in combination with gemcitabine treatment, the standard care for pancreatic cancer patients with metastatic or recurrent disease. The vaccination was well-tolerated with no vascular adverse events (such as bleeding, thromboembolism, or hypertension) reported. Immune responses at the injection site were observed in 83% of the vaccinated patients, but only 61% of them exhibited stimulation of epitope-specific cytotoxic T cells, with reduced frequency of epitope-specific Tregs. Disease control rate (DCR) was 67%, including patients with stable disease (SD) or partial response (PR), whereas 33% exhibited progressed disease (PD).

Similar results were shown in the use of either the HLA-A0201-restricted peptide VEGFR1-770 or the HLA-A2402-restricted peptide VEGFR1-1084 for the treatment of metastatic renal cell cancer (RCC). Out of the 18 patients examined, 15 developed CTL responses specific to the injected peptide (83%), regardless of the dose injected. Two of the cohort exhibited PR, and five showed SD for over 5 months, so that the DCR was 55% (68).

To test the feasibility of peptide vaccination in high-grade glioma patients (including glioblastoma, anaplastic astrocytoma and anaplastic oligodendroglioma), eight patients were vaccinated with HLA-A2402-restricted peptides derived from the VEGF receptors VEGFR1-1084 and VEGFR2-169. Most patients developed positive immune responses to the VEGFR1 peptide (87.5%) and VEGFR2 peptide (12.5%), but this was not correlated to overall survival. However, a negative correlation that was found between plasma IL-8 levels and overall survival may suggest the use of IL-8 levels as a biomarker for vaccination efficacy (69). The authors suggest that targeting VEGF receptors may be more efficient than targeting VEGF alone, as these receptors can bind all VEGF family members, and may promote the killing of VEGFR-expressing tumor cells and endothelial cells.

Multiple epitopes ("cocktail") vaccinations were tested in several studies. The pro-angiogenic VEGF receptors were targeted using a mixed "cocktail" vaccination that included the peptides VEGFR1-1084 and VEGFR2-169, with or without other antigens, and often in combination with a chemotherapeutic drug. No difference in the overall survival (OS) and progression free survival (PFS) was found if each peptide was injected in a different site or if all peptides were mixed together and injected in a single site (71). When patients were stratified between those that expressed the HLA-A2402 haplotype and those that did not, no significant change was observed (73, 74). The ability to generate a peptide-specific cellular immune response, which was tested by the IFNγ secretion of $CD8^+$ T cells that were stimulated *ex vivo* with the peptide in ELISPOT assay, was correlated to disease free survival (DFS) rate or disease control rate (DCR) (72, 73), suggesting that the activation of an immune response was responsible for the clinical effect. In most studies, high percentage of the patients exhibited positive CTL responses to at least one of the vaccinating peptides. In one study, patients that had positive CTL responses to the VEGR2-169 peptides, but not those with immune responses to VEGFRI-1084 peptide, had significantly better prognosis (70). In contrast, another study showed better OS in patients that had positive CTL responses to VEGFR1-1084 but not to VEGFR2-169 (73). Thus, additional studies are needed to determine which receptor is the preferred target.

NRG-TNF is a drug consisting of the human TNFα protein fused to the CNGRCG peptide that targets it to aminopeptidase N (CD13), an enzyme overexpressed on newly formed tumor endothelial cells (75). NRG-TNF alters the vascular barrier and allows the increased uptake of chemotherapeutic drugs by the tumor cells, and improves immune cell infiltration. In a phase I/II clinical study, NRG-TNF was administered to patients with metastatic melanoma that were resistant to other drugs, together with one of the two peptides that were derived from melanoma-associated antigens, according to their HLA-A haplotype restriction. One peptide (NA17.A2) was derived from a spliced form of N-acetylglucosaminyltransferase expressed on 50% of melanoma patients, and another peptide (MAGE-3.A1) was derived from chain A of the MAGE 3 protein expressed

TABLE 2 | Clinical trials for pro-angiogenic peptide vaccines.

Antigen and type of peptide	Cancer type	Adjuvant used	Positive CTL response	Clinical response	Phase	HLA restriction	Combination	References
Monotherapy								
VEGFR2-169 (9 aa)	Advance pancreatic cancer	Montanide ISA-51	11/18 (61%)	DCR 67%	I	A2402	Gemcitabine	(67)
VEGFR1-770 or VEGFR1-1084 (9 aa each):	Metastatic renal cell carcinoma	Montanide ISA-51	8/18 (83%)	SD (over 5 months)−8/18 (45%); PR−2/18 (11%)	I	A2402, A0201	None	(68)
Multiple epitope vaccines								
VEGFR1-1084 and VEGFR2-169 (9 aa each)	Advanced gliomas	Montanide ISA-51	7/8 (87/5%) to VEGFR1, 1/8 (12.5%) to VEGFR2	SD−25% (2/6) PD− 75% (6/8)	I	A2402	None	(69)
VEGFR1-1084 and VEGFR2-169 (9 aa each)	Advanced gastric cancer	Montanide ISA-51	18/22 (84%) to each of the peptides	PR−12/22 (55%) SD−10/22 (45%) DCR−100%	I/II	A2402	S-I and cisplatin	(70)
VEGFR1-1084, VEGFR2-169, RNF43-721, TOMM34-299, KOC1-508 (9–10 aa each)	Advances Coloreactal cancer (CRC)	Montanide ISA-51	18/18 (100%) to at least one of the peptides 10/18 (55%) to VEGFR1, 12/18 (66%) to VEGFR2	CR-1/18 (5.5%) SD-6/18 (33%) DCR 38.9%	I	A2402	None	(71)
VEGFR1-1084, VEGFR2-169, KIF20A-66 (9–10 aa each)	Resected pancreatic cancer	Montanide ISA-51	13/29 (44.8%) to VEGFR1 13/29 (44.8%) to VEGFR2	Median DFS of 15.8 months relative to 12 month of controls (only gemcitabine).	II	A2402	Gemcitabine	(72)
VEGFR1-1084, VEGFR2-169, KIF20A-66 (9–10 aa each)	Advanced pancreatic cancer	Montanide ISA-51	22/37 (59%) to VEGFR1 16/37 (43%) to VEGFR2	RR-12.1% PR-8/66 (12%) SD-41/66 (62%) DCR-74.2%	II	A2402	Gemcitabine	(73)
DEPDC1-294, URLC10-177, FoxM1-262, KIF20A-66, VEGERI-1084 (9–10 aa each)	Advanced gastric cancer	Montanide ISA-51	11/20 (55%) to VEGFR1	SD−10/22 (45%) PD−12/22 (55%)	II	A2402	None	(74)

CR, complete response; SD, stable disease; PR, partial response; PD, progressive disease; DFS, disease-free survival; DCR, disease control rate (usually SD + PR).

on 70% of melanoma patients (76). All patients had increased serum levels of the chemokines MCP-1 and MIP-1β, suggesting inflammation and increased infiltration of immune cells into tumors. Additionally, immunohistochemistry in some lesions showed increased infiltration of macrophages (76). 6 out of 7 patients showed positive T cell responses to the peptides or to other melanoma antigens (due to antigen spreading) in the peripheral blood, and long-term survival (above 4 months) was demonstrated in 4 out of 8 patients (76). These results demonstrate the benefit of combination therapy that target the tumor vasculature and provides immunotherapy against tumor antigens.

In all the studies mentioned above, no adverse effects of grade 3 or higher were observed, and all doses examined were well-tolerated. However, limited rate of more severe adverse responses, especially neutropenia, were observed in some of the studies when peptide vaccination was combined with chemotherapy (70, 72, 73). The most common effects were erythema and pain at the site of injection. Thus, in accordance with other studies that targeted a wide range of non-angiogenic targets, peptide vaccination seems to be safe and well-tolerated. Of interest, some studies indicated that a better clinical outcome was generally observed in patients with a strong injection site responses (ISR), sometime reaching significance (72, 73).

SUMMARY AND CONCLUSIONS

One of the problems in cancer immunotherapy is the set of defense mechanisms employed by the tumor to evade immune recognition, and especially its ability to alter antigens or lose their expression due to mutations. Especially pertinent to vaccination is the ability of tumors to reduce or lose the expression of HLA class I molecules, thereby avoiding efficient antigen presentation and immune response. As this makes targeting of tumor antigens more difficult, an alternative way might be to target antigens expressed on vascular ECs and induced in the tumor tissue by the angiogenic switch. This approach is effective even if these antigens are not expressed by the tumor cells, since ECs that stably express HLA molecules are the main targets of the vaccination, resulting in tumor cell suffocation and increased death due to reduced angiogenesis.

Using peptide vaccination is a promising approach to target angiogenesis. So far, targeting antigens by peptide vaccination in general, and attacking angiogenic targets in particular, have shown only limited therapeutic beneficial results, although most studies demonstrate stimulation of a peptide-specific immune response. However, all clinical studies exhibit safety and vaccines were well-tolerated with only mild adverse responses. Thus, once optimal conditions for vaccination are defined, peptide vaccination may be more advantageous than monoclonal antibodies that carry the risk of long-term ADA or rebound effect. These optimal conditions include target choice, peptide formulation, adjuvant and delivery systems, choice of patient populations that will better respond to treatment, and the vaccination regimen.

Target Choice

Lessons learnt from cancer peptide-vaccinations that target a variety of TAAs suggest that targeting of TAAs exhibits only limited efficacy. This is explained by tolerance that retains only a limited T cell repertoire with low affinity to TAAs, by the ability of tumors to escape immune recognition by reducing or losing expression of MHC/HLA class I molecules, and by the immunosuppressive TME. Most clinical trials targeting pro-angiogenic proteins focused on VEGF and VEGFRs. However, these targets are problematic, as they can be compensated for by other members of their family or other pro-angiogenic proteins. One approach could be to use multiple-epitope vaccines that would include VEGF, VEGFR1, VEGFR2, FGF-2, and additional pro-angiogenic targets injected together as a cocktail. Another approach would be to identify additional pro-angiogenic protein targets. Such proteins could affect ECM remodeling (e.g., heparanase), or be overexpressed on the tumor vasculature and/or tumor cells (e.g., EMMPRIN). Thus, since EMMPRIN is expressed on tumor cells, leukocytes (especially Tregs) and tumor vasculature, targeting it could directly and simultaneously attack tumor cells, disrupt tumor vascularization, and alleviate immune suppression. The ideal target would be a protein that is essential to tumor growth and dissemination, so that the tumor cannot afford to reduce its expression. Preferably, such a target would be expressed on both tumor cells and tumor vasculature.

Peptide Formulation

The vast majority of peptide vaccines tested so far, including those targeting angiogenic proteins, are based on short peptides, and only few studies used SLPs to target pro-angiogenic proteins. All of these studies, for the most part, did not yield tumor regression in pre-clinical studies or complete response in clinical studies. T cells that expand after vaccination *a priori* have only low affinity and avidity to tumor antigens, due to elimination of high affinity T cells by central and peripheral tolerance, and so are not sufficient to drive strong anti-tumor responses. Better results may be obtained by using modified peptides, especially the multiple antigenic peptide (MAP) modification. Modification of the peptide seems to be a crucial strategy to elicit a sufficiently strong immune response. Therefore, it is highly recommended to introduce modifications to the peptide formulation in future experiments. Future research should attempt to identify the best type of modification that would elicit a strong immune response against the modified peptide, thus overcoming tolerance, yet allowing cross-reactivity with the native antigen.

Adjuvant and Delivery Systems

Most studies used IFA or Montanide ISA-51 and only recently other compositions that include TLR ligands or GM-CSF are being evaluated. It seems that the choice of adjuvant may be critical in light of evidence demonstrating entrapment of T cells in the vaccination site, and it is still not fully understood whether this occurs only for short peptide vaccines or may also occur using SLPs or modified peptides. Therefore, much work should be devoted to identifying the optimal adjuvant for cancer peptide vaccines.

Patient Populations

Selection of patients for clinical studies is usually biased, limiting our possibility to evaluate vaccine efficiency. Patients that participate in clinical studies are often terminally ill, far-advanced patients with high grade and stage tumors and/or widespread metastases that have already shown refractoriness to treatments with chemotherapy or radiotherapy, and whose immune system is already compromised. Therefore, the window of opportunity to vaccinate efficiently is long-passed in these patients. It is conceivable that patients with early stage disease could potentially benefit more from peptide vaccination. Studies should look at the efficacy of vaccination in sub-populations according to the stage of the disease.

Vaccination Regimen

Usually peptide vaccination is performed as a standalone approach or a<underline >monotherapy, yielding only poor clinical benefits, and when combined with chemotherapy, improvement is noticeable. Therefore, future investigations should identify the best modality of treatment to combine with peptide vaccination, which would yield significant clinical improvement. Since peptide vaccination is about triggering the immune system and restoring its anti-tumoral effects, it is logical to examine a possible combination between peptide vaccination and checkpoint inhibitors, a combination likely to repolarize the immune system toward the desired effect. Experiments with monoclonal antibodies revealed that anti-VEGF inhibits the expression of checkpoint inhibitors such as PD-1, CTLA-4, LAG-3, and TIM-3, preventing the exhaustion of $CD8^+$ T cells, and suggesting a mechanism that could explain a synergistic effect of anti-PD-1 and anti-VEGF (77). In view of the recent success in combining checkpoint inhibitors with other anti-angiogenic treatment modalities (78), this combination approach might also be highly effective for anti-angiogenic peptide vaccines and should be explored further. Although data are lacking at the moment, it will be interesting to see future developments using a combination of neoantigen-derived peptides with peptides targeting the tumor vasculature, and to explore whether such combinations enhance the anti-tumoral response and increase clinical success.

Of note, pathological angiogenesis that results from an imbalance between pro- and anti-angiogenic factors is associated with many types of chronic inflammatory diseases. While cancer diseases are one form of chronic inflammation, angiogenesis is also essential to the progression of autoimmune and inflammatory diseases (79, 80). However, with the exception of our previously mentioned study on a DSS-induced colitis model (66), other studies on peptide vaccination targeting angiogenic proteins in autoimmune disease models were not found. Therefore, examining the potential of targeting angiogenesis in such conditions is strongly indicated.

In conclusion, the fact that most peptide vaccinations demonstrated poor clinical benefits is the main difficulty facing the development of new peptide vaccines. On the other hand, peptide vaccination is safe and well-tolerated, suggesting clear potential advantages over other modalities of treatment. The data presented here suggests that peptide vaccination, especially against angiogenic targets, is still a viable option, if peptides are modified, targets are well-selected and an optimal adjuvant is used. Additional possibilities of using peptide vaccines as adjuvant therapy to other treatment modalities still await more exploration. Still, targeting angiogenic proteins may be a double-edged sword, as these proteins may be physiologically expressed in normal tissues as well. In this case, stimulating the immune system against these proteins could risk triggering autoimmunity and cause catastrophic results. However, so far, peptide vaccination in general, and that of pro-angiogenic targets in particular, has been well-tolerated and showed no adverse responses, suggesting that the immune system is directed in a selective manner to the tumor site. The mechanisms that might explain such a phenomenon should be intensively studied. Once such mechanisms are better understood, they could be manipulated at need to avoid autoimmune diseases and promote the use of peptide vaccination for the treatment of cancer diseases.

AUTHOR CONTRIBUTIONS

MR collected the data, organized, drafted, and wrote the paper.

FUNDING

This manuscript was supported by the Israel Science Foundation (Grant No. 1392/14), and by the Israel Cancer Association (Grant No. 20180051/20191633 made available by the ICA USA Board of Directors).

REFERENCES

1. Sharma P, Allison JP. Immune checkpoint targetingin cancer therapy: toward combination strategies with curative potential. *Cell.* (2015) 161:205–14. doi: 10.1016/j.cell.2015.03.030
2. Baumeister SH, Freeman GJ, Dranoff G, Sharpe AH. Coinhibitory pathways in immunotherapy for cancer. *Annu Rev Immunol.* (2016) 34:539–73. doi: 10.1146/annurev-immunol-032414-112049
3. Carmeliet P, Jain RK. Molecular mechanisms and and clinical applications of angiogenesis. *Nature.* (2011) 473:298–307. doi: 10.1038/nature10144
4. Gacche RN. Compensatory angiogenesis and tumor refractoriness. *Oncogenesis.* (2015)4:e153. doi: 10.1038/oncsis.2015.14
5. Folkman J. Anti-angiogenesis: new concept for therapy of solid tumors. *Ann Surg.* (1972) 173:409–16. doi: 10.1097/00000658-197203000-00014
6. Sormendi S, Wielockx B. Hypoxia pathway proteins as central mediators of metabolism in the tumor cells and their microenvironment. *Front Immunol.* (2018) 9:40. doi: 10.3389/fimmu.2018.00040
7. Chouaib S, Umansky V, Kieda C. The role of hypoxia in shaping the recruitment of proangiogenic and immunosuppressive cells in the tumor microenvironment. *Contemp Oncol.* (2018) 22:7–13. doi: 10.5114/wo.2018.73874
8. Kim JY, Lee JY. Targeting tumor adaption to chronic hypoxia: implications for drug resistance, and how it can be overcome. *Int J Mol Sci.* (2017) 18:E1854. doi: 10.3390/ijms18091854

9. Meijer TWH, Kaanders JHAM, Span PN, Bussink J. Targeting hypoxia, HIF-1, and tumor glucose metabolism to improve radiotherapy efficacy. *Clin Cancer Res.* (2012) 18:5585–94. doi: 10.1158/1078-0432.CCR-12-0858
10. Wentink MQ, Hackeng TM, Tabruyn SP, Puijk WC, Schwamborn K, Altschuh D, et al. Targeted vaccination against the bevacizumab binding site on VEGF using 3D-structured peptides elicits efficient antitumor activity. *Proc Natl Acad Sci USA.* (2016) 113:12532–7. doi: 10.1073/pnas.1610258113
11. Wagner SC, Ichim TE, Ma H, Szymanski J, Perez JA, Lopez J, et al. Cancer anti-angiogenesis vaccines: is the tumor vasculature antigenically unique? *J Transl Med.* (2015) 13:340. doi: 10.1186/s12967-015-0688-5
12. Motz GT, Santoro SP, Wang L-P, Garrabrant T, Lastra RR, Hagemann IS, et al. Tumor endothelium FasL establishes a selective immune barrier promoting tolerance in tumors. *Nat Med.* (2014) 20:607–15. doi: 10.1038/nm.3541
13. Ruiz-Cabello F, Bernal M, Garrido F, Perea F, Aptsiauri N, Sánchez-Palencia A. The escape of cancer from T cell-mediated immune surveillance: HLA class I loss and tumor tissue architecture. *Vaccines.* (2017) 5:7. doi: 10.3390/vaccines5010007
14. Wada S, Tsunoda T, Baba T, Primus FJ, Kuwano H, Shibuya M, et al. Rationale for antiangiogenic cancer therapy with vaccination using epitope peptides derived from human vascular endothelial growth factor receptor 2. *Cancer Res.* (2005) 65:4939–46. doi: 10.1158/0008-5472.CAN-04-3759
15. Ebos JM, Kerbel RS. Antiangiogenic therapy: impact on invasion, disease progression, and metastasis. *Nat Rev Clin Oncol.* (2011) 8:210–21. doi: 10.1038/nrclinonc.2011.21
16. van Beijnum JR, Griffioen AW, Huijbers EJM, Thijssen VL, Nowak-Sliwinska P. The great escape; the hallmarks of resistance to antiangiogenic therapy. *Pharmacol Rev.* (2015) 67:441–61. doi: 10.1124/pr.114.010215
17. Abdel-Qadir H, Ethier JL, Lee DS, Thavendiranathan P, Amir E. Cardiovascular toxicity of angiogenesis inhibitors in treatment of malignancy: a systematic review and meta-analysis. *Cancer Treat Rev.* (2017) 53:120–7. doi: 10.1016/j.ctrv.2016.12.002
18. Haemmerle M, Bottsford-Miller J, Pradeep S, Taylor ML, Choi HJ, Hansen JM, et al. FAK regulates platelet extravasation and tumor growth after antiangiogenic therapy withdrawal. *J Clin Invest.* (2016) 126:1885–96. doi: 10.1172/JCI85086
19. Allen E, Missianen R, Bergers G. Trimming the vascular tree in tumors : metabolic and immune adaptations. *Cold Spring Harb Symp Quant Biol.* (2016) 81:21–9. doi: 10.1101/sqb.2016.81.030940
20. Zarrin B, Zarifi F, Vaseghi G, Javanmard SH. Acquired tumor resistance to antiangiogenic therapy: mechanisms at a glance. *J Res Med Sci.* (2017) 22:117–23. doi: 10.4103/jrms.JRMS_182_17
21. Al-Abd AM, Alamoudi AJ, Abdel-Naim AB, Neamatallah TA, Ashour OM. Anti-angiogenic agents for the treatment of solid tumors: potential pathways, therapy and current strategies – a review. *J Adv Res.* (2017) 8:591–605. doi: 10.1016/j.jare.2017.06.006
22. Abdollahi A, Folkman J. Evading tumor evasion: current concepts and perspectives of anti-angiogenic cancer therapy. *Drug Resist Updat.* (2010) 13:16–28. doi: 10.1016/j.drup.2009.12.001
23. Cheson BD. Angiogenesis inhibitors as therapeutic agents in cancer: challenges and future directions. *Semin Nucl Med.* (2016) 793:76–81. doi: 10.1016/j.ejphar.2016.10.039
24. Dunn GP, Old LJ, Schreiber RD. The Three Es of cancer immunoediting. *Annu Rev Immunol.* (2004) 22:329–60. doi: 10.1146/annurev.immunol.22.012703.104803
25. Zaenker P, Gray ES, Ziman MR. Autoantibody production in cancer—the humoral immune response toward autologous antigens in cancer patients. *Autoimmun Rev.* (2016) 15:477–83. doi: 10.1016/j.autrev.2016.01.017
26. Gubin MM, Zhang X, Schuster H, Caron E, Ward JP, Noguchi T, et al. Checkpoint blockade cancer immunotherapy targets tumour-specific mutant antigens. *Nature.* (2014) 515:577–81. doi: 10.1038/nature13988
27. Garcês S, Demengeot J. The immunogenicity of biologic therapies. *Curr Probl Dermatol.* (2018) 53:37–48. doi: 10.1159/000478077
28. Dubbs SB. The latest cancer agents and their complications. *Emerg Med Clin North Am.* (2018) 36:485–92. doi: 10.1016/j.emc.2018.04.006
29. Yamada A, Sasada T, Noguchi M, Itoh K. Next-generation peptide vaccines for advanced cancer. *Cancer Sci.* (2013) 104:15–21. doi: 10.1111/cas.12050
30. Bezu L, Kepp O, Cerrato G, Pol J, Fucikova J, Spisek R, et al. Trial watch: peptide-based vaccines in anticancer therapy. *Oncoimmunology.* (2018) 7:1–15. doi: 10.1080/2162402X.2018.1511506
31. Van Der Burg SH, Arens R, Ossendorp F, Van Hall T, Melief CJM. Vaccines for established cancer: overcoming the challenges posed by immune evasion. *Nat Rev Cancer.* (2016) 16:219–33. doi: 10.1038/nrc.2016.16
32. Araya RE, Goldszmid RS. IFNAR1 degradation: a new mechanism for tumor immune evasion? *Cancer Cell.* (2017) 31:161–3. doi: 10.1016/j.ccell.2017.01.012
33. Lee CH, Yelensky R, Jooss K, Chan TA. Update on tumor neoantigens and their utility: why it is good to be different. *Trends Immunol.* (2018) 39:536–48. doi: 10.1016/j.it.2018.04.005
34. Guo Y, Lei K, Tang L. Neoantigen vaccine delivery for personalized anticancer immunotherapy. *Front Immunol.* (2018) 9:1499. doi: 10.3389/fimmu.2018.01499
35. Buhrman JD, Slansky JE. Improving T cell responses to modified peptides in tumor vaccines. *Immunol Res.* (2013) 55:34–47. doi: 10.1007/s12026-012-8348-9
36. Melief CJM, van Hall T, Arens R, Ossendorp F, van der Burg SH. Therapeutic cancer vaccines. *J Clin Invest.* (2015) 125:3401–12. doi: 10.1172/JCI80009
37. Iero M, Filipazzi P, Castelli C, Belli F, Valdagni R, Parmiani G, et al. Modified peptides in anti-cancer vaccines: are we eventually improving anti-tumour immunity? *Cancer Immunol Immunother.* (2009) 58:1159–67. doi: 10.1007/s00262-008-0610-6
38. Buhrdman JD, Jordan KR, U'Ren L, Sprangue J, Kemmler CB, Slansky JE. Augmenting anti-tumor T cell responses to mimotope vaccination by boosting with native tumor antigens. *Cancer Res.* (2013) 73:74–85. doi: 10.1158/0008-5472.CAN-12-1005
39. Filipazzi P, Pilla L, Mariani L, Patuzzo R, Castelli C, Camisaschi C, et al. Limited induction of tumor cross-reactive T cells without a measurable clinical benefit in early melanoma patients vaccinated with human leukocyte antigen class I-modified peptides. *Clin Cancer Res.* (2012) 18:6485–96. doi: 10.1158/1078-0432.CCR-12-1516
40. Tam JP. Synthetic peptide vaccine design: synthesis and properties of a high-density multiple antigenic peptide system. *Proc Natl Acad Sci USA.* (1988) 85:5409–13. doi: 10.1073/pnas.85.15.5409
41. Falciani C, Pini A, Bracci L. Oligo-branched peptides for tumor targeting: from magic bullets to magic forks. *Expert Opin Biol Ther.* (2009) 9:171–8. doi: 10.1517/14712590802620501
42. Falciani C, Lozzi L, Pini A, Corti F, Fabbrini M, Bernini A, et al. Molecular basis of branched peptides resistance to enzyme proteolysis. *Chem Biol Drug Des.* (2007) 69:216–21. doi: 10.1111/j.1747-0285.2007.00487.x
43. Ciesielski MJ, Kazim AL, Barth RF, Fenstermaker RA. Cellular antitumor immune response to a branched lysine multiple antigenic peptide containing epitopes of a common tumor-specific antigen in a rat glioma model. *Cancer Immunol Immunother.* (2005) 54:107–19. doi: 10.1007/s00262-004-0576-y
44. Rahma OE, Ashtar E, Czystowska M, Szajnik ME, Wieckowski E, Bernstein S, et al. A gynecologic oncology group phase II trial of two p53 peptide vaccine approaches: subcutaneous injection and intravenous pulsed dendritic cells in high recurrence risk ovarian cancer patients. *Cancer Immunol Immunother.* (2012) 61:373–84. doi: 10.1007/s00262-011-1100-9
45. Neek M, Kim T Il, Wang SW. Protein-based nanoparticles in cancer vaccine development. *Nanomedicine.* (2019) 15:164–174. doi: 10.1016/j.nano.2018.09.004
46. Ye F, Hu Z, Mo F, Lai C, Yu X, Yang X, et al. The enhanced antitumor-specific immune response with mannose- and CpG-ODN-coated liposomes delivering TRP2 peptide. *Theranostics.* (2018) 8:1723–39. doi: 10.7150/thno.22056
47. Gouttefangeas C, Rammensee HG. Personalized cancer vaccines: adjuvants are important, too. *Cancer Immunol Immunother.* (2018) 67:1911–8. doi: 10.1007/s00262-018-2158-4
48. Hailemichael Y, Dai Z, Jaffarzad N, Ye Y, Medina MA, Huang XF, et al. Persistent antigen at vaccination sites induces tumor-specific CD8+ T cell sequestration, dysfunction and deletion. *Nat Med.* (2013) 19:465–72. doi: 10.1038/nm.3105
49. Hailemichael Y, Overwijk WW. Cancer vaccines: trafficking of tumor-specific T cells to tumor after therapeutic vaccination. *Int J Biochem Cell Biol.* (2014) 53:46–50. doi: 10.1016/j.biocel.2014.04.019

50. Khong H, Volmari A, Sharma M, Dai Z, Imo CS, Hailemichael Y, et al. Peptide vaccine formulation controls the duration of antigen presentation and magnitude of tumor-specific CD8 $^{+}$ T cell response. *J Immunol.* (2018) 200:3464–74. doi: 10.4049/jimmunol.1700467
51. Fernández A, Oliver L, Alvarez R, Fernández LE, Lee KP, Mesa C. Adjuvants and myeloid-derived suppressor cells: enemies or allies in therapeutic cancer vaccination. *Hum Vaccines Immunother.* (2014) 10:3251–60. doi: 10.4161/hv.29847
52. Arens R, van Hall T, van der Burg SH, Ossendorp F, Melief CJM. Prospects of combinatorial synthetic peptide vaccine-based immunotherapy against cancer. *Semin Immunol.* (2013) 25:182–90. doi: 10.1016/j.smim.2013.04.008
53. Kim JW, Kim TD, Hong BS, Kim OY, Yoon WH, Chae CB, et al. A serum-stable branched dimeric anti-VEGF peptide blocks tumor growth via anti-angiogenic activity. *Exp Mol Med.* (2010) 42:514–23. doi: 10.3858/emm.2010.42.7.052
54. Ishizaki H, Tsunoda T, Wada S, Yamauchi M, Shibuya M, Tahara H. Inhibition of tumor growth with antiangiogenic cancer vaccine using epitope peptides derived from human vascular endothelial growth factor receptor 1. *Clin Cancer Res.* (2006) 12:5841–9. doi: 10.1158/1078-0432.CCR-06-0750
55. Femel J, Huijbers EJM, Saupe F, Cedervall J, Zhang L, Roswall P, et al. Therapeutic vaccination against fibronectin ED-A attenuates progression of metastatic breast cancer. *Oncotarget.* (2014) 5:12418–27. doi: 10.18632/oncotarget.2628
56. Zhang J, Yang JM, Wang HJ, Ru GQ, Fan DM. Synthesized multiple antigenic polypeptide vaccine based on B-cell epitopes of human heparanase could elicit a potent antimetastatic effect on human hepatocellular carcinoma *in vivo*. *PLoS ONE.* (2013) 8:e52940. doi: 10.1371/journal.pone.0052940
57. Zhang J, Yang J, Cai Y, Jin N, Wang H, Yu T. Multiple antigenic polypeptide composed of heparanase B-cell epitopes shrinks human hepatocellular carcinoma in mice. *Oncol Rep.* (2015) 33:1248–56. doi: 10.3892/or.2014.3679
58. Plum SM, Holaday JW, Ruiz A, Madsen JW, Fogler WE, Fortier AH. Administration of a liposomal FGF-2 peptide vaccine leads to abrogation of FGF-2-mediated angiogenesis and tumor development. *Vaccine.* (2000) 19:1294–303. doi: 10.1016/S0264-410X(00)00210-3
59. Simanovich E, Brod V, Rahat MM, Drazdov E, Miriam W, Shakya J, et al. Inhibition of tumor growth and metastasis by EMMPRIN Multiple Antigenic Peptide (MAP) vaccination is mediated by immune modulation. *Oncoimmunology.* (2017) 6:e1261778. doi: 10.1080/2162402X.2016.1261778
60. Vicari D, Foy KC, Liotta EM, Kaumaya PTP. Engineered conformation-dependent VEGF peptide mimics are effective in inhibiting VEGF signaling pathways. *J Biol Chem.* (2011) 286:13612–25. doi: 10.1074/jbc.M110.216812
61. Foy KC, Miller MJ, Moldovan N, Carson WE, Kaumaya PTP. Combined vaccination with her-2 peptide followed by therapy with vegf peptide mimics exerts effective anti-tumor and anti-angiogenic effects *in vitro* and *in vivo*. *Oncoimmunology.* (2012) 1:1048–60. doi: 10.4161/onci.20708
62. Li W, Ran Y, Li M, Zhang K, Qin X, Xue X, et al. Mimotope vaccination for epitope-specific induction of anti-VEGF antibodies. *BMC Biotechnol.* (2013) 13:77. doi: 10.1186/1472-6750-13-77
63. Vlodavsky I, Gross-Cohen M, Weissmann M, Ilan N, Sanderson RD. Opposing functions of heparanase-1 and heparanase-2 in cancer progression. *Trends Biochem Sci.* (2018) 43:18–31. doi: 10.1016/j.tibs.2017.10.007
64. Ilan N, Vlodavsky I, Sanderson RD, Boyango I, Singh P, Gutter-Kapon L, et al. Heparanase: from basic research to therapeutic applications in cancer and inflammation. *Drug Resist Updat.* (2016) 29:54–75. doi: 10.1016/j.drup.2016.10.001
65. Walter M, Simanovich E, Brod V, Lahat N, Bitterman H, Rahat MA. An epitope-specific novel anti-EMMPRIN polyclonal antibody inhibits tumor progression. *Oncoimmunology.* (2015) 5:e1078056. doi: 10.1080/2162402X.2015.1078056
66. Simanovich E, Brod V, Rahat MA. Active vaccination with EMMPRIN-derived Multiple Antigenic Peptide (161-MAP) reduces angiogenesis in a Dextran Sodium Sulfate (DSS)-induced colitis model. *Front Immunol.* (2018) 9:2919. doi: 10.3389/fimmu.2018.02919
67. Miyazawa M, Ohsawa R, Tsunoda T, Hirono S, Kawai M, Tani M, et al. Phase I clinical trial using peptide vaccine for human vascular endothelial growth factor receptor 2 in combination with gemcitabine for patients with advanced pancreatic cancer. *Cancer Sci.* (2010) 101:433–9. doi: 10.1111/j.1349-7006.2009.01416.x
68. Yoshimura K, Minami T, Nozawa M, Uemura H. Phase i clinical trial of human vascular endothelial growth factor receptor 1 peptide vaccines for patients with metastatic renal cell carcinoma. *Br J Cancer.* (2013) 108:1260–6. doi: 10.1038/bjc.2013.90
69. Shibao S, Ueda R, Saito K, Kikuchi R, Nagashima H, Kojima A, et al. A pilot study of peptide vaccines for VEGF receptor 1 and 2 in patients with recurrent/progressive high grade glioma. *Oncotarget.* (2018) 9:21569–79. doi: 10.18632/oncotarget.25131
70. Masuzawa T, Fujiwara Y, Okada K, Nakamura A, Takiguchi S, Nakajima K, et al. Phase I/II study of S-1 plus cisplatin combined with peptide vaccines for human vascular endothelial growth factor receptor 1 and 2 in patients with advanced gastric cancer. *Int J Oncol.* (2012) 41:1297–304. doi: 10.3892/ijo.2012.1573
71. Hazama S, Nakamura Y, Takenouchi H, Suzuki N, Tsunedomi R, Inoue Y, et al. A phase I study of combination vaccine treatment of five therapeutic epitope-peptides for metastatic colorectal cancer; safety, immunological response, and clinical outcome. *J Transl Med.* (2014) 12:63–73. doi: 10.1186/1479-5876-12-63
72. Miyazawa M, Katsuda M, Maguchi H, Katanuma A, Ishii H, Ozaka M, et al. Phase II clinical trial using novel peptide cocktail vaccine as a postoperative adjuvant treatment for surgically resected pancreatic cancer patients. *Int J Cancer.* (2017) 140:973–82. doi: 10.1002/ijc.30510
73. Suzuki N, Hazama S, Iguchi H, Uesugi K, Tanaka H, Hirakawa K, et al. Phase II clinical trial of peptide cocktail therapy for patients with advanced pancreatic cancer: VENUS-PC study. *Cancer Sci.* (2017) 108:73–80. doi: 10.1111/cas.13113
74. Fujiwara Y, Okada K, Omori T, Sugimura K, Miyata H, Ohue M, et al. Multiple therapeutic peptide vaccines for patients with advanced gastric cancer. *Int J Oncol.* (2017) 50:1655–62. doi: 10.3892/ijo.2017.3955
75. Gregorc V, Santoro A, Bennicelli E, Punt CJA, Citterio G, Timmer-Bonte JNH, et al. Phase Ib study of NGR-hTNF, a selective vascular targeting agent, administered at low doses in combination with doxorubicin to patients with advanced solid tumours. *Br J Cancer.* (2009) 101:219–24. doi: 10.1038/sj.bjc.6605162
76. Parmiani G, Pilla L, Corti A, Doglioni C, Cimminiello C, Bellone M, et al. A pilot Phase I study combining peptide-based vaccination and NGR-hTNF vessel targeting therapy in metastatic melanoma. *Oncoimmunology.* (2014) 3:e963406. doi: 10.4161/21624011.2014.963406
77. Voron T, Colussi O, Marcheteau E, Pernot S, Nizard M, Pointet A-L, et al. VEGF-A modulates expression of inhibitory checkpoints on CD8 + T cells in tumors. *J Exp Med.* (2015) 212:139–48. doi: 10.1084/jem.20140559
78. Yi M, Jiao D, Qin S, Chu Q, Wu K, Li A. Synergistic effect of immune checkpoint blockade and anti-angiogenesis in cancer treatment. *Mol Cancer.* (2019) 18:1–12. doi: 10.1186/s12943-019-0974-6
79. Cantatore FP, Maruotti N, Corrado A, Ribatti D. Angiogenesis dysregulation in psoriatic arthritis : molecular mechanisms. *Biomed Res Int.* (2017) 2017:5312813. doi: 10.1155/2017/5312813
80. Veale DJ, Fearon U. What makes psoriatic and rheumatoid arthritis so different? *RMD Open.* (2015) 1:1–5. doi: 10.1136/rmdopen-2014-000025

Conflict of Interest Statement: MR is an inventor of a patent (US Grant US9688732B2, EP application EP2833900A4) related to peptide vaccination approach described in the manuscript.

frontiers in Immunology

MINI REVIEW
published: 22 January 2020
doi: 10.3389/fimmu.2019.02930

YKL-39 as a Potential New Target for Anti-Angiogenic Therapy in Cancer

Julia Kzhyshkowska[1,2,3]*, *Irina Larionova*[3,4] *and Tengfei Liu*[1]

[1] Medical Faculty Mannheim, Institute of Transfusion Medicine and Immunology, University of Heidelberg, Mannheim, Germany, [2] German Red Cross Blood Service Baden-Württemberg—Hessen, Mannheim, Germany, [3] Laboratory of Translational Cellular and Molecular Biomedicine, National Research Tomsk State University, Tomsk, Russia, [4] Cancer Research Institute, Tomsk National Research Medical Center of the Russian Academy of Sciences, Tomsk, Russia

YKL-39 belongs to the evolutionarily conserved family of Glyco_18-containing proteins composed of chitinases and chitinase-like proteins. Chitinase-like proteins (CLPs) are secreted lectins that lack hydrolytic activity due to the amino acid substitutions in their catalytic domain and combine the functions of cytokines and growth factors. One of the major cellular sources that produce CLPs in various pathologies, including cancer, are macrophages. Monocytes recruited to the tumor site and programmed by tumor cells differentiate into tumor-associated macrophages (TAMs), which are the primary source of pro-angiogenic factors. Tumor angiogenesis is a crucial process for supplying rapidly growing tumors with essential nutrients and oxygen. We recently determined that YKL-39 is produced by tumor-associated macrophages in breast cancer. YKL-39 acts as a strong chemotactic factor for monocytes and stimulates angiogenesis. Chemotherapy is a common strategy to reduce tumor size and aggressiveness before surgical intervention, but chemoresistance, resulting in the relapse of tumors, is a common clinical problem that is critical for survival in cancer patients. Accumulating evidence indicates that TAMs are essential regulators of chemoresistance. We have recently found that elevated levels of YKL-39 expression are indicative of the efficiency of the metastatic process in patients who undergo neoadjuvant chemotherapy. We suggest YKL-39 as a new target for anti-angiogenic therapy that can be combined with neoadjuvant chemotherapy to reduce chemoresistance and inhibit metastasis in breast cancer patients.

Keywords: YKL-39, chitinase-like proteins, cancer, angiogenesis, chemotactic activity, tumor-associated macrophages, neoadjuvant chemotherapy

OPEN ACCESS

Edited by:
Fabrizio Mattei,
Istituto Superiore di Sanità (ISS), Italy

Reviewed by:
Limin Zheng,
Sun Yat-sen University, China
Douglas Mc Clain Noonan,
University of Insubria, Italy

***Correspondence:**
Julia Kzhyshkowska
julia.kzhyshkowska@medma.uni-heidelberg.de

Specialty section:
This article was submitted to Cancer Immunity and Immunotherapy, a section of the journal Frontiers in Immunology

Received: *29 May 2019*
Accepted: *28 November 2019*
Published: *22 January 2020*

Citation:
Kzhyshkowska J, Larionova I and Liu T (2020) YKL-39 as a Potential New Target for Anti-Angiogenic Therapy in Cancer. Front. Immunol. 10:2930. doi: 10.3389/fimmu.2019.02930

INTRODUCTION

YKL-39 belongs to the family of Glyco_18-containing proteins composed of chitinases and chitinase-like proteins. Chitinases comprise the Glycosyl hydrolase (GH) 18 family; their name originates from their ability to cleave chitin polymers into oligosaccharides of different sizes and release monosaccharides from the end of chitin polymer (1, 2). Chitin is the second most abundant polysaccharide in nature (after cellulose) and is found in the cell walls of fungi and the exoskeletons of crustaceans and insects (3–5). The chitinases are produced by the lower life forms as a defense mechanism against infection with chitin-containing organisms (6, 7). Mammals cannot synthesize chitin, but several chitinases and chitinase-like proteins have been identified in rodents and in humans. In humans, two functional chitinases—Acidic Mammalian Chitinase (AMCase) and Chitotriosidase (CHIT1)—have been found. AMCase is induced by IL-13 and is found in

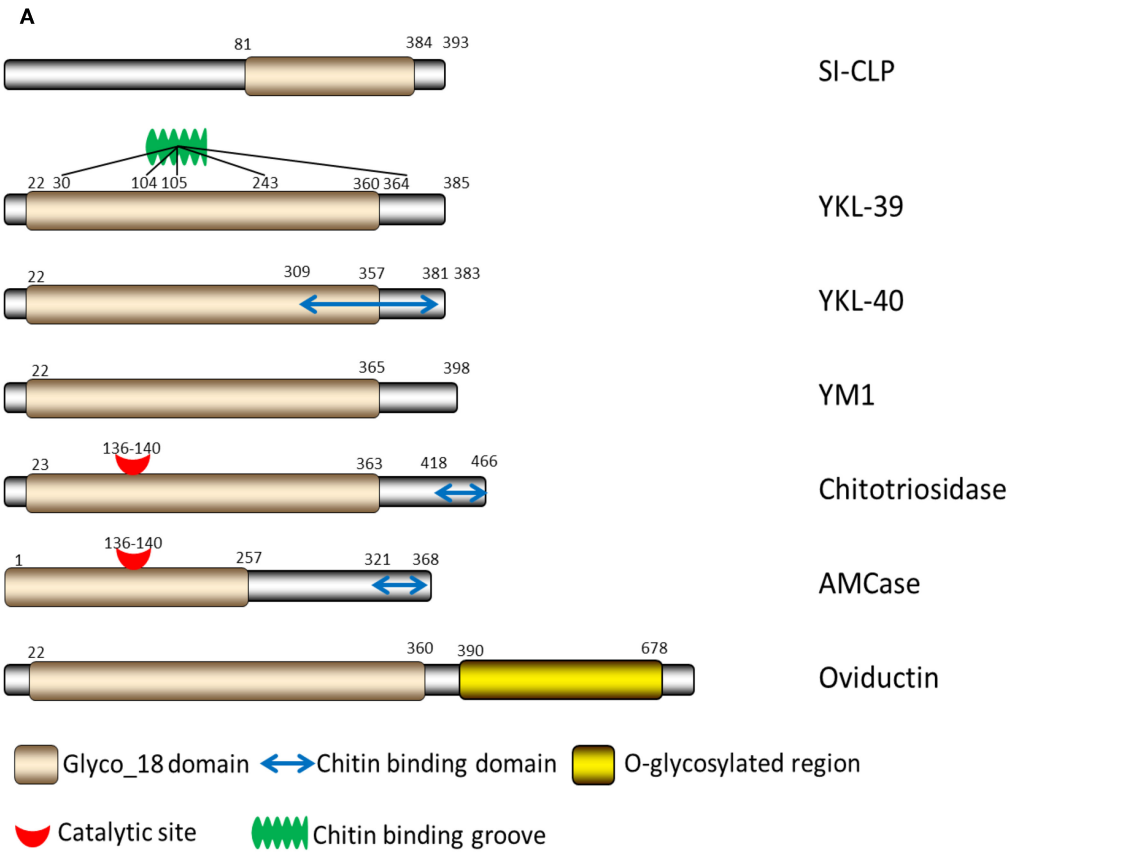

B

FDGIDIDWEYP	Glyco_18 prototype catalytic domain
1-186-FDGFVVEVMNQ-393	SI-CLP
1-131-FDGLDVSWIYP-385	YKL-39
1-131-FDGLDLAWLYP-383	YKL-40
1-131-FDGLNLDWQYP-398	YM-1
1-131-FDGLDLDWEYP-466	Chitotriosidase
1-131-FDGLDFDWEYP-368	AMCase
1-132-FDGLDLFFLYP-678	Oviductin

FIGURE 1 | Structure of mammalian chitinases and chitinase-like proteins. **(A)** Domain organization of Glyco_18-containing proteins. **(B)** Critical amino acids in catalytic sites of mammalian Glyco_18-containing proteins (12), Copyright by de Gruyter.

allergic inflammations such as asthma (8, 9). Chitotriosidase is expressed by phagocytic cells and is a biomarker for Gaucher's disease, a lysosomal storage disease that involves the dysfunctional metabolism of sphingolipids (10, 11).

Chitinase-like proteins (CLPs), as well as chitinases, possess Glyco_18 domains, but they lack enzymatic activity (12). In mammals, the following CLPs have been identified: YKL-40 (13), YKL-39 (14), SI-CLP (15), YM1, and YM2 (16). Of these, YKL-39 is present only in humans but absent in rodents, while YM1 and YM2 are only present in rodents (12).

CLPs lack enzymatic activity due to the substitution of the critical catalytic residue (glutamic acid) at the end of the DxxDxDxE conserved motif with either leucine, isoleucine, or tryptophan (**Figure 1**) (12).

The sugar-binding properties of CLPs are attributed to the Glyco_18 domain of CLPs (**Table 1**). Lectin properties define the interactions of CLPs with glycoproteins on the cell surface and with specific carbohydrate molecules in the extracellular matrix. For YKL-40, lectin properties have been identified to be critical for its interaction with syndecan-1 and αvβ3

TABLE 1 | Lectin properties of CLPs.

CLP	Carbohydrate-binding	Method of analysis	References
YKL-39	Chitooligosaccharides, (GlcNac)5, and (GlcNac)6	Glycan array screen and intrinsic tryptophan fluorescence	(17)
	Chitooligosaccharides	Isothermal titration calorimetry (ITC)	(18)
YKL-40	Type I collagen	Affinity chromatography and surface plasmon resonance	(19)
	Chitooligosaccharides	Protein X-ray crystallography	(20)
	(GlcNac)5 and (GlcNac)4	Western blotting	(21)
	Heparin	Heparin affinity and HPLC chromatograph	(22)
SI-CLP	Galactosamine, glucosamine, chitooligosacharide, (GlcNac)4, ribose, and mannose	Isothermal titration calorimetry (ITC)	(23)
YM1	Glucosamine, galactosamine, and glucosamine polymers	Surface plasmon resonance	(24)

integrin, resulting in the activation of the ERK1/2 pathway and vascular endothelial growth factor (VEGF) production in endothelial cells (25, 26). Moreover, SI-CLP was shown to bind lipopolysaccharide (LPS) *in vitro* and thereby to neutralize the toxic effect of LPS on macrophages (23). By applying a glycan microarray, performed at the Consortium of Functional Glycomics, the chitooligosaccharides were identified as the best ligands of YKL-39 (17). Structural analysis demonstrates that YKL-39 interacts with chitooligosaccharides through hydrogen bonds and hydrophobic interactions, and compared with other GH-18 members, YKL-39 has the least extended chitin-binding cleft (18). However, the biological relevance of these interactions is questionable, since chitin is not synthesized by mammals, and the tissue expression of YKL-39 rather precludes contact with chitooligosaccharides as a component of the nutrition or pathogens (17).

YKL-39 IDENTIFICATION AND EXPRESSION IN PATHOLOGY

YKL-39 was first identified when found to be produced in high amounts by synoviocytes and chondrocytes (14, 27) and was suggested as a circulating biomarker for osteoarthritis (OA) (14, 27, 28). Increased YKL-39 mRNA levels were also detected in the microglia of Alzheimer patients (29). The detection of YKL-39 in cerebrospinal fluid was suggested to be a potential prognostic biomarker in the early stage of multiple sclerosis (30, 31). Also, YKL-39 mRNA levels were significantly increased in the hippocampus in simian immunodeficiency virus encephalitis (SIVE) and HIV encephalitis (HIVE) (32). These data suggested the role of YKL-39 in both neurodegeneration and chronic inflammatory diseases of the brain. We have recently identified that YKL-39 is expressed in human breast cancer (33), and these data are discussed in the context of the role of CLPs in tumor progression and response to therapy in the following paragraphs.

BIOLOGICAL ACTIVITIES

Biological activities of chitinase-like proteins related to tumor progression include chemotactic activity, growth factor activity, induction of cytokine secretion, and stimulation of angiogenesis. YKL-39 was identified to combine monocyte chemotactic and pro-angiogenic activities (33), and these biological activities will be discussed in our review.

CHEMOTACTIC ACTIVITY

Several chitinase-like proteins were demonstrated to have chemotactic activities. YM1 was first identified as eosinophil chemotactic protein (ECF-L) (34). YM1 attracted T lymphocytes and bone marrow polymorphonuclear leukocytes *in vitro* and induced selective extravasation of eosinophils in a mouse model (34). Microglia-secreted YM1 was suggested to be involved in eosinophilic meningitis and meningoencephalitis caused by Angiostrongylus cantonensis infection (35). YM1 and YM2 were strongly induced in a mouse model for proliferative dermatitis characterized by the accumulation of eosinophils in the skin (36).

Human YKL-40 was reported to have chemotactic activity toward different cell types. Nishikawa et al. showed that YKL-40 is associated with vascular smooth muscle cell (VSMC) migration and invasion into the gelatinous matrix (22). YKL-40 expressed in human colon cancer SW480 cells enhanced the migration of human monocyte-like THP-1 cells and human umbilical vein endothelial cells (HUVEC). The expression of YKL-40 was associated with macrophage infiltration and micro-vessel density (MVD) in the tumors of human colorectal cancer patients and in a xenograft mouse model (37). YKL-40 was also found to contribute to the migration of bronchial smooth muscle cells indirectly by inducing the expression of IL-8 (38).

We have recently demonstrated that purified YKL-39 strongly induces the migration of freshly isolated human CD14+ monocytes (**Figure 2**) (33). YKL-39 was active at the concentration of 100 ng/ml corresponding to the biologically active concentration of YKL-40, 90.3 ± 8.2 ng/ml, in patients with OA (39). After 3 h of migration, the effect of YKL-39 was comparable to the effect of the major monocyte chemotactic factor CCL2 if used at the same concentration. Monocytes are intensively recruited into growing tumors by chemotactic factors secreted by tumor cells and stromal cells in the tumor microenvironment, where both tumor-associated macrophages (TAMs) and cancer cells serve as sources of chemotactic factors such as CCL2 (40, 41). Monocytes differentiate in the tumor tissue into tumor-associated macrophages, which are key inducers of the angiogenic switch (42). The strong chemotactic activity of YKL-39 makes it an attractive candidate to consider as a target to reduce monocyte recruitment into the tumor tissue.

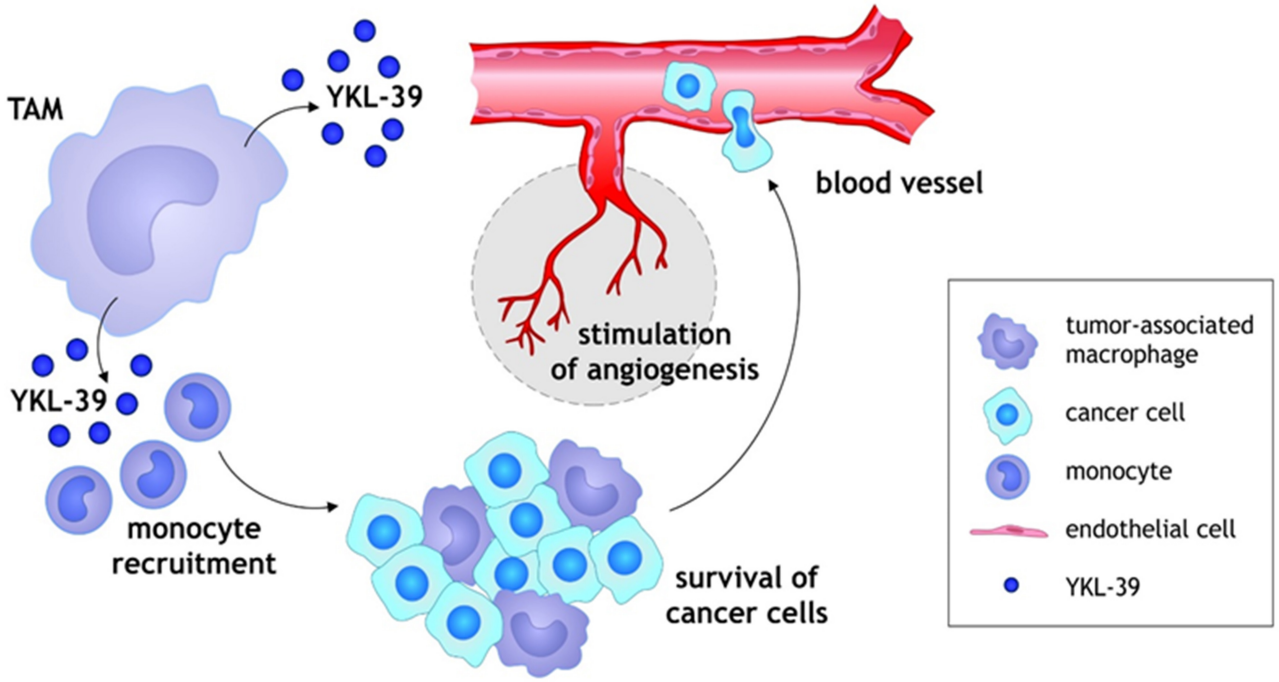

FIGURE 2 | Schematic illustration of YKL-39 activity in cancer. Monocytes are recruited into growing tumors by chemotactic factor YKL-39 secreted by TAMs in the tumor microenvironment, where TAMs support the survival and growth of cancer cells. Monocytes differentiate in the tumor tissue into TAMs, which are key inducers of the angiogenic switch. YKL-39 possesses pro-angiogenic activity and causes stimulation of angiogenesis that can lead to the intensive intravasation of cancer cells to the blood vessels.

ANGIOGENESIS

YKL-39 was identified by us as a strong pro-angiogenic factor *in vitro*. Tumor angiogenesis is a crucial process for supplying rapidly growing tumors with essential nutrients and oxygen (41). Monocytes recruited to the tumor site and programmed by tumor cells are known as TAMs, which are the primary source of pro-angiogenic factors (41, 43). TAMs produce a variety of pro-angiogenic factors under the hypoxic condition in tumor sites, for example, VEGF, which promotes migration of endothelial cells and macrophages toward tumor areas (40, 44).

VEGF is the prototypical proangiogenic factor that induces vascular permeability and increased migration and proliferation of endothelial cells, making it a major target for therapy (45). One of the main anti-angiogenic approaches is to block VEGF using a monoclonal antibody (bevacizumab). Other drugs include VEGF pathway inhibitors such as small-molecule tyrosine kinase inhibitors (sunitinib, sorafenib, pazopanib, regorafenib, lenvatinib, and vandetanib), a soluble VEGF decoy receptor (aflibercept), a human monoclonal antibody against VEGFR-2 (ramucirumab), and others (45, 46). Administering bevacizumab in combination with chemotherapeutic agents showed improved survival of patients with colorectal cancer, ovarian cancer, and lung cancer in comparison with chemotherapy alone (46–48). However, there is resistance against anti-VEGF medication, which includes several mechanisms, such as the activation and upregulation of alternative proangiogenic pathways, the recruitment of bone marrow-derived proangiogenic cells, and the adoption of alternative angiogenic mechanisms (45). Several studies have demonstrated TAM accumulation in the tumor mass after chemotherapy and antiangiogenic therapy. Thus, Dalton et al. showed that recruitment of macrophages to the TME after anti-VEGF treatment leads to tumor growth as a mechanism of resistance to therapy but that depletion of macrophages inhibited tumor growth and improved the survival of tumor-bearing mice (49). The vascular disrupting agent combretastatin A4-P causes the increased production of CSF-1, CCL2, and CXCL12 that increases monocyte recruitment and TAM accumulation in tumor sites (50). In mouse mammary tumors, chemotherapy increased the expression of CSF-1 by tumor cells, followed by the recruitment of macrophages (51). Thus, chemotherapy and anti-VEGF therapy have disadvantages such as TAM accumulation and treatment resistance, and additional new therapeutic approaches need to be developed.

Chitinase-like protein YKL-40 has already been shown to be involved in tumor angiogenesis in several studies. It was reported that gp38k (porcine homolog protein of YKL-40) promotes the migration and spreading of VSMCs *in vitro* (22). The expression of YKL-40 in MDA-MB-231 breast cancer cells and HCT-116 colon cancer cells is also associated with tube formation in an extensive angiogenic phenotype mouse model (26). Recombinant YKL-40 protein was also found to induce angiogenesis of vascular endothelial cells *in vitro* (52). A correlation between blood vessel density and YKL-40 expression has also been observed in

human breast cancer patients (53). The YKL-40-induced pro-angiogenic effect was VEGF-independent, suggesting that YKL-40 and VEGF individually promote endothelial cell angiogenesis (26). However, a long-term blockade of VEGF may result in angiogenic compensative tumor cell activities by inducing YKL-40 (54). It is most likely that blockade of one angiogenic factor induces the expression of other potent angiogenic factors to maintain tumor vascularization.

YKL-39 has a high structural similarity to YKL-40. Therefore, we considered that YKL-39 can act as a pro-angiogenic factor in cancer. We have performed tube formation assay using HUVEC cells and found that YKL-39 exerts a strong pro-angiogenenic effect through direct activation of vascular endothelial cells (**Figure 2**). Recombinant YKL-39 at a concentration of 100 ng/ml significantly induced tube formation in HUVEC cells *in vitro* (33). This data indicated that YKL-39 can directly induce angiogenesis and that YKL-39-expressing TAMs can serve as a source of angiogenic factors in the tumor microenvironment.

MACROPHAGES ARE A MAJOR SOURCE OF CHITINASE-LIKE PROTEINS

Pathological programming of macrophages is crucial for the development of major types of life-threatening disorders, including cancer and cardiovascular and neurodegenerative disorders (55–59). Macrophages regulate intratumoral immune responses and the progression of atherosclerosis by the secretion of cytokines, growth factors, enzymes, and extracellular matrix proteins (41, 55, 60). Two major directions of macrophage polarization are known: pro-inflammatory M1 macrophages with antitumor properties and anti-inflammatory M2 macrophages with pro-tumor functions. In most solid tumors, macrophages are represented by the M2 phenotype, which supports tumor growth, angiogenesis, and metastatic spread (61, 62). Macrophages serve as a major source of all murine and human chitinase-like proteins (**Table 2**). However, the expression of YKL-40 is not restricted to macrophages (TAMs) and has been found in human small cell lung cancer (63), microglia from Alzheimer's disease patients (29), and other cell types. The expression of SI-CLP was detected in peripheral blood mononuclear cells from rheumatoid arthritis (RA) patients (68).

Elevated levels of YKL-39 gene expression were detected in microglia of Alzheimer's patients (29). In *in vitro* experimental models, expression of CLPs depends on the activation state of macrophages (M1 or M2). YKL-40 expression is elevated during the differentiation process of human macrophages, and macrophage differentiation factors GM-CSF or M-CSF have been shown to induce YKL-40 expression (65, 70). It was identified that in human monocyte-derived macrophages, IFN-γ and LPS are strong inducers of YKL-40 gene expression (15, 67). In contrast, expression of SI-CLP is induced by IL-4 and dexamethasone on both the mRNA and protein levels in human monocyte-derived macrophages (15). YKL-39 expression is strongly induced by TGF-beta, an essential regulatory cytokine of the tumor microenvironment (33).

TABLE 2 | Expression of chitinase-like proteins in macrophages.

CLP	Macrophage type	Method of analysis	References
YKL-40	Human primary monocyte-derived macrophages stimulated by IFN-γ	RT-PCR	(15)
	Microglia in Alzheimer's disease patients	RT-PCR	(29)
	Human peritumoral macrophages and murine lung macrophages	RT-PCR	(63)
	Human macrophages in pulmonary sarcoid granulomas	Immunohistochemical staining	(64)
	Peritumoral macrophages in human small cell lung cancer	Immunohistochemical staining	(63)
	Human primary monocyte-derived macrophages stimulated by GM-CSF or M-CSF	RT-PCR/ELISA/ Immunofluorescence staining	(65)
	Murine pulmonary macrophages	RT-PCR/ELISA	(66)
	Human M1 polarized macrophages stimulated by LPS and IFN-γ	RT-PCR	(67)
SI-CLP	Human primary monocyte-derived macrophages stimulated by IL-4+dexamethasone	RT-PCR/Western blotting/Immunofluorescence staining	(15)
	Murine bone marrow-derived macrophages	RT-PCR/Western blotting	(68)
	PMA-treated THP-1 macrophages	RT-PCR/Western blotting	(68)
	THP-1, Mono-Mac-6 cells	RT-PCR/Western blotting	(15)
YKL-39	Human primary monocyte-derived macrophages stimulated by TGF-beta and IL-4	RT-PCR	(33, 69)
	Alternatively activated microglia in Alzheimer's disease patients	RT-PCR	(29)

The secretion of SI-CLP and YKL-39 at least partially depends on their transport into the secretory lysosomes, mediated by their intracellular sorting by stabilin-1 (15, 33). Lysosomes are organelles with complex functions involved in the cell death, immunity, signaling, and stress responses (71–73) that not only participate in digesting extracellular material internalized by endocytosis and intracellular components sequestered by autophagy but also secrete their contents by fusing with the plasma membrane (72). Two types of lysosome-contained proteins are necessary for their functions: soluble hydrolases and integral lysosomal membrane proteins. More than 60 hydrolases have been identified and characterized, some of which play an important role in tumor progression (72, 74). The best investigated lysosomal hydrolases are the cathepsin proteases,

which are subdivided into three groups based on the active site of the amino acids and the catalytic activity: serine cathepsins (cathepsins A and G), cysteine cathepsins (cathepsins B, C, F, and H), and aspartic cathepsins (cathepsins D and E) (72). It has been suggested that cathepsins could either promote or suppress tumor growth; the cytosolic cathepsins inhibit tumor growth by activating the apoptotic pathway (75), whereas, in contrast, the extracellular cathepsins promote tumor growth through degradation of basement membrane and activation of other pro-tumorigenic proteins (76). Cathepsins B and E have been proved to be involved in cancer progression and metastasis in different types of cancer, such as breast cancer and pancreatic cancer (69, 77). Glyco_18 domain-containing proteins were also found by us and others to be sorted via the endosomal/lysosomal system and secreted by activated macrophages (4, 15, 78). Chitotriosidase was seen to be comparable to cathepsin D in lysosomal vesicles in macrophages (78). We identified that LAMP+CD63+lysosomes are major sites of SI-CLP localization in human IL4 and dexamethasone-stimulated M2 macrophages (15). Sorting of newly synthesized SI-CLP from the biosynthetic to the lysosomal pathway was mediated by stabilin-1. Similarly, we found that YKL-39 is sorted into LAMP-1 positive and secretion-committed CD63 positive lysosomes in human IL-4+TGF-beta-stimulated macrophages (33). The mechanistic role of stabilin-1 in the intracellular sorting of YKL-39 was confirmed using the HEK293-YKL-39-FLAG cell line, where YKL-39 is miss-sorted into the globular structures and localized in the nuclear area. Transient overexpression of recombinant stabilin-1 in this model cell line resulted in the re-distribution of YKL-39 into the cytoplasm, and this effect was similar to our previously published data demonstrating the role of stabilin-1 in the intracellular sorting of SI-CLP in a H1299 cell model (15). Protein–protein interaction studies demonstrated that the extracellular fasciclin domain 7 domain of stabilin-1 directly interacts with SI-CLP and YKL-39 (15, 33). Therefore, YKL-39, similarly to SI-CLP, can be targeted by stabilin-1 into the lysosomal secretory pathway in human alternatively activated macrophages.

YKL-39 was identified by us to be produced by human macrophages *in vitro* and in the tumor microenvironment (33, 79). *In vitro*, TGFbeta was a key inducer of YKL-39 gene expression, and release in primary macrophages propagated up to 24 days (33). During tumor growth and progression, a significant amount of TGF-beta is produced by cancer and stromal cells and secreted into the tumor microenvironment (80). Increased expression of TGF-beta was shown to correlate with the malignancy of different cancers (81, 82). Therefore, TGF-beta is considered to play a major role in the initiation and progression of cancer by affecting the proliferation, apoptosis, and differentiation of cancer cells in the tumor microenvironment (83). Using a monoclonal-aYKL-39 antibody generated by us, we have identified that in human breast cancer, YKL-39 is expressed on TAMs, but, in contrast to YKL-40, not on cancer cells.

CHITINASE-LIKE PROTEINS IN CANCER

Accumulating data reveals that CLPs play a role in the progression of different types of cancer. Elevated levels of circulating YKL-40 are related to poor outcome or short disease-free survival in glioblastoma, melanoma, ovarian, breast, colon, lung, and prostate cancers in humans (52, 84–92). Moreover, in breast cancer, elevated serum levels of YKL-40 have been used as a prognostic biomarker (84). The adhesive and invasive abilities of U87MG glioblastoma cells were significantly inhibited when endogenous expression of YKL-40 was blocked (93). YKL-40 was also induced during pulmonary melanoma metastasis, and this induction was mediated by Sema7a (90, 94). Overexpression of YKL-40 and YM1/2 was observed in the pre-neoplastic phase of a latent membrane protein 1 (LMP1) viral oncogene-expressing transgenic mouse model, which is associated with carcinogenic progression (95). In breast cancer, YKL-40 may support cancer progression and facilitate angiogenesis, as experimental knock-down of YKL-40 in tumorigenic breast epithelial cell line D492HER2 resulted in reduced migration and invasion as well as reduced ability to induce angiogenesis *in vitro* (96). Targeting of YKL-40 as a potential therapeutic approach has been evaluated in melanoma and glioblastoma mouse models. Application of anti-YKL-40 antibody in the U87 glioblastoma mouse models resulted in the suppression of xenograft tumor growth as well as angiogenesis (97). However, an opposite result was seen in BALB/c-scid mice injected with human melanoma cells; the tumor growth was enhanced after anti-YKL-40 antibody treatment (98). The contradictory results between glioblastoma and melanoma mouse models can be explained by the different mouse strains and antibodies used in the studies.

SI-CLP was shown to induce the secretion of IL-1β, IL-6, IL-12, and IL-13 in PMA-treated THP-1 cells, suggesting that it may serve as a regulator of inflammation and in the tumor microenvironment (68). The regulatory effect of SI-CLP is not clear yet since the cytokines induced by SI-CLP can either promote (IL-1β, IL-6, IL-13) or suppress (IL-12) tumor progression (99, 100).

Information about the potential role of YKL-39 in cancer is still very limited. Serial Analysis of Gene Expression (SAGE) revealed that YKL-39 expression is elevated in the II–IV grades of glial tumors (101). The expression of YKL-39 was detected in the majority of glioblastomas (19 of 27 samples analyzed) by Northern blot analysis and demonstrated on the protein level by Western blotting (102). Our recent study has demonstrated that YKL-39 is expressed in human breast cancer, and its expression level were indicative of metastatic spread in patients who underwent neoadjuvant chemotherapy, as discussed below.

CHEMOTHERAPY, TAMs AND CHITINASE-LIKE PROTEINS

Chemotherapy (CT) is a common strategy for reducing tumor size and aggressiveness before surgical intervention (103). However, only a subset of patients respond efficiently to neoajuvant chemotherapy (NAC). Chemoresistance and

chemotherapy-induced immunosuppression can result in the relapse of tumors and are critical for survival in cancer patients (49, 104). Numerous studies have examined the molecular mechanisms that promote the chemoresistance of cancer cells, such as the induction of anti-apoptotic regulators, ABC transporters, aberrant transcription factor nuclear factor-κB (NF-κB) activity, and the mechanisms of damaged DNA repair (104–106). Evidence is accumulating that the tumor microenvironment, and TAMs in particular, is critical to the response to chemotherapy (107, 108). TAMs may contribute to resistance to therapy and facilitate tumor progression via macrophage-induced suppression of T cell immunity, maintenance of tumor cell survival, and stimulation of tumor revascularization (50, 108, 109). Chemotherapeutic agents can edit macrophages in tumor-protective or antitumor directions, where three major mechanisms must be considered: (1) changes in the macrophage phenotype; (2) induced recruitment of monocytes or macrophages to the tumor site; and (3) systemic depletion of monocytes/macrophages (110). Numerous data demonstrate that chemotherapy interacts with macrophages; however, the mechanisms of the direct action of chemotherapeutic drugs on TAMs, as well as the mechanisms of TAM-mediated chemoresistance in tumors, still require in-depth investigation. The profile of immune cell subpopulations in the tumor microenvironment can help to identify a group of patients that are more sensitive/or resistant to neoadjuvant chemotherapy to improve treatment regimens.

Several studies have identified correlations between levels of CLPs and the efficiency of chemotherapy. For example, a high plasma level of YKL-40 was associated with shorter progression-free survival (PFS) and shorter overall survival (OS) in 140 patients with chemotherapy-resistant ovarian cancer treated with bevacizumab (111). A similar result was obtained in prostate cancer, where high serum YKL-40 levels were associated with shorter OS and disease-specific survival (DSS) in 109 patients who received first-line treatment with docetaxel (DOC). Moreover, YKL-40 serum levels were significantly higher in DOC-resistant patients (112). In another study, 120 patients with small cell lung cancer with high levels of serum YKL-40 had a shorter PFS and OS than those with low levels of serum YKL-40 (113). YKL-40 levels were significantly decreased after chemotherapy (cisplatin with etoposide or cisplatin with irinotecan). However, patients with high serum YKL-40 showed a poorer response to chemotherapy than those patients with low serum YKL-40. Of the 81 patients with high serum YKL-40, only 46% responded to chemotherapy with either complete response or partial remission. Of 39 patients who had low serum YKL-40, 70% exhibited a response to chemotherapy ($p = 0.031$) (113). The question of the exact role of CLPs in the response of cancer cells, macrophages, and the intratumoral vasculature to chemotherapeutic agents remains open.

A recent study of 195 patients in the European cohort with pancreatic ductal adenocarcinoma indicated single-nucleotide polymorphisms (SNP) in YKL39 that was associated with tumor-associated survival after pancreatic resection. Individuals who were homozygous for the minor A allele of SNP rs684559 (YKL-39) had an increased risk for tumor-associated death compared with patients with at least 1 G allele of rs684559 (protective phenotype) (114). Our recent study for the first time demonstrated the prognostic role of YKL-39 in cancer metastasis in breast cancer patients after neoadjuvant therapy (33). In patients with metastases, the expression levels of YKL-39 in tumor tissue obtained after NAC were more than 6 times higher than in the patients without metastases. Significantly higher expression levels of YKL-39 were found in patients with stable disease or progressive disease than in patients with the objective response (partial response). Our data demonstrated that elevated levels of YKL-39 in tumor tissues after NAC are indicative of poor prognosis.

Taking into consideration that YKL-39 was demonstrated by us as a pro-angiogenic factor and chemoattractant for monocytes, we suggest that YKL-39 is a promising target for cancer therapy and that targeting of YKL-39 can be considered in combination with NAC in breast cancer patients in order to reduce the risk of metastasis formation.

AUTHOR CONTRIBUTIONS

JK has structured the article, analyzed the literature, and wrote the manuscript. IL has analyzed the literature and wrote the manuscript. TL has analyzed the literature and wrote the manuscript.

FUNDING

This work was supported by the Russian Scientific Foundation, grant #19-15-00151.

ACKNOWLEDGMENTS

Part of this work was published as the Ph.D. Thesis of TL, performed at the University of Heidelberg, Medical Faculty Mannheim, Institute of Transfusion Medicine and Immunology, which is available online at http://www.ub.uni-heidelberg.de/archiv/23511 (115).

REFERENCES

1. Boot RG, van Achterberg TA, van Aken BE, Renkema GH, Jacobs MJ, Aerts JM, et al. Strong induction of members of the chitinase family of proteins in atherosclerosis. *Arterioscler Thromb Vasc Biol.* (1999) 19:687–94. doi: 10.1161/01.ATV.19.3.687
2. Di Rosa M, Distefano G, Zorena K, Malaguarnera L. Chitinases and immunity: ancestral molecules with new functions. *Immunobiology.* (2016) 221:399–411. doi: 10.1016/j.imbio.2015.11.014
3. Tharanathan RN, Kittur FS. Chitin—the undisputed biomolecule of great potential. *Crit Rev Food Sci Nutr.* (2003) 43:61–87. doi: 10.1080/10408690390826455

4. Kzhyshkowska J, Gratchev A, Goerdt S. Human chitinases and chitinase-like proteins as indicators for inflammation and cancer. *Biomark Insights.* (2007) 2:128–46. doi: 10.1177/117727190700200023
5. Muzzarelli RA. Chitin: Oxford, UK: Pergamon Press (1977).
6. Elias JA, Homer RJ, Hamid Q, Lee CG. Chitinases and chitinase-like proteins in T H 2 inflammation and asthma. *J Allergy Clin Immunol.* (2005) 116:497–500. doi: 10.1016/j.jaci.2005.06.028
7. Mondal S, Baksi S, Koris A, Vatai G. Journey of enzymes in entomopathogenic fungi. *Pac Sci Rev A Nat Sci Eng.* (2016) 18:85–99. doi: 10.1016/j.psra.2016.10.001
8. Donnelly LE, Barnes PJ. Acidic mammalian chitinase–a potential target for asthma therapy. *Trends Pharmacol Sci.* (2004) 25:509–11. doi: 10.1016/j.tips.2004.08.002
9. Zhu Z, Zheng T, Homer RJ, Kim Y-K, Chen NY, Cohn L, et al. Acidic mammalian chitinase in asthmatic Th2 inflammation and IL-13 pathway activation. *Science.* (2004) 304:1678–82. doi: 10.1126/science.1095336
10. Cox T. Gaucher disease: understanding the molecular pathogenesis of sphingolipidoses. *J Inherit Metab Dis.* (2001) 24:106–21. doi: 10.1023/a:1012496514170
11. Raskovalova T, Deegan PB, Yang R, Pavlova E, Stirnemann J, Labarère J, et al. Plasma chitotriosidase activity versus CCL18 level for assessing type I Gaucher disease severity: protocol for a systematic review with meta-analysis of individual participant data. *Syst Rev.* (2017) 6:87. doi: 10.1186/s13643-017-0483-x
12. Kzhyshkowska J, Yin S, Liu T, Riabov V, Mitrofanova I. Role of chitinase-like proteins in cancer. *Biol Chem.* (2016) 397:231–47. doi: 10.1515/hsz-2015-0269
13. Volck B, Price PA, Johansen JS, Sørensen O, Benfield TL, Nielsen HJ, et al. YKL-40, a mammalian member of the chitinase family, is a matrix protein of specific granules in human neutrophils. *Proc Assoc Am Phys.* (1998) 110:351–60.
14. Hu B, Trinh K, Figueira WF, Price PA. Isolation and sequence of a novel human chondrocyte protein related to mammalian members of the chitinase protein family. *J Biol Chem.* (1996) 271:19415–20. doi: 10.1074/jbc.271.32.19415
15. Kzhyshkowska J, Mamidi S, Gratchev A, Kremmer E, Schmuttermaier C, Krusell L, et al. Novel stabilin-1 interacting chitinase-like protein (SI-CLP) is up-regulated in alternatively activated macrophages and secreted via lysosomal pathway. *Blood.* (2006) 107 3221–3228. doi: 10.1182/blood-2005-07-2843
16. Jin H, Copeland N, Gilbert D, Jenkins N, Kirkpatrick R, Rosenberg M. Genetic characterization of the murine Ym1 gene and identification of a cluster of highly homologous genes. *Genomics.* (1996) 54 316–322. doi: 10.1006/geno.1998.5593
17. Schimpl M, Rush CL, Betou M, Eggleston IM, Recklies AD, Van Aalten DM. Human YKL-39 is a pseudo-chitinase with retained chitooligosaccharide-binding properties. *Biochem J.* (2012) 446:149–57. doi: 10.1042/BJ20120377
18. Ranok A, Wongsantichon J, Robinson RC, Suginta W. Structural and thermodynamic insights into chitooligosaccharide binding to human cartilage chitinase 3-like protein 2 (CHI3L2 or YKL-39). *J Biol Chem.* (2015) 290:2617–29. doi: 10.1074/jbc.M114.588905
19. Bigg HF, Wait R, Rowan AD, Cawston TE. The mammalian chitinase-like lectin, YKL-40, binds specifically to type I collagen and modulates the rate of type I collagen fibril formation. *J Biol Chem.* (2006) 281:21082–95. doi: 10.1074/jbc.M601153200
20. Fusetti F, Pijning T, Kalk KH, Bos E, Dijkstra BW. Crystal structure and carbohydrate-binding properties of the human cartilage glycoprotein-39. *J Biol Chem.* (2003)278:37753–60. doi: 10.1074/jbc.M303137200
21. Renkema GH, Boot RG, Au FL, Donker-Koopman WE, Strijland A, Muijsers AO. Chitotriosidase, a chitinase, and the 39-kDa human cartilage glycoprotein, a chitin-binding lectin, are homologues of family 18 glycosyl hydrolases secreted by human macrophages. *Eur J Biochem.* (1998) 251:504–9. doi: 10.1046/j.1432-1327.1998.2510504.x
22. Nishikawa KC, Millis AJ (2003). gp38k (CHI3L1) is a novel adhesion and migration factor for vascular cells. *Exp Cell Res.* (2003) 287:79–87. doi: 10.1016/S0014-4827(03)00069-7
23. Meng G, Zhao Y, Bai X, Liu Y, Green TJ, Luo M, et al. Structure of human stabilin-1 interacting chitinase-like protein (SI-CLP) reveals a saccharide-binding cleft with lower sugar-binding selectivity. *J Biol Chem.* (2010) 285:39898–904. doi: 10.1074/jbc.M110.130781
24. Chang N-CA, Hung S-I, Hwa K-Y, Kato I, Chen J-E, Liu C-H, et al. A macrophage protein, Ym1, transiently expressed during inflammation is a novel mammalian lectin. *J Biol Chem.* (2001) 276:17497–506. doi: 10.1074/jbc.M010417200
25. Francescone RA, Scully S, Faibish M, Taylor SL, Oh D, Moral L, et al. Role of YKL-40 in the angiogenesis, radioresistance, and progression of glioblastoma. *J Biol Chem.* (2011) 286:15332–43. doi: 10.1074/jbc.M110.212514
26. Shao R, Hamel K, Petersen L, Cao Q, Arenas RB, Bigelow C, et al. YKL-40, a secreted glycoprotein, promotes tumor angiogenesis. *Oncogene.* (2009) 28:4456–68. doi: 10.1038/onc.2009.292
27. Knorr T, Obermayr F, Bartnik E, Zien A, Aigner T. YKL-39 (chitinase 3-like protein 2), but not YKL-40 (chitinase 3-like protein 1), is up regulated in osteoarthritic chondrocytes. *Ann Rheum Dis.* (2003) 62:995–8. doi: 10.1136/ard.62.10.995
28. Steck E, Breit S, Breusch SJ, Axt M, Richter W. Enhanced expression of the human chitinase 3-like 2 gene (YKL-39) but not chitinase 3-like 1 gene (YKL-40) in osteoarthritic cartilage. *Biochem Biophys Res Commun.* (2002) 299:109–15. doi: 10.1016/S0006-291X(02)02585-8
29. Colton CA, Mott RT, Sharpe H, Xu Q, Van Nostrand WE, Vitek MP. Expression profiles for macrophage alternative activation genes in AD and in mouse models of AD. *J Neuroinflammation.* (2006) 3:27. doi: 10.1186/1742-2094-3-27
30. Hinsinger G, Galéotti N, Nabholz N, Urbach S, Rigau V, Demattei C, et al. Chitinase 3-like proteins as diagnostic and prognostic biomarkers of multiple sclerosis. *Mult Scler.* (2015) 21:1251–61. doi: 10.1177/1352458514561906
31. Møllgaard M, Degn M, Sellebjerg F, Frederiksen J, Modvig S. Cerebrospinal fluid chitinase-3-like 2 and chitotriosidase are potential prognostic biomarkers in early multiple sclerosis. *Eur J Neurol.* (2016) 23:898–905. doi: 10.1111/ene.12960
32. Sanfilippo C, Nunnari G, Calcagno A, Malaguarnera L, Blennow K, Zetterberg H, et al. The chitinases expression is related to Simian Immunodeficiency Virus Encephalitis (SIVE) and in HIV encephalitis (HIVE). *Virus Res.* (2017) 227:220–30. doi: 10.1016/j.virusres.2016.10.012
33. Liu T, Larionova I, Litviakov N, Riabov V, Zavyalova M, Tsyganov M, et al. Tumor-associated macrophages in human breast cancer produce new monocyte attracting and pro-angiogenic factor YKL-39 indicative for increased metastasis after neoadjuvant chemotherapy. *Oncoimmunology.* (2018) 7:e1436922. doi: 10.1080/2162402X.2018.1436922
34. Owhashi M, Arita H, Hayai N. Identification of a novel eosinophil chemotactic cytokine (ECF-L) as a chitinase family protein. *J Biol Chem.* (2000) 275:1279–86. doi: 10.1074/jbc.275.2.1279
35. Zhao J, Lv Z, Wang F, Wei J, Zhang Q, Li S, et al. Ym1, an eosinophilic chemotactic factor, participates in the brain inflammation induced by *Angiostrongylus cantonensis* in mice. *Parasitol Res.* (2013) 112:2689–95. doi: 10.1007/s00436-013-3436-x
36. HogenEsch H, Dunham A, Seymour R, Renninger M, Sundberg JP. Expression of chitinase-like proteins in the skin of chronic proliferative dermatitis (cpdm/cpdm) mice. *Exp Dermatol.* (2006) 15:808–14. doi: 10.1111/j.1600-0625.2006.00483.x
37. Kawada M, Seno H, Kanda K, Nakanishi Y, Akitake R, Komekado H, et al. Chitinase 3-like 1 promotes macrophage recruitment and angiogenesis in colorectal cancer. *Oncogene.* (2012) 31:3111–23. doi: 10.1038/onc.2011.498
38. Tang H, Sun Y, Shi Z, Huang H, Fang Z, Chen J, et al. YKL-40 induces IL-8 expression from bronchial epithelium via MAPK (JNK and ERK) and NF-κB pathways, causing bronchial smooth muscle proliferation and migration. *J Immunol.* (2013) 190:438–46. doi: 10.4049/jimmunol.1201827
39. Conrozier T, Carlier M, Mathieu P, Colson F, Debard A, Richard S, et al. Serum levels of YKL-40 and C reactive protein in patients with hip osteoarthritis and healthy subjects: a cross sectional study. *Ann Rheum Dis.* (2000) 59:828–31. doi: 10.1136/ard.59.10.828
40. Quail DF, Joyce JA. Microenvironmental regulation of tumor progression and metastasis. *Nat Med.* (2013) 19:1423–37. doi: 10.1038/nm.3394

41. Riabov V, Gudima A, Wang N, Mickley A, Orekhov A, Kzhyshkowska J. Role of tumor associated macrophages in tumor angiogenesis and lymphangiogenesis. *Front Physiol.* (2014) 5:75. doi: 10.3389/fphys.2014.00075
42. Lin EY, Pollard JW. Tumor-associated macrophages press the angiogenic switch in breast cancer. *Cancer Res.* (2007) 67:5064–6. doi: 10.1158/0008-5472.CAN-07-0912
43. Nishida N, Yano H, Nishida T, Kamura T, Kojiro M. Angiogenesis in cancer. *Vasc Health Risk Manag.* (2006) 2:213–9. doi: 10.2147/vhrm.2006.2.3.213
44. Casazza A, Di Conza G, Wenes M, Finisguerra V, Deschoemaeker S, Mazzone M. Tumor stroma: a complexity dictated by the hypoxic tumor microenvironment. *Oncogene.* (2014) 33:1743–54. doi: 10.1038/onc.2013.121
45. Rosen LS. VEGF-targeted therapy: therapeutic potential and recent advances. *Oncologist.* (2005) 10:382–91. doi: 10.1634/theoncologist.10-6-382
46. Chelariu-Raicu A, Coleman RL, Sood AK. Anti-angiogenesis therapy in ovarian cancer: which patient is it most likely to benefit? *Oncology*. (2019) 33:629378.
47. Hurwitz H, Fehrenbacher L, Novotny W, Cartwright T, Hainsworth J, Heim W, et al. Bevacizumab plus irinotecan, fluorouracil, and leucovorin for metastatic colorectal cancer. *N Engl J Med.* (2004) 350:2335–42. doi: 10.1056/NEJMoa032691
48. Johnson DH, Fehrenbacher L, Novotny WF, Herbst RS, Nemunaitis JJ, Jablons DM, et al. Randomized phase II trial comparing bevacizumab plus carboplatin and paclitaxel with carboplatin and paclitaxel alone in previously untreated locally advanced or metastatic non-small-cell lung cancer. *J Clin Oncol*. (2004) 22:2184–91. doi: 10.1200/JCO.2004.11.022
49. Dalton HJ, Pradeep S, McGuire M, Hailemichael Y, Ma S, Lyons Y, et al. Macrophages facilitate resistance to anti-VEGF therapy by altered VEGFR expression. *Clin Cancer Res.* (2017) 23:7034–46. doi: 10.1158/1078-0432.CCR-17-0647
50. Hughes R, Qian BZ, Rowan C, Muthana M, Keklikoglou I, Olson OC, et al. Perivascular M2 macrophages stimulate tumor relapse after chemotherapy. *Cancer Res.* (2015) 75:3479–91. doi: 10.1158/0008-5472.CAN-14-3587
51. De Palma M, Lewis CE. Macrophages limit chemotherapy. *Cancer Discov*. (2011) 1:54–67. doi: 10.1038/472303a
52. Shao R. YKL-40 acts as an angiogenic factor to promote tumor angiogenesis. *Front Physiol.* (2013) 4:122. doi: 10.3389/fphys.2013.00122
53. Shao R, Cao Q, Arenas R, Bigelow C, Bentley B, Yan W. Breast cancer expression of YKL-40 correlates with tumour grade, poor differentiation, and other cancer markers. *Br J Cancer.* (2011) 105:1203–9. doi: 10.1038/bjc.2011.347
54. Saidi A, Javerzat S, Bellahcene A, De Vos J, Bello L, Castronovo V, et al. Experimental anti-angiogenesis causes upregulation of genes associated with poor survival in glioblastoma. *Int J Cancer.* (2008) 122:2187–98. doi: 10.1002/ijc.23313
55. Kzhyshkowska J, Neyen C, Gordon S. Role of macrophage scavenger receptors in atherosclerosis. *Immunobiology.* (2012) 217:492–502. doi: 10.1016/j.imbio.2012.02.015
56. Oishi Y, Manabe I. Macrophages in age-related chronic inflammatory diseases. *NPJ Aging Mech Dis.* (2016) 2:16018. doi: 10.1038/npjamd.2016.18
57. Dehne N, Mora J, Namgaladze D, Weigert A, Brüne B. Cancer cell and macrophage cross-talk in the tumor microenvironment. *Curr Opin Pharmacol.* (2017) 35:12–19. doi: 10.1016/j.coph.2017.04.007
58. Goswami KK, Ghosh T, Ghosh S, Sarkar M, Bose A, Baral R. Tumor promoting role of anti-tumor macrophages in tumor microenvironment. *Cell Immunol.* (2017) 316:1–10. doi: 10.1016/j.cellimm.2017.04.005
59. Gisterå A, Hansson GK. The immunology of atherosclerosis. *Nat Rev Nephrol.* (2017) 13:368–80. doi: 10.1038/nrneph.2017.51
60. Rhee I. Diverse macrophages polarization in tumor microenvironment. *Arch Pharm Res.* (2016) 39:1588–96. doi: 10.1007/s12272-016-0820-y
61. Franklin RA, Li MO. Ontogeny of tumor-associated macrophages and its implication in cancer regulation. *Trends Cancer.* (2016) 2:20–34. doi: 10.1016/j.trecan.2015.11.004
62. Raggi F, Pelassa S, Pierobon D, Penco F, Gattorno M, Novelli F, et al. Regulation of human macrophage M1-M2 polarization balance by hypoxia and the triggering receptor expressed on myeloid cells-1. *Front Immunol.* (2017) 8:1097. doi: 10.3389/fimmu.2017.01097
63. Junker N, Johansen JS, Andersen CB, Kristjansen PE. Expression of YKL-40 by peritumoral macrophages in human small cell lung cancer. *Lung Cancer.* (2005) 48:223–31. doi: 10.1016/j.lungcan.2004.11.011
64. Johansen JS, Milman N, Hansen M, Garbarsch C, Price PA, Graudal N. Increased serum YKL-40 in patients with pulmonary sarcoidosis—a potential marker of disease activity? *Respir Med.* (2005) 99:396–402. doi: 10.1016/j.rmed.2004.09.016
65. Kunz L, van't Wout E, van Schadewijk A, Postma D, Kerstjens H, Sterk P, et al. Regulation of YKL-40 expression by corticosteroids: effect on pro-inflammatory macrophages *in vitro* and its modulation in COPD *in vivo*. *Respir Res.* (2015) 16:154. doi: 10.1186/s12931-015-0314-3
66. Sohn MH, Kang MJ, Matsuura H, Bhandari V, Chen NY, Lee CG, et al. The chitinase-like proteins breast regression protein-39 and YKL-40 regulate hyperoxia-induced acute lung injury. *Am J Respir Crit Care Med.* (2010) 182:918–28. doi: 10.1164/rccm.200912-1793OC
67. Di Rosa M, Malaguarnera G, De Gregorio C, Drago F, Malaguarnera L. Evaluation of CHI3L-1 and CHIT-1 expression in differentiated and polarized macrophages. *Inflammation.* (2013) 36:482–92. doi: 10.1007/s10753-012-9569-8
68. Xiao W, Meng G, Zhao Y, Yuan H, Li T, Peng Y, et al. Human secreted stabilin-1-interacting chitinase-like protein aggravates the inflammation associated with rheumatoid arthritis and is a potential macrophage inflammatory regulator in rodents. *Arthritis Rheumatol.* (2014) 66:1141–52. doi: 10.1002/art.38356
69. Keliher EJ, Reiner T, Earley S, Klubnick J, Tassa C, Lee AJ, et al. Targeting cathepsin E in pancreatic cancer by a small molecule allows *in vivo* detection. *Neoplasia.* (2013) 15:684–93. doi: 10.1593/neo.13276
70. Rehli M, Nille H-H, Ammon C, Langmann S, Schwarzfischer L, Andreesen R, et al. Transcriptional regulation of CHI3L1, a marker gene for late stages of macrophage differentiation. *J Biol Chem.* (2003) 278:44058–67. doi: 10.1074/jbc.M306792200
71. Appelqvist H, Wäster P, Kågedal K, Öllinger K. The lysosome: from waste bag to potential therapeutic target. *J Mol Cell Biol.* (2013) 5:214–26. doi: 10.1093/jmcb/mjt022
72. Piao S, Amaravadi RK. Targeting the lysosome in cancer. *Ann N Y Acad Sci.* (2016) 1371:45–54. doi: 10.1111/nyas.12953
73. Wartosch L, Bright NA, Luzio JP. Lysosomes. *Curr Biol.* (2015) 25:R315–6. doi: 10.1016/j.cub.2015.02.027
74. Schröder BA, Wrocklage C, Hasilik A, Saftig P. The proteome of lysosomes. *Proteomics.* (2010) 10:4053–76. doi: 10.1002/pmic.201000196
75. Olson OC, Joyce JA. Cysteine cathepsin proteases: regulators of cancer progression and therapeutic response. *Nat Rev Cancer.* (2015) 15:712–29. doi: 10.1038/nrc4027
76. Repnik U, Stoka V, Turk V, Turk B. Lysosomes and lysosomal cathepsins in cell death. *Biochim Biophys Acta.* (2012) 1824:22–33. doi: 10.1016/j.bbapap.2011.08.016
77. Bengsch F, Buck A, Günther S, Seiz J, Tacke M, Pfeifer D, et al. Cell type-dependent pathogenic functions of overexpressed human cathepsin B in murine breast cancer progression. *Oncogene.* (2014) 33:4474–84. doi: 10.1038/onc.2013.395
78. Renkema GH, Boot RG, Strijland A, Donker-Koopman WE, Berg M, Muijsers AO, et al. Synthesis, sorting, and processing into distinct isoforms of human macrophage chitotriosidase. *Eur J Biochem.* (1997) 244:279–85. doi: 10.1111/j.1432-1033.1997.00279.x
79. Gratchev A, Schmuttermaier C, Mamidi S, Gooi L, Goerdt S, Kzhyshkowska J. Expression of osteoarthritis marker YKL-39 is stimulated by transforming growth factor beta (TGF-beta) and IL-4 in differentiating macrophages. *Biomark Insights.* (2008) 3:39–44. doi: 10.1177/117727190800300003
80. Pickup M, Novitskiy S, Moses HL. The roles of TGF beta in the tumour microenvironment. *Nat Rev Cancer.* (2013) 13:788–99. doi: 10.1038/nrc3603
81. Derynck R, Akhurst RJ, Balmain A. TGF-β signaling in tumor suppression and cancer progression. *Nat Genet.* (2001) 29:117–29. doi: 10.1038/ng1001-117
82. Katsuno Y, Lamouille S, Derynck R. TGF-β signaling and epithelial–mesenchymal transition in cancer progression. *Curr Opin Oncol.* (2013) 25:76–84. doi: 10.1097/CCO.0b013e32835b6371

83. Cantelli G, Crosas-Molist E, Georgouli M, Sanz-Moreno V. TGFb-induced transcription in cancer. *Semin Cancer Biol.* (2017) 42:60–9. doi: 10.1016/j.semcancer.2016.08.009
84. Cintin C, Johansen J, Christensen IJ, Price P, Sørensen S, Nielsen HJ. Serum YKL-40 and colorectal cancer. *Br J Cancer.* (1999) 79:1494–9. doi: 10.1038/sj.bjc.6690238
85. Høgdall EV, Ringsholt M, Høgdall CK, Christensen IJ, Johansen JS, Kjaer SK, et al. YKL-40 tissue expression and plasma levels in patients with ovarian cancer. *BMC Cancer.* (2009) 9:8. doi: 10.1186/1471-2407-9-8
86. Hormigo A, Gu B, Karimi S, Riedel E, Panageas KS, Edgar MA, et al. YKL-40 and matrix metalloproteinase-9 as potential serum biomarkers for patients with high-grade gliomas. *Clin Cancer Res.* (2006) 12:5698–704. doi: 10.1158/1078-0432.CCR-06-0181
87. Iwamoto FM, Hottinger AF, Karimi S, Riedel E, Dantis J, Jahdi M, et al. Serum YKL-40 is a marker of prognosis and disease status in high-grade gliomas. *Neuro Oncol.* (2011) 13:1244–51. doi: 10.1093/neuonc/nor117
88. Johansen JS, Brasso K, Iversen P, Teisner B, Garnero P, Price PA, et al. Changes of biochemical markers of bone turnover and YKL-40 following hormonal treatment for metastatic prostate cancer are related to survival. *Clin Cancer Res.* (2007) 13:3244–9. doi: 10.1158/1078-0432.CCR-06-2616
89. Libreros S, Iragavarapu-Charyulu V. YKL-40/CHI3L1 drives inflammation on the road of tumor progression. *J Leukoc Biol.* (2015) 98:931–6. doi: 10.1189/jlb.3VMR0415-142R
90. Ma B, Herzog EL, Lee CG, Peng X, Lee C-M, Chen X, et al. Role of chitinase 3–like-1 and semaphorin 7a in pulmonary melanoma metastasis. *Cancer Res.* (2015) 75:487–96. doi: 10.1158/0008-5472.CAN-13-3339
91. Schmidt H, Johansen JS, Gehl J, Geertsen PF, Fode K, von der Maase H. Elevated serum level of YKL-40 is an independent prognostic factor for poor survival in patients with metastatic melanoma. *Cancer.* (2006) 106:1130–9. doi: 10.1002/cncr.21678
92. Wan G, Xiang L, Sun X, Wang X, Li H, Ge W, et al. Elevated YKL-40 expression is associated with a poor prognosis in breast cancer patients. *Oncotarget.* (2017) 8:5382–91. doi: 10.18632/oncotarget.14280
93. Ku BM, Lee YK, Ryu J, Jeong JY, Choi J, Eun KM, et al. CHI3L1 (YKL-40) is expressed in human gliomas and regulates the invasion, growth and survival of glioma cells. *Int J Cancer.* (2011) 128:1316–26. doi: 10.1002/ijc.25466
94. He CH, Lee CG, Cruz CSD, Lee C-M, Zhou Y, Ahangari F, et al. Chitinase 3-like 1 regulates cellular and tissue responses via IL-13 receptor α2. *Cell Rep.* (2013) 4:830–41. doi: 10.1016/j.celrep.2013.07.032
95. Qureshi AM, Hannigan A, Campbell D, Nixon C, Wilson JB. Chitinase-like proteins are autoantigens in a model of inflammation-promoted incipient neoplasia. *Genes Cancer*. (2011) 2:74–87. doi: 10.1177/1947601911402681
96. Morera E, Steinhäuser SS, Budkova Z, Ingthorsson S, Kricker J, Krueger A, et al. YKL-40/CHI3L1 facilitates migration and invasion in HER2 overexpressing breast epithelial progenitor cells and generates a niche for capillary-like network formation. *In Vitro Cell Dev Biol Anim.* (2019) 55:838–53. doi: 10.1007/s11626-019-00403-x
97. Faibish M, Francescone R, Bentley B, Yan W, Shao R. A YKL-40–neutralizing antibody blocks tumor angiogenesis and progression: a potential therapeutic agent in cancers. *Mol Cancer Ther.* (2011) 10:742–51. doi: 10.1158/1535-7163.MCT-10-0868
98. Salamon J, Hoffmann T, Elies E, Peldschus K, Johansen JS, Lüers G, et al. Antibody directed against human YKL-40 increases tumor volume in a human melanoma xenograft model in scid mice. *PLoS ONE.* (2014) 9:e95822. doi: 10.1371/journal.pone.0095822
99. Fujisawa T, Joshi BH, Puri RK. IL-13 regulates cancer invasion and metastasis through IL-13Rα2 via ERK/AP-1 pathway in mouse model of human ovarian cancer. *Int J Cancer.* (2012) 131:344–56. doi: 10.1002/ijc.26366
100. Voronov E, Dotan S, Krelin Y, Song X, Elkabets M, Carmi Y, et al. Unique versus redundant functions of IL-1α and IL-1β in the tumor microenvironment. *Front Immunol.* (2013) 4:177. doi: 10.3389/fimmu.2013.00177
101. Kavsan V, Shostak K, Dmitrenko V, Zozulya Y, Rozumenko V, Demotes-Mainard J. Characterization of genes with increased expression in human glioblastomas. *Tsitol Genet.* (2005) 39:37–49. doi: 10.1016/j.canlet.2004.07.001
102. Kavsan V, Dmitrenko V, Boyko O, Filonenko V, Avdeev S, Areshkov P, et al. Overexpression of YKL-39 gene in glial brain tumors. *Scholarly Res Exchange.* (2008) 2008:814849. doi: 10.3814/2008/814849
103. Rubovszky G, Horváth Z. Recent advances in the neoadjuvant treatment of breast cancer. *J Breast Cancer.* (2017) 20:119–31. doi: 10.4048/jbc.2017.20.2.119
104. Baghdadi M, Wada H, Nakanishi S, Abe H, Han N, Putra WE, et al. Chemotherapy-induced IL-34 enhances immunosuppression by tumor-associated macrophages and mediates survival of chemoresistant lung cancer cells. *J Clin Pathol.* (2012) 65:159–63. doi: 10.1158/0008-5472.CAN-16-1170
105. Harrison DJ. Molecular mechanisms of drug resistance in tumours. *J Pathol.* (1995) 175:7–12. doi: 10.1002/path.1711750103
106. Gottesman MM, Fojo T, Bates SE. Multidrug resistance in cancer: role of ATP–dependent transporters. *Nat Rev Cancer*. (2002) 2:48. doi: 10.1038/nrc706
107. Noy R, Pollard JW. Tumor-associated macrophages: from mechanisms to therapy. *Immunity.* (2014) 41:49–61. doi: 10.1016/j.immuni.2014.09.021
108. Mantovani A, Allavena P. The interaction of anticancer therapies with tumor-associated macrophages. *J Exp Med.* (2015) 212:435–45. doi: 10.1084/jem.20150295
109. Dijkgraaf EM, Heusinkveld M, Tummers B, Vogelpoel LTC, Goedemans R, Jha V, et al. Chemotherapy alters monocyte differentiation to favor generation of cancer-supporting M2 macrophages in the tumor microenvironment. *Cancer Res.* (2013) 73:2480–92. doi: 10.1158/0008-5472.CAN-12-3542
110. Larionova I, Cherdyntseva N, Liu T, Patysheva M, Rakina M, Kzhyshkowska J. Interaction of tumor-associated macrophages and cancer chemotherapy. *Oncoimmunology.* (2019) 8:1596004. doi: 10.1080/2162402X.2019.1596004
111. Boisen MK, Madsen CV, Dehlendorff C, Jakobsen A, Johansen JS, Steffensen KD. The prognostic value of plasma YKL-40 in patients with chemotherapy-resistant ovarian cancer treated with bevacizumab. *Int J Gynecol Cancer.* (2016) 26:1390–8. doi: 10.1097/IGC.0000000000000798
112. Darr C, Krafft U, Hadaschik B, Tschirdewahn S, Sevcenco S, Csizmarik A, et al. The role of YKL-40 in predicting resistance to docetaxel chemotherapy in prostate cancer. *Urol Int.* (2018) 101:65–73. doi: 10.1159/000489891
113. Xu CH, Yu LK, Hao KK. Serum YKL-40 level is associated with the chemotherapy response and prognosis of patients with small cell lung cancer. *PLoS ONE.* (2014) 9:e96384. doi: 10.1371/journal.pone.0096384
114. Dimitrakopoulos C, Vrugt B, Flury R, Schraml P, Knippschild U, Wild P, et al. Identification and validation of a biomarker signature in patients with resectable pancreatic cancer via genome-wide screening for functional genetic variants. *JAMA Surg.* (2019) 154:e190484. doi: 10.1001/jamasurg.2019.0484
115. Liu T. *Analysis of macrophage production and biological activity of chitinase-like protein YKL-39.* Thesis. University of Heidelberg. Available online at: https://archiv.ub.uni-heidelberg.de/volltextserver/23511/

Conflict of Interest: The authors declare that the research was conducted in the absence of any commercial or financial relationships that could be construed as a potential conflict of interest.

frontiers in Immunology

REVIEW
published: 05 March 2020
doi: 10.3389/fimmu.2020.00346

Semaphorins in Angiogenesis and Autoimmune Diseases: Therapeutic Targets?

Vijaya Iragavarapu-Charyulu, Ewa Wojcikiewicz and Alexandra Urdaneta*

Department of Biomedical Sciences, Florida Atlantic University, Boca Raton, FL, United States

The axonal guidance molecules, semaphorins, have been described to function both physiologically and pathologically outside of the nervous system. In this review, we focus on the vertebrate semaphorins found in classes 3 through 7 and their roles in vascular development and autoimmune diseases. Recent studies indicate that while some of these vertebrate semaphorins promote angiogenesis, others have an angiostatic function. Since some semaphorins are also expressed by different immune cells and are known to modulate immune responses, they have been implicated in autoimmune disorders such as multiple sclerosis, rheumatoid arthritis, systemic lupus erythematosus and systemic sclerosis. We conclude this review by addressing strategies targeting semaphorins as potential therapeutic agents for angiogenesis and autoimmune diseases.

Keywords: semaphorin, neuropilins, plexins, angiogenesis, angiostatic, autoimmunity, MOG, targeted therapy

OPEN ACCESS

Edited by:
Kutty Selva Nandakumar, Southern Medical University, China

Reviewed by:
Luca Tamagnone, Institute for Cancer Research and Treatment (IRCC), Italy
Yves Lepelletier, Université Paris Descartes, France

****Correspondence:***
Vijaya Iragavarapu-Charyulu
iragavar@health.fau.edu

Specialty section:
This article was submitted to Autoimmune and Autoinflammatory Disorders, a section of the journal Frontiers in Immunology

Received: *28 May 2019*
Accepted: *12 February 2020*
Published: *05 March 2020*

Citation:
Iragavarapu-Charyulu V, Wojcikiewicz E and Urdaneta A (2020) Semaphorins in Angiogenesis and Autoimmune Diseases: Therapeutic Targets? Front. Immunol. 11:346. doi: 10.3389/fimmu.2020.00346

INTRODUCTION

Semaphorins consist of a large family of conserved proteins originally described as axon guidance molecules during the development of the nervous system. These molecules are now known to be expressed in other adult tissues and function outside of the nervous system (1). Semaphorins since have been discovered to have pleiotropic effects in both health and disease. Semaphorins and their receptors have widespread functional impact physiologically and pathologically as they participate in immune regulation, extracellular matrix remodeling, organogenesis, and angiogenesis (2–4). These molecules therefore play crucial roles in pathophysiology of diseases such as cancer, systemic lupus erythematosus, rheumatoid arthritis, psoriasis, arthritis, proliferative retinopathy, and atherosclerosis among others (5–10). In this review, we discuss semaphorin's structure, receptors, signaling and downstream effects on pathophysiology. We then highlight the roles of semaphorins with respect to angiogenesis and autoimmune disease. We conclude with an emphasis on the role of semaphorins in angiogenesis and autoimmune disease and explore the possibility of targeting semaphorins and their receptors to ameliorate angiogenesis and regulate immune functions.

STRUCTURE, RECEPTORS, AND SIGNALING

The semaphorin family is divided into eight classes, with invertebrate semaphorins belonging to classes 1 and 2, the vertebrate semaphorins being found in classes 3–7, and the viral semaphorins in class 8 (**Figure 1**). The Sema domain of semaphorins contains approximately

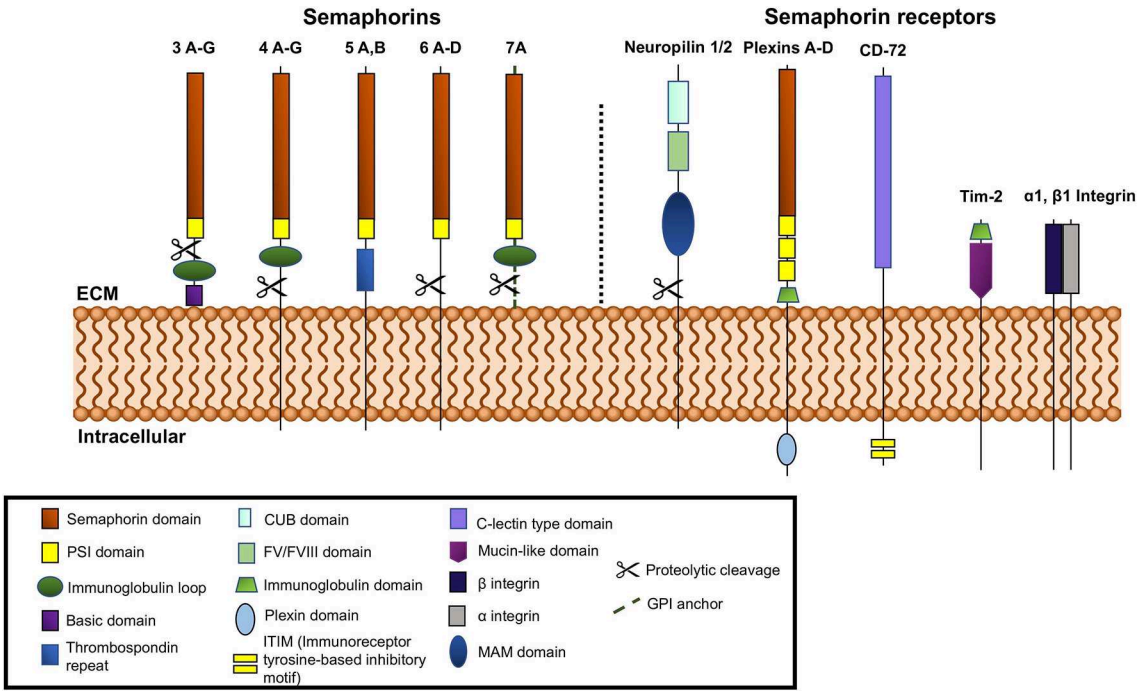

FIGURE 1 | Schematic representation of vertebrate semaphorins and semaphorin receptors. Class 3 is secreted, Classes 4-6 are transmembrane and Class 7 is GPI anchored. Cleavable semaphorins are Sema3, 4, 6, and 7. Receptors for semaphorins are shown on the right side of the figure, neuropilins, plexins, Tim-2, and α1β1 integrin.

500 amino acids (1). At the carboxy terminus of the Sema domain, all semaphorins also contain a Plexin-semaphorin-integrin (PSI) domain (11). Variations in the C-terminal motifs joining the PSI domain are the key differentiating factor among semaphorins (12). The C-terminus of vertebrate Sema3, 4, and 7 contains an immunoglobulin loop. Sema3 (A-G) contains a basic domain and Sema5 (A-C) contains thrombospondin repeats on their C termini, respectively. Class 3 semaphorins are secreted, classes 4, 5, and 6 are membrane bound and class 7 is the only member that is GPI-anchored (13) (**Figure 1**). Semaphorins 3, 4, 6, and 7A are susceptible to cleavage by matrix metalloproteinases and adamlysin family proteases (14, 15).

Neuropilins and Plexins serve as semaphorin receptors and are the means through which semaphorins can participate in signal transduction (16–19). Both are transmembrane proteins, with extracellular domains capable of interaction with the semaphorins which can dimerize to mediate their function. Most semaphorins can interact with Plexins directly, while almost all of the class 3 semaphorins (except 3E) bind neuropilins, which form complexes with type A Plexins or Plexin D1. The plexins are required to transduce the signals (13, 16, 20, 21). There are two known neuropilins, -1 and -2 (16, 17) (**Figure 1**). Both have short intracellular domains. Their interaction with Plexins, which possess a longer intracellular segment, facilitates their involvement in the transduction of pro-angiogenic signals. The extracellular segment of neuropilins is also the site of binding for VEGF, HGF (hepatocyte growth factor), FGF-2, PDGF-B, TGF-β and other ligands (22–24). The Plexins can more robustly participate in signal transduction via their longer intracellular GTP-ase activating domain (GAP domain). The intracellular GAP domain interacts with GTP-ases directly. Plexins are subdivided into classes A, B, C, and D (**Figure 1**) and interact directly with semaphorins from classes 4, 5, 6, and 7 and Sema3E (25, 26). Plexins A (1–4) and D interact with neuropilins 1 and 2 (25, 26).

Semaphorins are a family of proteins that were initially established as repellent cues in axonal guidance and synapse formation during embryogenesis. It is now known that they not only exert a repulsive effect in axonal guidance but, they can also be attractive axonal cues. Sema3A has repellent effects on neurons while Sema3C is known as an attractant. The other members in this family, Sema3D, Sema3E, and Sema3F have both repellent and chemoattractant effects on axons (27, 28). Semaphorin 4A has been shown to function as a chemoattractant, likely working in concert with other neurotrophic factors to promote neurite outgrowth (29). Sema5A, on the other hand, has been shown to have both attractive and repulsive functions during development (30, 31). Of class semaphorins, Sema6A and Sema6B were shown to have chemorepulsive activity via interaction with Plexin A4 in various models of development and angiogenesis (32–34). Although Sema7A promotes axon growth, chemotropic effect was not evident in a model of rat olfactory bulb explant (35). In addition to their role in axonal guidance, semaphorins also play a role in the periphery in regulating angiogenesis and immune responses.

ROLE OF SEMAPHORINS IN ANGIOGENESIS

Semaphorins play a significant role in vascular development through the promotion or inhibition of angiogenesis. A balance between pro- and anti-angiogenic signals determine the progression of new blood vessel sprouting. Similar to their function in axonal guidance, semaphorins guide endothelial cells toward tube formation for angiogenesis. Pro-angiogenic semaphorins include Sema3C, Sema4A, Sema4D, Sema6D, and Sema7A, while angiostatic semaphorins include Sema3A, Sema3B, Sema3D, Sema3E, and Sema3F (**Table 1**). Although Sema3C and Sema4A have been shown to have pro-angiogenic activity, they also were reported to function as anti-angiogenic molecules (13, 53) (**Table 1**).

Class 3 semaphorins are for the most part anti-angiogenic. Class 3 semaphorins exert angiogenic effects through interactions with co-receptors neuropilin-1, -2 (NRP-1,−2) and vascular endothelial growth factor (VEGF) receptor family. Semaphorins 3A, 3B, 3D, 3E, and 3F are exclusively anti-angiogenic (**Table 1**). The anti-angiogenic activity of Sema3A was demonstrated using cultured rat aortic rings. Sema3A inhibited capillary sprouting and it was further shown to inhibit endothelial cell migration (36). Using an oxygen-induced retinopathy mouse model, Yu et al. showed that injection of the intravitreous region with Sema3A reduced neovascularized areas and decreased abnormal vessel growth (37). Acevedo et al. showed that Sema3A interferes with VEGF-induced angiogenesis (38). Recently, in a mouse model of bronchial asthma by Adi et al. have shown that treatment of mice with Sema3A reduced inflammatory cell infiltration in bronchioles and angiogenesis was significantly decreased compared to the untreated controls (39). Sema3A and Sema3F are characterized as anti-angiogenic by competing with VEGF in binding to endothelial cell expressed neuropilins (NRP-1/2), the co-receptors for VEGF family (40). Further, Guttmann-Raviv et al. found that co-expression of Sema3A and Sema3F repel endothelial cells more potently than either one of the semaphorins alone (40). Sema3B also was found to have anti-angiogenic activity via NRP-1/-2 which resulted in the repelling of endothelial cells, induction of apoptosis, and inhibition of tube formation (41). Rolny et al. determined the role of Sema3B in tumor angiogenesis and found a reduction in angiogenesis in mice injected with Sema3B transduced tumor cells (42). Similarly, Sema3D/NRP-1 activity was found to inhibit cell motility and tube formation in endothelial cells (47). In contrast, Sema3E was determined to be anti-angiogenic via Plexin-D1, and not NRP signaling on endothelial cells *in vitro* and *in vivo* (63). Sakurai et al. reported that Sema3E's anti-angiogenic activity can be attributed to its inactivation of R-Ras and stimulation of Arf6 factors which affect integrin activity and inhibit endothelial cell adhesion (63). Other studies have also elucidated Sema3E/Plexin-D1's activity to work as a regulatory mechanism for VEGF-induced angiogenesis by modulating the ratio of endothelial tip and stalk cells (24). Studies with Sema $3E^{-/-}$ mice revealed the important role that avascular zones generated by Sema3E play in guiding cardiac vessel development (48). Further, in a rat model of ischemic stroke, it was shown that Sema3E/Plexin-D1 signaling inhibited angiogenesis through regulation of endothelial dynamic delta-like 4 molecule (64).

Within class 3 semaphorins, Sema3C is one of the exceptions due to its bifunctional activity as both a pro-angiogenic and anti-angiogenic factor (13, 43, 45, 65). *In vitro* studies showed Sema3C to induce endothelial cell proliferation, adhesion and directional migration (43). However, other studies report Sema3C to be significantly anti-angiogenic (13, 45). Pathologic angiogenesis was shown to be inhibited by Sema3C in an oxygen-induced retinopathy model (45). Further, these authors showed that Sema3C inhibits endothelial tube formation when Human Umbelical Vein Cells were cultured with Sema3C conditioned medium. The anti-angiogenic activity of Sema3C was shown by overexpressing Sema3C in U87 glioblastoma cells and assessing formation of neovasculature in chick chorioallantoic membranes (CAM). Sema3C overexpressing U87 cells did not induce new vessels while control U87 cells had extensive vessels on CAMs (66). Therefore, the effects of this semaphorin may be environment dependent and are ultimately controversial. Sema3F contrary to majority of class 3 semaphorins, was shown to promote extraembryonic angiogenesis via inhibition of Myc-regulated thrombospondin 1 in yolk sac epithelial cells (50). In contrast, other studies showed that Sema3F is expressed in the avascular outer region of retina and that it exerts anti-angiogenic effects on the retinal and choroidal capillaries (51).

Within class 4 semaphorins, Sema4D was found to have pro-angiogenic effects. Both soluble and membrane-bound forms of Sema4D have been described as pro-angiogenic by signaling through endothelial receptors, Plexin-B1 and Plexin-B2. Interaction of Sema4D with Plexin-B1 stabilizes vasculature. Sema4D has been shown to have potent angiogenic effects both *in vitro* and *in vivo* by inducing endothelial cell chemotaxis, tube formation, cytoskeletal rearrangements, and vessel growth (55, 56). Increased levels of Sema4D have been correlated with poor prognosis in studies of leukemia and mammary carcinoma (67–69). Interestingly, this semaphorin has been shown to play a role in vasculogenic mimicry in a non-small cell lung cancer model. Xia et al. found that the interaction of Sema4D with PlexinB1 promoted vasculogenic mimicry while inhibition of Sema4D decreased vasculature (70). In contrast to Sema4D, Sema4A was found to have dual activity as both a pro- and anti-angiogenic factor. The pro-angiogenic effect of Sema4A in the context of tumor is indirectly mediated by signaling through Plexin-D1-expressing macrophages, which induce VEGF-A expression and thereby enhance tumor vasculature (52). However, depending on the environment, Sema4A inhibits angiogenesis using the same receptor, Plexin-D1 (53). Therefore, the role of Sema4A in tumors is still controversial.

The only member in class 5 semaphorins reported to have angiogenic activity is Sema5A. This semaphorin has been shown to be necessary for normal cranial vasculature development and be a regulator of angiogenesis by promoting endothelial cell migration and proliferation, while also reducing apoptosis (57, 58).

TABLE 1 | The role of semaphorins in mediating angiogenesis and autoimmune diseases.

Semaphorin	Angiogenesis	References
Semaphorin 3A	↓	(36–40)
Semaphorin 3B	↓	(41, 42)
Semaphorin 3C	↓↑	↑(43, 44)
		↓(13, 45, 46)
Semaphorin 3D	↓	(47)
Semaphorin 3E	↓	(48, 49)
Semaphorin 3F	↓↑	↓(40, 50)
		↑(51)
Semaphorin 4A	↓↑	↑(52)
		↓(53)
		↓↑(54)
Semaphorin 4D	↑	(55, 56)
Semaphorin 5A	↑	(57, 58)
Semaphorin 6D	↑	(59)
Semaphorin 7A	↑	(60–62)

↓*Anti-angiogenic;* ↑*Pro-angiogenic.*

Among class 6 semaphorins, Sema6D acts by binding to a receptor complex composed of PlexinA1 and either Off Track (OTK) or VEGFR2. Binding of Sema6D to these receptor complexes results in varying effects during cardiac development including, endothelial cell repulsion or attraction, respectively (2). In models of gastric cancer, signaling due to Sema6D and Plexin-A1/VEGFR2 interaction results in effects similar to VEGF binding alone. In addition, Sema6D/Plexin-A1 expression is positively correlated with the expression of VEGFR2, therefore contributing to its angiogenic and tumorigenic properties (59). Poor prognosis of gastric cancer has been correlated with Sema6D expression and increased angiogenesis (59) (**Table 1**).

Class 7 semaphorins have also been found to have pro-angiogenic effects (**Table 1**). In particular, Sema7A was determined to mediate angiogenesis through signaling via Plexin-C1 and β1 integrins. Using a corneal neovascularization model, Ghanem et al. showed that Sema7A is expressed in vascularized corneas and that basic fibroblastic growth factor (bFGF) enhances the expression of Sema7A (60). The pro-angiogenic function of Sema7A in promoting intraplaque neovascularization was found to be mediated through β1 integrin and activation of VEGFA/VEGFR2 (61). Tumor angiogenesis is regulated by stromal cells such as macrophages, neutrophils and cancer associated fibroblasts (71). Tumor angiogenesis is affected by infiltration of leukocytes, e.g., tumor associated macrophages (TAMs) (72). Due to its chemotactic effects, Sema7A could attract TAMs which could then regulate angiogenesis in the tumor microenvironment (73). Garcia-Areas et al. delineated the angiogenic role of Sema7A in promoting tumor growth. In this study, it was shown that co-culture of Sema7A with macrophages induces the production of angiogenic chemokines, CCL2, CXCL2/MIP2. Further, implantation of Sema7A gene-silenced mammary tumor cells resulted in decreased *in vivo* tumor angiogenesis compared to the wild type tumors (62). Thus, in the context of tumor, Sema7A could promote angiogenesis in multiple ways. Further, Black et al. revealed a novel role for Sema7A in promoting lymphangiogenesis in breast cancer and reported that loss of Sema7A reduces both tumor cell invasion and activation of β1-integrin receptor (74).

ROLE OF SEMAPHORINS IN AUTOIMMUNE DISEASE

Semaphorins through interaction with their receptors, in addition to playing a role in angiogenesis, regulate immune homeostasis, and tissue inflammation. Neuropilins are important for the initiation of the primary immune response as NRP-1 has been shown to mediate contact between DCs and T cells in the immunologic synapse (75). Autoimmune disorders are characterized by dysregulated immune responses associated with decreased T regulatory cells and overactive responses by B and T cells against self-molecules. T regulatory development is guided by the transcription factor, Foxp3 (76). In a mouse model, it was shown that T_{reg} cells express NRP-1. However, it is important to note NRP-1 is not a marker of human Foxp3 T_{reg} cells (77). The interaction of NRP-1 with immune cell-expressed Sema4A in mice further potentiates T_{reg} cell function (78). Further, peripheral tolerance is also maintained by dendritic cells that could prevent activation of self-reactive cells which can then lead to inhibition of autoimmunity. The receptors expressed at the immunological synapse between dendritic cells (DCs) and T cells can therefore affect the outcome between development of tolerance or autoimmune response (79).

Semaphorins, Sema3A, Sema3E, Sema4A, Sema4D, Sema5A, Sema6D, and Sema7A may be considered as "immune semaphorins" since they are involved in physiological and pathological immune responses (80). Autoimmune diseases, such as systemic lupus erythematosus (SLE), rheumatoid arthritis (RA), multiple sclerosis (MS), and systemic sclerosis or scleroderma (SSc), are characterized by chronic inflammation and subsequent tissue damage resulting from cellular and humoral immune responses to self-antigens. Inflammation affects the expression of semaphorins and their receptors and recent studies show that several members of the semaphorin family are aberrantly expressed in autoimmune disorders (**Table 2**) (89, 90). In this review, we focus on immune semaphorins as one of the mediators of autoimmune diseases.

The secreted class 3 semaphorins modulate immune responses by binding and signaling through neuropilins and their association with Plexins. The members of the semaphorin 3 family that function in pathogenesis of autoimmune diseases are Sema3A, Sema3C, Sema3E, and Sema3F. Sema3A is a potent immunoregulatory molecule and has been shown to suppress the over-activity of T and B lymphocytes (91–93). Activation of naïve T cells requires an immunological synapse with dendritic

TABLE 2 | The role of semaphorins in mediating autoimmune diseases.

Semaphorin	Autoimmune disease	References
Semaphorin 3A	Rheumatoid Arthritis (RA), asthma, systemic sclerosis (SSc), Multiple Sclerosis (MS), systemic lupus erythematosus (SLE)	(81, 82)
Semaphorin 3C	RA	(83)
Semaphorin 3E	SSc	(49)
Semaphorin 3F	MS	(84)
Semaphorin 4A	Experimental autoimmune encephalomyelitis (EAE), MS, RA	(85)
Semaphorin 4D	MS/EAE, RA	(85–87)
Semaphorin 5A	RA	(88)
Semaphorin 6D	EAE	(21)
Semaphorin 7A	RA, MS/EAE, SSc, COPD	(85)

cells in the secondary lymphoid organs. The immunosuppressive role of Sema3A on T cell proliferation was first described by Lepelletier et al. (94). NRP-1, the Sema3A receptor expressed by activated T cells and DCs., was found to play an important role in forming DC-T cell synapse (75). Lepelletier et al. found that the high levels of Sema3A produced in the later stage of DC-T cells co-cultures inhibited T cell proliferation. Thus, the induced Sema3A expression by both DCs and T cells during the latter part of the immune response could be regulating this response (94). Either neutralization by blocking antibodies or by an antagonist peptide of Sema3A increased T cell proliferation (94). These authors have shown that the immunomodulatory function of Sema3A is mediated by actin cytoskeleton reorganization that has downstream effects on signal transduction (94) (**Figure 2B**). Solomon et al. have shown that NRP-1 attenuates autoreactivity of myelin oligodendrocyte glycoprotein (MOG)-induced experimental autoimmune encephalitis (EAE) and that lack of NRP-1 aggravates the disease (95). Furthermore, Lepellier et al. have also shown that both Sema3A and Galectin-1 expressed by mesenchymal stem cells inhibit T cell proliferation through NRP-1 binding (96).

Other studies have shown that Sema3A downregulates T cell activation and modulates immune responses through activation of T regulatory cells (81). Further, co-culture of B regulatory cells with Sema3A upregulated expression of CD72 and enhanced the production of immunoregulatory cytokines, IL-10 and TGF-β (97) (**Figure 2B**). More significantly, culturing of Sema3A with cytosine-phosphodiester-guanine oligodeoxynucleotides (CpG-ODN)-stimulated B cells from SLE patients resulted in decreased TLR-9 expression that could then have an effect on cytokine production profile (98). Several studies have linked pathogenesis of autoimmune diseases to lower Sema3A levels and serum levels were reported to inversely correlate with disease activity of SLE, RA and SSc (81, 97–99) (**Table 2**). Catalano reported downregulation of Sema3A in T cells from RA patients (91). Further, transient ectopic expression of Sema3A inhibited clinical manifestation of collagen induced arthritis (91). Rezaeepoor et al. found that serum levels of Sema3A and its expression in peripheral blood mononuclear cells were significantly decreased in MS patients compared to normal subjects (100). In contrast, Williams et al. showed an increase in expression of Sema3A at the inflammatory regions from brains of human patients (84). It is possible that Sema3A is involved in the regeneration of oligodendrocytes, and deregulation of Sema3A could impair recruitment of oligodendrocyte precursors preventing repair. T helper cell differentiation and transmigration through the blood brain barrier are also detrimental in mediating pathogenesis of MS. Lack of Sema3A or its receptors resulted in impaired T cell priming and studies show that inhibiting immune cell migration prevents MS relapse (85). These studies indicate that Sema3A downregulates autoimmune disease by suppressing both B and T cell activity (93). The role of Sema3A in SSc is unclear, while some studies have shown reduced expression of Sema3A in serum and in regulatory T cells, others did not detect any differences in expression levels between SSc patients and normal individuals (81, 82).

Another member of class 3 semaphorins, Sema3C, has been implicated in RA (**Table 2**). Miller et al. showed that synovial tissue samples from RA patients were positive for Sema3C and synovial macrophages and fibroblasts were found to express Sema3C by immunofluorescence (83). In contrast to decreased Sema3A levels in SSc, elevated levels of Sema3E were found in both serum and skin from SSc patients (49) (**Table 2**). Impaired angiogenic response following tissue ischemia and hypoxia is an important feature of SSc (101). Thus, the anti-angiogenic effect of the Sema3E and Plexin-D1 interaction results in the dysregulation of vascular tone control and may contribute to pathogenesis of SSc. The last member of the semaphorin 3 family implicated in autoimmunity is Sema3F. The transcripts of Sema3F were upregulated in the brains of MS patients and in experimental models of demyelination (84, 102). Increased Sema3F expression was associated with glial cell infiltrates in the inflammatory lesions (84). These authors suggested Sema3F expression influences oligodendrocyte precursor cell recruitment that could promote re-myelination.

Class 4 semaphorins also play a role in autoimmune diseases (**Table 2**). The effects of Sema4 members are mediated by binding to class B Plexins, Tim-2, CD72, NRP-1, and NRP-2 among others (4, 103–106) (**Figure 1**). Additionally, Sema4A and Sema4D may be cleaved producing soluble forms (21). Both of these semaphorins have been associated with pathology of RA. Levels of Sema4A and Sema4D are increased in serum and synovial fluid of RA patients (87, 107). These elevated levels have been positively correlated with serum levels of inflammatory cytokines, TNF-α and IL-6 (107). Sema4A is expressed in activated T cells and DCs and plays a critical role in the immune system as it is involved in antigen-specific T helper cell responses (108, 109). Pathogenesis of MS is mediated in part by dysregulated helper T cells. Since Sema4A plays a role in T helper cell differentiation, it has been associated with pathogenesis of MS. Further, the use of anti-Sema4A (anti-CD100) monoclonal antibodies significantly suppressed the development of EAE (108). Others have shown that mice lacking Sema4A have diminished TH1 responses; this suggests that these mice may be less prone to EAE, which is mediated by TH1 cells (109). Another member of class 4 semaphorins which is

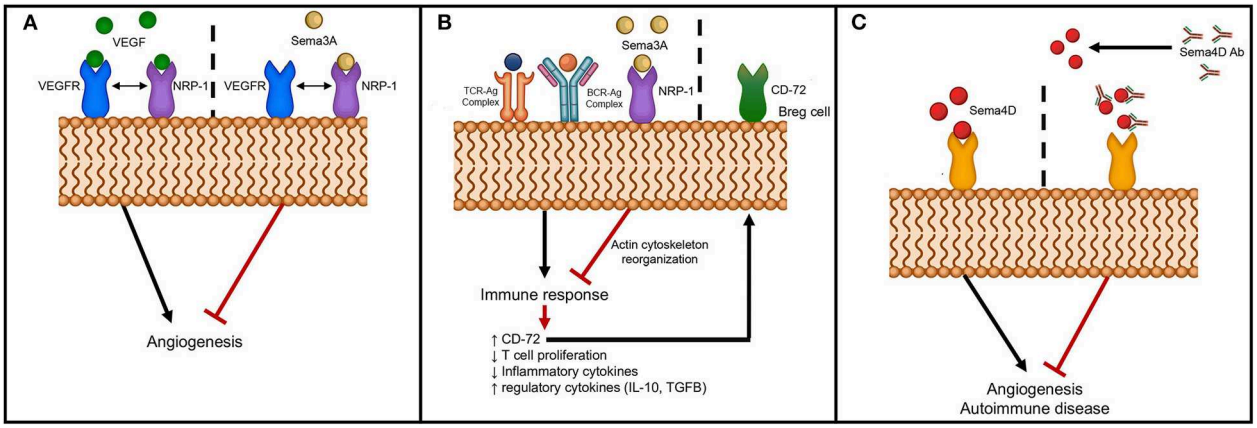

FIGURE 2 | Schematic of semaphorin interaction with receptors to modulate angiogenesis and autoimmunity. **(A)** Sema3A interferes with angiogenesis through binding to NRP-1, the co-receptor for VEGFR; **(B)** Sema3A dampens immune response through binding to NRP-1 with downstream effects on actin cytoskeletal reorganization and upregulation of CD72 on B regulatory cells; and **(C)** Inhibition of angiogenesis and autoimmunity by neutralizing anti-Sema4D antibody.

implicated in autoimmune disease is Sema4D. While Sema4D is expressed at low levels in B cells, it is expressed at higher levels in T cells. The interaction of T cell expressed Sema4D with CD72 on DCs augments T cell activation (110, 111) (**Table 2**). By binding to Plexin B1 and CD72, Sema4D promotes activation of B cells to induce antibody production and antigen specific T cells (86, 110, 112). Okuno et al. demonstrated attenuation of MOG-specific EAE development by adoptive transfer of MOG-specific T cells into Plexin-B1 deficient mice, which indicates the role of the Sema4D-Plexin B1 interaction in pathogenesis of EAE (88).

Among class 5 semaphorins, Sema5A is the only member thus far that has been associated with autoimmune disease (**Table 2**). High levels of secreted Sema5A were found in circulation of patients with RA (113). Further, treatment of primary T cells and NK cells with soluble form of recombinant Sema5A resulted in increased proliferation and secretion of proinflammatory TH1 and TH17 cytokines (113).

A class 6 semaphorin, Sema6D, is expressed in lymphoid populations including T, B and NK cells. O'Connor et al. studied the regulation of T cells by Sema6D, the stimulation of which resulted in enhanced Sema6D expression (114). Sema6D interacts with Plexin A1 and TREM-1/DAP12 complex to activate T cells and generate antigen specific T cells (85). In mice lacking Plexin A1, production of antigen-specific T cells is defective. Therefore, these mice are less prone to developing EAE (21). These studies suggest a potential role for Sema6D in the development of MS.

Semaphorin 7A, an immune semaphorin, plays an important role in regulating innate immune cells. In the immune system, Sema7A is expressed by activated T lymphocytes and stimulates not only monocytes, but also macrophages to produce proinflammatory cytokines. Sema7A was found to induce the production of proinflammatory cytokines through monocytes (73) and activated T-cells (4) (**Figure 1**). By binding to α1β1 integrin in both monocytes (115) and T cells, Sema7A activates the MAP kinase pathway (43, 115). This finding departs from the notion that semaphorins signal only through Plexins and neuropilins, the traditional semaphorin receptors. As a GPI-anchored protein, Sema7A is recruited to lipid rafts that accumulate at the immunological synapse between T cells and macrophages. Direct immunization of Sema7A-deficient mice with MOG peptide and adoptive transfer of antigen-specific Sema7A-deficient T cells do not induce T-cell-mediated immune responses (115). Sema7A-knockout mice resist the development of inflammation after hapten-induced contact hypersensitivity (85). In human studies, Sema7A has been shown to be involved in chronic inflammatory diseases like chronic obstructive pulmonary disease (COPD) (116) and RA (117) (**Table 2**).

In addition to its role in the immune response, Sema7A, the only GPI-anchored semaphorin, functions as a chemoattractant and stimulates neuronal migration. Other semaphorins such as Sema4D (118), Sema4C (119), and Sema6A (120) have also been shown to promote neuronal migration. More importantly, Sema7A promotes dendricity not only in axons (35), but also in melanocytes (121), osteoclasts (122), activated T-cells (4), and monocytes (73). Expression of Sema7A has also been associated with fibrosis, inflammation and immune modulation, and is shown to play a role in RA, MS and SSc (123–125) (**Table 2**).

Sema7A is cleaved off the membrane by ADAM-17 (15). In patients with RA, the elevated levels of soluble Sema7A in both serum and synovial fluid have been correlated with disease severity (99, 125). Xie et al. showed that soluble Sema7A activates TH1 cells resulting in increased production of the inflammatory cytokines IL-6 and IL-17 that could contribute to pathogenesis of RA (125). Costa et al. studied the expression of Sema7A in lesions of MS patients and correlated the levels to the severity of the inflammation in the lesions (126). Using an EAE mouse model, Gutierrez-Franco et al. elucidated the role of Sema7A in MS by comparing demyelination or cell death in Sema7A deficient mice with wild type mice. Mice deficient in Sema7A had impaired inflammatory cellular infiltrates into the central

nervous system and reduced demyelination compared to wild type littermates (124). Further, decreased circulating levels of Sema7A have been associated with patients with SLE compared to healthy controls (99).

Sema7A is also an important regulator of tissue remodeling by inducing fibrosis (116, 127). A pulmonary fibrosis study showed that expression of Sema7A and its receptors, Plexin C1 and α1β1 integrins, are induced by TGF-β1 contributing to TGF-β1-derived fibrosis and tissue remodeling mediated by the PI3K/AKT pathway (116). Similarly, recent studies found Sema7A in astrocytes and, accumulation of Sema7A in fibrotic tissue following spinal cord injury via activation the PI3K/AKT pathway (127). Sema7A knockout mice crossed with TGF-β1 overexpressing transgenic mice exhibited decreased severity in lung fibrosis compared to TGF-β1 overexpressing transgenic control mice (123). Collagen-producing fibrocytes and B cells expressing Sema7A contribute to pulmonary fibrosis and thus could lead to SSc (123).

TARGETING SEMAPHORINS TO CONTROL ANGIOGENESIS AND AUTOIMMUNE DISEASES

Numerous studies have implicated semaphorins as therapeutic targets for angiogenesis and autoimmune diseases. However, the strategies depend on various factors. For example, semaphorins can either promote or inhibit angiogenesis depending on the receptor they engage with, whether it is a transmembrane or a secreted molecule, and which signaling pathways are activated. Further, semaphorin signaling is modulated by the receptor and co-receptor complex. Thus, different combinations of receptor complexes can affect signaling pathways to result in altered cytokine production, cell proliferation and migration and, ultimately, causing either angiogenesis or angiostasis. Similarly, dysregulated immune responses contributing to autoimmune disorders are also affected by transmembrane *vs.* secreted semaphorins, the receptors engaged and the signaling pathways activated. All of these factors must be considered when designing therapeutic strategies. So, what are some of the possible strategies to control angiogenesis and/or autoimmune diseases mediated by semaphorins? Some strategies include the use of soluble semaphorins, small molecules or blocking antibodies to inhibit signaling, and antagonist peptides to inhibit sema-receptor complexes. Addressed in this review are soluble semaphorins and antibodies to ameliorate angiogenesis and autoimmune disease.

Studies show that Class 3 semaphorins have anti-angiogenic activity (128–130). Sema3A, -C, and E have all been shown to be anti-angiogenic. Thus, class 3 semaphorins have been used as "physiological vascular normalizing agents" for anti-cancer therapy and thereby, aid in enhancing the efficacy and overcoming acquired resistance to anti-angiogenic therapies (130). *In vitro* studies show that migration of endothelial cells cultured in the presence of angiogenic inducers is inhibited by Sema3A and Sema3F (38, 129, 131). In mouse models of cancer, systemic delivery of Sema3A impaired angiogenesis and metastasis (128). A possible mechanism by which Sema3A inhibits angiogenesis is by competing for neuropilin, a co-receptor for VEGF (**Figure 2A**). Anti-angiogenic activity of Sema3E is mediated through Plexin D1 to regulate endothelial cells and development of vasculature (132). Sema3E-plexin D1 interaction inhibits angiogenesis by suppressing the VEGF signaling pathway (133). It may be postulated that semphorins such as Sema3A or Sema3E can be used as anti-angiogenic agents to block the pro-angiogenic activity of semaphorins such as Sema4A or Sema4D. Using an oxygen-induced retinopathy model, Yang et al. found that local administration of Sema3C inhibits pathological angiogenesis (45). Further, both tumor angiogenesis and lymphangiogenesis were inhibited by the stabilized form of Sema3C (65). In a glioblastoma model, ectopic expression of Sema3D or Sema3E reduced tumor growth (134). Using a RipTag2 pancreatic tumor model, Tamagnone et al. showed inhibition of tumor angiogenesis by administering Sema3E via an Alzet pump delivery system (135). These studies indicate that semaphorins may be used as therapeutic agents to regulate angiogenesis. However, a potential problem with the use of semaphorins as treatment agents for angiogenesis are the possible side effects, e.g., those caused by suppressing the VEGF pathway by Sema3E/Plexin D1.

In terms of its possible use in treating autoimmune diseases, Sema3A is a viable candidate as it has been shown to have immunoregulatory activities on both innate and adaptive immunity (136). Treatment with Sema3A and subsequent binding to NRP-1 suppresses the immune response and also enhances B regulatory cells by upregulating CD72 (137) (**Figure 2B**). In a mouse model of RA, overexpression of Sema3A partially attenuated disease progression (91). Further, treatment of mice with Sema3A was beneficial in that it reduced lupus nephritis (136). Behar et al. showed that increased Sema3A expression on B regulatory cells and that addition of Sema3A to activated B cells resulted in downregulation of TLR-9 expression (136). Sema3A could therefore be added to the arsenal of treatment options for MS, SLE and other autoimmune disorders.

Antibodies provide an attractive treatment option to directly target specific molecules to block the action of semaphorins and thus, reduce angiogenesis or suppress autoimmune diseases. However, there are difficulties in targeting semaphorins due to: (1) the conserved Sema domain in semaphorins and Plexins; (2) redundancy in semaphorins; and (3) receptors that bind to molecules other than semaphorins. Despite these difficulties, antibodies have been designed and manufactured providing positive results. Semaphorins interact with their receptors, neuropilins, and Plexins, to mediate the downstream effects. Studies have shown that targeting neuropilins, Plexins, or semaphorins with specific antibodies results in decreased angiogenesis. Semaphorin 4D blocking antibody was used to assess the level of inhibition of angiogenesis *in vitro* and *in vivo*. Reduced vessel counts were observed in mice that received anti-sema4D antibodies indicating reduced angiogenesis (56) (**Figure 2C**). Kong et al. using anti-NRP-1 peptide in both *in vitro* and *in vivo* studies found suppression of VEGF-induced angiogenesis and experimental arthritis (138).

Blocking of semaphorins and preventing interaction with their receptors provides a unique strategy to inhibit autoimmune

diseases. It is known that CD4 T cells proliferate and differentiate into TH1 or TH2 cells when presented with an antigen by DCs. TH1 cells not only promote cell-mediated immunity but are involved in development of autoimmune disease. NRP-1 is one of the molecules involved in stabilization of DC-T cell interaction (75). Incubation of either T cells or DCs with NRP-1 antibodies reduced T cell proliferation. This could have implications in developing treatment options for autoimmune diseases. Using an *in vivo* experimental model of axotomy of the rat optic nerve, Shirvan et al. demonstrated that injecting anti-Sema3A antibodies inhibited retinal ganglion cell loss and neuronal protection from degeneration was observed (139). These studies led to the use of the semaphorin antibodies and peptides as possible treatment options for immune mediated diseases. Administration of anti-Sema4A monoclonal antibodies during MOG-induced EAE blocked the development of EAE (108). Other studies have shown that use of neutralizing anti-Sema4D antibodies in treating EAE and RA decreased disease severity (140). Fisher et al. determined that anti-Sema4D antibodies ameliorate collagen-induced arthritis and reduced inflammation in a collagen-induced arthritis model (140). In other studies, administration of anti-Sema4D reduced the severity of RA (107), and using anti-Sema7A antibodies, Xie et al. reported inhibition of collagen induced arthritis (125) (**Figure 2C**). Using antibodies as therapeutics, one must be cognizant of off-target effects on vasculature, vascularized organs, brain, and spinal cord. In addition to antibodies peptides targeting semaphorin receptors may be an alternative strategy to ameliorate autoimmune diseases. A recent study used Plexin-A1 antagonist to counteract the anti-migratory effect of Sema3A in oligodendrocytes. It was shown that blocking PlexinA1, the receptor of Sema3A enhanced myelin content and thus locomotor activity in an *in vivo* model of EAE (141).

CONCLUSION

Considering that the field of study of semaphorins is relatively new, tremendous progress has been made in understanding their roles in various diseases affected by angiogenesis and autoimmune reactivities. Designing effective strategies to reduce pathogenicity associated with these molecules is crucial. In this review, we discussed the role of immune semaphorins, Sema3A, 3C, 3E, 3F, 4A, 4D, 5A, 6D, and 7A in angiogenesis and autoimmune diseases. We then highlighted the inhibition of semaphorins or their receptors in ameliorating angiogenesis and autoimmune diseases.

AUTHOR CONTRIBUTIONS

VI-C selected the topic and wrote the introduction, autoimmune disease, and therapeutic approach and conclusion sections. EW wrote the semaphorin structure and signaling and prepared the Table. AU wrote the angiogenesis section and prepared **Figures 1**, **2**. All of the authors critically read and edited the manuscript.

FUNDING

This work was supported by Private donation from Pancreatic Cancer Foundation.

REFERENCES

1. Kolodkin AL, Matthes DJ, Goodman CS. The semaphorin genes encode a family of transmembrane and secreted growth cone guidance molecules. *Cell*. (1993) 75:1389–99. doi: 10.1016/0092-8674(93)90625-Z
2. Toyofuku T, Zhang H, Kumanogoh A, Takegahara N, Suto F, Kamei J, et al. Dual roles of Sema6D in cardiac morphogenesis through region-specific association of its receptor, Plexin-A1, with off-track and vascular endothelial growth factor receptor type 2. *Genes Dev*. (2004) 18:435–47. doi: 10.1101/gad.1167304
3. Bielenberg DR, Pettaway CA, Takashima S, Klagsbrun M. Neuropilins in neoplasms: expression, regulation, and function. *Exp Cell Res*. (2006) 312:584–93. doi: 10.1016/j.yexcr.2005.11.024
4. Suzuki K, Kumanogoh A, Kikutani H. Semaphorins and their receptors in immune cell interactions. *Nat Immunol*. (2008) 9:17–23. doi: 10.1038/ni1553
5. Adamis AP, Miller JW, Bernal MT, D'Amico DJ, Folkman J, Yeo TK, et al. Increased vascular endothelial growth factor levels in the vitreous of eyes with proliferative diabetic retinopathy. *Am J Ophthalmol*. (1994) 118:445–50. doi: 10.1016/S0002-9394(14)75794-0
6. Folkman J. Angiogenesis in cancer, vascular, rheumatoid and other disease. *Nat Med*. (1995) 1:27–31. doi: 10.1038/nm0195-27
7. Couffinhal T, Kearney M, Witzenbichler B, Chen D, Murohara T, Losordo DW, et al. Vascular endothelial growth factor/vascular permeability factor (VEGF/VPF) in normal and atherosclerotic human arteries. *Am J Pathol*. (1997) 150:1673–85.
8. Carmeliet P. Angiogenesis in health and disease. *Nat Med*. (2003) 9:653–60. doi: 10.1038/nm0603-653
9. MacDonald IJ, Liu SC, Su CM, Wang YH, Tsai CH, Tang CH. Implications of angiogenesis involvement in arthritis. *Int J Mol Sci*. (2018) 19:E2012. doi: 10.3390/ijms19072012
10. Zhong W, Montana M, Santosa SM, Isjwara ID, Huang YH, Han KY, et al. Angiogenesis and lymphangiogenesis in corneal transplantation-a review. *Surv Ophthalmol*. (2018) 63:453–79. doi: 10.1016/j.survophthal.2017.12.008
11. Love CA, Harlos K, Mavaddat N, Davis SJ, Stuart DI, Jones EY, et al. The ligand-binding face of the semaphorins revealed by the high-resolution crystal structure of SEMA4D. *Nat Struct Biol*. (2003) 10:843–8. doi: 10.1038/nsb977
12. Zhou Y, Gunput RA, Pasterkamp RJ. Semaphorin signaling: progress made and promises ahead. *Trends Biochem Sci*. (2008) 33:161–70. doi: 10.1016/j.tibs.2008.01.006
13. Toledano S, Nir-Zvi I, Engelman R, Kessler O, Neufeld G. Class-3 semaphorins and their receptors: potent multifunctional modulators of tumor progression. *Int J Mol Sci*. (2019) 20:556. doi: 10.3390/ijms20030556
14. Basile JR, Holmbeck K, Bugge TH, Gutkind JS. MT1-MMP controls tumor-induced angiogenesis through the release of semaphorin 4D. *J Biol Chem*. (2007) 282:6899–905. doi: 10.1074/jbc.M609570200
15. Fong KP, Barry C, Tran AN, Traxler EA, Wannemacher KM, Tang HY, et al. Deciphering the human platelet sheddome. *Blood*. (2011) 117:e15–26. doi: 10.1182/blood-2010-05-283838
16. Chen H, Chedotal A, He Z, Goodman CS, Tessier-Lavigne M. Neuropilin-2, a novel member of the neuropilin family, is a high affinity receptor for the semaphorins Sema E and Sema IV but not Sema III. *Neuron*. (1997) 19:547–59. doi: 10.1016/S0896-6273(00)80371-2
17. He Z, Tessier-Lavigne M. Neuropilin is a receptor for the axonal chemorepellent Semaphorin III. *Cell*. (1997) 90:739–51. doi: 10.1016/S0092-8674(00)80534-6

18. Comeau MR, Johnson R, DuBose RF, Petersen M, Gearing P, VandenBos T, et al. A poxvirus-encoded semaphorin induces cytokine production from monocytes and binds to a novel cellular semaphorin receptor, VESPR. *Immunity*. (1998) 8:473–82. doi: 10.1016/S1074-7613(00)80552-X
19. Winberg ML, Noordermeer JN, Tamagnone L, Comoglio PM, Spriggs MK, Tessier-Lavigne M, et al. Plexin A is a neuronal semaphorin receptor that controls axon guidance. *Cell*. (1998) 95:903–16. doi: 10.1016/S0092-8674(00)81715-8
20. Kolodkin AL, Levengood DV, Rowe EG, Tai YT, Giger RJ, Ginty DD. Neuropilin is a semaphorin III receptor. *Cell*. (1997) 90:753–62. doi: 10.1016/S0092-8674(00)80535-8
21. Nishide M, Kumanogoh A. The role of semaphorins in immune responses and autoimmune rheumatic diseases. *Nat Rev Rheumatol*. (2018) 14:19–31. doi: 10.1038/nrrheum.2017.201
22. Gagnon ML, Bielenberg DR, Gechtman Z, Miao HQ, Takashima S, Soker S, et al. Identification of a natural soluble neuropilin-1 that binds vascular endothelial growth factor: *in vivo* expression and antitumor activity. *Proc Natl Acad Sci USA*. (2000) 97:2573–8. doi: 10.1073/pnas.040337597
23. Gu C, Rodriguez ER, Reimert DV, Shu T, Fritzsch B, Richards LJ, et al. Neuropilin-1 conveys semaphorin and VEGF signaling during neural and cardiovascular development. *Dev Cell*. (2003) 5:45–57. doi: 10.1016/S1534-5807(03)00169-2
24. Kim J, Oh WJ, Gaiano N, Yoshida Y, Gu C. Semaphorin 3E-Plexin-D1 signaling regulates VEGF function in developmental angiogenesis via a feedback mechanism. *Genes Dev*. (2011) 25:1399–411. doi: 10.1101/gad.2042011
25. Neufeld G, Kessler O. The semaphorins: versatile regulators of tumour progression and tumour angiogenesis. *Nat Rev Cancer*. (2008) 8:632–45. doi: 10.1038/nrc2404
26. Neufeld G, Sabag AD, Rabinovicz N, Kessler O. Semaphorins in angiogenesis and tumor progression. *Cold Spring Harb Perspect Med*. (2012) 2:a006718. doi: 10.1101/cshperspect.a006718
27. Chauvet S, Cohen S, Yoshida Y, Fekrane L, Livet J, Gayet O, et al. Gating of Sema3E/PlexinD1 signaling by neuropilin-1 switches axonal repulsion to attraction during brain development. *Neuron*. (2007) 56:807–22. doi: 10.1016/j.neuron.2007.10.019
28. Koncina E, Roth L, Gonthier B, Bagnard D. Role of semaphorins during axon growth and guidance. *Adv Exp Med Biol*. (2007) 621:50–64. doi: 10.1007/978-0-387-76715-4_4
29. Ishii H, Kubo T, Kumanogoh A, Yamashita T. Th1 cells promote neurite outgrowth from cortical neurons via a mechanism dependent on semaphorins. *Biochem Biophys Res Commun*. (2010) 402:168–72. doi: 10.1016/j.bbrc.2010.10.029
30. Kantor DB, Chivatakarn O, Peer KL, Oster SF, Inatani M, Hansen MJ, et al. Semaphorin 5A is a bifunctional axon guidance cue regulated by heparan and chondroitin sulfate proteoglycans. *Neuron*. (2004) 44:961–75. doi: 10.1016/j.neuron.2004.12.002
31. Lin L, Lesnick TG, Maraganore DM, Isacson O. Axon guidance and synaptic maintenance: preclinical markers for neurodegenerative disease and therapeutics. *Trends Neurosci*. (2009) 32:142–9. doi: 10.1016/j.tins.2008.11.006
32. Suto F, Ito K, Uemura M, Shimizu M, Shinkawa Y, Sanbo M, et al. Plexin-a4 mediates axon-repulsive activities of both secreted and transmembrane semaphorins and plays roles in nerve fiber guidance. *J Neurosci*. (2005) 25:3628–37. doi: 10.1523/JNEUROSCI.4480-04.2005
33. Suto F, Tsuboi M, Kamiya H, Mizuno H, Kiyama Y, Komai S, et al. Interactions between plexin-A2, plexin-A4, and semaphorin 6A control lamina-restricted projection of hippocampal mossy fibers. *Neuron*. (2007) 53:535–47. doi: 10.1016/j.neuron.2007.01.028
34. Curley JL, Catig GC, Horn-Ranney EL, Moore MJ. Sensory axon guidance with semaphorin 6A and nerve growth factor in a biomimetic choice point model. *Biofabrication*. (2014) 6:035026. doi: 10.1088/1758-5082/6/3/035026
35. Pasterkamp RJ, Peschon JJ, Spriggs MK, Kolodkin AL. Semaphorin 7A promotes axon outgrowth through integrins and MAPKs. *Nature*. (2003) 424:398–405. doi: 10.1038/nature01790
36. Miao HQ, Soker S, Feiner L, Alonso JL, Raper JA, Klagsbrun M. Neuropilin-1 mediates collapsin-1/semaphorin III inhibition of endothelial cell motility: functional competition of collapsin-1 and vascular endothelial growth factor-165. *J Cell Biol*. (1999) 146:233–42. doi: 10.1083/jcb.146.1.233
37. Yu W, Bai Y, Han N, Wang F, Zhao M, Huang L, et al. Inhibition of pathological retinal neovascularization by semaphorin 3A. *Mol Vis*. (2013) 19:1397–405.
38. Acevedo LM, Barillas S, Weis SM, Gothert JR, Cheresh DA. Semaphorin 3A suppresses VEGF-mediated angiogenesis yet acts as a vascular permeability factor. *Blood*. (2008) 111:2674–80. doi: 10.1182/blood-2007-08-110205
39. Adi SD, Eiza N, Bejar J, Shefer H, Toledano S, Kessler O, et al. Semaphorin 3A Is Effective in Reducing Both Inflammation and Angiogenesis in a Mouse Model of Bronchial Asthma. *Front Immunol*. (2019) 10:550. doi: 10.3389/fimmu.2019.00550
40. Guttmann-Raviv N, Shraga-Heled N, Varshavsky A, Guimaraes-Sternberg C, Kessler O, Neufeld G. Semaphorin-3A and semaphorin-3F work together to repel endothelial cells and to inhibit their survival by induction of apoptosis. *J Biol Chem*. (2007) 282:26294–305. doi: 10.1074/jbc.M609711200
41. Varshavsky A, Kessler O, Abramovitch S, Kigel B, Zaffryar S, Akiri G, et al. Semaphorin-3B is an angiogenesis inhibitor that is inactivated by furin-like pro-protein convertases. *Cancer Res*. (2008) 68:6922–31. doi: 10.1158/0008-5472.CAN-07-5408
42. Rolny C, Capparuccia L, Casazza A, Mazzone M, Vallario A, Cignetti A, et al. The tumor suppressor semaphorin 3B triggers a prometastatic program mediated by interleukin 8 and the tumor microenvironment. *J Exp Med*. (2008) 205:1155–71. doi: 10.1084/jem.20072509
43. Banu N, Teichman J, Dunlap-Brown M, Villegas G, Tufro A. Semaphorin 3C regulates endothelial cell function by increasing integrin activity. *FASEB J*. (2006) 20:2150–2. doi: 10.1096/fj.05-5698fje
44. Maione FF, Molla C, Meda R, Latini L, Zentilin M, Giacca G. et al. Semaphorin 3A is an endogenous angiogenesis inhibitor that blocks tumor growth and normalizes tumor vasculature in transgenic mouse models. *J Clin Invest*. (2009). 119:3356–72. doi: 10.1172/JCI36308
45. Yang WJ, Hu J, Uemura A, Tetzlaff F, Augustin HG, Fischer A. Semaphorin-3C signals through Neuropilin-1 and PlexinD1 receptors to inhibit pathological angiogenesis. *EMBO Mol Med*. (2015) 7:1267–84. doi: 10.15252/emmm.201404922
46. Toledano SH, Lu A, Palacio K, Ziv O, Kessler S, Schaal G, et al. Barak. A sema3c mutant resistant to cleavage by furin (fr-sema3c) inhibits choroidal neovascularization. *PLoS One*. (2016). 11:e0168122. doi: 10.1371/journal.pone.0168122
47. Aghajanian H, Choi C, Ho VC, Gupta M, Singh MK, Epstein JA. Semaphorin 3d and semaphorin 3e direct endothelial motility through distinct molecular signaling pathways. *J Biol Chem*. (2014) 289:17971–9. doi: 10.1074/jbc.M113.544833
48. Meadows SM, Fletcher PJ, Moran C, Xu K, Neufeld G, Chauvet S, et al. Integration of repulsive guidance cues generates avascular zones that shape mammalian blood vessels. *Circ Res*. (2012) 110:34–46. doi: 10.1161/CIRCRESAHA.111.249847
49. Mazzotta C, Romano E, Bruni C, Manetti M, Lepri G, Bellando-Randone S, et al. Plexin-D1/Semaphorin 3E pathway may contribute to dysregulation of vascular tone control and defective angiogenesis in systemic sclerosis. *Arthritis Res Ther*. (2015) 17:221. doi: 10.1186/s13075-015-0749-4
50. Regano D, Visintin A, Clapero F, Bussolino F, Valdembri D, Maione F, et al. Sema3F (Semaphorin 3F) selectively drives an extraembryonic proangiogenic program. *Arterioscler Thromb Vasc Biol*. (2017) 37:1710–21. doi: 10.1161/ATVBAHA.117.308226
51. Buehler A, Sitaras N, Favret S, Bucher F, Berger S, Pielen A, et al. Semaphorin 3F forms an anti-angiogenic barrier in outer retina. *FEBS Lett*. (2013) 587:1650–5. doi: 10.1016/j.febslet.2013.04.008
52. Meda C, Molla F, De Pizzol M, Regano D, Maione F, Capano S, et al. Semaphorin 4A exerts a proangiogenic effect by enhancing vascular endothelial growth factor-A expression in macrophages. *J Immunol*. (2012) 188:4081–92. doi: 10.4049/jimmunol.1101435
53. Toyofuku T, Yabuki M, Kamei J, Kamei M, Makino N, Kumanogoh A, et al. Semaphorin-4A, an activator for T-cell-mediated immunity, suppresses angiogenesis via Plexin-D1. *EMBO J*. (2007) 26:1373–84. doi: 10.1038/sj.emboj.7601589

54. Iyer AS, Chapoval SP. Neuroimmune semaphorin 4a in cancer angiogenesis and inflammation: a promoter or a suppressor? *Int J Mol Sci*. (2018). 20:E124. doi: 10.3390/ijms20010124
55. Conrotto P, Valdembri D, Corso S, Serini G, Tamagnone L, Comoglio PM, et al. Sema4D induces angiogenesis through met recruitment by Plexin B1. *Blood*. (2005) 105:4321–9. doi: 10.1182/blood-2004-07-2885
56. Zhou H, Binmadi NO, Yang YH, Proia P, Basile JR. Semaphorin 4D cooperates with VEGF to promote angiogenesis and tumor progression. *Angiogenesis*. (2012) 15:391–407. doi: 10.1007/s10456-012-9268-y
57. Fiore R, Rahim B, Christoffels VM, Moorman AF, Puschel AW. Inactivation of the Sema5a gene results in embryonic lethality and defective remodeling of the cranial vascular system. *Mol Cell Biol*. (2005) 25:2310–9. doi: 10.1128/MCB.25.6.2310-2319.2005
58. Sadanandam A, Rosenbaugh EG, Singh S, Varney M, Singh RK. Semaphorin 5A promotes angiogenesis by increasing endothelial cell proliferation, migration, and decreasing apoptosis. *Microvasc Res*. (2010) 79:1–9. doi: 10.1016/j.mvr.2009.10.005
59. Lu Y, Xu Q, Chen L, Zuo Y, Liu S, Hu Y, et al. Expression of semaphorin 6D and its receptor plexin-A1 in gastric cancer and their association with tumor angiogenesis. *Oncol Lett*. (2016) 12:3967–74. doi: 10.3892/ol.2016.5208
60. Ghanem RC, Han KY, Rojas J, Ozturk O, Kim DJ, Jain S, et al. Semaphorin 7A promotes angiogenesis in an experimental corneal neovascularization model. *Curr Eye Res*. (2011) 36:989–96. doi: 10.3109/02713683.2011.593730
61. Hu S, Liu Y, You T, Zhu L. Semaphorin 7A promotes VEGFA/VEGFR2-mediated angiogenesis and intraplaque neovascularization in ApoE(-/-) mice. *Front Physiol*. (2018) 9:1718. doi: 10.3389/fphys.2018.01718
62. Garcia-Areas R, Libreros S, Amat S, Keating P, Carrio R, Robinson P, et al. Semaphorin7A promotes tumor growth and exerts a pro-angiogenic effect in macrophages of mammary tumor-bearing mice. *Front Physiol*. (2014) 5:17. doi: 10.3389/fphys.2014.00017
63. Sakurai A, Gavard J, Annas-Linhares Y, Basile JR, Amornphimoltham P, Palmby TR, et al. Semaphorin 3E initiates antiangiogenic signaling through plexin D1 by regulating Arf6 and R-Ras. *Mol Cell Biol*. (2010) 30:3086–98. doi: 10.1128/MCB.01652-09
64. Zhou YF, Chen AQ, Wu JH, Mao L, Xia YP, Jin HJ, et al. Sema3E/PlexinD1 signaling inhibits postischemic angiogenesis by regulating endothelial DLL4 and filopodia formation in a rat model of ischemic stroke. *FASEB J*. (2019) 33:4947–61. doi: 10.1096/fj.201801706RR
65. Mumblat Y, Kessler O, Ilan N, Neufeld G. Full-length semaphorin-3C is an inhibitor of tumor lymphangiogenesis and metastasis. *Cancer Res*. (2015) 75:2177–86. doi: 10.1158/0008-5472.CAN-14-2464
66. Valiulyte I, Curkunaviciute R, Ribokaite L, Kazlauskas A, Vaitkeviciute M, Skauminas K, et al. The anti-tumorigenic activity of Sema3C in the chick embryo chorioallantoic membrane model. *Int J Mol Sci*. (2019) 20:E5672. doi: 10.3390/ijms20225672
67. Granziero L, Circosta P, Scielzo C, Frisaldi E, Stella S, Geuna M, et al. CD100/Plexin-B1 interactions sustain proliferation and survival of normal and leukemic CD5+ B lymphocytes. *Blood*. (2003) 101:1962–9. doi: 10.1182/blood-2002-05-1339
68. Deaglio S, Vaisitti T, Bergui L, Bonello L, Horenstein AL, Tamagnone L, et al. CD38 and CD100 lead a network of surface receptors relaying positive signals for B-CLL growth and survival. *Blood*. (2005) 105:3042–50. doi: 10.1182/blood-2004-10-3873
69. Evans EE, Jonason ASJr, Bussler H, Torno S, Veeraraghavan J, Reilly C, et al. Antibody blockade of semaphorin 4D promotes immune infiltration into tumor and enhances response to other immunomodulatory therapies. *Cancer Immunol Res*. (2015) 3:689–701. doi: 10.1158/2326-6066.CIR-14-0171
70. Xia Y, Cai XY, Fan JQ, Zhang LL, Ren JH, Li ZY, et al. The role of sema4D in vasculogenic mimicry formation in non-small cell lung cancer and the underlying mechanisms. *Int J Cancer*. (2019) 144:2227–38. doi: 10.1002/ijc.31958
71. Hanahan D, Coussens LM. Accessories to the crime: functions of cells recruited to the tumor microenvironment. *Cancer Cell*. (2012) 21:309–22. doi: 10.1016/j.ccr.2012.02.022
72. Suarez-Lopez L, Sriram G, Kong YW, Morandell S, Merrick KA, Hernandez Y, et al. MK2 contributes to tumor progression by promoting M2 macrophage polarization and tumor angiogenesis. *Proc Natl Acad Sci USA*. (2018) 115:E4236–44. doi: 10.1073/pnas.1722020115
73. Holmes S, Downs AM, Fosberry A, Hayes PD, Michalovich D, Murdoch P, et al. Sema7A is a potent monocyte stimulator. *Scand J Immunol*. (2002) 56:270–5. doi: 10.1046/j.1365-3083.2002.01129.x
74. Black SA, Nelson AC, Gurule NJ, Futscher BW, Lyons TR. Semaphorin 7a exerts pleiotropic effects to promote breast tumor progression. *Oncogene*. (2016) 35:5170–8. doi: 10.1038/onc.2016.49
75. Tordjman R, Lepelletier Y, Lemarchandel V, Cambot M, Gaulard P, Hermine O, et al. A neuronal receptor, neuropilin-1, is essential for the initiation of the primary immune response. *Nat Immunol*. (2002) 3:477–82. doi: 10.1038/ni789
76. Fontenot JD, Gavin MA, Rudensky AY. Foxp3 programs the development and function of $CD4^+CD25^+$ regulatory T cells. *Nat Immunol*. (2003) 4:330–6. doi: 10.1038/ni904
77. Milpied P, Renand A, Bruneau JDA, Mendes-da-Cruz Jacquelin S, Asnafi V, Rubio MT, et al. Neuropilin-1 is not a marker of human $Foxp3^+$ Treg. *Eur J Immunol*. (2009) 39:1466–71. doi: 10.1002/eji.200839040
78. Delgoffe GM, Woo SR, Turnis ME, Gravano DM, Guy C, Overacre AE, et al. Stability and function of regulatory T cells is maintained by a neuropilin-1-semaphorin-4a axis. *Nature*. (2013) 501:252–6. doi: 10.1038/nature12428
79. Audiger C, Rahman MJ, Yun TJ, Tarbell KV, Lesage S. The Importance of Dendritic Cells in Maintaining Immune Tolerance. *J Immunol*. (2017) 198:2223–31. doi: 10.4049/jimmunol.1601629
80. Takegahara N, Kumanogoh A, Kikutani H. Semaphorins: a new class of immunoregulatory molecules. *Philos Trans R Soc Lond B Biol Sci*. (2005) 360:1673–80. doi: 10.1098/rstb.2005.1696
81. Rimar D, Nov Y, Rosner I, Slobodin G, Rozenbaum M, Halasz K, et al. Semaphorin 3A: an immunoregulator in systemic sclerosis. *Rheumatol Int*. (2015) 35:1625–30. doi: 10.1007/s00296-015-3269-2
82. Romano E, Chora I, Manetti M, Mazzotta C, Rosa I, Bellando-Randone S, et al. Decreased expression of neuropilin-1 as a novel key factor contributing to peripheral microvasculopathy and defective angiogenesis in systemic sclerosis. *Ann Rheum Dis*. (2016) 75:1541–9. doi: 10.1136/annrheumdis-2015-207483
83. Miller LE, Weidler C, Falk W, Angele P, Schaumburger J, Scholmerich J, et al. Increased prevalence of semaphorin 3C, a repellent of sympathetic nerve fibers, in the synovial tissue of patients with rheumatoid arthritis. *Arthritis Rheum*. (2004) 50:1156–63. doi: 10.1002/art.20110
84. Williams A, Piaton G, Aigrot MS, Belhadi A, Theaudin M, Petermann F, et al. Semaphorin 3A and 3F: key players in myelin repair in multiple sclerosis? *Brain*. (2007) 130(Pt 10):2554–65. doi: 10.1093/brain/awm202
85. Okuno T, Nakatsuji Y, Kumanogoh A. The role of immune semaphorins in multiple sclerosis. *FEBS Lett*. (2011) 585:3829–35. doi: 10.1016/j.febslet.2011.03.033
86. Shi W, Kumanogoh A, Watanabe C, Uchida J, Wang X, Yasui T, et al. The class IV semaphorin CD100 plays nonredundant roles in the immune system: defective B and T cell activation in CD100-deficient mice. *Immunity*. (2000) 13:633–42. doi: 10.1016/S1074-7613(00)00063-7
87. Wang L, Song G, Zheng Y, Tan W, Pan J, Zhao Y, et al. Expression of Semaphorin 4A and its potential role in rheumatoid arthritis. *Arthritis Res Ther*. (2015) 17:227. doi: 10.1186/s13075-015-0734-y
88. Okuno T, Nakatsuji Y, Moriya M, Takamatsu H, Nojima S, Takegahara N, et al. Roles of Sema4D-plexin-B1 interactions in the central nervous system for pathogenesis of experimental autoimmune encephalomyelitis. *J Immunol*. (2010) 184:1499–506. doi: 10.4049/jimmunol.0903302
89. Mizui M, Kumanogoh A, Kikutani H. Immune semaphorins: novel features of neural guidance molecules. *J Clin Immunol*. (2009) 29:1–11. doi: 10.1007/s10875-008-9263-7
90. Garcia S. Role of semaphorins in immunopathologies and rheumatic diseases. *Int J Mol Sci*. (2019) 20:E374. doi: 10.3390/ijms20020374
91. Catalano A. The neuroimmune semaphorin-3A reduces inflammation and progression of experimental autoimmune arthritis. *J Immunol*. (2010) 185:6373–83. doi: 10.4049/jimmunol.0903527
92. Cozacov R, Halasz K, Haj T, Vadasz Z. Semaphorin 3A: is a key player in the pathogenesis of asthma. *Clin Immunol*. (2017) 184:70–2. doi: 10.1016/j.clim.2017.05.011

93. Liu LN, Li XM, Ye DQ, Pan HF. Emerging role of semaphorin-3A in autoimmune diseases. *Inflammopharmacology*. (2018) 26:655–65. doi: 10.1007/s10787-018-0484-y
94. Lepelletier Y, Moura IC, Hadj-Slimane R, Renand A, Fiorentino S, Baude C, et al. Immunosuppressive role of semaphorin-3A on T cell proliferation is mediated by inhibition of actin cytoskeleton reorganization. *Eur J Immunol*. (2006) 36:1782–93. doi: 10.1002/eji.200535601
95. Solomon BD, Mueller C, Chae WJ, Alabanza LM, Bynoe MS. Neuropilin-1 attenuates autoreactivity in experimental autoimmune encephalomyelitis. *Proc Natl Acad Sci USA*. (2011) 108:2040–5. doi: 10.1073/pnas.1008721108
96. Lepelletier Y, Lecourt S, Renand A, Arnulf B, Vanneaux V, Fermand JP, et al. Galectin-1 and semaphorin-3A are two soluble factors conferring T-cell immunosuppression to bone marrow mesenchymal stem cell. *Stem Cells Dev*. (2010) 19:1075–9. doi: 10.1089/scd.2009.0212
97. Vadasz Z, Toubi E. Semaphorin 3A - a marker for disease activity and a potential putative disease-modifying treatment in systemic lupus erythematosus. *Lupus*. (2012) 21:1266–70. doi: 10.1177/0961203312456753
98. Vadasz Z, Haj T, Halasz K, Rosner I, Slobodin G, Attias D, et al. Semaphorin 3A is a marker for disease activity and a potential immunoregulator in systemic lupus erythematosus. *Arthritis Res Ther*. (2012) 14:R146. doi: 10.1186/ar3881
99. Wang P, Mao YM, Liu LN, Zhao CN, Li XM, Pan HF. Decreased expression of semaphorin 3A and semaphorin 7A levels and its association with systemic lupus erythematosus. *Immunol Invest*. (2020) 49:69–80. doi: 10.1080/08820139.2019.1649280
100. Rezaeepoor M, Shapoori S, Ganjalikhani-Hakemi M, Etemadifar M, Alsahebfosoul F, Eskandari N, et al. Decreased expression of Sema3A, an immune modulator, in blood sample of multiple sclerosis patients. *Gene*. (2017) 610:59–63. doi: 10.1016/j.gene.2017.02.013
101. Matucci-Cerinic M, Kahaleh B, Wigley FM. Review: evidence that systemic sclerosis is a vascular disease. *Arthritis Rheum*. (2013) 65:1953–62. doi: 10.1002/art.37988
102. Piaton G, Aigrot MS, Williams A, Moyon S, Tepavcevic V, Moutkine I, et al. Class 3 semaphorins influence oligodendrocyte precursor recruitment and remyelination in adult central nervous system. *Brain*. (2011) 134(Pt 4):1156–67. doi: 10.1093/brain/awr022
103. Tamagnone L, Artigiani S, Chen H, He Z, Ming GI, Song H, et al. Plexins are a large family of receptors for transmembrane, secreted, and GPI-anchored semaphorins in vertebrates. *Cell*. (1999) 99:71–80. doi: 10.1016/S0092-8674(00)80063-X
104. Kumanogoh A, Kikutani H. Immune semaphorins: a new area of semaphorin research. *J Cell Sci*. (2003) 116(Pt 17):3463–70. doi: 10.1242/jcs.00674
105. Witherden DA, Watanabe M, Garijo O, Rieder SE, Sarkisyan G, Cronin SJ, et al. The CD100 receptor interacts with its plexin B2 ligand to regulate epidermal gammadelta T cell function. *Immunity*. (2012) 37:314–25. doi: 10.1016/j.immuni.2012.05.026
106. Alto LT, Terman JR. Semaphorins and their Signaling Mechanisms. *Methods Mol Biol*. (2017) 1493:1–25. doi: 10.1007/978-1-4939-6448-2_1
107. Yoshida Y, Ogata A, Kang S, Ebina K, Shi K, Nojima S, et al. Semaphorin 4D contributes to rheumatoid arthritis by inducing inflammatory cytokine production: pathogenic and therapeutic implications. *Arthritis Rheumatol*. (2015) 67:1481–90. doi: 10.1002/art.39086
108. Kumanogoh A, Marukawa S, Suzuki K, Takegahara N, Watanabe CE, Ch'ng Ishida I, et al. Class IV semaphorin Sema4A enhances T-cell activation and interacts with Tim-2. *Nature*. (2002) 419:629–33. doi: 10.1038/nature01037
109. Kumanogoh A, Shikina T, Suzuki K, Uematsu S, Yukawa K, Kashiwamura S, et al. Nonredundant roles of Sema4A in the immune system: defective T cell priming and Th1/Th2 regulation in Sema4A-deficient mice. *Immunity*. (2005) 22:305–16. doi: 10.1016/j.immuni.2005.01.014
110. Kumanogoh A, Watanabe C, Lee I, Wang X, Shi W, Araki H, et al. Identification of CD72 as a lymphocyte receptor for the class IV semaphorin CD100: a novel mechanism for regulating B cell signaling. *Immunity*. (2000) 13:621–31. doi: 10.1016/S1074-7613(00)00062-5
111. Takamatsu H, Okuno T, Kumanogoh A. Regulation of immune cell responses by semaphorins and their receptors. *Cell Mol Immunol*. (2010) 7:83–8. doi: 10.1038/cmi.2009.111
112. Kumanogoh A, Suzuki KE, Ch'ng Watanabe C, Marukawa S, Takegahara N, Ishida I, et al. Requirement for the lymphocyte semaphorin, CD100, in the induction of antigen-specific T cells and the maturation of dendritic cells. *J Immunol*. (2002) 169:1175–81. doi: 10.4049/jimmunol.169.3.1175
113. Gras C, Eiz-Vesper B, Jaimes Y, Immenschuh S, Jacobs R, Witte T, et al. Secreted semaphorin 5A activates immune effector cells and is a biomarker for rheumatoid arthritis. *Arthritis Rheumatol*. (2014) 66:1461–71. doi: 10.1002/art.38425
114. O'Connor BP, Eun SY, Ye Z, Zozulya AL, Lich JD, Moore CB, et al. Semaphorin 6D regulates the late phase of CD4+ T cell primary immune responses. *Proc Natl Acad Sci USA*. (2008) 105:13015–20. doi: 10.1073/pnas.0803386105
115. Suzuki K, Okuno T, Yamamoto M, Pasterkamp RJ, Takegahara N, Takamatsu H, et al. Semaphorin 7A initiates T-cell-mediated inflammatory responses through alpha1beta1 integrin. *Nature*. (2007) 446:680–4. doi: 10.1038/nature05652
116. Kang HR, Lee CG, Homer RJ, Elias JA. Semaphorin 7A plays a critical role in TGF-beta1-induced pulmonary fibrosis. *J Exp Med*. (2007) 204:1083–93. doi: 10.1084/jem.20061273
117. Kim CW, Cho EH, Lee YJ, Kim YH, Hah YS, Kim DR. Disease-specific proteins from rheumatoid arthritis patients. *J Korean Med Sci*. (2006) 21:478–84. doi: 10.3346/jkms.2006.21.3.478
118. Giacobini P, Messina A, Morello F, Ferraris N, Corso S, Penachioni J, et al. Semaphorin 4D regulates gonadotropin hormone-releasing hormone-1 neuronal migration through PlexinB1-Met complex. *J Cell Biol*. (2008) 183:555–66. doi: 10.1083/jcb.200806160
119. Deng S, Hirschberg A, Worzfeld T, Penachioni JY, Korostylev A, Swiercz JM, et al. Plexin-B2, but not Plexin-B1, critically modulates neuronal migration and patterning of the developing nervous system *in vivo*. *J Neurosci*. (2007) 27:6333–47. doi: 10.1523/JNEUROSCI.5381-06.2007
120. Belle M, Parray A, Belle M, Chedotal A, Nguyen-Ba-Charvet KT. PlexinA2 and Sema6A are required for retinal progenitor cell migration. *Dev Growth Differ*. (2016) 58:492–502. doi: 10.1111/dgd.12298
121. Scott GA, McClelland LA, Fricke AF. Semaphorin 7a promotes spreading and dendricity in human melanocytes through beta1-integrins. *J Invest Dermatol*. (2008) 128:151–61. doi: 10.1038/sj.jid.5700974
122. Delorme G, Saltel F, Bonnelye E, Jurdic P, Machuca-Gayet I. Expression and function of semaphorin 7A in bone cells. *Biol Cell*. (2005) 97:589–97. doi: 10.1042/BC20040103
123. Gan Y, Reilkoff R, Peng X, Russell T, Chen Q, Mathai SK, et al. Role of semaphorin 7a signaling in transforming growth factor beta1-induced lung fibrosis and scleroderma-related interstitial lung disease. *Arthritis Rheum*. (2011) 63:2484–94. doi: 10.1002/art.30386
124. Gutierrez-Franco A, Eixarch H, Costa C, Gil V, Castillo M, Calvo-Barreiro L, et al. Semaphorin 7A as a potential therapeutic target for multiple sclerosis. *Mol Neurobiol*. (2017) 54:4820–31. doi: 10.1007/s12035-016-0154-2
125. Xie J, Wang H. Semaphorin 7A as a potential immune regulator and promising therapeutic target in rheumatoid arthritis. *Arthritis Res Ther*. (2017) 19:10. doi: 10.1186/s13075-016-1217-5
126. Costa C, Martinez-Saez E, Gutierrez-Franco A, Eixarch H, Castro Z, Ortega-Aznar A, et al. Expression of semaphorin 3A, semaphorin 7A and their receptors in multiple sclerosis lesions. *Mult Scler*. (2015) 21:1632–43. doi: 10.1177/1352458515599848
127. Kopp MA, Brommer B, Gatzemeier N, Schwab JM, Pruss H. Spinal cord injury induces differential expression of the profibrotic semaphorin 7A in the developing and mature glial scar. *Glia*. (2010) 58:1748–56. doi: 10.1002/glia.21045
128. Casazza A, Fu X, Johansson I, Capparuccia L, Andersson F, Giustacchini A, et al. Systemic and targeted delivery of semaphorin 3A inhibits tumor angiogenesis and progression in mouse tumor models. *Arterioscler Thromb Vasc Biol*. (2011) 31:741–9. doi: 10.1161/ATVBAHA.110.211920
129. Kessler O, Shraga-Heled N, Lange T, Gutmann-Raviv N, Sabo E, Baruch L, et al. Semaphorin-3F is an inhibitor of tumor angiogenesis. *Cancer Res*. (2004) 64:1008–15. doi: 10.1158/0008-5472.CAN-03-3090
130. Serini G, Bussolino F, Maione F, Giraudo E. Class 3 semaphorins: physiological vascular normalizing agents for anti-cancer therapy. *J Intern Med*. (2013) 273:138–55. doi: 10.1111/joim.12017
131. Bielenberg DR, Hida Y, Shimizu A, Kaipainen A, Kreuter M, Kim CC, et al. Semaphorin 3F, a chemorepulsant for endothelial cells, induces a poorly

vascularized, encapsulated, nonmetastatic tumor phenotype. *J Clin Invest*. (2004) 114:1260–71. doi: 10.1172/JCI21378

132. Gu C, Yoshida Y, Livet J, Reimert DV, Mann F, Merte J, et al. Semaphorin 3E and plexin-D1 control vascular pattern independently of neuropilins. *Science*. (2005) 307:265–8. doi: 10.1126/science.1105416
133. Moriya J, Minamino T, Tateno K, Okada S, Uemura A, Shimizu I, et al. Inhibition of semaphorin as a novel strategy for therapeutic angiogenesis. *Circ Res*. (2010) 106:391–8. doi: 10.1161/CIRCRESAHA.109.210815
134. Sabag AD, Bode J, Fink D, Kigel B, Kugler W, Neufeld G. Semaphorin-3D and semaphorin-3E inhibit the development of tumors from glioblastoma cells implanted in the cortex of the brain. *PLoS ONE*. (2012) 7:e42912. doi: 10.1371/journal.pone.0042912
135. Casazza A, Kigel B, Maione F, Capparuccia L, Kessler O, Giraudo E, et al. Tumour growth inhibition and anti-metastatic activity of a mutated furin-resistant Semaphorin 3E isoform. *EMBO Mol Med*. (2012) 4:234–50. doi: 10.1002/emmm.201100205
136. Bejar J, Kessler O, Sabag AD, Sabo E, Itzhak OB, Neufeld G, et al. Semaphorin3A: a potential therapeutic tool for lupus nephritis. *Front Immunol*. (2018) 9:634. doi: 10.3389/fimmu.2018.00634
137. Vadasz Z, Haj T, Balbir A, Peri R, Rosner I, Slobodin G, et al. A regulatory role for CD72 expression on B cells in systemic lupus erythematosus. *Semin Arthritis Rheum*. (2014) 43:767–71. doi: 10.1016/j.semarthrit.2013.11.010
138. Kong JS, Yoo SA, Kim JW, Yang SP, Chae CB, Tarallo V, et al. Anti-neuropilin-1 peptide inhibition of synoviocyte survival, angiogenesis, and experimental arthritis. *Arthritis Rheum*. (2010) 62:179–90. doi: 10.1002/art.27243
139. Shirvan A, Kimron M, Holdengreber V, Ziv I, Ben-Shaul Y, Melamed S, et al. Anti-semaphorin 3A antibodies rescue retinal ganglion cells from cell death following optic nerve axotomy. *J Biol Chem*. (2002) 277:49799–807. doi: 10.1074/jbc.M204793200
140. Fisher TL, Seils J, Reilly C, Litwin V, Green L, Salkowitz-Bokal J, et al. Saturation monitoring of VX15/2503, a novel semaphorin 4D-specific antibody, in clinical trials. *Cytometry B Clin Cytom*. (2016) 90:199–208. doi: 10.1002/cyto.b.21338
141. Biname F, Pham-Van LD, Spenle C, Jolivel V, Birmpili D, Meyer LA, et al. Disruption of Sema3A/Plexin-A1 inhibitory signalling in oligodendrocytes as a therapeutic strategy to promote remyelination. *EMBO Mol Med*. (2019) 11:e10378. doi: 10.15252/emmm.201910378

Conflict of Interest: The authors declare that the research was conducted in the absence of any commercial or financial relationships that could be construed as a potential conflict of interest.

Advantages of publishing in Frontiers

OPEN ACCESS
Articles are free to read for greatest visibility and readership

FAST PUBLICATION
Around 90 days from submission to decision

HIGH QUALITY PEER-REVIEW
Rigorous, collaborative, and constructive peer-review

TRANSPARENT PEER-REVIEW
Editors and reviewers acknowledged by name on published articles

Frontiers
Avenue du Tribunal-Fédéral 34
1005 Lausanne | Switzerland

Visit us: www.frontiersin.org
Contact us: info@frontiersin.org | +41 21 510 17 00

REPRODUCIBILITY OF RESEARCH
Support open data and methods to enhance research reproducibility

DIGITAL PUBLISHING
Articles designed for optimal readership across devices

FOLLOW US
@frontiersin

IMPACT METRICS
Advanced article metrics track visibility across digital media

EXTENSIVE PROMOTION
Marketing and promotion of impactful research

LOOP RESEARCH NETWORK
Our network increases your article's readership